The Dissertation Committee for Nikhil Jayant Kavimandan certifies that this is the approved version of the following dissertation:

In vitro and In vivo Behavior of Insulin Delivery Systems Based on Poly(ethylene glycol)-Grafted Poly(methacrylic acid) Hydrogels

Committee:

Nicholas A. Peppas, Supervisor

Robert Williams III

Benny Freeman

Lynn Loo

Christine Schmidt

In vitro and In vivo Behavior of Insulin Delivery Systems Based on Poly(ethylene glycol)-Grafted Poly(methacrylic acid) Hydrogels

by

Nikhil Jayant Kavimandan, B. Chem.

Dissertation

Presented to the Faculty of the Graduate School of

the University of Texas at Austin

in Partial Fulfillment

of the Requirements

for the Degree of

Doctor of Philosophy

The University of Texas at Austin

May, 2005

To My Loving Wife Reena,

For Your Constant Support and Understanding.

ACKNOWLEDGEMENTS

I would like to take this opportunity to thank Professor Nicholas Peppas for his constant support during the course of my Ph.D. I have learnt many valuable things about professional life from him that will help me immensely in my career path. I would also like to thank Prof. Morishita, Prof. Takayama and Prof. Nagai, for their constant support during my stay in Japan. I am also grateful to my dissertation committee members: Professors Robert Williams, Benny Freeman, Christine Schmidt, and Lynn Loo. I would like to thank Dr. Atul Khare of Baxter Healthcare, for his guidance and help.

I feel extremely fortunate to have worked with some wonderful colleagues during my work: Jennifer, Ebru, Christina, Bumsang, Mark, Dave, Jay, Zach, Nicki, Kristy, Hunter, Brock, Dan, Don, Terry, Jeff, Omar, and others. I would like to thank Elena Losi, who helped me immensely during the finishing stages of my work. I am also grateful to my friends in Japan: Tetsu, Chiba, Goto, Onuki, and others for their love and affection.

I would also like to thank my friends and family members who were always there for me, in person, or in spirit, when I needed them.

Finally, I would like to dedicate this work to my wife, who probably deserves this Ph.D. as much as I do, for her immense patience and understanding.

In vitro and In vivo Behavior of Insulin Delivery Systems Based on Poly(ethylene glycol)-Grafted Poly(methacrylic acid) Hydrogels

Publication No. _____

Nikhil Jayant Kavimandan, Ph.D.

The University of Texas at Austin, 2005

Supervisor: Nicholas A. Peppas

Developing oral insulin formulations for the treatment of diabetes can greatly improve the quality of life of the patients. Many different approaches have been investigated to address the problems associated with oral insulin delivery, but the bioavailability of oral insulin is still low, even in some of the most successful formulations. Insulin is rapidly degraded by the enzymes in the GI tract and is not transported across the epithelial barrier easily. The oral insulin formulation developed in this work makes use of complexation hydrogels for oral delivery of insulin bioconjugates. The insulin bioconjugates synthesized in this work consist of insulin bound to transferrin molecule which can be uptaken by the epithelial cells. These conjugates can increase the permeability of insulin across the epithelial barrier by receptor-mediated transcytosis. The transferrin in the conjugate is also shown to stabilize insulin in the presence of intestinal enzymes.

Use of complexation hydrogels for delivery of insulin-transferrin conjugate may greatly increase the bioavailability of oral insulin. This is because, the complexation hydrogels are known to exhibit characteristics that make them ideal candidates for oral protein delivery. For example, it is shown in this work that the hydrogels can increase the retention of the therapeutic protein in the small intestine. They can also inhibit the degradation of insulin in the GI tract. Thus, combination of these two approaches provides an innovative platform for oral insulin delivery.

TABLE OF CONTENTS

CHAPTER 1

INTRODUCTION

Increasing number of therapeutic agents emerging from the rapid growth of biotechnological research component of pharmaceutical drug discovery are macromolecules such as proteins. However, difficulties encountered in administration of these proteins limit their clinical applicability. Currently the most common way of administering therapeutic proteins is through injections. This route of administration is typically painful, and suffers from low patient compliance for the treatment. Thus, new and improved methods of administration are being constantly developed.

Insulin therapy is at the heart of protein delivery research. Insulin is a protein of immense importance because of its role in the treatment of diabetes, which is growing into epidemic proportions in many developing countries. The options currently available for administration of insulin are mostly limited to insulin injections through needles. Hence other routes of administration such as pulmonary, dermal, buccal, and oral are currently being investigated. Oral route remains the preferred mode of administration because of the ease and cost effectiveness of oral dosage formulations. Oral administration is also linked to increase in patient compliance and overall increase in the efficacy of treatment.

However, the enzymatic instability of insulin in the GI tract and its inability

to traverse the intestinal barrier severely reduce the fraction of orally administered insulin that reaches the blood stream (bioavailability).

In this work we have developed an oral insulin formulation based on complexation hydrogels used as delivery vehicles for insulin-bioconjugates. The complexation hydrogels developed in our laboratory are shown to be promising candidates for oral insulin administration. These hydrogels come under the class of environment-sensitive hydrogels, and specifically, they show pH-dependent swelling behavior. The hydrogel is synthesized by UV-initiated free radical polymerization of methacrylic acid (MAA) and methoxy-terminated poly(ethylene glycol) monomethacrylate PEGMA and consists of crosslinked PMAA grafted with PEG chains, henceforth designated as P(MAA-g-EG). The success of this delivery system for insulin is due to the ability of the carriers to protect the protein from degradation in the harsh conditions encountered in the GI tract. These hydrogels also exhibit potential to stick to the intestinal mucus and increase the residence time of the drug in the GI tract.

The objectives of this work are given in Chapter 3. Experimental investigation of gastrointestinal distribution and retention of the microparticles was performed here. The ability of microparticles to protect insulin degradation in the GI tract was also studied. These studies are presented in Chapter 6 and Chapter 7. The ability of the microparticles to change the permeability of model intestinal epithelium was also investigated in this work. This study is given in Chapter 4. One important factor that limits the bioavailability of orally

administered insulin is its inability to efficiently traverse the intestinal epithelium. Thus, understanding of mechanisms of insulin transport across the cellular barrier is important for development of effective delivery systems. In vitro evaluation of transport mechanism was carried out using confocal microscopy and the results are presented in Chapter 5. Chapters 8 through Chapter 10 deal with the development of oral formulation based on complexation hydrogels used as oral delivery vehicle for insulin-transferrin conjugates. The synthesis and characterization of insulin-transferrin conjugate is discussed in Chapter 8. Optimization of the polymer carriers for delivery of the conjugates is presented in Chapter 9. These conjugates are shown to improve the permeability of insulin across in vitro model of intestinal epithelium. These cellular studies are discussed in Chapter 10. In Chapter 1 an overview of diabetes treatment and insulin therapy is presented with focus on oral insulin delivery.

CHAPTER 2

BACKGROUND

Major innovations in the drug delivery field have surfaced in recent years. Oral administration of therapeutic agents is the preferred means of delivering drugs because of ease of administration, low cost and high patient compliance. However, formulating a drug for oral delivery is a complicated process. Poor intrinsic protein permeability as a result of large molecular weight, degradation by proteolytic enzymes in the stomach and in the small intestine, and chemical instability are some of the major hurdles for developing effective formulations for delivery of peptides and proteins. Although there are several success stories in the development and commercialization of oral dosage forms for small molecules, very few oral delivery systems have been developed for proteins and peptides. The oral formulation of cyclosporin [1] is one of the very few examples of successful development of oral formulations for peptide drugs.

In this chapter we will discuss novel methods for administration of insulin for the treatment of diabetes. Since its initial administration to humans in 1922, insulin has been the cornerstone of type 1 diabetes. Conventionally, insulin is administered by subcutaneous injections which mimic, as close as possible, secretion of insulin by healthy pancreas. However, due to compliance-related issues and other complications, more acceptable delivery systems are highly desirable. An overview of diabetes mellitus and novel ways of treating this

disease are included here. Special attention is given to oral insulin delivery which is the focus of this work.

2.1 Diabetes Mellitus

Diabetes is characterized by the body's inability to produce or properly use insulin. Diabetes mellitus is a metabolic disorder of multiple aetiology characterized by chronic hyperglycaemia with disturbances of carbohydrate, fat and protein metabolism resulting from defects in insulin secretion, insulin action, or both [2]. There are 18.2 million people in the United States, or 6.3% of the population, who have diabetes [3]. Diabetes mellitus is occurring in epidemic proportions in many developing and newly industrialized countries [4]. Globally, it is now one of the most common non-communicable diseases and is the fourth or fifth leading cause of death in most developed countries [5]. The global burden of diabetes is estimated to rise from about 118 million in 1995 to 220 million in 2010 and 300 million in 2025 [6, 7].

The aetiological types of diabetes are designated as type 1, type 2 diabetes and other specific types of diabetes resulting from genetic defects of β-cell function, genetic defects in insulin action, endocrinopathies (resulting from over secretion of insulin antagonizing hormones), infections and drug- or chemically induced diabetes [2]. Further, in nearly 3 to 5 % of all pregnancies, women develop gestational diabetes [8].

Type 1 diabetes can be classified as autoimmune diabetes mellitus or idiopathic Type 1 diabetes. Autoimmune diabetes mellitus is characterized by the autoimmune mediated destruction of the insulin secreting pancreatic β-cells [2]. Individuals suffering from this form of Type 1 diabetes typically become dependent on insulin for survival and are at a risk of ketoacidosis, a condition resulting from extremely high levels of blood glucose (over 249 mg/dl) wherein the body begins to burn fat and muscle for energy which causes release of ketone bodies in the bloodstream. Idiopathic Type 1 diabetes is a diabetes of unknown origin. Some of the patients suffering from this disease have permanent insulin deficiency and are prone to ketoacidosis, but this form of diabetes shows no evidence of autoimmunity [2, 3].

Type 2 is the most common form of diabetes and is characterized by disorders of insulin action and insulin secretion, either of which may be the predominant feature [2]. Individuals suffering from this form of diabetes are typically resistant to the action of insulin [2, 9]. According to the American Diabetes Association (ADA), nearly 16 million individuals in the United States have type 2 diabetes while about one-third of those people are not aware that they have the disease [3]. This is primarily because the hyperglycemia is often not severe enough to be symptomatic. Ketoacidosis is relatively infrequent in this type of diabetes. Nevertheless individuals suffering from this form of diabetes are at increased risk of developing macrovascular and microvascular complications. If untreated, type 2 diabetes can cause serious complications, including kidney

failure, blindness, heart attack, lower-limb amputation [10]. Fortunately, in many cases, type 2 diabetes can be adequately controlled through a combination of proper nutrition and exercise. However, some people with type 2 diabetes do require oral medications or insulin injections.

To determine if a patient is normal, pre-diabetic or diabetic, health care providers conduct a fasting plasma glucose test (FPG) or an oral glucose tolerance test (OGTT) [11]. Either test can be used to diagnose pre-diabetes or diabetes. Pre-diabetes, characterized by a glucose level between that of a healthy individual and a diabetic patient, is also called impaired glucose tolerance (IGT) or impaired fasting glucose (IFG) [12].

The FPG test is easier, faster, and less expensive to perform. With the FPG test, a fasting blood glucose level between 100 and 125 mg/dl indicates pre-diabetes. A person with a fasting blood glucose level of 126 mg/dl or higher is considered diabetic [2, 11].

In the OGTT test, a person's blood glucose level is measured after a fast and two hours after drinking a glucose-rich beverage (2h-PG value). Two-hour blood glucose level of 140-199 mg/dl signals pre-diabetes, whereas the two-hour blood glucose level of >200 mg/dl, signals diabetes [2, 11]. Although the OGTT (which consists of an FPG and 2-h PG value) is recognized as a valid way to diagnose diabetes, the use of the test for diagnostic purposes in clinical practice is limited because of its inconvenience, less reproducibility, greater cost [11, 13].

The most common form of type 1 diabetes treatment is insulin therapy which is described in the next section. Some of the important areas of therapeutic treatment of diabetes that are currently being explored are discussed here.

Curative therapy for diabetes mellitus mainly implies replacement of functional insulin-producing pancreatic beta cells, with pancreas or islet-cell transplants. This is the only replacement therapy that can improve metabolic control other than conventional and intensive insulin therapy [14]. Transplantation can be performed either by implantation of the pancreatic organ or by implantation of only the pancreatic islets of Langerhans. Until recently, pancreas transplantation was considered to be the only viable procedure for autonomous regulation of glucose level [14, 15]. However, to avoid pancreatic graft rejection, transplantation has to be coupled with lifelong immunosuppression which itself can cause severe side effect as increased susceptibility to viral, fungal, and bacterial infections, and increased risk for the development of malignancies [14, 16, 17].

Islet transplants are beneficial compared to implantation of pancreatic organ since they avoid the need for major surgical procedures. A small mass of islet cells can be delivered to the liver through intraportal infusion. The procedure for islet cell transplantation was initially successful in small animal models, but was not effective in humans [18, 19]. However, Shapiro et al. [20] recently developed a new immunosuppressive regimen and reported a 100% success

rate in achieving insulin independence through islet transplantation in 7 long term diabetic patients. Unfortunately, like pancreatic graft transplants, islet transplantation also suffers from the necessity of lifelong immunosuppression. Another limitation of islet cell transplantation procedures is the need for adequate supply of donor islet cells. One solution to this problem that is currently an area of active research is differentiation of embryonic stem cells into the insulin secreting islet cells by manipulating the culture conditions [18, 21]. However, the precise factors and conditions that convert progenitor stem cells into the desired mature β-cells are not yet fully understood [22].

Researchers have sought to circumvent the need for immunosuppressant regimen in islet transplantation by encapsulation of the islet cells by semipermeable membrane that protects the grafts from the host immune system [23, 24]. In addition to being immunoprotective, these membranes also have to be mechanically stable, biocompatible and sufficiently permeable to insulin and should also allow oxygenation of the encapsulated cells.

2.2 Insulin and Insulin Therapy

In 1889, von Mehring and Minkowski showed that ligation of the pancreas in dog caused diabetes [25]. This lead to an intensive search for the active component that the pancreas was producing that was involved in preventing the development of diabetes. In 1922 Banting and Best successfully extracted

insulin. For more than a decade following its discovery, insulin was used in the form of crude extracts of the pancreas of cow, pig or sheep for diabetes treatment [26]. Insulin was first purified by crystallization in the presence of zinc in 1936 [27].

Sanger in 1955 elucidated the primary structure of insulin [28]. Although the amino acid sequence of insulin varies among different species, certain sequences are highly conserved [29]. The sequences porcine insulin and human insulin are almost identical, differing by only one amino acid whereas bovine insulin differs by three amino acids from the human analog. However, none of the variations in the amino acid sequence are at sites crucial for the activity and function of insulin [29].

When insulin is synthesized by the beta cells of the pancreas, it is produced as a large preproharmone. This preproharmone has a molecular weight of about 11,500. It is cleaved within the cisternae of the endoplasmic reticulum of the β-cells to form proinsulin which has a molecular weight of about 9,000. This molecule then splits into two pieces: insulin, with a molecular weight of 5,808 in humans, and C-peptide, before being secreted outside the cells through the secretory granules. The secreted insulin has 31 amino acid long B chain and the 20 amino acid long A chain which are locked in their relative conformation by two disulfide bonds. The cleaved and secreted insulin is 51 amino acids long and has a hydrodynamic radius of about 20 Å [30].

The plasma glucose level is maintained within a very narrow range of 3.5-7.0 mmol/L in spite of wide fluctuations introduced by food intake, exercise, other physiological and physiological disturbances [31]. This glucose homeostasis is achieved by regulating release and inhibition of glucagons and insulin, both secreted by the pancreatic cells.

Increase in blood glucose triggers secretion of insulin from the pancreas. Insulin secreted from the pancreas is infused via the portal vein to the liver, where it leads to an increase in the storage of glucose with a concomitant decrease in hepatic glucose release to the circulation [32]. Insulin circulates in the blood with plasma half life of about 6 minutes, so that it is almost entirely cleared from the circulation within 10-15 minutes. The freely circulating insulin then acts on several peripheral tissues including muscle, liver and fat tissue by binding to the specific insulin receptors on cells.

An Insulin receptor is a hetero-tetramer with a molecular weight of about 300,000. The two alpha subunits lie entirely outside of the cell membrane and the two beta subunits penetrate through the cell membrane. Insulin binding to the alpha subunits on the outside of the cell triggers autophosphorylation of the beta subunits on several tyrosine residues protruding into the cytoplasm.

The activated beta subunits then phosphorylate and activate IRS-1. IRS-1 is an enzyme and a key mediator of insulin's biological activity. Following this, various intracellular regulators are recruited to IRS-1 and this initiates a regulatory cascade of signals with each molecule binding to IRS-1 activating its

own complex cascade [33]. This finally leads to increase in the permeability of cell membranes to glucose and glucose uptake increases. This increased uptake of glucose due to insulin binding occurs in the muscle cells, adipose cells, and other types of cells in the body constituting about 80 percent of all the cells.

In addition to its role in uptake of glucose, insulin also stimulates conversion of carbohydrate or proteins to fat (lipogenesis), and increases amino acid transport into cells. It also stimulates growth, DNA synthesis, and cell replication.

In the absence of curative therapy for the treatment of diabetes, insulin replacement therapy is required for all people with type 1 diabetes [34]. Benefits of insulin therapy in patients with type 2 diabetes are also well recognized now [35-37]. Intensive glucose control delays the onset and retards the progression of microvascular and macrovascular diseases in patients with type 2 diabetes [38]. Insulin therapy is, therefore, central to management of patients with diabetes. With the development and approval of recombinant technologies for insulin production, human insulin could be made biosynthetically which became the preferred method of insulin production. This also led to the development of mutant insulin analogues having improved pharmacokinetic properties for subcutaneous administration [39-41]. However, for over 80 years injection or infusion of insulin into the subcutaneous (s.c.) tissue has been the only route of insulin delivery used in clinical practice. This mimics, as close as possible, secretion of insulin by healthy pancreas.

Recent developments of improved injection devices, such as insulin pens, and very sharp needles, have reduced the pain associated with the injection therapy to a considerable extent. But even with these developments, injection therapy still requires the handling of a device and is associated with pain. This often results in low patience compliance to the therapy. Clinical studies have shown that because of the non-compliance related issues, even on insulin treatment, a significant percentage of patients fail to attain lasting glycemic control [32].Further, this route of insulin administration has associated side effects, such as hyperinsulinemia and localized deposition of insulin that lead to local hypertrophy and fat deposits at injection sites [42].

Thus there is great interest today in developing formulations that deliver insulin through other routes of administration. These alternative routes of insulin administration are discussed in the following section.

2.3 Alternative Routes of Insulin Administration

The current recommended intensive insulin therapy regimens involve multiple subcutaneous insulin injections everyday. These increases compliance constrains on patients to a great extent and reduce the overall efficacy of treatment. Hence, as discussed above, non-invasive insulin formulations that mimic physiological secretion of insulin as a means of maintaining the glucose homeostasis are highly desirable. Recent advances in alternative routes of

administration as an approach to improve insulin therapy are discussed here. Investigated delivery systems for insulin therapy mainly include transdermal, nasal, buccal, pulmonary and oral delivery systems.

2.3.1 Transdermal delivery

Large, hydrophilic macromolecules such as insulin cannot efficiently permeate the skin. This skin impermeability is mainly due to the intercellular lipid layer of the stratum corneum [43]. Thus, the delivery approaches targeted at improving the transdermal delivery of drugs involve breaking down or removing the lipid barrier by chemical, electrical or physical methods [44]. Iontophoresis, low-frequency ultrasound, or chemical agents acting as vesicles are some of the methodologies investigated. In Iontophoresis, low-level electric current is used to enhance the permeability of the drug across the stratum corneum and the permeability of insulin depends on the net charge of the insulin molecule [45, 46]. However the potential of this methodology has only been demonstrated in animal studies and the amount of insulin transferred across the skin was barely enough to meet basal insulin requirement [44].

Low-frequency ultrasound (20-150 kHz) has been shown to be more effective by causing several-fold increase in macromolecular permeability [47]. However, even with this technique, insulin delivery rates may not be sufficient for physiological replacement of insulin [48]. Combined use of iontophoresis and

ultrasound has been proposed as an approach for increasing macromolecular transfer across the skin barrier [49].

Another approach involves incorporating insulin into vesicles made of soybean phosphatidylcholine, called transfersomes. Transfersomes are highly deformable and as a result are able to pass through pores smaller than their size with permeability similar to water [50]. It was observed that transformers transport insulin with 50% bioefficiency compared to subcutaneous injection. However, more recent studies have been unable to reproduce these findings [44]. Despite a number of techniques that have been investigated, so far, dermal insulin methodologies have not resulted in reproducible and acceptable transfer of insulin across the highly efficient skin barrier [44].

2.3.2 Intranasal Delivery

The nasal mucosa is characterized by large surface area for drug absorption (about 150 cm^2), high coverage density of the epithelium by microvilli, and a rich, vascularized subepithelium [51]. The drugs entering through this route directly enter the systemic circulation, thus avoiding hepatic first-pass metabolism. Nasal absorption also provides for rapid attainment of therapeutic blood levels, and quicker onset of pharmacological activity [52]. The main barriers to absorption include the very active mucociliary clearance, enzyme activity, low permeability and low pH of the nasal epithelium. In addition, little information is available on the influence of nasal pathology on the efficacy of

insulin administration [51, 53]. Small molecular weight molecules such as oxytocin (MW 1,007) and calcitonin (MW3,431) have been successfully delivered via the nasal route [54], but reproducible and reliable intranasal delivery methodology for insulin has not been developed.

The observed low bioavailability of insulin administered via the intranasal route often necessitates use of absorption enhancers. However many of these enhancers have been known to cause damage to the nasal mucosa. Use of lecithin, bile salts or laureth-9 as absorption enhancers for nasal absorption enhancement caused nasal irritation in patients [48, 55, 56]. Even with the use of absorption enhancers, reproducible and reliable insulin delivery has not been achieved.

Intranasal insulin administration with a medium-chain phospholipid (didecanoyl-L-alpha-phosphatidylcholine) as an absorption enhancer was observed to cause rapid increase in the serum insulin concentration in healthy individuals, reaching glucose reducing peak in 20-45 min [57, 58]. Pharmacological bioavailability, corrected for the endogenously produced insulin for the nasal formulation, was 8.3% relative to an intravenous bolus injection [58]. Administered insulin also exhibited a faster time-course of absorption when compared to subcutaneous injection. This makes intranasal administration a particularly attractive option for prandial insulin replacement.

However, subsequent studies failed to confirm these initial positive results [59]. Potential damage to the nasal mucosa and nasal irritation, especially in the

long-term treatment regimen and high rates of treatment failure are the main obstacles in clinical application of intranasal insulin delivery [44, 48].

2.3.3 Buccal Delivery

Buccal mucosa offers an interesting portal of administration for both systemic and local delivery of therapeutic agents. The oral mucosa consists of a non-keratinized area (sublingual, and buccal mucosa) and the keratinized area (the gum or gingiva, the palatal mucosa, and the inner side of the lips). The non-keratinized regions are generally more permeable as compared to the keratinized areas [60]. The oral cavity has a large surface area for absorption (100– 200 cm^2), is richly vascularized and has little proteolytic activity. It has fewer proteolytic enzymes than the oral, nasal, vaginal and rectal administration areas [61]. The predominant peptidases found in the buccal mucosa are aminopeptidases. The proteolytic enzymes such as trypsin, chymotrypsin and pepsin, which are present in the gastric and intestinal fluids, are largely absent [60, 62]. The factors limiting insulin absorption via the buccal route are the relatively thick multi-layered buccal barrier, the high rate of mucus turnover and the proteolytic degradation. Strategies investigated to improve absorption of insulin include use of absorption enhancers, bioadhesive systems and enzyme inhibitors [60, 63, 64].

Recently, Generex (Toronto, Canada) demonstrated efficacy of a buccal insulin delivery system based on an oral insulin spray which administers insulin in

the form of a high-velocity, fine particle aerosol directly into the patient's mouth. The particles consist of mixed micelles made from absorption enhancers that encapsulate insulin [65]. The fast moving, fine particles are able to penetrate a thin membrane that guards the surface area in direct contact with the blob circulation. Combined with the effect of absorption enhancers, the penetrating particles cause a rapid increase in the uptake of insulin into the systemic circulation [66]. The administered insulin appears in the circulation within 10 minutes of application. Bioavailability of 7 to 8% was determined in a proof-of-concept study involving type 2 diabetic patients and the insulin peak was reached in about 30 min after application. The subcutaneously injected insulin reached the absorption peak in about 60 minutes [65]. More clinical and toxicological data is required to establish the efficacy of this system.

2.3.4 Pulmonary Delivery

The respiratory tract offers a high area for drug absorption, a thin epithelial membrane and a rich vasculature. It also lacks effective mucociliary clearance and is highly immunotolerant. In addition, this route of administration also eliminates the first-pass hepatic metabolism [59]. This makes the lungs an attractive option for drug delivery [51, 67]. Inhalers are typically used for pulmonary insulin delivery, which enables the drug to reach the deep-lung, from where it can be quickly absorbed into the circulation. The factors that need to be controlled for optimizing insulin delivery include the type of propellant used, the

air flow speed, the losses within the device, the particle size and drug deposition into the throat and bronchial tubes [48]. Particle size and velocity greatly influence the deep-lung deposition of the inhaled protein [67]. Several pulmonary insulin delivery systems including Exubera, being jointly developed by Nektar Therapeutics, Pfizer and Aventis, the AERx, developed by Aradigm Corporation and Novo Nordisk and AIR developed by Alkermes and Eli Lilly, are in development and in phase III testing [42-Cefalu]. Two of these devices, Exubera and AERx are in phase III testing and show efficacy comparable to subcutaneous insulin [48, 68, 69]. In some studies however, it was observed that patients treated with inhaled insulin had increased insulin antibody levels, but these levels thus far have not been related to any significant clinical change [48, 70]. Adverse effects of the treatment on pulmonary function are also a cause of concern [71]. Safety and tolerability issues need to be addressed for this treatment to be clinically applicable.

Of all the routes of delivering drugs, the oral route is the most desirable. This route of administration results in higher patient compliance than any other route of administration. If successful, this delivery system will solve the current non-compliance related problems associated with insulin injections. The attractiveness of this delivery system has led to several attempts to develop oral insulin formulations [59]. Another great advantage of this route of administration is that insulin delivered via the oral route mimics more closely the endogenous

secretion of insulin. Insulin absorbed from the intestinal epithelium reaches the liver through the portal vein and can have a direct effect on the hepatic glucose production. This mode of distribution is highly appropriate, since the liver plays an important role in maintaining glucose homeostasis in the bloodstream, taking up and storing the energy in carbohydrates in the form of glycogen. Parenterally administered insulin mainly targets the peripheral tissue rather than the liver with pharmacokinetics that do not replicate the normal dynamics of endogenous insulin release [32]. A detailed description of the challenges associated with oral administration of proteins, and attempted solutions are included in section 2.4.

2.4 Oral Delivery of Proteins

Oral delivery formulation for insulin is highly desirable from a patient compliance point of view and other considerations discussed above. However, only a small portion of insulin administered orally reaches the blood stream, mainly due to extensive degradation of the protein in the gastrointestinal tract. Further, large size and hydrophilicity of the molecule greatly limits its transport across the intestinal epithelium. No specific transport mechanism is present for the passage of insulin cross the intestinal cell monolayer. Insulin molecules that are unable to cross the intestinal barrier thus get further exposed to the intestinal proteolytic activity, this in turn reduces the bioavailability of the protein. Owing to

these factors, less than 0.5% of the orally administered insulin typically reaches the systemic circulation.

For many years researchers have tried to find a solution to these problems and in effect increase the oral bioavailability of insulin. The investigated approaches include use of permeation enhancers, protease inhibitors [72-74], or concomitant administration of permeation enhancers and protease inhibitors, chitosan coatings to stabilize the protein and improve cellular permeability [75], entrapment of insulin within microparticles [76], and protein modification to make it resistant to proteolytic attack and more permeable across the epithelium [77, 78]. Some of these promising approaches are discussed in detail in Section 2.4.2. The physiology of the GI tract in relation to oral protein delivery is discussed in the Section 2.4.1.

2.4.1 Physiology of the Gastrointestinal Tract

To maintain a constant state of homeostasis, the body needs to constantly replace nutrient molecules, and replenish water and electrolytes that are lost through urine, sweat and other means. The digestive system helps achieve this by continually supplying the body with energy-rich nutrients, water and electrolytes from the external environment. In most cases, the digestive tract itself does not directly regulate the uptake and transfer of these components based on the body's requirement, but optimizes the digestion and absorption of the ingested food. This is achieved by the movement of the ingested food

through the GI tract, digestion of the ingested food by secretion of the digestive juices, absorption of the digested components, water and electrolytes, and movement of absorbed components away from the digestive tract by blood circulation.

The process of digestion converts complex food matter into simpler and smaller fragments that can be absorbed by the cells lining the GI tract to be utilized for various bodily functions. The digestive juices are emptied into the lumen of the digestive tract by the exocrine glands via the tubular channels formed by the duct cells. Specific enzymes in these secretions digest the energy-rich foodstuff which can be primarily classified into carbohydrates, fats and proteins. Proteins of therapeutic value, such as insulin, are broken down into smaller peptide fragments and finally into individual amino acids rendering them biologically inactive. The specific physiology of the stomach and intestine in relation to oral protein delivery as discussed below.

2.4.1.1 Gastric and Intestinal Environment

Degradation of proteins during their transit from mouth, the pharynx and the esophagus is minimal. The secretions of the salivary glands contain mucus, amylase and lysozyme. Digestion in the mouth is limited to initiation of polysaccharides hydrolysis into disaccharides by amylase. No absorption of food material occurs in the mouth. The secretions of esophagus are entirely mucoid in character and maintain a well lubricated esophageal lumen. Mucus secreted by

the esophagus protects the esophageal wall from damage due to food. The entire movement of food through the pharynx and esophagus takes between 6-10 seconds.

After traveling through the esophagus the food reaches the stomach where it is stored and digestion of the ingested food begins. Based on anatomical and histological characteristics, the stomach is divided into the fundus (part of stomach that lies above the esophageal opening), the body (middle portion) and the antrum (lowermost part of the stomach characterized by thick muscles). The three regions coordinate and control the motility function of stomach. The digestive juices of the stomach are mainly secreted by gastric (or oxyntic) glands. These glands are responsible for secretion of hydrochloric acid and pepsinogen and mucus along with other components.

Other exocrine glands present in the gastric mucosa are the pyloric glands. These mainly secrete mucus and some pepsinogen. The oxyntic glands are mainly present in on the inside surface of the body on the fundus (oxyntic mucosa) whereas the pyloric glands are present in the pyloric gland area lining the antral surface. Pepsinogen, the inactive precursor of pepsin, is converted into pepsin by the HCl secreted by the oxyntic glands. This then leads to autocatalytic conversion of pepsinogen into pepsin, which is the main digestive enzyme of the stomach. Pepsin is active at low pH but is rapidly inactivated above pH 5.0. Pepsin acts at specific amide bonds within protein molecules and convert them into smaller peptide fragments.

It is most efficient in cleaving amino acid linkages involving the aromatic amino acids, phenylalanine, tryptophan, and tyrosine.

No absorption of foodstuff takes place through the stomach. Food components digested in the stomach are still large fragments and hence cannot get absorbed through the gastric mucosa. Most of the digestion and absorption occurs in the small intestine. The small intestine is divided into three sections: the duodenum, the jejunum and the ileum [79]. The small intestine secretions themselves do not contribute significantly to the process of digestion. Although the intestinal cells do secrete digestive enzymes (such as aminopeptidase), they mainly act in the brush border of the epithelial cells. The exocrine glands in the small intestine mainly secrete mucus that lines the inside of the intestinal wall. Protein digestion activity of the small intestine mainly comes from the pancreatic secretions.

The gastric contents, on emptying into the upper portion of the small intestine (duodenum), mix with the juices in the small intestine and also with the secretions of the pancreas. The secretions of the pancreas come from the exocrine pancreatic acinar cells. These cells form sac-like structures with the duct cells forming channels leading to the pancreatic duct. The secretions of the pancreas mix with the bile duct coming from the liver before mixing into the intestinal contents.

The acinar cells are responsible for the secretion of proteolytic enzymes (protein digestion), pancreatic amylase (carbohydrate digestion), and pancreatic

lipase (fat digestion). The duct cells secrete large amounts of sodium bicarbonate ($NaHCO_3$) that neutralizes the acidity of the contents emptied by the stomach. The proteolytic enzyme secretions from the pancreas contain trypsinogen, chymotrypsinogen and procarboxypeptidase. Trypsinogen is converted by an autocatalytic reaction to its active form, trypsin, by an enzyme called enterokinase present in the wall of the duodenum. Trypsin then converts chymotrypsin and procarboxypeptidase into their active analogues. Trypsin is the most abundant of the three enzymes.

Each of these enzymes acts on specific amino acid linkages and convert the peptide fragments (formed by pepsin digestion) into small peptides and amino acids. Trypsin cleaves the peptide bonds where the carboxyl group comes from arginine or lysine residue, whereas chymotrypsin specifically breaks the peptide bonds where the carboxyl group is donated by tyrosine, phenylalanine, tryptophan, methionine, or leucine. Due to the high specificity of trypsin for amino acid linkages, it is commonly used as a reagent in unambiguous cleavage of proteins.

2.4.1.2 The Intestinal Epithelial Cell Barrier

The epithelial tissue consists of cells specialized in exchange of materials between the external environment and the internal host milieu. Since these cells form the boundary between the external and the internal environment, the transport across these cells is highly regulated and passage of only selective

components is allowed. Most of the absorption of nutrients is completed in the duodenum and the jejunum. The small intestinal absorptive epithelium is remarkably well adapted for absorption of nutrients from the lumen. The inner surface of the intestine forms macroscopic circular folds, called valvulae conniventes that increase the surface area for absorption threefold. Each of these folds has microscopic fingerlike projections called villi that result in a 10-fold increase in the surface area. The villus surface is covered by the absorptive epithelial cells along with some mucous cells. The epithelial cells form hairlike projections on the luminal side called the microvilli that further increase the absorptive area 20-fold. Enzymatic secretions of the small intestine are active within these brush borders. Thus these macroscopic and microscopic projections together increase the surface area nearly 600-folds compared to a hollow cylinder of similar dimensions or about 250 m^2.

Nutrients, such as amino acids and sugars, enter the circulation by crossing the epithelium covering the villi. Each villus contains a blunt-ended lymphatic capillary bed and a blunt-ended lymphatic vessel called the central lacteal. It also has a network of capillaries which absorb the molecules transported across the epithelial cells. The intestinal capillaries converge into venules and the hepatic portal vein that take the absorbed molecules to the liver. Fats, instead of being transported into the capillaries, are absorbed into the lymphatic vessels that rapidly flow into the blood via the thoracic duct.

The small intestinal epithelium is highly differentiated and consists of six distinct cell types: the enterocytes or absorptive cells, mucin producing goblet cells, endocrine cells, paneth cells, M cells and tuft and cup cells [80]. Epithelial cells are the most common type of cells in the intestinal cell monolayer. The epithelial cells are organized as polarized monolayer, which provides a permeability barrier between two distinct environments. Disruption of this highly regulated polarized cell barrier can cause passage of toxic luminal contents to the systemic circulation.

The epithelial cells are circumferentially tied to one another by intercellular junctional complexes. These include the tight junctions or zonula occludens, zonula adherens, and desmosomes [81, 82]. The tight junctions, which appear as a series of fusion points involving the outer leaflets of the plasma membranes, attach the adjacent cells to one another at the apical region of the cells. A century ago, these complexes were thought to be absolute and unregulated barriers in the paracellular space [82]. Physiological studies of the past several decades have shown the tight junctions to be dynamic structures, able to respond to extracellular environmental changes. They are composed of the transmembrane proteins occludin and claudin, and cytoplasmic plaque proteins zonula occludens (ZO)-1, ZO-2, ZO-3, cingulin, and 7H6 [82].

Next to the tight junction lies the adherens junction, in which cadherins act as adhesion receptors. The cadherins are a group of functionally related glycoproteins responsible for the calcium-dependent cell-to-cell adhesion.

The transcellular pathway is limited to those molecules which have specific mechanisms of active or facilitated transport, such as receptors-mediated endocytosis, wherein the molecules recognize specific receptors presented on the cell surface and get endocytosed in the form of endocytotic vesicles. The absorption of large and hydrophilic macromolecules is almost exclusively limited to the paracellular pathway, which consists of aqueous pores created by the cellular tight junctions [80]. However, under normal conditions, this pathway is restricted to molecules with molecular radii less than 11 Å [83].

The development of efficacious delivery systems based on well-regulated modulation of the tight junctions by absorption enhancers has not been very successful, mainly due to lack of comprehensive understanding of the function of the tight junctions. Some drug delivery approaches based on this approach are discussed in section 2.4.2.2

2.4.2 Strategies for Enhancing the Protein Oral Bioavailability

The strategies for enhancing the oral bioavailability of proteins can mainly be categorized into two subsets. The first subset includes approaches that aim at reversibly changing the intestinal environment so as to make it more favorable for the stability and transport of the protein molecule across the intestinal epithelium. The term *'intestinal environment'* is used here to include the lumen of the stomach and the intestine, and the intestinal epithelium. The second subset includes those approaches where the protein molecule is modified, typically by

covalent modifications, so that it can better resist the proteolytic degradation and can permeate the intestinal epithelium effectively. Some specific examples each of these approaches are discussed below.

2.4.2.1 Changing the Intestinal Milieu for Improved Absorption

As pointed out earlier, the reduced bioavailability of proteins from the oral route is mainly due to their extensive degradation in the gastric and intestinal fluids and to some extent, in the brush border of the epithelial cells, and also due to their limited permeability across the intestinal epithelial barrier. Thus, inhibition of the degradative functions of the proteolytic enzymes or an overall increase in the paracellular or transcellular permeability of the epithelium may result in significant increase in the bioavailability of orally administered proteins. Some approaches based on this methodology are highlighted here.

1. Permeation Enhancers, Protease Inhibitors and the Zonula Occludens Toxin

Permeation enhancers and protease inhibitors have been extensively studied to overcome the barriers to oral protein and peptide delivery. Penetration enhancers act on the intestinal epithelium and increase the permeability of the membrane by either the paracellular or the transcellular pathway. Representative examples of this class of compounds include substances like surfactants, fatty acids, bile salts, and chelators such as ethylene diamine tetra acetate (EDTA). Many gel-forming polymers such as polycarbophil, also act as permeation

enhancers by binding the extracellular Ca^{2+}. Fatty acids, bile salts and surfactants mostly increase the fluidity of the lipid bilayer of the cell membranes thus making them more permeable. Local toxicity to the epithelium in the gastrointestinal tract is a major concern in using these systems in pharmaceutical products.

Intracellular Ca^{2+} plays an important role in regulating the tight junctional permeability [84]. Thus, compounds, such as EDTA, that can bind the extracellular Ca^{2+} thus lowering the intracellular Ca^{2+} concentration, can act as permeation enhancers by rendering the paracellular pathway more permeable. Some of these enhancers, however, can locally damage the intestinal mucosa and even enter the systemic circulation, leading to systemic toxic effects. Thus, damage to the epithelium and changes in the intestinal morphology, especially in the long term multi-dosing regimen, as would be required in diabetes treatment, are major concerns in clinical use of these agents. Another disadvantage of these compounds is their non-specificity in permeation enhancement. Increased permeability of the epithelium may also allow toxins and biological pathogens in the intestinal lumen to pass into the systemic circulation.

Aprotinin, soybean trypsin inhibitors and polycarbophil are representative examples of protease inhibitors. By forming reversible stoichiometric enzyme inhibitor-complexes, aprotinin acts as an inhibitor of human trypsin and chymotrypsin. Concomitant administration of insulin with aprotinin and soybean trypsin inhibitors has been shown to induce hypoglycemic effect [73, 74].

Polyacrylates such as Carbopol 934P and polycarbophil, which are typically used as bioadhesives, are also known to inhibit the activity of trypsin and chymotrypsin in a calcium-dependent manner [85, 86]. Bai et al. [87] showed that in-situ absorption of insulin was improved by carbomer polymers and also induced a significant decline in blood glucose levels.

However, these enzyme inhibitors have a toxic potential caused by the inhibition of digestive enzymes, which can further cause incomplete digestion of the nutritive proteins. In addition, the inhibitory action can cause increased secretion of these enzymes by a feed-back regulation [73, 88]. Studies have shown that this feed-back regulation leads to both hypertrophy and hyperplasia of the pancreas. Prolonged administration of soybean trypsin inhibitor can lead to invasive carcinoma [73].

One of the recent additions to the class of absorption enhancers is zonla occludens toxin (Zot), a protein secreted by *Vibrio cholerae* [89]. This toxin induces modifications of cytoskeletal organization, specifically at the actin filament of the zonula occludens which leads to opening of the tight junctions causing increased permeability. This permeability increase is reversible, time- and dose-dependent and is restricted to jejunal and ileal sections of the small intestine owing to the presence of receptors for the protein in those sections [72]. Studies with diabetic animals have shown that insulin administered with 5 µg Zot and $NaHCO_3$ to neutralize the gastric acidity, induced a hypoglycemic effect comparable to that caused by subcutaneously administered insulin. This is a

promising approach to improving oral bioavailability of insulin, but it suffers from the same safety and specificity issues that limit the use of other permeation enhancers discussed above.

Thus, attempts to increase the oral bioavailability of proteins using permeation enhancers and protease inhibitors have not resulted in an acceptable delivery system. Potential side effect of this methodology has limited its clinical applicability [90].

2. Complexation Hydrogels in Protein and Peptide Delivery

Much attention has been focused on developing stimuli-sensitive hydrogels that exhibit dramatic changes in network structure or swelling behavior in response to change in pH, temperature, electric field, and ionic strength [91-93]. Most of these systems rely on the sensitive nature of specific interpolymeric complexation within the hydrogels. By exploiting the sensitive nature of these hydrogels, external (magnetic field, laser) or internal triggers (pH, ionic strength changes) can be used for temporally and/or spatially targeted delivery of biomolecules within the body. Delivery systems can also be designed to release macromolecules in response to increased concentration of a specific compound [94, 95], or changes in the surrounding environment.

We have developed hydrogen bonding, copolymer networks of poly(methacrylic acid) grafted with poly(ethylene glycol) (P(MAA-g-EG)) as oral delivery systems for peptides and proteins. The polymer complexes are prepared

by free radical solution polymerization [85] or dispersion polymerization [96] of methacrylic acid and methoxy-terminated poly(ethylene glycol) monomethacrylate with tetra(ethylene glycol) dimethacrylate added to provide crosslinks in the network structure.

These materials exhibit pH-dependent swelling behavior due to the formation/dissociation of interpolymer complexes [97, 98]. In acidic media, interpolymer complexes form due to hydrogen bonding between the graft PEG chains and the methacrylic acid units. These complexes serve as temporary, physical crosslinks and cause the gels to be in the collapsed conformation. The pK_a of PMAA is about 4.8; thus at neutral pH the MAA groups in the network are almost entirely deprotonated. The hydrogen bonds present at low pH dissociate at near neutral pH resulting in swelling of the network structure. The equilibrium swelling characteristics of the polymer network depend on the composition of the polymer.

Lowman and Peppas [98] studied the effects of copolymer composition and the pH of the surrounding medium on the network structure and the drug release characteristics. Hydrogels comprising MAA and EG in equimolar amounts exhibit maximum change in the mesh size or the correlation length of the network due to the pH shift. With an increase in the amount of MAA in the network, the average mesh size in the acidic media increases owing to the absence of physical crosslinks arising from MAA-EG interactions. Depending on the pH of the surrounding medium, the average mesh size in a network with MAA: EG ratio of

1:1 changes by a factor of 3 between deswollen to swollen states, which corresponds to a 10-fold change in the effective area for diffusion of the drug. This results in a change in the diffusion coefficient of the drug by two orders of magnitude [99]. Thus these hydrogels are ideal for the oral delivery of peptides and proteins due to the large change in network structure over a small pH range.

In the acidic environment of the stomach, the drugs would be trapped in the collapsed gel and protected from degradation by digestive enzymes in the stomach. However, in the near-neutral environment in the intestine where the drugs could be absorbed, the peptides and proteins can be readily released. In addition, the macromolecular polymer structure and the polymer composition can be altered by changing parameters such as the nature of the crosslinker, the crosslinking density, and relative amounts of monomers added, to achieve diffusion-controlled delivery of proteins and peptides of therapeutic interests.

These complexation hydrogels can also inhibit the activity of Ca^{2+} dependent proteolytic enzymes [85]. As discussed in chapter 8, these hydrogels can also protect the entrapped protein in gastric fluid. Further, the bioactive agent released from the polymer formulations in intestinal fluid is significantly protected from the proteolytic attack. These polymer networks also exhibit mucoadhesive characteristics due to the PEG chains which interact with the mucus layer lining the epithelial cells. This mucoadhesive behavior is advantageous since it results in release of the drug at the site of absorption and also increases the residence time of the drug in the small intestine.

The aforementioned characteristics make these copolymers ideal carriers for oral delivery of proteins and peptides. We have successfully demonstrated application of this system in oral delivery of insulin in the diabetic rat models. Insulin can be incorporated into the polymer microparticles by partitioning from a concentrated solution followed by acidification to collapse the microparticles.

Upon exposure to acidic environment, most of the entrapped insulin remains trapped inside and less than 10% of insulin is released from the microparticles. But when the pH of the surrounding medium rises to the physiological pH in the small intestine, insulin trapped inside the network is released rapidly [100]. In addition to exhibiting a pH-responsive behavior, these polymer matrices also serve to stabilize the entrapped insulin [101]. The PEG chains present in the network serve to maintain the biological activity of the insulin by stabilizing the drug and preventing binding to ionizable MAA backbone [99, 101].

The effectiveness of this system in delivering insulin was evident from the observed hypoglycemic effect upon oral administration in the diabetic rat studies [102]. The blood glucose levels in diabetic rats were lowered by up to 40% for more than 8h. Transport studies using Caco-2 cells, a widely used in vitro model for intestinal absorption of drugs [103], have also proven the efficacy of the polymeric system [104]. The particles induced Ca^{2+} concentration-dependent lowering on the transepithelial electrical resistance (TEER) due to the reversible opening of the tight junctions [96, 104], resulting in an increase in the permeability coefficient of insulin across the cell monolayer. Whether or not a

similar permeation enhancing effect is responsible for the improved oral bioavailability of insulin in animals is not clear.

2.4.2.2 Drug Modification Strategies

As mentioned previously, some of the approaches for improving the oral bioavailability of therapeutic proteins and peptides by transiently modulating the tight junctions between the cells suffer from possibility of side effects such as systemic toxicity and damage to the epithelium. The potentially invasive nature of this approach combined with the lack of precise control over the tight junction permeability limits its clinical applicability. A promising alternative to this approach are the drug modification strategies. The distinguishing feature of these approaches is that instead of altering the physiological conditions for improved stability and epithelial transport of protein molecule, the protein itself is modified to increase bioavailability. As a specific example, a novel methodology, which utilizes receptor-mediated transcytosis of extracellular proteins, is discussed here.

Receptor-mediated endocytosis for improved oral delivery:

Receptor-mediated endocytosis of proteins is being investigated as a specific, non-invasive alternative to facilitate intestinal absorption of drugs [105]. Receptor-mediated endocytosis is a pathway for selective and efficient cellular uptake of specific macromolecules required for various cell processes from the extracellular milieu. During this process, the binding of receptor to a ligand

triggers intracellular signaling pathways which lead to endocytosis of the receptor-ligand complex in membrane-derived vesicles. After endocytosis, the receptor-ligand complex encounters the acidic pH in the early endosomal compartments [106], which may lead to (i) uncoupling of the ligand-receptor complex due to changes in the conformation of receptor proteins followed by recycling of the receptor to the cell membrane, or (ii) degradation of the receptor in lysosomes. The endocytosed ligands that dissociate from their receptors in the early endosomes are usually degraded in the lysosomes. Some ligands, however, remain bound to the receptors and hence share the fate of their bound receptors.

Depending on the specific type of the receptor proteins, the receptors along with the bound ligand may be recycled to the same plasma membrane domain from which they came, get degraded in the lysosomes, or get transported to a different domain of the membrane, as in the polarized epithelial and endothelial cells. The last process is called transcytosis and is of particular interest from drug delivery standpoint. By coupling therapeutic proteins to the ligand molecules that can recognize specific receptors on the epithelial cell monolayers, transcellular delivery of these macromolecular biopharmaceuticals may be achieved. Since only those molecules that are conjugated to the ligands are transcytosed, this process eliminates the potential side effects associated to the unspecific transport by the paracellular pathway. Transferrin and lectin receptor mediated protein delivery systems are discussed here.

1. Transferrin-mediated drug delivery

Transferrin is a single-chain protein with molecular weight of approximately ~80 kDa [107]. Serum transferrin is involved in uptake of iron by the cells and tissues. Transferrin receptors (TfRs) have been widely explored for receptor-mediated delivery of anticancer agents [107, 108], in enhancing the transport of drugs across the blood brain barrier [109, 110], and more recently, across the epithelial cells of the intestine [77].

TfR is a homodimer expressed by many cell types including the human intestinal cells. TfR binds iron-bound transferrin (holo-transferrin) on the cell surface. This binding is sensed by the cells which results in an uptake of the Tf-TfR complex. Triggered by the change in the endosomal pH, the ligand-bound transferrin then looses its bound iron and the complex is recycled to the cell surface where iron-free transferrin (apo-transferrin) is released. In polarized cells such as the epithelial and endothelial cells, transferrin can be transcytosed from the apical to the basolateral membrane [111]. This mechanism is exploited in TfR-mediated drug delivery across the blood brain barrier as well as the epithelial barrier of the small intestine.

Transferrin receptors are present at high densities in human GI epithelium [112], and transferrin can resist tryptic and chymotryptic degradation [113]. Shen and co-workers [114] were the first to utilize the potential of TfR-mediated transport in improving oral delivery of therapeutic agents. They conjugated

transferrin to insulin via disulfide linkages and demonstrated that the conjugation resulted in 5- to 15-fold increase in insulin transport across Caco-2 cell monolayer [115]. As pointed out earlier, since this enhancement is specific for the conjugated protein, viz. insulin, and takes place without causing the tight junctions to open even momentarily, this approach is most desirable in terms of toxicity and damage to the epithelium.

Following successful in vitro studies, Shen and co-workers [77] demonstrated that insulin-transferrin conjugate, when administered orally to diabetic rats, caused slow but prolonged hypoglycemic effect. In-Tf conjugate after oral administration as well as after subcutaneous injection caused a delayed but prolonged glucose reducing activity as compared to native insulin after subcutaneous injection. Subcutaneously administered In-Tf conjugate maintained low blood glucose levels for at least 4 times longer than unconjugated insulin. While this might be beneficial in terms of the frequency of dosage, the reasons behind this behavior is not fully understood.

The authors have also presented data suggesting that the disulfide linkage between the two proteins can be reduced in the liver following its absorption into the portal vein. The approach thus makes use of transferrin for overcoming the transport barrier of the small intestine after which free insulin can be released to perform its physiological system.

The observation that the intact conjugate is able to reach the systemic circulation intact, suggests that the insulin conjugated to transferrin is able to

overcome proteolytic attack during transit in the GI tract and across the epithelial cells. In vitro studies with simulated gastric and intestinal fluids can shed light on the conjugates ability to shield insulin from proteolytic attack.

2. Lectin-mediated drug delivery

Lectins are a class of structurally diverse proteins of non-immune origin that are characterized by their ability to specifically bind carbohydrates [116]. They are primarily found in seeds, but are also present in animals, plants and microorganisms. Lectins have been studied widely for oral delivery applications because of their relatively good resistance to the acidic pH and enzymatic degradation and presence of binding sites in the gastrointestinal tract [117, 118]. While some lectins such as phaseolus vulgaris agglutinin (PHA) from raw kidney beans have been known to cause dietary toxicity [119, 120] and are unsuitable for drug delivery applications, variety of other lectins such as wheat germ agglutinin (WGA) *Triticum vulgare* [117] and tomato lectin (TL) from *Lycopersicum esculentum* [121] are natural component of our diet and bind to intestinal mucosa without any obvious deleterious effects.

Use of lectins in improving the residence time of the drug carrier particulate systems has been the subject of a number of excellent reviews [122-125]. Recent work on the use of WGA-protein conjugates for improving the uptake and transcytosis of proteins across the epithelial cell barrier of the gut is discussed here.

WGA is a dimeric protein with two subunits containing two or four carbohydrate-combining sites [126]. It specifically binds N-acetylglucosamine and sialic acid residues. Wheat germ contains approximately 300 mg WGA/kg and hence the peroral toxicity that can result from long term oral administration of WGA may be negligible [127]. Further the lectin can resist degradation due to proteolytic attack upon exposure to the gastrointestinal enzymes [117]. These characteristics and the presence of N-acetylglucosamine containing oligosaccharides in the glycocalyx of the intestinal mucosa make WGA a promising candidate for enhancing oral bioavailability of drug candidates.

Binding studies of WGA using Caco-2 cells, mucus producing HT-29 cells and HT-8 cells have revealed that it exhibits low nonspecific proteinaceous binding to the cell surfaces and high affinity for oligosaccharides present on the cell surfaces [128]. In an interesting study, Gabor and co-workers examined whether WGA can improve the binding and uptake of a model fluorescently labeled BSA (F-BSA), by the Caco-2 cells [127]. They observed that WGA in the conjugated form was able to bind specifically to the oligosaccharides on the cell surface and the conjugate was uptaken by the cells by an energy dependent mechanism.

This is an important result since it demonstrates the potential of lectin mediated delivery in improving the transcellular transport of proteins across the epithelium. However, there are concerns about the cellular fate of the uptaken conjugate. The conjugate accumulated within lysosomal compartment where it

was degraded. The degraded products diffused into the cytosol and finally appeared in the extracellular medium. Thus, even though lectins can resist degradation due to proteolytic attack, the conjugated protein drug is still susceptible to degradation by the enzymes in the lysosomes. In addition, the stability of such conjugates in the gastrointestinal environment is an unaddressed issue.

One important consideration here is the size of the protein under consideration that is conjugated to the lectin. WGA is 147 kDa, whereas BSA is 68 kDa protein. Since BSA is a large molecule, the lectin may not be able to protect bound protein by creating a steric hindrance to the proteolytic attack. But if a smaller protein such as insulin (5.8 kDa with hydrodynamic radius of approximately 20 Å) is conjugated to WGA, the lectin might shield the bound protein from proteolytic attack and hence improve its stability during transit in the GI tract and through the cellular barrier.

2.5 Conclusions

A variety of approaches have emerged in the recent past for designing oral delivery systems for therapeutic proteins and peptides, although a clinically viable solution to this long standing problem still alludes the scientific community. These approaches come from such diverse research disciplines as biomaterials, conjugation chemistry, nanotechnology, cell biology, and employ different

methodologies for solving the same problem. Some of these strategies have distinguishing beneficial characteristics that make them good candidates for oral protein delivery. Interfacing different strategies to combine the benefits of novel approaches is an interesting new possibility.

References

1 Tan, K. K., Trull, A. K., Uttridge, J. A. and Wallwork, J. (1995) Relative bioavailability of cyclosporin from conventional and microemulsion formulations in heart-lung transplant candidates with cystic fibrosis. Eur J Clin Pharmacol **48**, 285-289

2 Definition, diagnosis and classification of diabetes mellitus and its complications. Report of a WHO consultation, Part 1: diagnosis and classification of diabetes mellitus, World Health Organization, Geneva, 1999.

3 McCarthy, A. A. (2004) New approaches to diabetes disease control, insulin delivery, and monitoring. Chem Biol **11**, 1597-1598

4 Simpson, R. W., Shaw, J. E. and Zimmet, P. Z. (2003) The prevention of type 2 diabetes--lifestyle change or pharmacotherapy? A challenge for the 21st century. Diabetes Res Clin Pract **59**, 165-180

5 Park, K. S. (2004) Prevention of type 2 diabetes mellitus from the viewpoint of genetics. Diabetes Res Clin Pract **66 Suppl 1**, S33-35

6 Amos, A. F., McCarty, D. J. and Zimmet, P. (1997) The rising global burden of diabetes and its complications: estimates and projections to the year 2010. Diabet Med **14 Suppl 5**, S1-85

7 King, H., Aubert, R. E. and Herman, W. H. (1998) Global burden of diabetes, 1995-2025: prevalence, numerical estimates, and projections. Diabetes Care **21**, 1414-1431

8 Gabbe, S. G. and Graves, C. R. (2003) Management of diabetes mellitus complicating pregnancy. Obstet Gynecol **102**, 857-868

9 Lillioja, S., Mott, D. M., Spraul, M., Ferraro, R., Foley, J. E., Ravussin, E., Knowler, W. C., Bennett, P. H. and Bogardus, C. (1993) Insulin resistance and insulin secretory dysfunction as precursors of non-insulin-dependent diabetes mellitus. Prospective studies of Pima Indians. N Engl J Med **329**, 1988-1992

10 Anthony, S., Odgers, T. and Kelly, W. (2004) Health promotion and health education about diabetes mellitus. J R Soc Health **124**, 70-73

11 Genuth, S., Alberti, K. G., Bennett, P., Buse, J., Defronzo, R., Kahn, R., Kitzmiller, J., Knowler, W. C., Lebovitz, H., Lernmark, A., Nathan, D., Palmer, J., Rizza, R., Saudek, C., Shaw, J., Steffes, M., Stern, M., Tuomilehto, J. and Zimmet, P. (2003) Follow-up report on the diagnosis of diabetes mellitus. Diabetes Care **26**, 3160-3167

12 Benjamin, S. M., Valdez, R., Geiss, L. S., Rolka, D. B. and Narayan, K. M. (2003) Estimated number of adults with prediabetes in the US in 2000: opportunities for prevention. Diabetes Care **26**, 645-649

13 Stern, M. P., Williams, K. and Haffner, S. M. (2002) Identification of persons at high risk for type 2 diabetes mellitus: do we need the oral glucose tolerance test? Ann Intern Med **136**, 575-581

14 de Groot, M., Schuurs, T. A. and van Schilfgaarde, R. (2004) Causes of limited survival of microencapsulated pancreatic islet grafts. J Surg Res **121**, 141-150

15 McChesney, L. P. (1999) Advances in pancreas transplantation for the treatment of diabetes. Dis Mon **45**, 88-100

16 Vial, T. and Descotes, J. (2003) Immunosuppressive drugs and cancer. Toxicology **185**, 229-240

17 Penn, I. (2000) Post-transplant malignancy: the role of immunosuppression. Drug Saf **23**, 101-113

18 Street, C. N., Sipione, S., Helms, L., Binette, T., Rajotte, R. V., Bleackley, R. C. and Korbutt, G. S. (2004) Stem cell-based approaches to solving the problem of tissue supply for islet transplantation in type 1 diabetes. Int J Biochem Cell Biol **36**, 667-683

19 Ballinger, W. F. and Lacy, P. E. (1972) Transplantation of intact pancreatic islets in rats. Surgery **72**, 175-186

20 Shapiro, A. M., Lakey, J. R., Ryan, E. A., Korbutt, G. S., Toth, E., Warnock, G. L., Kneteman, N. M. and Rajotte, R. V. (2000) Islet transplantation in seven patients with type 1 diabetes mellitus using a glucocorticoid-free immunosuppressive regimen. N Engl J Med **343**, 230-238

21 Hussain, M. A. and Theise, N. D. (2004) Stem-cell therapy for diabetes mellitus. Lancet **364**, 203-205

22 Bouwens, L. (2004) Islet morphogenesis and stem cell markers. Cell Biochem Biophys **40**, 81-88

23 Soon-Shiong, P. (1999) Treatment of type I diabetes using encapsulated islets. Adv Drug Deliv Rev **35**, 259-270

24 Opara, E. C. and Kendall, W. F., Jr. (2002) Immunoisolation techniques for islet cell transplantation. Expert Opin Biol Ther **2**, 503-511

25 Stuart-Harris, C. H. (1958) The frontiers of medicine. Lancet **2**, 427-430

26 Dominguez, L. J. and Licata, G. (2001) [The discovery of insulin: what really happened 80 years ago]. Ann Ital Med Int **16**, 155-162

27 Scott, D. A. (1934) Crystalline Insulin. Biochem J **28**, 1592-1602

28 Sanger, F. (1959) Chemistry of insulin; determination of the structure of insulin opens the way to greater understanding of life processes. Science **129**, 1340-1344

29 Mohan, V. (2002) Which Insulin to Use? Human or Animal? Current Science **83**, 1544-1547

30 Oliva, A., Farina, J. and Llabres, M. (2000) Development of two high-performance liquid chromatographic methods for the analysis and characterization of insulin and its degradation products in pharmaceutical preparations. J Chromatogr B Biomed Sci Appl **749**, 25-34

31 Owens, D. R., Zinman, B. and Bolli, G. B. (2001) Insulins today and beyond. Lancet **358**, 739-746

32 Arbit, E. (2004) The physiological rationale for oral insulin administration. Diabetes Technol Ther **6**, 510-517

33 Hill, R. A., Strat, A. L., Hughes, N. J., Kokta, T. J., Dodson, M. V. and Gertler, A. (2004) Early insulin signaling cascade in a model of oxidative skeletal muscle: mouse Sol8 cell line. Biochim Biophys Acta **1693**, 205-211

34 McAulay, V. and Frier, B. M. (2003) Insulin analogues and other developments in insulin therapy for diabetes. Expert Opin Pharmacother **4**, 1141-1156

35 UK Prospective Diabetes Study Group. Intensive blood-glucose control with sulphonylureas or insulin compared with conventional treatment and risk of complications in patients with type 2 diabetes (UKPDS 33). (1998) In Lancet, pp. 837-853

36 Ohkubo, Y., Kishikawa, H., Araki, E., Miyata, T., Isami, S., Motoyoshi, S., Kojima, Y., Furuyoshi, N. and Shichiri, M. (1995) Intensive insulin therapy prevents the progression of diabetic microvascular complications in Japanese patients with non-insulin-dependent diabetes mellitus: a randomized prospective 6-year study. Diabetes Res Clin Pract **28**, 103-117

37 Malmberg, K. (1997) Prospective randomised study of intensive insulin treatment on long term survival after acute myocardial infarction in patients with diabetes mellitus. DIGAMI (Diabetes Mellitus, Insulin Glucose Infusion in Acute Myocardial Infarction) Study Group. Bmj **314**, 1512-1515

38 Mudaliar, S. and Edelman, S. V. (2001) Insulin therapy in type 2 diabetes. Endocrinol Metab Clin North Am **30**, 935-982

39 Barnett, A. H. and Owens, D. R. (1997) Insulin analogues. Lancet **349**, 47-51

40 Bolli, G. B., Di Marchi, R. D., Park, G. D., Pramming, S. and Koivisto, V. A. (1999) Insulin analogues and their potential in the management of diabetes mellitus. Diabetologia **42**, 1151-1167

41 Brange, J. and Volund, A. (1999) Insulin analogs with improved pharmacokinetic profiles. Adv Drug Deliv Rev **35**, 307-335

42 Skyler, J. S. (1986) Lessons from studies of insulin pharmacokinetics. Diabetes Care **9**, 666-668

43 Foldvari, M. (2000) Non-invasive administration of drugs through the skin: challenges in delivery system design. Pharm Sci Technol Today **3**, 417-425

44 Owens, D. R., Zinman, B. and Bolli, G. (2003) Alternative routes of insulin delivery. Diabet Med **20**, 886-898

45 Stephen, R. L., Petelenz, T. J. and Jacobsen, S. C. (1984) Potential novel methods for insulin administration: I. Iontophoresis. Biomed Biochim Acta **43**, 553-558

46 Langkjaer, L., Brange, J., Grodsky, G. M. and Guy, R. H. (1998) Iontophoresis of monomeric insulin analogues in vitro: effects of insulin charge and skin pretreatment. J Control Rel **51**, 47-56

47 Mitragotri, S., Blankschtein, D. and Langer, R. (1995) Ultrasound-mediated transdermal protein delivery. Science **269**, 850-853

48 Cefalu, W. T. (2004) Concept, strategies, and feasibility of noninvasive insulin delivery. Diabetes Care **27**, 239-246

49 Le, L., Kost, J. and Mitragotri, S. (2000) Combined effect of low-frequency ultrasound and iontophoresis: applications for transdermal heparin delivery. Pharm Res **17**, 1151-1154

50 Cevc, G., Gebauer, D., Stieber, J., Schatzlein, A. and Blume, G. (1998) Ultraflexible vesicles, Transfersomes, have an extremely low pore penetration resistance and transport therapeutic amounts of insulin across the intact mammalian skin. Biochim Biophys Acta **1368**, 201-215

51 Owens, D. R. (2002) New horizons--alternative routes for insulin therapy. Nat Rev Drug Discov **1**, 529-540

52 Kissel, T. and Werner, U. (1998) Nasal delivery of peptides: an in vitro cell culture model for the investigation of transport and metabolism in human nasal epithelium. J Control Rel **53**, 195-203

53 Hayakawa, E., Yamamoto, A., Shoji, Y. and Lee, V. H. (1989) Effect of sodium glycocholate and polyoxyethylene-9-lauryl ether on the hydrolysis of varying concentrations of insulin in the nasal homogenates of the albino rabbit. Life Sci **45**, 167-174

54 Sayani, A. P. and Chien, Y. W. (1996) Systemic delivery of peptides and proteins across absorptive mucosae. Crit Rev Ther Drug Carrier Syst **13**, 85-184

55 Gordon, G. S., Moses, A. C., Silver, R. D., Flier, J. S. and Carey, M. C. (1985) Nasal absorption of insulin: enhancement by hydrophobic bile salts. Proc Natl Acad Sci U S A **82**, 7419-7423

56 Salzman, R., Manson, J. E., Griffing, G. T., Kimmerle, R., Ruderman, N., McCall, A., Stoltz, E. I., Mullin, C., Small, D., Armstrong, J. and et al. (1985) Intranasal aerosolized insulin. Mixed-meal studies and long-term use in type I diabetes. N Engl J Med **312**, 1078-1084

57 Nolte, M. S., Taboga, C., Salamon, E., Moses, A., Longenecker, J., Flier, J. and Karam, J. H. (1990) Biological activity of nasally administered insulin in normal subjects. Horm Metab Res **22**, 170-174

58 Drejer, K., Vaag, A., Bech, K., Hansen, P., Sorensen, A. R. and Mygind, N. (1992) Intranasal administration of insulin with phospholipid as absorption enhancer: pharmacokinetics in normal subjects. Diabet Med **9**, 335-340

59 Heinemann, L., Pfutzner, A. and Heise, T. (2001) Alternative routes of administration as an approach to improve insulin therapy: update on dermal, oral, nasal and pulmonary insulin delivery. Curr Pharm Des **7**, 1327-1351

60 Veuillez, F., Kalia, Y. N., Jacques, Y., Deshusses, J. and Buri, P. (2001) Factors and strategies for improving buccal absorption of peptides. Eur J Pharm Biopharm **51**, 93-109

61 Lee, V. H. L. and Yamamoto, A. (1989) Penetration and enzymatic barriers to peptide and protein absorption. Adv Drug Deliv Rev **4**, 171-207

62 Stratford, R. E. and Lee, V. H. L. (1986) Aminopeptidase activity in homogenates of various absorptive mucosae m the albino rabbit: implications in peptide delivery. Int J Pharm **30**, 73-82

63 Nagai, T. (1986) Topical mucosal adhesive dosage forms. Med Res Rev **6**, 227-242

64 Aungst, B. J. and Rogers, N. J. (1988) Site dependence of absorption-promoting actions of laureth-9, Na salicylate, Na2EDTA, and aprotinin on rectal, nasal, and buccal insulin delivery. Pharm Res **5**, 305-308

65 Guevara-Aguirre, J., Guevara, M., Saavedra, J., Mihic, M. and Modi, P. (2004) Oral spray insulin in treatment of type 2 diabetes: a comparison of efficacy of the oral spray insulin (Oralin) with subcutaneous (SC) insulin injection, a proof of concept study. Diabetes Metab Res Rev **20**, 472-478

66 Modi, P., Mihic, M. and Lewin, A. (2002) The evolving role of oral insulin in the treatment of diabetes using a novel RapidMist System. Diabetes Metab Res Rev **18 Suppl 1**, S38-42

67 Patton, J. S., Bukar, J. and Nagarajan, S. (1999) Inhaled insulin. Adv Drug Deliv Rev **35**, 235-247

68 Skyler, J. S., Cefalu, W. T., Kourides, I. A., Landschulz, W. H., Balagtas, C. C., Cheng, S. L. and Gelfand, R. A. (2001) Efficacy of inhaled human insulin in type 1 diabetes mellitus: a randomised proof-of-concept study. Lancet **357**, 331-335

69 Hermansen, K., Ronnemaa, T., Petersen, A. H., Bellaire, S. and Adamson, U. (2004) Intensive therapy with inhaled insulin via the AERx insulin diabetes management system: a 12-week proof-of-concept trial in patients with type 2 diabetes. Diabetes Care **27**, 162-167

70 Stoever, J. A. and Palmer, J. P. (2002) Inhaled insulin and insulin antibodies: a new twist to an old debate. Diabetes Technol Ther **4**, 157-161

71 Cefalu, W. T., Rosenstock, J. and Bindra, S. (2002) Inhaled insulin: a novel route for insulin delivery. Expert Opin Investig Drugs **11**, 687-691

72 Fasano, A. and Uzzau, S. (1997) Modulation of intestinal tight junctions by Zonula occludens toxin permits enteral administration of insulin and other macromolecules in an animal model. J Clin Invest **99**, 1158-1164

73 Bernkop-Schnurch, A. (1998) The use of inhibitory agents to overcome the enzymatic barrier to perorally administered therapeutic peptides and proteins. J Control Rel **52**, 1-16

74 Morishita, M., Morishita, I., Takayama, K., Machida, Y. and Nagai, T. (1993) Site-dependent effect of aprotinin, sodium caprate, Na2EDTA and sodium glycocholate on intestinal absorption of insulin. Biol Pharm Bull **16**, 68-72

75 Wu, Z. H., Ping, Q. N., Wei, Y. and Lai, J. M. (2004) Hypoglycemic efficacy of chitosan-coated insulin liposomes after oral administration in mice. Acta Pharmacol Sin **25**, 966-972

76 Sajeesh, S. and Sharma, C. P. (2004) Poly methacrylic acid-alginate semi-IPN microparticles for oral delivery of insulin: a preliminary investigation. J Biomater Appl **19**, 35-45

77 Xia, C. Q., Wang, J. and Shen, W. C. (2000) Hypoglycemic effect of insulin-transferrin conjugate in streptozotocin-induced diabetic rats. J Pharmacol Exp Ther **295**, 594-600

78 Clement, S., Dandona, P., Still, J. G. and Kosutic, G. (2004) Oral modified insulin (HIM2) in patients with type 1 diabetes mellitus: results from a phase I/II clinical trial. Metabolism **53**, 54-58

79 Ganong, W. (1995) Review of medical physiology. Appleton & Lange, Stamford, CT

80 Madara, J. L. and Trier, J. S. (1986) Functional morphology of the mucosa of the small intestine. In Physiology of the Gastrointestinal Tract (Johnson, L. R., ed.), pp. 1209-1250, Raven Press, New York

81 Denker, B. M. and Nigam, S. K. (1998) Molecular structure and assembly of the tight junction. Am J Physiol **274**, F1-9

82 Anderson, J. M. and Van Itallie, C. M. (1995) Tight junctions and the molecular basis for regulation of paracellular permeability. Am J Physiol **269**, G467-475

83 Fasano, A. (1998) Novel approaches for oral delivery of macromolecules. J Pharm Sci **87**, 1351-1356

84 Kan, K. S. and Coleman, R. (1988) The calcium ionophore A23187 increases the tight-junctional permeability in rat liver. Biochem J **256**, 1039-1041

85 Madsen, F. and Peppas, N. A. (1999) Complexation graft copolymer networks: swelling properties, calcium binding and proteolytic enzyme inhibition. Biomaterials **20**, 1701-1708

86 LuBen, H. L., Rentel, C. O., Kotze, A. F., Lehr, C. M., de Boer, A. G., Verhoef, J. C. and Junginger, H. E. (1997) Mucoadhesive polymers in peroral peptide drug delivery. IV. Polycarbophil and chitosan are potent enhancers of peptide transport across intestinal mucosae in vitro. J Control Rel **45**, 15-23

87 Bai, J. P., Chang, L. L. and Guo, J. H. (1996) Effects of polyacrylic polymers on the degradation of insulin and peptide drugs by chymotrypsin and trypsin. J Pharm Pharmacol **48**, 17-21

88 Reseland, J. E., Holm, H., Jacobsen, M. B., Jenssen, T. G. and Hanssen, L. E. (1996) Proteinase inhibitors induce selective stimulation of human trypsin and chymotrypsin secretion. J Nutr **126**, 634-642

89 Baudry, B., Fasano, A., Ketley, J. and Kaper, J. B. (1992) Cloning of a gene (zot) encoding a new toxin produced by Vibrio cholerae. Infect Immun **60**, 428-434

90 Lee, V. H., Yamamoto, A. and Kompella, U. B. (1991) Mucosal penetration enhancers for facilitation of peptide and protein drug absorption. Crit Rev Ther Drug Carrier Syst **8**, 91-192

91 Qiu, Y. and Park, K. (2001) Environment-sensitive hydrogels for drug delivery. Adv Drug Deliv Rev **53**, 321-339

92 Mun, G. A., Nurkeeva, Z. S., Khutoryanskiy, V. V., Sergaziyev, A. D. and Rosiak, J. M. (2002) Radiation synthesis of temperature-responsive hydrogels by copolymerization of [2-(methacryloyloxy)ethyl]trimethylammonium chloride with N-isopropylacrylamide. Radiation Physics and Chemistry **65**, 67-70

93 Nam, I. K., Mun, G. A., Urkimbaeva, P. I. and Nurkeeva, Z. S. (2003) Gamma-induced synthesis of hydrogels of vinyl ethers with stimuli-sensitive behavior. Radiation Physics and Chemistry **66**, 281-287

94 Podual, K., Doyle, F. J., 3rd and Peppas, N. A. (2000) Dynamic behavior of glucose oxidase-containing microparticles of poly(ethylene glycol)-grafted cationic hydrogels in an environment of changing pH. Biomaterials **21**, 1439-1450

95 Goldraich, M. and Kost, J. (1993) Glucose-sensitive polymeric matrices for controlled drug delivery. Clin Mater **13**, 135-142

96 Torres-Lugo, M., Garcia, M., Record, R. and Peppas, N. A. (2002) Physicochemical behavior and cytotoxic effects of p(methacrylic acid-g-ethylene glycol) nanospheres for oral delivery of proteins. J Control Rel **80**, 197-205

97 Peppas, N. A. and Klier, J. (1991) Controlled release by using poly(methacrylic acid-g-ethylene glycol) hydrogels. J Control Rel **16**, 203-214

98 Lowman, A. M. and Peppas, N. A. (1997) Analysis of the Complexation/Decomplexation Phenomena in Graft Copolymer Networks. Macromolecules **30**, 4959 -4965

99 Peppas, N. A., Lowman, A. M. (1998) Protein Delivery from Novel Bioadhesive Complexation Hydrogels. In Protein and Peptide Drug Research (Frøkjær, S., Christup, L., Krogsgaard-Larsen, P., ed.), pp. 206-216, Munksgaard, Copenhagen

100 Morishita, M., Lowman, A. M., Takayama, K., Nagai, T. and Peppas, N. A. (2002) Elucidation of the mechanism of incorporation of insulin in controlled release systems based on complexation polymers. J Control Rel **81**, 25-32

101 Lowman, A. M. M., M.; Peppas, N. A.; Nagai, T. (1998) Novel Bioadhesive Complexation Networks for Oral Protein Drug Delivery. In Materials for Controlled Release Applications (McCulloch, I., Shalaby, S. W., ed.), pp. 156-164, American Chemical Society, Washington, DC

102 Lowman, A. M., Morishita, M., Kajita, M., Nagai, T. and Peppas, N. A. (1999) Oral delivery of insulin using pH-responsive complexation gels. J Pharm Sci **88**, 933-937

103 Rubas, W., Cromwell, M. E., Shahrokh, Z., Villagran, J., Nguyen, T. N., Wellton, M., Nguyen, T. H. and Mrsny, R. J. (1996) Flux measurements across Caco-2 monolayers may predict transport in human large intestinal tissue. J Pharm Sci **85**, 165-169

104 Ichikawa, H. and Peppas, N. A. (2003) Novel complexation hydrogels for oral peptide delivery: In vitro evaluation of their cytocompatibility and insulin-transport enhancing effects using Caco-2 cell monolayers. J Biomed Mat Res **67A**, 609-617

105 Shen, W.-C., Wan, J. and Ekrami, H. (1992) (C) Means to enhance penetration: (3) Enhancement of polypeptide and protein absorption by macromolecular carriers via endocytosis and transcytosis. Adv Drug Deliv Rev **8**, 93-113

106 Mellman, I., Fuchs, R. and Helenius, A. (1986) Acidification of the endocytic and exocytic pathways. Annl Rev Biochem **55**, 663-700

107 Singh, M. (1999) Transferrin As A targeting ligand for liposomes and anticancer drugs. Curr Pharm Des **5**, 443-451

108 Beyer, U., Roth, T., Schumacher, P., Maier, G., Unold, A., Frahm, A. W., Fiebig, H. H., Unger, C. and Kratz, F. (1998) Synthesis and in vitro efficacy of transferrin conjugates of the anticancer drug chlorambucil. J Med Chem **41**, 2701-2708

109 Broadwell, R. D., Baker-Cairns, B. J., Friden, P. M., Oliver, C. and Villegas, J. C. (1996) Transcytosis of protein through the mammalian cerebral epithelium and endothelium. III. Receptor-mediated transcytosis through the blood-brain barrier of blood-borne transferrin and antibody against the transferrin receptor. Exp Neurol **142**, 47-65

110 Qian, Z. M., Li, H., Sun, H. and Ho, K. (2002) Targeted drug delivery via the transferrin receptor-mediated endocytosis pathway. Pharmacol Rev **54**, 561-587

111 Jones, A. T., Gumbleton, M. and Duncan, R. (2003) Understanding endocytic pathways and intracellular trafficking: a prerequisite for effective design of advanced drug delivery systems. Adv Drug Deliv Rev **55**, 1353-1357

112 Banerjee, D., Flanagan, P. R., Cluett, J. and Valberg, L. S. (1986) Transferrin receptors in the human gastrointestinal tract. Relationship to body iron stores. Gastroenterology **91**, 861-869

113 Azari, P. R. and Feeney, R. E. (1958) Resistance of metal complexes of conalbumin and transferrin to proteolysis and to thermal denaturation. J Biol Chem **232**, 293-302

114 Wan, J., Taub, M. E., Shah, D. and Shen, W. C. (1992) Brefeldin A enhances receptor-mediated transcytosis of transferrin in filter-grown Madin-Darby canine kidney cells. J Biol Chem **267**, 13446-13450

115 Shah, D. and Shen, W. C. (1996) Transcellular delivery of an insulin-transferrin conjugate in enterocyte-like Caco-2 cells. J Pharm Sci **85**, 1306-1311

116 Rini, J. M. (1995) Lectin structure. Biophysical J **24**, 551-577

117 Gabor, F., Wirth, M., Jurkovich, B., Haberl, I., Theyer, G., Walcher, G. and Hamilton, G. (1997) Lectin-mediated bioadhesion: Proteolytic stability and binding-characteristics of wheat germ agglutinin and Solanum tuberosum lectin on Caco-2, HT-29 and human colonocytes. J Control Rel **49**, 27-37

118 Naisbett, B., Woodley, J. and Department of Biological Sciences, U. o. K. S. U. K. (1990) Binding of tomato lectin to the intestinal mucosa and its potential for oral drug delivery. Biochemical Society transactions. **18(5)**, 879-880

119 Noah, N. D., Bender, A. E., Reaidi, G. B. and Gilbert, R. J. (1980) Food poisoning from raw red kidney beans. British Medical Journal **281**, 236-237

120 Lafont, J., Rouanet, J. M., Gabrion, J., Assouad, J. L., Zambonino Infante, J. L. and Besancon, P. (1988) Duodenal toxicity of dietary Phaseolus vulgaris lectins in the rat: an integrative assay. Digestion **41**, 83-93

121 Kilpatrick, D. C., Pusztai, A., Grant, G., Graham, C. and Ewen, S. W. B. (1985) Tomato lectin resists digestion in the mammalian alimentary canal and binds to intestinal villi without deleterious effects. FEBS Letters **185**, 299-305

122 Lehr, C. M. (2000) Lectin-mediated drug delivery: the second generation of bioadhesives. J Control Rel **65**, 19-29

123 Ponchel, G. and Irache, J. (1998) Specific and non-specific bioadhesive particulate systems for oral delivery to the gastrointestinal tract. Adv Drug Deliv Rev **34**, 191-219

124 Woodley, J. (2001) Bioadhesion: new possibilities for drug administration? Clin Pharmacokinet **40**, 77-84

125 Clark, M. A., Hirst, B. H. and Jepson, M. A. (2000) Lectin-mediated mucosal delivery of drugs and microparticles. Adv Drug Deliv Rev **43**, 207-223

126 Nagahora, H., Harata, K., Muraki, M. and Jigami, Y. (1995) Site-directed mutagenesis and sugar-binding properties of the wheat germ agglutinin mutants Tyr73Phe and Phe116Tyr. Eur J Biochem **233**, 27-34

127 Gabor, F., Schwarzbauer, A. and Wirth, M. (2002) Lectin-mediated drug delivery: binding and uptake of BSA-WGA conjugates using the Caco-2 model. Int J Pharm **237**, 227-239

128 Gabor, F., Stangl, M. and Wirth, M. (1998) Lectin-mediated bioadhesion: binding characteristics of plant lectins on the enterocyte-like cell lines Caco-2, HT-29 and HCT-8. J Control Rel **55**, 131-142

CHAPTER 3

OBJECTIVES

Development of oral delivery formulations for therapeutic proteins and peptides is of great interest to the pharmaceutical industry. Successful oral delivery of therapeutic proteins such as insulin, can greatly improve the efficacy of treatment of diseases, and improve the quality of life of patients. However, the challenges in developing oral protein formulations largely remain unaddressed and a universally acceptable solution to those challenges still eludes the scientific community. Some significant advances have been made in the recent past, that have led to better ways of addressing the challenges of oral protein delivery.

Use of complexation hydrogels developed in our laboratory has been proposed as a promising alternative for oral insulin delivery. Hydrogels-based delivery systems effectively address some of the key challenges in protein delivery. However, better understanding of how the hydrogel-based oral formulations function is desired for developing better ways to enhance oral bioavailability of proteins. As discussed in Chapter 2, some of the other investigated strategies, such as the use of transferrin specific receptor-mediated transcytotic pathway, address the issue of low protein bioavailability through other specific means.

The overall goal of this work was to evaluate the effectiveness complexation hydrogels in addressing some key problems in oral protein delivery

and to design a system based on integrating the hydrogels with other effective strategies for oral protein delivery. The specific goals of this research are outlined below:

(1) *Evaluation of the synergistic effect of complexation hydrogels and permeation enhancers on the permeability of in vitro cell culture models of the intestinal epithelium.*

(2) *Investigation of the mechanisms of transport of insulin across the model intestinal cell monolayers.*

(3) *Evaluation of the contribution of PEG chains in the P(MAA-g-EG) particles towards increased retention of the polymer particles in the GI tract.*

(4) *Investigation of the ability of the microparticles to protect insulin from degradation in the gastric and intestinal environment.*

(5) *Investigation and optimization of the synthesis conditions and characterization of insulin-transferrin conjugates.*

(6) *Optimization of the P(MAA-g-EG) microparticle carriers for delivery of the insulin-transferrin conjugates.*

(7) *Cellular evaluation of the formulations based on complexation hydrogels for oral delivery of insulin-transferrin conjugates.*

CHAPTER 4

SYNERGISTIC EFFECT OF PERMEATION ENHANCERS AND COMPLEXATION HYDROGELS ON THE CELL MONOLAYER

4.1 Introduction

Transport of a drug across the intestinal epithelium is greatly influenced by its physiochemical characteristics. Typically, peptides that have molecular weight greater than 500, are charged at the intestinal pH, and tend to hydrogen bond, diffuse poorly across the epithelial barrier via the transcellular passive diffusion pathway [1]. Paracellular transport, as described previously, is size dependent and hence the paracellular diffusion of structurally complex proteins, such as insulin is negligible [2]. Thus, any enhancement in the paracellular transport of a protein will require improved control over the opening of the tight junctions.

Various methods based on this rationale have been explored to improve the transport of therapeutic proteins across the intestinal epithelium. A common method has been the use of permeation enhancers, like detergents, fatty acids or bile salts, which open the intercellular tight junctions and hence increase the transport of insulin across the intestinal membrane [3]. However, potential for damage to the epithelia and toxicity is a major concern since the approach is not selective towards the drug molecule of interest and undesirable luminal contents can also be transported into the blood stream[4-6].

This potential disadvantage of the methodology may be addressed by achieving a tight control over permeability of the tight junctions. A delivery system which can reversibly open the tight junctions only for a short period of time so that only the drug can be transported across the intestinal epithelium is highly desirable. Thus, the end goal of these approaches is an oral delivery formulation, which, after reaching the upper small intestine, will precisely control opening and closing of the tight junctions so that only the protein of interest can cross the intestinal barrier to reach the blood stream. By inducing rapid reversibility of the tight junction opening, any non-specific transport of undesirable components may be greatly restricted, thus avoiding the toxicity associated with this approach.

Various permeation enhancers have been investigated for their ability to increase the transport of large molecules across the intestinal cell monolayer. Most of these enhancers act by opening the tight junctions between the cells [7, 29]. However, precise control over opening and closing of the tight junctions has not been achieved yet.

It has been shown that P(MAA-g-EG) based complexation hydrogels can reversibly open the tight junctions between Caco-2 cells. This property of the hydrogels is believed to be associated with their ability to bind free Ca^{2+} when placed in contact with Caco-2 cells. Reduction in extracellular Ca^{2+} concentration is believed to cause opening of the tight junctions. Thus, the complexation hydrogels reversibly open the tight junctions between the cells by reducing free Ca^{2+} concentrations and any improvement in the ability of the hydrogels to

control opening and closing of the tight junctions may greatly increase the oral bioavailability of insulin released from the hydrogel formulation. It was the focus of this work to investigate if complexation hydrogels used in conjunction with a model paracellular enhancer exhibit better control over the tight junction permeability.

One absorption enhancer that is relatively well-studied and used clinically Japan with no reports of side effects is sodium caprate [7-9]. It is the sodium salt of capric acid, a 10-carbon saturated fatty acid, that constitutes 2-3% of the fatty acids in dairy products [10]. Sodium caprate facilitates transport via the transcellular route through membrane perturbation and via the paracellular route through the opening of the tight junctions, which are mediated by the contraction of calmodulin-dependent actin microfilaments, causing by elevation of intracellular calcium ion levels [8, 9]. Ultrastructural studies of Caco-2 monolayers after exposure to sodium caprate showed dilatations in the tight junctions in rat and hamster small intestine [11, 12].

Tomita et al. [13] showed that sodium caprate induced increase in paracellular permeability via a calcium-mediated contraction of the perijunctional actin microfilaments. Sakai et al. [14] examined the changes in intracellular calcium ion level and histomorphology of actin filaments in Caco-2 cell monolayer in the presence of sodium caprate. Sodium caprate induced changes in the intracellular calcium concentration and significantly changed the actin filament structure in a reversible manner. It was postulated that the paracellular

permeability enhancing effect of sodium caprate was due the alteration in the cytoskeletal actin filaments which are provoked by changes in the intracellular calcium ion levels [14]. Further, sodium caprate is non-toxic when used in concentrations below 13 mM [15].

Hence, sodium caprate was used as a model paracellular enhancer for these studies. The objective was to investigate if the combination of the complexation hydrogels and the specific enhancing agent results into a better delivery system. The synergistic effect of sodium caprate and P(MAA-g-EG) microparticles on the permeability of the Caco-2 cell monolayer was investigated. The permeability of the cell monolayer was measured in terms of the transepithelial electric resistance (TEER) value of the monolayer[16, 17]. Concentrations of sodium caprate used for this work have been shown to reversibly reduce the TEER values of the Caco-2 cell monolayer [18].

4.2 Materials and Methods

Preparation of Polymer Microparticles: P(MAA-g-EG) hydrogels were prepared by free radical solution UV-polymerization of methacrylic acid (MAA) and poly(ethylene glycol) ether monomethacrylate (PEGMA). The monomers were mixed in the molar ratio of 1:1 (MAA:EG). The MAA (Aldrich Chemical Company, Milwaukee, WI) was vacuum distilled at 47°C/25 mmHg to remove the inhibitor

hydroquinone monomethyl ethere. PEGMA (Polysciences, Inc. Warrington, PA) was used as received.

PEGMA with PEG molecular weight of 1000 was used in this synthesis. Tetra(ethylene glycol) dimethacrylate (TEGDMA) (Polysciences, Inc. Warrington, PA) was used as the crosslinking agent and was added in the amount of 0.75 % moles of the total amount of monomers. The photoinitiator, Irgacure-184 (Ciba-Geigy Co. Hawthorne, NY) was added in the amount of 0.1wt % of the total amount of monomers. To inhibit autoacceleration in the polymerization reaction, monomer mixture was diluted with a mixture of 50 % v/v ethanol and deionized water (Milli-Q Plus system, Millipore). Nitrogen was bubbled through the well-mixed solution for 15 minutes to remove dissolved oxygen, which acts as a free radical scavenger. The mixture was then carefully poured between microscope slides (75 x 50 x 1 mm) (Fisher, Pittsburgh PA) separated by Teflon spacers with a thickness of 0.9 mm. The glass slides were then placed in a nitrogen atmosphere under a UV light source of 16 mW/cm^2 at 365 nm for 30 minutes. After the completion of the reaction, the polymer films were washed in deionized water for approximately 7 days in order to remove unreacted monomers, crosslinking agent, initiator and sol fraction. After washing the polymer films were dried at room temperature for a day and then placed in a vacuum oven at 27 °C for 2 days. The dry polymer films were then crushed by using a mortar and pestle and then sieved to 150-212 μm by using the corresponding. All the

particles were stored in a closed 5 mL glass vials inside a desiccator until further use.

Preparation of Caco-2 cell monolayer: Caco-2 cell cultures were grown in 6-well Transwell plates (4.71 cm^2/well) (Costar, Corning Incorp., Corning NY) with DMEM culture media for 21 to 24 days until they achieved a constant TEER value, which indicated that the tight junctions had formed in the monolayer [26,27]. The media was changed every other day. The electrical resistance was monitored using a voltmeter with a chopstick electrode (World Precision Instrument, Sarasota, FL). The culturing cell density was 2.35 x 10^5 cells/well. Each well consisted of two chambers: the apical (top) and the basolateral (bottom), which were separated by membrane with 0.45 μm pore size.

TEER Measurement Studies: The medium used for these studies was Hanks' balanced salt solution, HBSS containing Ca^{2+}. Before the measurements, the cell membranes were allowed to equilibrate for one hour with the experimental medium, HBSS containing Ca^{2+}. After this period, the cell monolayer achieved a constant electrical resistance after the change of medium. The electrical resistance was monitored using a voltmeter with a chopstick electrode.

After the equilibration period, the apical chamber media was removed and replaced by fresh HBSS containing the sodium caprate with or without pre-swollen microparticles. The microparticles were used in concentration of 5 mg/ml and sodium caprate was used in two different concentrations of 1 mg/ml and 0.5 mg/ml. Both these concentrations were used with or without the microparticles.

The TEER, of the cell monolayer was measured at different time intervals. The temperature was kept constant at 37 ^{0}C during the entire course of the experiment. While measuring TEER, the experimental plates were placed on a heated mat (Barnstead Thermolyne, size 6 x15 in, model LAB1611003, Duburque, Iowa) with a voltage controller (Glass-Col®, Terre Haute, IN) in a laminar flow hood. After incubation for 90 minutes, the HBSS containing sodium caprate and/or microparticles was removed, the cells were gently washed with HBSS and fresh HBSS was introduced on both apical and the basolateral sides. TEER readings were taken for 3 hours to study the reversible effect on tight junctions.

4. 3 Results and Discussion

Changes in the tight junction permeability in the presence of sodium caprate and P(MAA-g-EG) microparticles was studied by monitoring the TEER values of the cell monolayer. The TEER value is a quantitative measure of resistance to ion transport across the epithelium and hence the permeability of the tight junctions. Reversibility in opening of the tight junctions is a desired characteristic for designing a delivery system. P(MAA-g-EG) microparticles have been shown to reversibly reduce the TEER value of the Caco-2 cell monolayer [18]. Sodium caprate has also been shown to reversibly reduce the TEER values of Caco-2 cell monolayer in the concentration range of 0-1mg/ml [33]. Hence,

reduction in TEER values in the presence of both the microparticles and sodium caprate was studied here.

Percentage TEER value was calculated as

$$TEER\% = \frac{\left(R_t - R_{w/o}\right)}{\left(R_o - R_{w/o}\right)} \times 100 \quad (4.1)$$

Here, R_t is the measured electrical resistance at any time, $R_{w/o}$ is the electrical resistance in absence of cell monolayer, R_o is the initial resistance value.

Fig 4.1 shows the effect of microparticles and sodium caprate on the TEER values of Caco-2 cell monolayer. First 90 minutes show the effect of polymer solution and sodium caprate. Fresh HBSS was introduced after 90 minutes to study the reversible effect on TEER values.

Controls (cell monolayer without any microparticles or sodium caprate) showed some drop in TEER after introduction of fresh HBSS at 90 minutes and took longer time than expected to reach the initial value of TEER. As expected, both polymer and sodium caprate induced reversible decrease in TEER of the cell monolayer. However, when the microparticles and sodium caprate were placed together in the epical side, the synergistic effect of the two caused a sudden, irreversible decrease in TEER values. The pattern was almost identical for both 1 mg/ml and 0.5 mg/ml solutions of sodium caprate. In most cases, the combination of microparticles and sodium caprate caused detachment of the cell

monolayer from the pore membrane at around 85-90 minutes. This indicated that P(MAA-g-EG) microparticles and sodium caprate did not act independently. One affected the functioning of the other. Possible interaction between the microparticles and sodium caprate could have precipitated the sodium caprate on the cell monolayer creating high local concentrations of the salt. High concentrations of sodium caprate can open the tight junctions irreversibly [33]. This seems to be the most likely cause of the observed irreversible reduction in TEER values.

4.4 Conclusions

The combination of the enhancing agent and the microparticles did not result in an effective delivery system for protein molecules. Sodium caprate and P(MAA-g-EG) microparticles caused irreversible damage to the epithelium. Thus a formulation which contains permeation enhancers and the microparticles, if administered orally, can cause severe damage to the epithelia. Hence this line of investigation was abandoned and we turned our attention to the other, non-invasive mechanism of improving the transport of proteins across the epithelium. These studies are discussed in Chapter 8, 9 and 10.

References

1 Aungst, B. J., Saitoh, H., Burcham, D. L., Huang, S. M., Mousa, S. A. and Hussain, M. A. (1996) Enhancement of the intestinal absorption of peptides and non-peptides. J Control Rel **41**, 19-31

2 Uchiyama, T., Sugiyama, T., Quan, Y. S., Kotani, A., Okada, N., Fujita, T., Muranishi, S. and Yamamoto, A. (1999) Enhanced permeability of insulin across the rat intestinal membrane by various absorption enhancers: their intestinal mucosal toxicity and absorption-enhancing mechanism of n-lauryl-beta-D-maltopyranoside. J Pharm Pharmacol **51**, 1241-1250

3 Lee, V. H., Yamamoto, A. and Kompella, U. B. (1991) Mucosal penetration enhancers for facilitation of peptide and protein drug absorption. Crit Rev Ther Drug Carrier Syst **8**, 91-192

4 Ward, P. D., Tippin, T. K. and Thakker, D. R. (2000) Enhancing paracellular permeability by modulating epithelial tight junctions. Pharm. Sci. Technol. Today **3**, 346-358

5 Fix, J. A. (1996) Strategies for delivery of peptides utilizing absorption-enhancing agents. J Pharm Sci **85**, 1282-1285

6 Aungst, B. J. (2000) Intestinal permeation enhancers. J Pharm Sci **89**, 429-442

7 Anderberg, E. K., Lindmark, T. and Artursson, P. (1993) Sodium caprate elicits dilatations in human intestinal tight junctions and enhances drug absorption by the paracellular route. Pharm Res **10**, 857-864

8 Tomita, M., Shiga, M., Hayashi, M. and Awazu, S. (1988) Enhancement of colonic drug absorption by the paracellular permeation route. Pharm Res **5**, 341-346

9 Tomita, M., Hayashi, M., Horie, T., Ishizawa, T. and Awazu, S. (1988) Enhancement of colonic drug absorption by the transcellular permeation route. Pharm Res **5**, 786-789

10 Soderholm, J. D., Oman, H., Blomquist, L., Veen, J., Lindmark, T. and Olaison, G. (1998) Reversible increase in tight junction permeability to macromolecules in rat ileal mucosa in vitro by sodium caprate, a constituent of milk fat. Dig Dis Sci **43**, 1547-1552

11 Lindmark, T., Nikkila, T. and Artursson, P. (1995) Mechanisms of absorption enhancement by medium chain fatty acids in intestinal epithelial Caco-2 cell monolayers. J Pharmacol Exp Ther **275**, 958-964

12 Madara, J. L. and Pappenheimer, J. R. (1987) Structural basis for physiological regulation of paracellular pathways in intestinal epithelia. J Membr Biol **100**, 149-164

13 Tomita, M., Hayashi, M. and Awazu, S. (1994) Comparison of absorption-enhancing effect between sodium caprate and disodium ethylenediaminetetraacetate in Caco-2 cells. Biol Pharm Bull **17**, 753-755

14 Sakai, M., Imai, T., Ohtake, H., Azuma, H. and Otagiri, M. (1998) Effects of absorption enhancers on cytoskeletal actin filaments in Caco-2 cell monolayers. Life Sci **63**, 45-54

15 Lindmark, T., Schipper, N., Lazorova, L., de Boer, A. G. and Artursson, P. (1998) Absorption enhancement in intestinal epithelial Caco-2 monolayers by sodium caprate: assessment of molecular weight dependence and demonstration of transport routes. J Drug Target **5**, 215-223

16 Frizzell, R. A. and Schultz, S. G. (1972) Ionic conductances of extracellular shunt pathway in rabbit ileum. Influence of shunt on transmural sodium transport and electrical potential differences. J Gen Physiol **59**, 318-346

17 Schultz, S. G. and Frizzell, R. A. (1976) Ionic permeability of epithelial tissues. Biochim Biophys Acta **443**, 181-189

18 Sakai, M., Imai, T., Ohtake, H., Azuma, H. and Otagiri, M. (1997) Effects of absorption enhancers on the transport of model compounds in Caco-2 cell monolayers: assessment by confocal laser scanning microscopy. J Pharm Sci **86**, 779-785

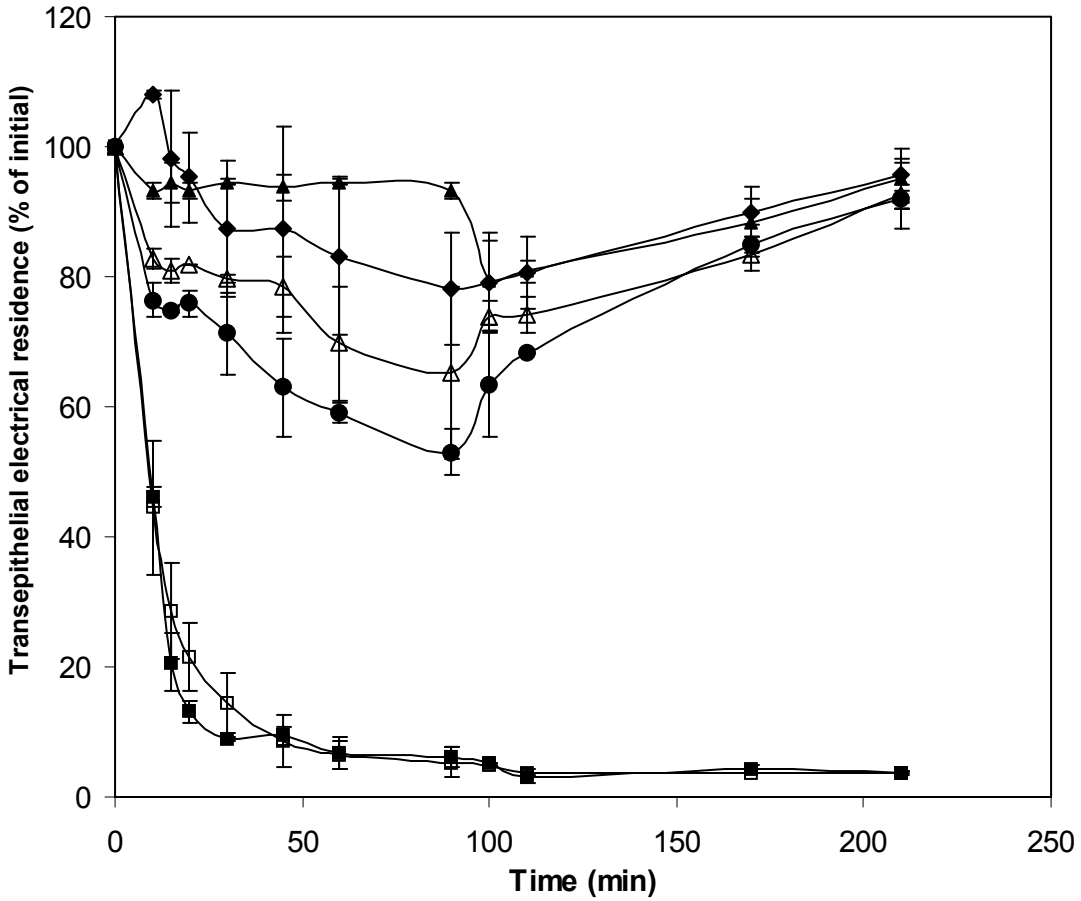

Fig. 4.1. Transepithelial electrical resistance (TEER) plotted against time. Combined effect of sodium caprate and P(MAA-g-EG) particles on transepithelial electrical resistance of Caco-2 cell monolayer. Polymer particles with initial feed ratio MAA:EG of 1:1 and PEG molecular weight of 1000 were used in the experiment. (▲)control, (♦) polymer(5mg/ml), (Δ) sodium caprate(0.5mg/ml), (●)sodium caprate(1mg/ml), (□)polymer (5mg/ml) and sodium caprate (0.5mg/ml) and (■)polymer (5mg/ml) and sodium caprate (1mg/ml). Solutions were replaced by fresh HBSS at 90 min. The experiments were carried out at a constant temperature of 37^0C. Error bars represent one standard deviation, n=3.

CHAPTER 5

EXPERIMENTAL INVESTIGATION OF TRANSPORT MECHANISMS OF INSULIN ACROSS THE CELL MONOLAYER

5.1 Introduction

As described in Section 2.4.1, the transport of therapeutic agents such as proteins across the intestinal gut wall may take place via various pathways [1]. The transport can occur primarily through the cell membrane of the enterocytes (transcellular transport) or via the tight junctions between the cells (paracellular transport). The transcellular passive diffusion pathway is mostly limited to drugs that are non-polar, and are lipid soluble, are not charged at the physiological pH of the small intestinal lumen. The octanol-water system is typically used as a reference system for biological partitioning in drug design work. Drug lipophilicity is estimated by determining the drug's octanol-water partition coefficient [2]. Insulin has low lipophilicity with an octanol-water partition coefficient of about 0.0215 [3]. Further, the iso-electric point of insulin is around 5 and hence insulin is negatively charged at the neutral pH of the small intestine. Thus, entry into the cell membrane is unfavorable. The primary pathway available for transport of insulin across the epithelium is the aqueous paracellular pathway.

One additional pathway available for the transcellular transport of proteins is the receptor mediated endocytosis, wherein, the protein molecules bind specific receptors presented on the cell surface. The ligand-receptor complex is

then endocytosed into the cells by the process of receptor mediated endocytosis. The transport of molecules via this pathway is considerably faster than the passive diffusion pathway.

Insulin receptors have been identified in the basolateral membranes of dog intestinal mucosa, in the mouse intestinal cells and in the membrane of Caco-2 cells [4-6]. The precise role of these receptors in the GI tract remains unclear. Kendzierski et al. [7, 8] analyzed the ability of the gut to make insulin. It was suggested that the insulin receptors might be involved in an autocrine or paracrine role of the insulin made in the gut. Intracellular immunoreactivity towards insulin was found in glandular cells in the stomach and colon but no immunoreactivity was found in the small intestine [7]. In addition, the preproinsulin mRNA was detected in similar cells in the stomach and colon. Insulin produced in the gut may function in controlling cell division, secretion of other peptides, or motility and absorption.

Importantly, insulin has been reported to be absorbed into the rat ileal epithelium in the presence of permeation enhancers and protease inhibitors [9-11]. By applying protein A-gold immunocytochemical technique, Bendayan et al. [9] showed that insulin was uptaken into endocytotic vesicles and was routed to the basolateral side of the ileal membrane via the trans-side of the Golgi-apparatus. A similar pathway of the insulin uptake and transport was also observed in normal and diabetic rats [12]. In addition to this, an insulin-degrading enzyme (IDE), a thiol metalloprotease, has been identified in the cytosol of the

rat intestinal enterocytes constituting upto 92% of total insulin-degrading activity [13]. These results indicate that the ligand-specific receptor-mediated transcellular pathway may be functional in protein transport across the intestinal epithelium.

Thus both the paracellular and transcellular pathways could be functional in insulin transport across the intestinal epithelium. However, because of the endosomal degradation and the degradation due to the IDE, the contribution of the transcellular pathway to the insulin flux across the intestinal mucosa would be negligible [13].

The precise mechanism of insulin transport across the epithelium when delivered using the P(MAA-g-EG) microparticles is not clear. The polymeric microparticles have been shown to reversibly reduce the transepithelial electrical resistance (TEER) of the Caco-2 cell monolayer [14], which is a measure of the integrity of the tight junctions between the cells. This opening of the tight junctions by P(MAA-g-PEG) microparticles has been attributed to their ability to bind free calcium. Any significant decrease in calcium concentration of the medium surrounding the epithelial cells opens the tight junctions [15, 16]. This suggests that the microparticles facilitate the paracellular transport of insulin. It is, however, unclear whether this is the only mechanism by which insulin can be transported across the epithelium. Understanding the precise mechanism of enhancement in insulin transport in the presence polymeric microparticles is critical to improving the oral bioavailability of the protein.

In this study, the transport mechanism of fluorescein isothiocynate insulin (FITC-insulin) (Sigma, St. Louis, MO) across the Caco-2 cell monolayer in the presence of P(MAA-g-EG) microparticles was investigated by using confocal laser scanning microscopy. In order to distinguish between intracellular and paracellular insulin, the cells were labeled using Nile Red dye (Sigma, St. Louis, Mo), a lipophilic dye used to label the cell membranes.

5.2 Materials and Methods

Preparation of Polymer Microparticles: P(MAA-g-EG) hydrogels were prepared by free radical solution UV-polymerization of methacrylic acid (MAA) and poly(ethylene glycol) ether monomethacrylate (PEGMA). The monomers were mixed in the molar ratio of 1:1 (MAA:EG). The MAA (Aldrich Chemical Company, Milwaukee, WI) was vacuum distilled at 47°C/25 mmHg to remove the inhibitor hydroquinone monomethyl ethere. PEGMA (Polysciences, Inc. Warrington, PA) was used as received.

PEGMA with PEG molecular weight of 1000 was used in this synthesis. Tetra(ethylene glycol) dimethacrylate (TEGDMA) (Polysciences, Inc. Warrington, PA) was used as the crosslinking agent and was added in the amount of 0.75 % moles of the total amount of monomers. The photoinitiator, 1-hydroxy-cyclohexl-phenylketone, (Irgacure-184) (Ciba-Geigy Co. Hawthorne, NY) was added in the amount of 0.1 wt % of the total amount of monomers. To inhibit autoacceleration

in the polymerization reaction, the monomer mixture was diluted with a mixture of 50 % v/v ethanol and deionized water (Milli-Q Plus system, Millipore). Nitrogen was bubbled through the well-mixed solution for 15 minutes to remove dissolved oxygen, which acts as a free radical scavenger. The mixture was then carefully poured between microscope slides (75 x 50 x 1 mm) (Fisher, Pittsburgh PA) separated by Teflon spacers with a thickness of 0.9 mm. The glass slides were then placed in a nitrogen atmosphere under a UV light source of 16 mW/cm^2 at 365 nm for 30 minutes.

After the completion of the reaction, the polymer films were washed in deionized water for approximately 7 days in order to remove unreacted monomers, crosslinking agent, initiator and sol fraction. After washing, the polymer films were dried at room temperature for a day and then placed in a vacuum oven at 27 °C for 2 days. The dry polymer films were then crushed by using a mortar and pestle and sieved to 150-212 μm. All the particles were stored in a closed 5 mL glass vials inside a desiccator until further use.

Development of Caco-2 cell monolayer: The cells were cultured in 75 cm^2 culturing flasks (VWR Scientific, West Chester, PA) with 10 mL of Dulbecco's Modified MEM, culture media, DMEM (Bio Fluids, Biosource International). The seeding density for cultivation was $2.5x10^5$ cells/flask. Cells were maintained in an incubator at 37 °C temperature, 95 % relative humidity, and 5 % CO_2. The culture medium was replaced with fresh medium every other day for about 6 or 7 days, until the cells reached 70-80% confluency. A passage operation was

performed after the cells reached 60-80% confluency. In the passage operation, the cells were detached from the culturing flask by trypsinization, counted and transferred with the desired seeding density to a new culturing flask or experimental wells. In these cells studies, cells with passage numbers between 60 and 65 were used.

For transport studies, Caco-2 cells were grown in 6-well Transwell® plates (4.71 cm^2/well) (Costar, Corning Incorp., Corning NY). The culturing cell density was 2.35 x 10^5 cells/well. The cells were grown in a DMEM culture media containing fetal bovine serum (FBS) for 21 to 24 days until they achieved a constant transepithelial electrical resistance, which indicated that the tight junctions had formed in the monolayer [17, 18]. The medium was changed every other day and the electrical resistance was monitored using a voltmeter with a chopstick electrode (World Precision Instrument, Sarasota, FL). The experimental setup is shown in Figure 5.1. Each well consisted of two chambers: the apical (top) and the basolateral (bottom), which were separated by membrane with 3.0 μm pore size. The medium used for these studies was Hanks' balanced salt solution, HBSS containing Ca^{2+}.

Confocal Microscopy Analysis of FITC-insulin Transport: Cell membranes were allowed to equilibrate for one hour with the experimental medium, HBSS with Ca^{2+}, prior to the initiation of the experiment. HBSS containing Ca^{2+} was used since the absence of Ca^{2+} from the medium itself can cause opening of the tight

junctions. After this period, the cell monolayer achieved a constant electrical resistance after the change of the medium.

The culturing medium from the wells was removed and substituted by HBSS-containing FITC-insulin with or without pre-swollen microspheres. The wells were then incubated for 120 min and Nile Red dye (Sigma, St. Louis, MO) was applied on the apical and the basolateral sides of each well. The final concentration of Nile Red dye was 5 μL/ml. The cells were incubated for 5 minutes for labeling the membranes. The experimental medium was then removed and the membranes were gently rinsed with fresh media. The cells were fixed by incubation with 3.7% formaldehyde in Dulbecco's modified Phospshate Buffer Saline, DPBS modified (VWR Scientific, West Chester, PA) for 10 minutes. After fixation, the formaldehyde solution was removed and cells were gently washed with HBSS. The membrane was removed from the plastic insert by cutting it with a scalpel. It was then placed on a microscope slide, covered with a cover slip and placed under the microscope. The equipment consisted of a MRC 1024 with a Nikkon Diaphot 300 (BioRAd, Hercules,CA).

5. 3 Results and Discussion

Confocal laser scanning microscopy experiments were performed to visualize the transport of FITC-insulin across Caco-2 cell monolayer in the presence or in the absence of P(MAA-g-EG) microparticles. Nile Red dye was

used to label the membrane in order to clearly distinguish between paracellular and transcellular insulin in the images.

Figures 5.2 to 5.3 illustrate the results obtained from confocal laser scanning microscope. Each figure is presents two X-Y images, the first one showing FITC-insulin (green) and Nile Red dye (red) and the second one showing the transmission image. Figure 5.2 shows a control Caco-2 cell monolayer (not incubated with FITC-insulin) labeled with the Nile Red dye. The dye successfully labeled the cell membranes, although some dye diffused inside the cells. The images are not very clear, primarily because high concentration of the labeling solution was used and the washing process after the labeling was not efficient in removing the excess dye. Based on this observation, lower concentration of the labeling solution was used to label the cells in the subsequent experiments. This experiment established the ability of Nile Red dye to stain the cell membrane of Caco-2 cells in a confluent monolayer.

Figure 5.3 shows confocal laser scanning microscope images of FITC-insulin placed on the basolateral side of cell membrane without any microparticles. Some important conclusions can be drawn from these images. The examination of images indicated that FITC-insulin present in the inter-cellular spaces can itself be used to visualize the cell membranes. Hence, the need for a lipophilic dye such as the Nile Dye in order to distinguish between the paracellular and transcellular insulin was eliminated. The images also revealed that some FITC-insulin was present inside the cells.

This insulin can be seen in the form of green dots localized in the intracellular spaces. Such green dots were seen predominantly in the X-Y sections near the apical and the basolateral sides of cell monolayer. As discussed in section 5.1, the insulin receptors present on the cells could be functional in absorbing the labeled insulin into the cells. However, no insulin was seen in the transcellular spaces in the optical sections near the basolateral membrane. This indicates that the insulin that entered the cells via the paracellular route was not able to reach the basolateral side. This could be either because of the degradation of protein in the endosomal vesicles or due to the degradation by the insulin degrading enzyme. Hence the transcellular component of the insulin transport is either extremely low or entirely absent.

Figure 5.4 shows images of FITC-insulin placed on the basolateral side of the cell membrane with microparticles. The FITC-insulin was again located in the paracellular spaces. The intensity of fluorescence was only slightly higher as compared to the membrane incubated with FITC-insulin without any microparticles. Probable cause of this increase in the intensity is enhancement in the paracellular transport of insulin because of the presence of the microparticles. Interestingly, the green dots indicating transcellular insulin were not so prominent in these monolayers compared to the monolayer incubated with FITC-insulin only. The reasons behind the absence of FITC-insulin localized in the transcellular were not clear. This could be because clear images were not obtained with microparticles for focal planes near the apical side since emission

due to excess concentration of Nile Dye was picked up in the channel for FITC-insulin. This made it difficult to analyze the optical planes near the apical region for the signal from transcellular FITC-insulin. This excess emission, also called bleed over, can also be noticed in Figure 5.4

5.4 Conclusions

Confocal microscopy studies were performed to evaluate the transport mechanisms of insulin across the Caco-2 cell monolayers. It was shown that the paracellular pathway was the predominant route of insulin transport across the monolayers in the presence or absence of the microparticles. The transcellular component for insulin transport was almost entirely absent even though uptake of insulin by the cells was observed. This is an important consideration in employing strategies to increase the flux of insulin across the Caco-2 cell monolayers and across the intestinal epithelium. It is suggested that insulin-degrading enzyme inhibitors such as N-ethylmaleimide, 1,10-phenanthroline, and EDTA may be used to achieve improved insulin absorption in the intestine [13]. However, such inhibitors may have adverse effect on the functioning of the intestinal enzymes and may also cause permanent damage to the epithelium. Based on the observations from the confocal microscopy investigations presented here, we targeted transcellular pathway for improving insulin permeability. The details of this approach are discussed in detail in Chapters 8, 9, and 10.

References

1 Balimane, P. V., Chong, S. and Morrison, R. A. (2000) Current methodologies used for evaluation of intestinal permeability and absorption. J Pharmacol Toxicol Methods **44**, 301-312

2 Smith, R. N., Hansch, C. and Ames, M. M. (1975) Selection of a reference partitioning system for drug design work. J Pharm Sci **64**, 599-606

3 Lee, V. H. (1988) Enzymatic barriers to peptide and protein absorption. Crit Rev Ther Drug Carrier Syst **5**, 69-97

4 Gingerich, R. L., Gilbert, W. R., Comens, P. G. and Gavin, J. R., 3rd (1987) Identification and characterization of insulin receptors in basolateral membranes of dog intestinal mucosa. Diabetes **36**, 1124-1129

5 Gallo-Payet, N. and Hugon, J. S. (1984) Insulin receptors in isolated adult mouse intestinal cells: studies in vivo and in organ culture. Endocrinology **114**, 1885-1892

6 Pillion, D. J., Ganapathy, V. and Leibach, F. H. (1985) Identification of insulin receptors on the mucosal surface of colon epithelial cells. J Biol Chem **260**, 5244-5247

7 Kendzierski, K. S., Pansky, B., Budd, G. C. and Saffran, M. (2000) Evidence for biosynthesis of preproinsulin in gut of rat. Endocrine **13**, 353-359

8 Saffran, M., Pansky, B., Budd, G. C. and Williams, F. (1997) Insulin and the gastrointestinal tract. J Control Rel **46**, 89-98

9 Bendayan, M., Ziv, E., Ben-Sasson, R., Bar-On, H. and Kidron, M. (1990) Morpho-cytochemical and biochemical evidence for insulin absorption by the rat ileal epithelium. Diabetologia **33**, 197-204

10 Ziv, E., Lior, O. and Kidron, M. (1987) Absorption of protein via the intestinal wall. A quantitative model. Biochem Pharmacol **36**, 1035-1039

11 Morishita, M., Morishita, I., Takayama, K., Machida, Y. and Nagai, T. (1993) Site-dependent effect of aprotinin, sodium caprate, Na2EDTA and sodium glycocholate on intestinal absorption of insulin. Biol Pharm Bull **16**, 68-72

12 Bendayan, M., Ziv, E., Gingras, D., Ben-Sasson, R., Bar-On, H. and Kidron, M. (1994) Biochemical and morpho-cytochemical evidence for the intestinal absorption of insulin in control and diabetic rats. Comparison between the effectiveness of duodenal and colon mucosa. Diabetologia **37**, 119-126

13 Bai, J. P. and Chang, L. L. (1995) Transepithelial transport of insulin: I. Insulin degradation by insulin-degrading enzyme in small intestinal epithelium. Pharm Res **12**, 1171-1175

14 Foss, A. C., Goto, T., Morishita, M. and Peppas, N. A. (2004) Development of acrylic-based copolymers for oral insulin delivery. Eur J Pharm Biopharm **57**, 163-169

15 Lacaz-Vieira, F. (1997) Calcium site specificity. Early Ca2+-related tight junction events. J Gen Physiol **110**, 727-740

16 Sedar, A. W. and Forte, J. G. (1964) Effects Of Calcium Depletion On The Junctional Complex Between Oxyntic Cells Of Gastric Glands. J Cell Biol **22**, 173-188

17 Gumbiner, B. (1987) Structure, biochemistry, and assembly of epithelial tight junctions. Am J Physiol **253**, C749-758

18 Denker, B. M. and Nigam, S. K. (1998) Molecular structure and assembly of the tight junction. Am J Physiol **274**, F1-9

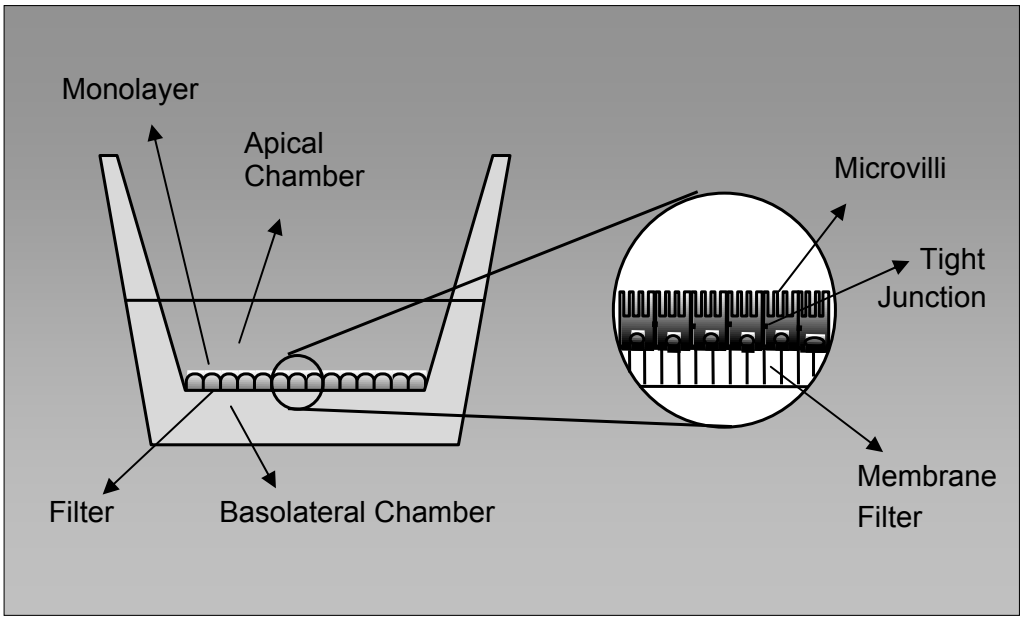

Figure 5.1 Experimental setup for transport studies using Caco-2 cell monolayers. The cells were seeded on the Transwell plates and grown for 21 days to form fully differentiated cell monolayer (adapted from the PhD thesis of Ichikawa Hidehi)

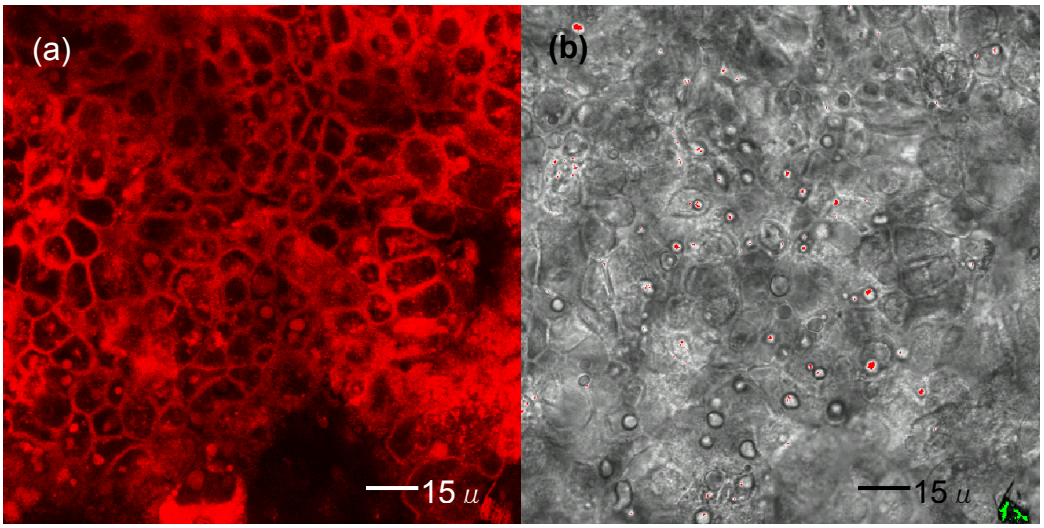

Fig. 5.2 Confocal laser scanning microscopy images of cells incubated with Nile Red dye. The combination of images (X-Y sections) illustrates (a) Nile Red dye (red) labeling the cells, (b) transmission image. The Nile Red dye is seen labeling the paracellular spaces but the dye can also be seen entering the cells

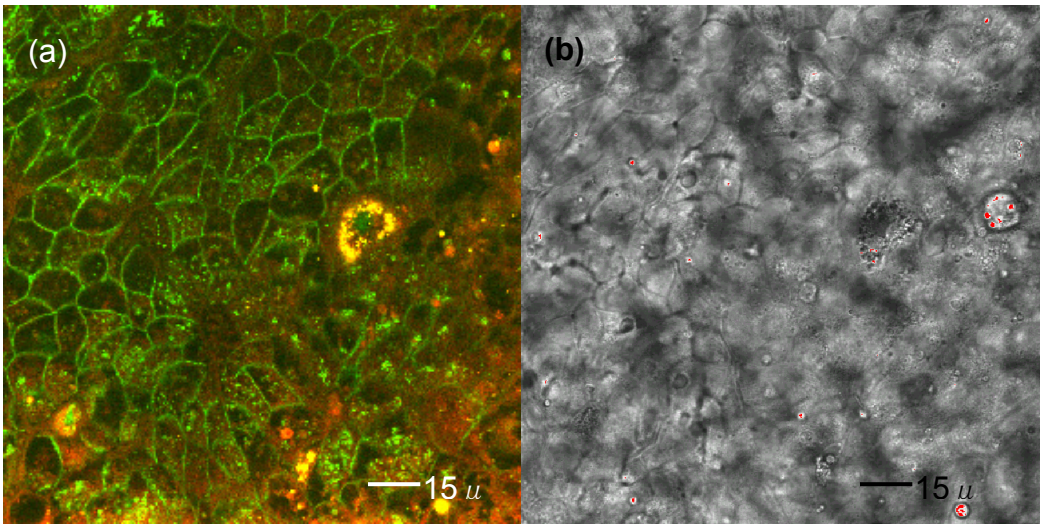

Fig. 5.3 Confocal laser scanning microscopy images cell monolayers with FITC-insulin. The cells were incubated with FITC-insulin without microsphere suspension. The cell monolayer was labeled with Nile Red dye. The combination of images (X-Y sections) illustrates (a) Nile Red dye (red) and FITC-insulin (green) co-labeling the cells, (b) transmission image. The enclosed spaces indicate insulin entering the paracellular spaces and the green dots inside the cells represent insulin uptaken by the cells.

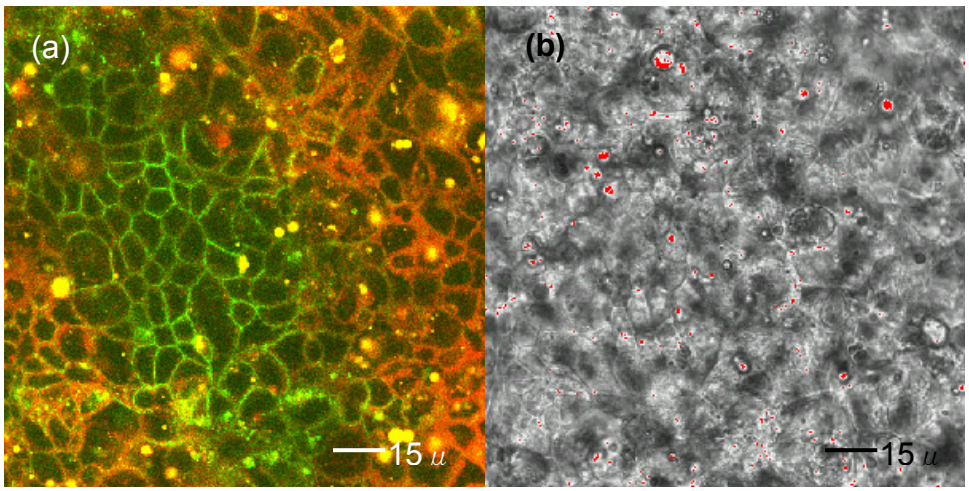

Fig. 5.4 Confocal laser scanning microscopy images cell monolayers with FITC-insulin and microparticles. The cells were incubated with FITC-insulin with microsphere suspension and labeled with Nile Red dye. The combination of images (X-Y sections) illustrates (a) Nile Red dye (red) and FITC-insulin (green) co-labeling the cells, (b) transmission image.

CHAPTER 6

GASTROINTESTINAL DISTRIBUTION AND RETENTION OF POLYMER MICROPARTICLES

6.1 Introduction

One of the most important attributes of the complexation hydrogels used as vehicles for oral delivery is their ability to prolong the residence time of the drug at the site of absorption, e.g., the upper small intestine. The polymer particles can interact favorably with the mucosal layer lining the gut wall and delay direct clearance of the formulation through the GI tract. If the drug is protected from proteolytic digestion in the small intestine, the increase in residence time can significantly enhance the bioavailability of the drug. The objective of this work was to evaluate the mucoadhesive properties of the complexation hydrogels in animal model and to study the GI transit of the polymeric carriers.

Bioadhesion is an interfacial phenomenon in which two materials, at least one of which is biological, are held together by means of interfacial forces [1, 2]. The term ‘mucoadhesion’ refers to the property of bioadhesion exhibited by certain polymers which become adhesive on hydration and hence can be used for targeting a drug to a particular region of the body for extended periods of time [1-3]. Thus, the goal of mucoadhesive drug delivery systems is to increase the

residence time of therapeutic molecules at the specific sites within the GI tract, for absorption of the drug into the circulation [4, 5].

There is a great interest in developing artificial carriers than can enhance the residence time of drug molecules at particular section of the GI tract. In the last few years, a large number of mucoadhesive systems have been developed including superporous hydrogel composite-based systems [6], lipid-based nanocarriers [7], thiolated poly(methacrylic acid)-starch compositions [8], chitosan-based carriers [9-11].

Complexation hydrogels developed in our laboratory are one of the most promising mucoadhesive systems for targeted oral delivery of therapeutic proteins [5]. It is believed that in these systems, PEG tethers attached to the polymer network act as adhesion promoters to enhance the mucoadhesive behavior of the carriers.

The use of adhesion promoters to achieve improved bioadhesion was first proposed by Peppas and co-workers [12-17]. Favorable interactions of the pendent PEG chains in the P(MAA-g-EG) polymer networks with the intestinal mucosa can increase the residence time of the carriers in the GI tract. However, the mucoadhesive characteristics of the hydrogels in the GI tract have not been studied in vivo. Understanding how the polymeric carriers travel through the GI tract and interact with the gastrointestinal mucosa is critical to developing approaches that will further increase the bioavailability of therapeutic proteins delivered orally by the complexation hydrogels. Hence, the objective of this study

was to evaluate the effect of PEG chains on the GI transit profile and retention properties of the complexation hydrogels.

Primarily, two techniques are employed for studying the GI transit profiles of drug carriers, including gamma scintigraphy [18], and radiolabeling of the drug carriers [9]. In this work, we developed a fluorescence spectroscopy-based method for evaluating the GI transit profiles of P(MAA-g-EG) microparticles.

6.2 Materials and Methods

Synthesis and characterization of fluorescently labeled polymer microparticles: Fluorescently labeled microparticles were prepared by incorporating PolyFluor® 407 (Polysciences, Inc. Warrington, PA), a fluorescent monomer (9-Anthracenylmethyl methacrylate; excitation wavelength 362nm, emission wavelength 407nm), into the polymer network during the polymerization reaction.

Polymer films were prepared by UV-initiated free radical solution polymerization of methacrylic acid (MAA) (Aldrich Chemical Company, Milwaukee, WI) and poly(ethylene glycol) ether monomethacrylate (PEGMA) (Polysciences, Inc. Warrington, PA). PEGMA was used as received whereas MAA was vacuum distilled at 47°C/25 mmHg to remove the inhibitor hydroquinone monomethyl ether.

The monomers were mixed in the molar ratio of 1:1 or 1:0 (MAA:EG). PEGMA with PEG molecular weight of 1000 was used in this synthesis. The

fluorescent monomer was added in 0.1 mol% of the total monomer Tetra(ethylene glycol) dimethacrylate (TEGDMA) (Polysciences, Inc. Warrington, PA) was used as the crosslinking agent and was added in the amount of 0.75 % moles of the total amount of monomers. The photoinitiator, Irgacure-184 (Ciba-Geigy Co. Hawthorne, NY) was added in the amount of 0.1wt % of the total amount of monomers.

To inhibit autoacceleration in the polymerization reaction, monomer mixture was diluted with a mixture of 50 % v/v ethanol and deionized water (Milli-Q Plus system, Millipore). Oxygen dissolved in the monomer mixture, which acts as free radical scavenger was removed by bubbling the monomer solution with nitrogen for 25 minutes. The mixture was then pipetted into glass plates (75 x 50 x 1 mm) (Fisher, Pittsburgh PA) separated by Teflon spacers with a thickness of 0.9 mm. The polymerization was carried out by exposing the glass plates containing the monomer mixture to a UV light (16 mW/cm^2 at 365 nm) under nitrogen environment for 30 minutes. After the completion of the reaction, the polymer films were washed in deionized water for approximately 7 days in order to remove unreacted monomers, crosslinking agent, initiator and sol fraction. The polymer films were protected from light during the washing step. After washing the polymer films were dried at room temperature for a day and then placed in a vacuum oven at 27 °C for 2 days. The dry polymer films were then crushed by using a mortar and pestle and then sieved to <53 μm. All the particles were stored in dark in closed 5 ml glass vials inside a desiccator until further use.

The labeled microparticles were compared with the control microparticles (no fluorescent monomer), by fluorescent microscopy. Both the control and the labeled microparticles were analyzed with a fluorescent microscope (Eclipse 600, Nikon Corporation, Tokyo, Japan) with a 5 x objective. The exposure time was 100 msec for the labeled particles and 1000 msec for the control particles. Figure 6.2 shows the comparison of the control and labeled particles.

Distribution of the labeled microparticles in the GI tract: Male Wistar rats (180-200 g) were fasted for 48 hours before the experiment with free access to water. During the experimental period, the rats were housed in cages and given water ad libitum. The rats were restrained in a supine position during administration without anesthesia. 50 mg of the labeled microparticles suspended in 2 mL phosphate-buffered saline (PBS, pH=7.4) were administered orally using a sonde needle. The rats were sacrificed by sodium pentobarbital overdose at 10 min, 0.5, 1, 2, 4, and 8 h after the administration of the microparticles and the abdomen was cut open along the median line. The stomach, small intestine and colon were excised and the small intestine was further divided into five equal segments. Each segment was opened lengthwise and the mucus was collected. The collected samples were added to 0.01 wt% sodium deoxycholate solution in PBS to dissolve the mucus. Fluorescence associated with the samples due to the hydrogels was measured by a fluorescence spectrophotometer at excitation wavelength of 355 nm and emission wavelength of 410 nm.

GI Retention of the polymer microparticles: The mucoadhesion of the fluorescent microparticles was evaluated by in situ loop method. The mucoadhesion was measured in stomach and the duodenum. Male Wistar rats (180-200 g) were fasted for 24 hours before the experiment. The rats were anaesthetised by intraperitoneal administration of 50 mg/kg sodium pentobarbital and rested in supine position. The particle suspension as prepared by adding the microparticles to PBS solution. The abdomen was opened along the median line and the stomach and the duodenum (10 cm intestinal segment from the pylorus), were ligated after insertion of tubings for administration of the particle suspension. After 5 min, the stomach was perfused with HCl-KCl buffer and the duodenum was perfused with PBS buffer at approximately 1 ml/min for 10 min. The buffers used for perfusion were prewarmed at 37 ^{o}C. The fluorescence in the perfusate was measured as described above. The percent of particles retained due to mucoadhesion, R_m was defined as:

$$R_m\,(\%) = \frac{\text{Dosing amount (mg)} - \text{Amount of unadhered microparticles (mg)}}{\text{Dosing amount (mg)}} \times 100 \qquad (6.1)$$

6.3 Results and Discussion

In this work, the GI retention properties of the complexation hydrogels were characterized. Specifically, the effect of PEG chains on the GI transit profile and the retention of the the polymeric carriers was studied. The property of the PEG containing polymer networks to adhere to the mucus has been extensively studied in our laboratory. De Ascentiis et al. [13] showed that the mucoadhesive properties of poly(2-hydroxyethyl methacrylate) (PHEMA) was significantly increased due to the incorporation of poly(ethylene oxide) into the network. In this work, the adhesion of the PHEMA microspheres to the jejunal section of Sprague-Dawley rats was shown to double due to the incorporation of the PEO chains in the microspheres. The increased adhesion was attributed to a significant increase of the PEO chains penetrating across the mucosal tissue.

Huang et al. [16] compared the work of adhesion for P(MAA-g-EG) polymer gel containing 1:1 molar ratio of MAA:EG and gelled bovine submaxillary gland mucin. The work of adhesion was significantly higher at pH 7.4 compared to pH3.2. It was concluded that the increased adhesion of the polymer gel was primarily due to the interaction between the PEG chains and the mucus and not due to the hydrogen bonding by the carboxyl groups.

In this work, we analyzed the GI transit profiles of PMMA microparticles with the P(MAA-g-EG) microparticles containing 1:1 molar ratio of MAA:EG. The GI retention of these formulations was also evaluated by in situ closed loop

method. To visualize the transit of microparticles through the GI tract in animal model, the particles were labeled using a fluorescent monomer (Figure 6.1). Figure 6.2 shows the comparison of labeled and control microparticles. As seen from these images, the fluorescent monomer was uniformly distributed in the polymer particles enabling quantitative determination of the microparticles.

Figure 6.3 and 6.4 show GI transit profiles of the microparticles containing 1:1 and 1:0 ratio of MAA/EG microparticles. The results are summarized in Table 6.1. The crosslinked PMAA hydrogel microparticles (1:0 ratio of MAA:EG) immediately passed through the stomach and reached the distal small intestine. In contrast, the P(MAA-g-EG) microparticles containing (1:1 ratio of MAA:EG) remained in the stomach for extended period and transited slowly to the distal part of the small intestine. The gastric emptying rate following administration of P(MAA-g-EG)(1:1 MAA:EG) hydrogel microparticles was lower than that of PMAA microparticles. These results indicated that the molar ratio of P(MAA-g-EG) affected the GI transit profile.

To further understand the reasons behind the increased transit time of the particles containing 1:1 molar ratio of MAA:EG particles in the gastric environment, we evaluated the retention of the particles by in situ closed loop technique. In this technique, a specific section of the GI tract is isolated and the experiments are performed in that segment. Labeled microparticles were directly administered into the isolated stomach and the duodenum segments, and after 5 minutes the non-adherent microparticles were removed by perfusion with buffer

solutions. The retention of the particles, R_m, defined here as the percentage of the microparticles adhering to the GI segment after perfusion, was calculated for 1:1 and 1:0 MAA:EG microparticles. These results are shown in Figure 6.5. The polymer microparticles containing 1:1 molar ratio of MAA:EG had higher value of R_m compared to the crosslinked PMMA microparticles. Interestingly this increase in the mucoadhesiveness due to the presence of the PEG chains was seen in both stomach and in the small intestine.

The exact reasons for this enhanced retention are unclear. One of the reasons could be that in these studies, the microparticles were administered as a suspension in a 2 ml PBS buffer. Although the time between addition of the microparticles to the buffer and the administration of the suspension was minimal (2-5 min), some of the particles in the suspension may have been pre-swollen. The PEG chains in these pre-swollen microparticles could interact with the gastric mucosa, thus increasing the retention of the microparticles. This seems to be the most probable reason for the enhancement in mucoadhesiveness due to the presence of the PEG chains.

The observed phenomenon may also be explained from the analysis of the complexation behavior of the 1:1 MAA:EG hydrogels under low pH conditions. The degree of complexation (β) in these hydrogels was defined by Lowman and Peppas [19] as the number repeating units of the graft chain participating in the complexes divided by the total number of backbone units in the material. The number of backbone units in the materials is the number of

methacrylic acid (MAA) units and the number of graft chain units is defined as the number of ethylene glycol (EG) repeating units. By definition the value of β can be between 0 and 1. For the polymer containing 1:1 molar ratio of MAA:EG, the maximum possible value of β (β_{max}) is 1. By performing small deformation test measurements, Lowman and Peppas [19] experimentally determined the value of β_{max} to be 0.21 at pH 3.0. This means that in even at the low pH of the stomach, some of the PEG chains in the network are free to interact with the mucus and can potentially increase the mucoadhesiveness of the formulation.

More importantly, the PEG chains increased the mucoadhesiveness of the microparticles at the near neutral pH of the small intestine. This is very important since it implies that the polymer carriers can increase the residence time of the loaded protein in the upper section of the intestine, which is the targeted site for absorption. The problem of mucoadhesiveness of the particles in the stomach can be addressed by placing the protein loaded particles inside a capsule covered with coatings that dissolve at the pH of the small intestine [20-22]. This would release the protein carriers directly into the upper small intestine where the particles can enhance the residence time of the formulation.

6.4 Conclusions

In this work, we demonstrated the ability of the PEG chains in the complexation hydrogels to enhance the retention of the particles in the GI tract.

The PEG chains were shown to affect the GI transit profiles of the hydrogels by improving their retention capacity. This property of the carriers is highly desired in the oral delivery applications, since increasing the residence time of therapeutic protein at the targeted site of absorption can significantly improve the fraction of orally administered protein that reaches the blood circulation. Further, if the carriers are able to interact with the intestinal mucosa, and provide a burst release of the protein, high local concentrations of the drug may be achieved in the microenvironment of the brush border. This can improve the protein bioavailability in two ways. First, the high concentration gradient across the epithelium can drive the protein across the cellular barrier. Secondly, the protein molecules released in the microenvironment of the brush border may be protected from degradation due to luminal enzymes such as trypsin and chymotrypsin.

References

1 Chowdary, K. P. and Rao, Y. S. (2004) Mucoadhesive microspheres for controlled drug delivery. Biol Pharm Bull **27**, 1717-1724

2 Chowdary, K. P. and Rao, Y. S. (2003) Design and in vitro and in vivo evaluation of mucoadhesive microcapsules of glipizide for oral controlled release: a technical note. AAPS PharmSciTech **4**, E39

3 Miyazaki, Y., Ogihara, K., Yakou, S., Nagai, T. and Takayama, K. (2003) In vitro and in vivo evaluation of mucoadhesive microspheres consisting of dextran derivatives and cellulose acetate butyrate. Int J Pharm **258**, 21-29

4 Peppas, N. A., Lowman, A. M. (1998) Protein Delivery from Novel Bioadhesive Complexation Hydrogels. In Protein and Peptide Drug Research (Frøkjær, S., Christup, L., Krogsgaard-Larsen, P., ed.), pp. 206-216, Munksgaard, Copenhagen

5 Peppas, N. A. (2004) Devices based on intelligent biopolymers for oral protein delivery. Int J Pharm **277**, 11-17

6 Dorkoosh, F. A., Stokkel, M. P., Blok, D., Borchard, G., Rafiee-Tehrani, M., Verhoef, J. C. and Junginger, H. E. (2004) Feasibility study on the retention of superporous hydrogel composite polymer in the intestinal tract of man using scintigraphy. J Control Release **99**, 199-206

7 Lamprecht, A., Saumet, J. L., Roux, J. and Benoit, J. P. (2004) Lipid nanocarriers as drug delivery system for ibuprofen in pain treatment. Int J Pharm **278**, 407-414

8 Bernkop-Schnurch, A., Konig, V., Leitner, V. M., Krauland, A. H. and Brodnik, I. (2004) Preparation and characterisation of thiolated poly(methacrylic acid)-starch compositions. Eur J Pharm Biopharm **57**, 219-224

9 Torrado, S., Prada, P., de la Torre, P. M. and Torrado, S. (2004) Chitosan-poly(acrylic) acid polyionic complex: in vivo study to demonstrate prolonged gastric retention. Biomaterials **25**, 917-923

10 de la Torre, P. M., Torrado, G. and Torrado, S. (2005) Poly (acrylic acid) chitosan interpolymer complexes for stomach controlled antibiotic delivery. J Biomed Mater Res B Appl Biomater **72**, 191-197

11 de la Torre, P. M., Enobakhare, Y., Torrado, G. and Torrado, S. (2003) Release of amoxicillin from polyionic complexes of chitosan and poly(acrylic acid). Study of polymer/polymer and polymer/drug interactions within the network structure. Biomaterials **24**, 1499-1506

12 De Ascentiis, A., Bettini, R., Colombo, P. and Peppas, N. A. (1996) [Mucoadhesive properties of hydrophilic polymer microparticles]. Boll Chim Farm **135**, 101-103

13 DeAscentiis, A., de Grazia, J. L., Bowman, C. N., Colombo, P. and Peppas, N. A. (1995) Mucoadhesion of poly(2-hydroxyethyl methacrylate) is improved when linear poly(ethylene oxide) chains are added to the polymer network. J Control Rel **33**, 197-201

14 DeAscentiis, A., Colombo, P. and Peppas, N. A. (1995) Screening of potentially mucoadhesive polymer microparticles in contact with rat intestinal mucosa. J Pharmacol Biopharmacol **41**, 229-334

15 Sahlin, J. J. and Peppas, N. A. (1997) Enhanced hydrogel adhesion by polymer interdiffusion: use of linear poly(ethylene glycol) as an adhesion promoter. J Biomater Sci Polym Ed **8**, 421-436

16 Huang, Y., Leobandung, W., Foss, A. and Peppas, N. A. (2000) Molecular aspects of muco- and bioadhesion: tethered structures and site-specific surfaces. J Control Rel **65**, 63-71

17 Peppas, N. A., Huang, Y., Torres-Lugo, M., Ward, J. H. and Zhang, J. (2000) Physicochemical foundations and structural design of hydrogels in medicine and biology. Annu Rev Biomed Eng **2**, 9-29

18 Sato, Y., Kawashima, Y., Takeuchi, H., Yamamoto, H. and Fujibayashi, Y. (2004) Pharmacoscintigraphic evaluation of riboflavin-containing microballoons for a floating controlled drug delivery system in healthy humans. J Control Rel **98**, 75-85

19 Lowman, A. M. and Peppas, N. A. (1997) Analysis of the Complexation/Decomplexation Phenomena in Graft Copolymer Networks. Macromolecules **30**, 4959 -4965

20 Palmieri, G. F., Michelini, S., Di Martino, P. and Martelli, S. (2000) Polymers with pH-dependent solubility: possibility of use in the formulation of gastroresistant and controlled-release matrix tablets. Drug Dev Ind Pharm **26**, 837-845

21 Gupta, V. K., Beckert, T. E. and Price, J. C. (2001) A novel pH- and time-based multi-unit potential colonic drug delivery system. I. Development. Int J Pharm **213**, 83-91

22 Gupta, V. K., Assmus, M. W., Beckert, T. E. and Price, J. C. (2001) A novel pH- and time-based multi-unit potential colonic drug delivery system. II. Optimization of multiple response variables. Int J Pharm **213**, 93-102

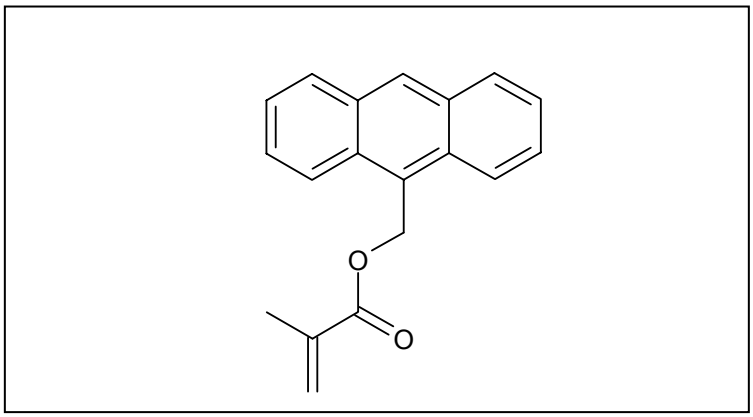

Figure 6.1 9-anthracenylmethyl methacrylate (PolyFluor ® 407); a fluorescent monomer that was used to label the P(MAA-g-EG) microparticles. The monomer was added to the monomer mixture at 0.1 mol% and polymerized by UV free radical polymerization.

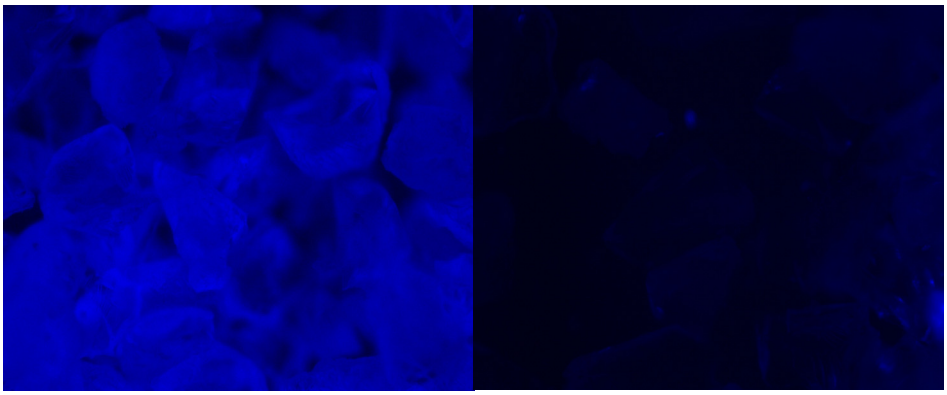

Figure 6.2 Comparison of the fluorescently labeled microparticles with the control particles. P(MAA-g-EG) microparticles containing 1:1 MAA:EG microparticles were labeled with 9-anthracenylmethyl methacrylate (PolyFluor ® 407) and sieved to 150-212 μm. (a) Labeled P(MAA-g-EG) microparticles: 150-212 μm, 5X, exposure time 100 ms; (b) Unlabeled P(MAA-g-EG) microparticles: 150-212 μm, 5 X, exposure time 1000 ms. The fluorescent images were obtained with a fluorescent microscope.

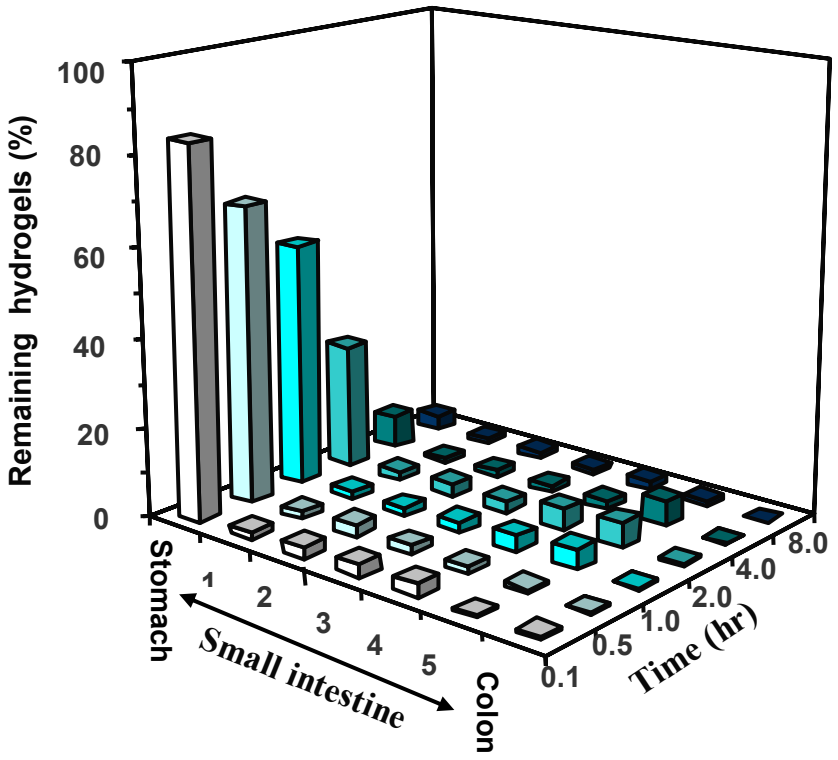

Figure 6.3 GI transit profile of the P(MAA-g-EG) 1:1 MAA:EG microparticles. The z-axis shows microparticles remaining in the segments of GI tract (x-axis) as a percentage of microparticles administered orally. 50 mg of the fluorescently labeled microparticles (<53 μm) were administered orally via a sonde needle and the animals were sacrificed at different time intervals (y-axis). The small intestine was divided into 5 segments of equal length. The mucus was removed from the segments of the GI tract and dissolved in 0.1 wt% sodium deoxycholate solution in PBS. Fluorescence associated with the samples was measured by fluorescence spectrophotometer at excitation wavelength of 355 nm and emission wavelength of 410 nm. Each value represents mean of three values.

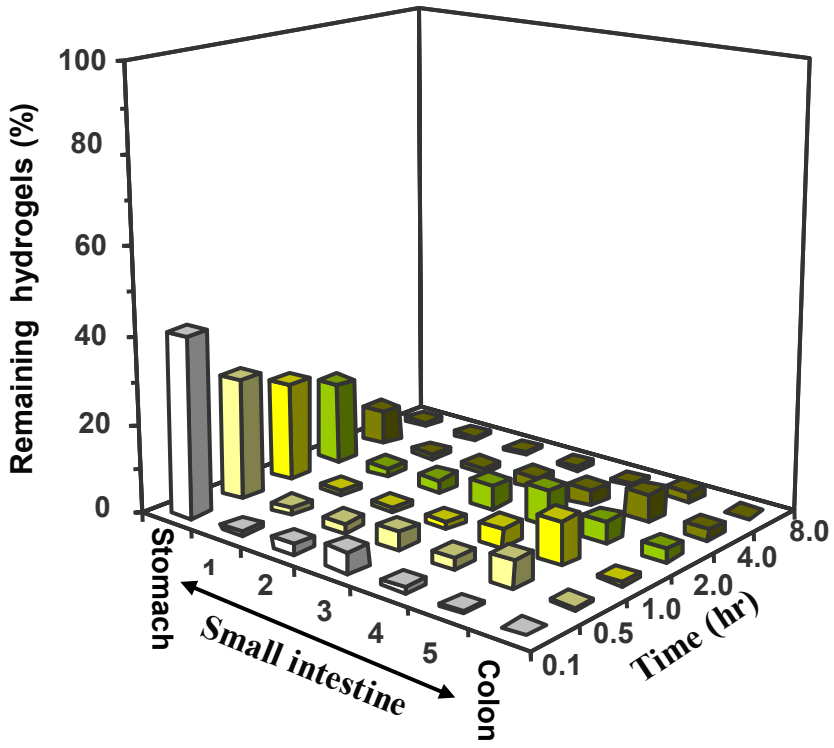

Figure 6.4 GI transit profile of the P(MAA-g-EG) 1:0 MAA:EG microparticles. The z-axis shows microparticles remaining in the segments of GI tract (x-axis) as a percentage of microparticles administered orally. 50 mg of the fluorescently labeled microparticles (<53 μm) were administered orally via a sonde needle and the animals were sacrificed at different time intervals (y-axis). The mucus was removed from the segments of the GI tract and dissolved in 0.1 wt% sodium deoxycholate solution in PBS. Fluorescence associated with the samples was measured by fluorescence spectrophotometer at excitation wavelength of 355 nm and emission wavelength of 410 nm. Each value represents mean of three values.

Table 6.1 Gastrointestinal distribution of fluorescently labeled P(MAA-g-EG) (MAA :EG 1:1, and 1:0) microparticles. Particles present in the stomach, small intestine and the colon are expressed as a percentage of total particles recovered in the GI tract. The rats were sacrificed at 0.5, 1, 2, 4, 8 hours after the oral administration.

	P(MAA-g-EG) 1:1 MAA:EG particles			**P(MAA-g-EG) 1:0 MAA:EG particles**		
	Stomach	Small Intestine	Colon	Stomach	Small Intestine	Colon
0.5hr	88.5 ±3.25	11.3 ±0.19	0.83 ±0.14	26.3 ±2.3	29.1 ±1.7	1.1 ±2.6
1hr	79.2 ±6.57	20.3 ±1.93	0.90 ±0.16	20.9 ±3.2	36.2 ±3.7	2.1 ±0.4
2hr	60.6 ±6.71	38.4 ±2.77	0.97 ±0.12	18.4 ±4.1	42.8 ±3.2	4.5 ±1.0
4hr	39.0 ±2.21	60.3 ±2.50	0.73 ±0.14	8.9 ±1.1	29.4 ±2.5	4.3 ±1.0
8hr	32.5 ±1.00	66.0 ±1.06	1.5 ±0.09	1.3 ±0.7	10.4 ±1.3	0 ±0.4

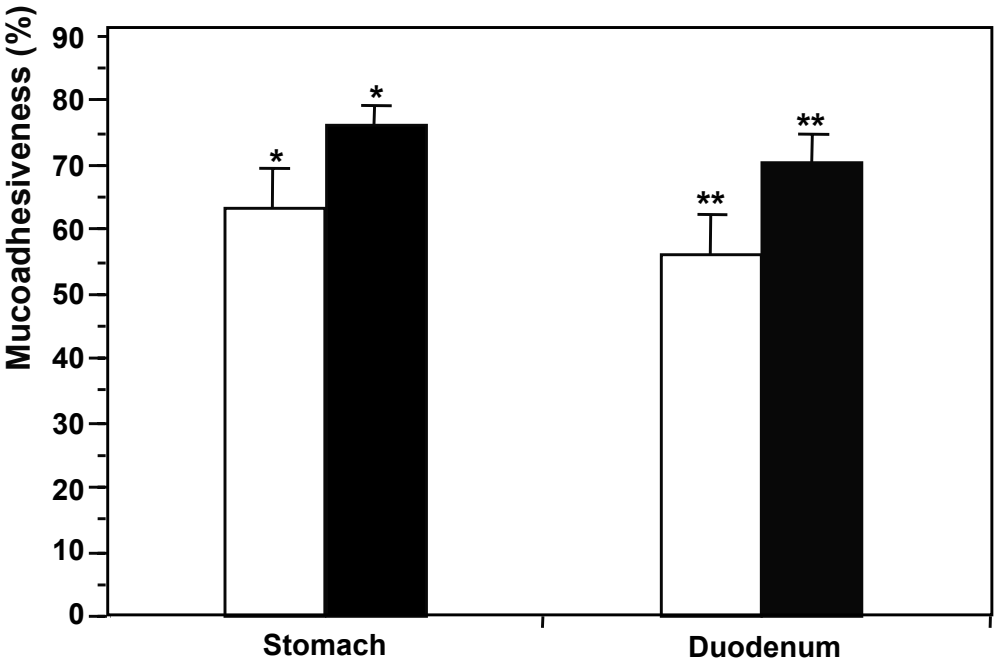

Figure 6.5 Retention of the fluorescently labeled microparticles in the stomach and the duodenum. 50 mg of the fluorescently labeled microparticles (<53 μm) suspended in PBS were administered directly to the stomach or the duodenum and the non-adherent microparticles were washed after 5 min by perfusion HCl-KCl buffer or PBS buffer, respectively. Fluorescence of the perfusate buffers was measured and retention of the particles was calculated (Eg 6.1). P(MAA-g-EG) microparticles with 1:1 MAA:EG (black) were compared with 1:0 (MAA:EG) (white) Error bars represent one standard deviation (n=3). Statistical difference: **, * $p<0.05$.

CHAPTER 7

INSULIN PROTECTION BY COMPLEXATION HYDROGELS IN THE GI TRACT

7.1 Introduction

One of the most desirable characteristics of the complexation hydrogels that make them excellent carriers for oral delivery of proteins is their ability to protect the protein drugs from proteolytic attack during their transit through the GI tract. In the absence of any mechanism to prevent protein digestion in the GI tract, the bioavailability of orally administered therapeutic proteins is typically low [1, 2]. It was the object of this study to evaluate the protection of insulin by the complexation hydrogels in the gastric and intestinal environment.

The complexation hydrogels exhibit pH-dependent swelling behavior due to the formation/dissociation of interpolymer complexes [3-5]. The interpolymeric hydrogen-bonding complexes between etheric groups of the graft PEG chains and the acid protons of the PMAA network at low pH result in low mesh size of the network. The low mesh size severely limits the diffusion of drug into the gastric environment, and the drug is protected within the network structure. On exposure to the near-neutral pH environment of the intestine, the network swells to a high degree and results in burst release of the entrapped drug. In the neutral environment of the small intestine, ionized carboxylic acid groups of PMAA can bind free Ca^{2+}. Therefore, the acidic groups in the polymeric network may

contribute to depletion of free calcium. Madsen and Peppas [6] showed that the complexation hydrogels can bind calcium at the pH of the small intestine and inhibit the activity of the calcium-dependent intestinal enzymes.

In previous studies, the oral administration of insulin-loaded P(MAA-g-EG) hydrogels demonstrated significant insulin absorption and glucose reduction in healthy and diabetic rats [7-9]. This implies that P(MAA-g-EG) hydrogels have a direct mucosal absorption enhancing effect on insulin. However, the precise mechanisms behind the improvement in oral insulin bioavailability have not been fully elucidated. Therefore, the aim of this study was to evaluate the ability of P(MAA-g-EG) hydrogels to protect the incorporated insulin from proteolytic degradation in the gastric and intestinal enzyme fluids obtained from Wistar rats. Understanding the mechanisms by which the hydrogel carriers can prevent insulin from getting degraded in the GI tract can help in formulating strategies to improve the oral bioavailability of insulin using complexation hydrogels. Polymers networks with three different compositions were used in this study: polymers with the initial monomer feed ratio of 1:1 for MAA:EG (designated henceforth as 1:1 MAA:EG polymer), polymers with the initial monomer feed ratio of 4:1 for MAA:EG (designated henceforth as 4:1 MAA:EG polymer) and polymers with the initial monomer feed ratio of 1:0 for MAA:EG (designated as 1:0 MAA:EG polymer. This was done to understand the mechanisms by which the polymer networks protect insulin from gastric and intestinal degradation

7.2 Materials and Methods

Preparation of Polymer Microparticles: P(MAA-g-EG) hydrogels prepared by free radical solution UV-polymerization of methacrylic acid (MAA) (Sigma, St. Louis, MO)and poly(ethylene glycol) ether monomethacrylate (PEGMA) with PEG molecular weight of 1000 (Polysciences, Warrington, PA). Tetra(ethylene glycol) dimethacrylate (TEGDMA) (Polysciences, Warrington, PA) was added at 1 mol% of the total monomer and 2 wt % of 2,2-dimethoxy-2-phenyl acetophenone (DMPA) was used as the initiator (Sigma-Aldrich, Chemie, Steinheim, Germany).

The copolymers were synthesized with the monomer feed ratio of 1:1, 4:1 and 1:0 MAA:EG. Nitrogen was bubbled through the solution for 30 min to remove dissolved oxygen. The monomer mixture was pipetted between two glass plates separated by 0.9 mm Teflon spacers and the plates were exposed to UV light at 1mW/cm^2 for 30 minutes. After the completion of the reaction, the polymer film was washed in deionized water for 7 days to remove unreacted monomer. All the copolymers were crushed and sieved to < 53 μm sizes after drying.

Insulin Loading of Polymer Microparticles: Recombinant human insulin (26 IU/ mg) (Wako Pure Chemical, Osaka, Japan) was incorporated into the polymer particles by equilibrium partitioning. 140 mg of polymer microparticles (1:1, 4:1, and 1:0) were added to 20 ml of PBS containing specific amount of insulin. The mixture was stirred for 2 hours at 37 ^{0}C. The particles were then collapsed by

addition of 20 ml of 0.1N HCl and were allowed to equilibrate for 5 min. The loading mixture was then filtered through 1.0 μm pore size filter (47 mm; Advantec, Japan) and washed with 10 ml DI water. The particles were dried under vacuum and stored at 4 ^{o}C until further use. All the insulin loaded microparticles (ILPs) were loaded so as to contain 60 μg insulin in 1 mg ILP. The loading efficiency was determined by measuring the concentration of insulin before and after the loading procedure by HPLC. Each sample was directly injected into a HPLC system composed of a pump (LC-10AS, Shimadzu Co. Ltd., Kyoto, Japan), a UV detector (SPD-10AV, Shimadzu), an integrator (C-R3A, Shimadzu) and a GL-PACK Nucleosil 100-5C_{18} column (150 x4.6 mm i.d.). The mobile phase was acetonitrile-0.1% trifluoroacetic acid in deionized water–sodium chloride (31:69:0.58, v/v/w). The flow rate was 1.2 ml/min and the peaks were detected at 220 nm. The loading efficiency was calculated as:

$$Partitioning\ efficiency\ = \frac{C_i - C_0}{C_i} \times 100 \qquad \ldots(6.1)$$

Here C_i was the concentration of insulin in solution before the loading study and C_o was the concentration of insulin in solution after the loading study.

Preparation of the gastric and intestinal fluids: Male Wistar rats weighing 200-300g were fasted for 24 hours and anesthetized by intraperitoneal administration of 50 mg/kg sodium pentobarbital. The rats were secured to the operating table

in a supine position and midline abdominal incision was performed. The pylorus and the cardia were clamped. The stomach was then excised and washed with saline water. A sonde needle was carefully inserted into the stomach from the pylorus and 2.5 ml HCl-KCl buffer (pH 1.2) was injected into the stomach. The contents of the stomach were mixed by shaking and the gastric fluid was withdrawn. This procedure was repeated two times so that 5 ml of the gastric fluid solution was obtained. The gastric fluid solution thus obtained was centrifuged at 3000 r.p.m. at 4 ^{0}C for 15 minutes. The total protein concentration of the purified gastric fluid was determined (Protein Quantification Kit, Dojindo Molecular Technologies, Inc. Gaithersburg, MD USA), since the enzyme concentration itself cannot be easily determined.

To remove the intestinal fluid, a sonde needle was inserted into the upper portion of the small intestine and the intestine was cannulated on the lower side to remove the intestinal fluid. 20 ml PBS buffer (pH 7.4) was slowly injected through the sonde needle and the intestinal fluid solution was collected from the cannula. The collected fluid was centrifuged at 3000 r.p.m. at 4 ^{0}C for 15 minutes. The intestinal fluid has high lipid contents which may interfere with the HPLC analysis of insulin. Hence this efflux was treated with two volumes of methylene chloride to remove the lipids. Two volumes of methylene chloride were mixed with the intestinal fluid and shaken vigorously for 1 minute. Following this, the mixture was centrifuged at 3000 r.p.m. for 5 minutes and the intestinal fluid was separated. The purification step was repeated 4 times [10]. In case of

the gastric fluid the lipid content is very low so this step was not necessary. The total protein concentration of the purified intestinal fluid was determined using the Protein Quantification Kit. To compare the results from different sets of insulin degradation studies, the concentration of the gastric or intestinal enzyme fluid was adjusted so that 50% of the initial insulin degraded in 30 min. For protein binding study and calcium deprivation study, the intestinal fluid was diluted with PBS to yield a protein concentration of 400-500 μg/ml as determined by the Protein Quantification.

7.2.1 Gastric Degradation of Insulin

Two sets of studies were performed to analyze the effect of polymer particles on insulin degradation by the gastric fluid. The ability of the insulin-loaded microparticles to protect the entrapped insulin was evaluated. In the second set of studies, the effect of polymer composition on the protease inhibition activity of the polymer particles was analyzed by studying the degradation of insulin in the presence of the microparticles.

Protection of entrapped insulin in gastric fluid by the complexation hydrogels: 2 ml of the gastric enzyme solution was incubated for 15 min at 37 ^{0}C. 10 mg of insulin-loaded polymer particles was added to the enzyme solution and the mixture was incubated for 1 h. Following incubation, the solution was centrifuged at 3000 r.p.m. for 5 min and the supernatant was removed to separate the particles. 40 ml PBS (pH 7.0) was then added to the particles and the total

amount of insulin released from the microparticles in 3 hours was measured by HPLC. For the control experiments, the amount of insulin equal to the amount incorporated in ILPs, was exposed to 2 ml of gastric fluid at 37 ^{0}C for 1 h.

Protease inhibition by the complexation hydrogels: 1900 µL of the gastric solution was incubated for 37 ^{0}C for 15 minutes. P(MAA-g-EG) microparticles (MAA:EG = 1:1, 4:1, 1:0) were added to the enzyme solution and immediately after the addition of microparticles, 100µl insulin solution (4 mg/ml) was added to this solution. Samples of 50 µl were withdrawn at predetermined time intervals after addition of the insulin solution. The enzyme activity in the withdrawn samples was completely inhibited by addition of 50µL of ice-cold acetonitrile solution (acetonitrile: 0.1 % trifluoroacetic acid (TFA): urea=31:69:0.16, v/v/w). The samples were then analyzed by HPLC to determine the amount of insulin remaining in the solution at different time intervals. Insulin remaining as a percentage of the initial insulin present in the solution was plotted against time and compared with the control (no polymer). The degradation rate was determined from the slope of the semi log plot of percentage insulin remaining plotted against time.

7.2.2 Intestinal Degradation of Insulin

In this study, insulin degradation in the intestinal fluid treated with polymer microparticles was evaluated. The ability of the insulin-loaded microparticles to protect the insulin released in the intestinal fluid solution was also analyzed.

Insulin-loaded polymer microparticles with 1:1, 4:1 and 1:0 MAA:EG, were used in these experiments. Further, the calcium binding and protein binding of the complexation hydrogels in the intestinal fluid solution was also studied.

Insulin degradation by polymer-treated intestinal fluid: 2 ml of the intestinal fluid was incubated at 37 ^{0}C for 15 min. 10 mg of P(MAA-g-EG) microparticles (1:1, 4:1, 1:0 MAA:EG) or Carbopol 934P were added to the fluid and incubated at 37 ^{0}C for 1 h. Following incubation, the particles were separated by centrifugation at 3000 rpm for 5 min and supernatant was collected. The pH of the fluid was adjusted to 7.4, and insulin solution was added, which contained 2 mg/ml insulin. At predetermined time points up to 30 min, 50 µl of samples were withdrawn from the incubation mixture. The samples were analyzed after adding 50 µl of ice-cold acetonitrile solutin (acetonitrile: 0.1 % TFA=31:69, v/v) to terminate the reaction.

Protein binding by the hydrogels in the intestinal fluid: 2 ml of the intestinal fluid was incubated at 37 ^{0}C for 15 min. 10 mg of P(MAA-g-EG) microparticles (1:1, 4:1, 1:0 MAA:EG) or Carbopol 934P were added to the fluid and incubated at 37 ^{0}C for 1 h. The concentration of protein in the fluid was then determined by the Protein Quantification Kit.

Calcium binding by the hydrogels in the intestinal fluid: 2 ml of the intestinal fluid was incubated at 37 ^{0}C for 15 min. 10 mg of P(MAA-g-EG) microparticles (1:1, 4:1, 1:0 MAA:EG) or Carbopol 934P were added to the intestinal fluid and incubated at 37 ^{0}C for 1 h. The concentration of calcium in the fluid was determined using Calcium test kit (Wako, Japan).

Degradation of insulin released from the microparticles in the intestinal fluid: P(MAA-g-EG) microparticles with 1:1, 4:1 and 1:0 MAA:EG typically have different loading efficiencies. Hence, the loading efficiencies of the microparticles were adjusted by changing the initial insulin concentration of the loading solution such that all the compositions tested released the same amount of insulin under the experimental conditions. This step was necessary to compare the enzyme inhibitory effect of the three different polymer formulations studied.

A sample of 20 ml of the intestinal enzyme solution was incubated for 15 minutes at 37 ^{0}C. Insulin-loaded particles (10 mg) were added to the enzyme solution and 50 μL samples were withdrawn at predetermined time intervals up to 60 min. After adding 50 μl of ice-cold acetonitrile solutin (acetonitrile: 0.1 % TFA=31:69, v/v) to terminate the reaction, the samples were analyzed by HPLC. The fractional release of insulin from ILPs, defined as the ratio of the amount released at any time, M_t, to the total amount of insulin released after 1 h, M_∞, was calculated.

Additionally, 20 ml of the intestinal fluid containing 0.01 mmol Ca^{2+} was incubated at 37 ^{0}C for 15 min. 10 mg of ILPs (MAA:EG=1:1) were added to the fluid and incubated at 37 ^{0}C. At predetermined time points up to 60 min, 50 μl of samples were withdrawn from the incubation mixture. After adding 50 μl of ice-cold acetonitrile solution (acetonitrile: 0.1 % TFA=31:69, v/v), the samples were then analyzed by HPLC.

Statistical analysis: Each value was expressed as the mean ± S.D. For group comparisons, the one-way layout ANOVA with duplication was applied. Significant differences in the mean values were evaluated by the Student's unpaired *t*-test. A *p* value of less than 0.05 was considered significant.

7.3 Results and Discussion

7.3.1 Insulin protection in gastric fluid by the hydrogels

By using the gastric and intestinal fluids directly extracted from rats, we were able to evaluate the ability of the polymeric carrier to protect insulin under conditions similar to those in the GI environment. To understand the mechanisms of insulin protection in the gastric fluid, and further the effect of polymer composition on the insulin protection ability of the network, we studied (i) the degradation of insulin entrapped inside the polymer particles by the gastric enzymes, and (ii) the direct inhibition of the proteolytic activity in the gastric fluid by the polymer carriers.

7.3.1.1 Protection of the entrapped insulin by complexation hydrogels

In order to examine the insulin protection ability of the complexation hydrogels in the harsh environment of the stomach, the native insulin and ILP were treated with the gastric fluid. After the treatment in gastric fluid, insulin

remaining inside the particles was measured. The results are shown in Figure 7.1 for hydrogels with different molar ratios of MAA and EG repeating units.

The unprotected insulin in the control experiment was rapidly degraded in the gastric fluid and only 20 % of the insulin remained after 1 h. In contrast, more than 80 % of the insulin remained undegraded in all the three ILPs. It is evident that all the three hydrogel compositions were effective in protecting the entrapped insulin from enzymatic degradation. Morishita et al. [11] reported that at pH 1.2, only 6 % of the insulin was released from the P(MAA-g-EG) hydrogels with 1:1 molar ratio of MAA:EG repeating units as the hydrogel was in a collapsed state [11], suggesting that the ability of the P(MAA-g-EG) hydrogel to protect the entrapped insulin can be chiefly attributed to the ineffective diffusion of insulin out of the hydrogels at low pH. On the other hand, it has been reported that the P(MAA-g-EG) hydrogels containing 4:1 or 1:0 molar ratio of MAA:EG released almost 30-40 % of the insulin in 1 h at pH 1.2 [11]. However in the present studies, even the crosslinked PMMA or 4:1 MAA:EG particles hydrogels effectively prevented the degradation of entrapped insulin. One of the reasons for this observation could be that the experimental conditions, such as the release volume, were different from that of Morishita's study [11], these results imply that other factors may play a critical role in the insulin protection ability.

7.3.1.2 Insulin protection by direct inhibition of gastric enzymes by complexation hydrogels

To further characterize the protection ability of the hydrogels, we investigated whether P(MAA-g-EG) microparticles could directly inhibit the gastric enzymes, thus preventing insulin degradation. Insulin was incubated in the gastric fluid in the presence or absence of P(MAA-g-EG) microparticles at 37 ^{0}C. The results are shown in Figure 7.2(a). The degradation rate constants were determined from the slopes. These results are shown in Figure 7.2(b). As expected, insulin was rapidly degraded in the absence of microparticles. Interestingly, even in the presence of P(MAA-g-EG) hydrogel with 1:1 molar ratio of MAA:EG repeating units the degradation rate constant did not change significantly and less than 20 % of insulin was present at 60 min. The calculated degradation rate constants for insulin with or without the 1:1 hydrogels were 1.45 ± 0.05 × 10^{-2} min^{-1} and 1.42 ± 0.17 × 10^{-2} min^{-1}, respectively. On the other hand, in the presence of P(MAA-g-EG) microparticles with 4:1 and 1:0 molar ratio of MAA:EG repeating units, insulin remaining at 1 h increased significantly and the degradation rate constants were 0.64 ± 0.03 × 10^{-2} min^{-1} and 0.32 ± 0.06 × 10^{-2} min^{-1}, respectively.

Figure 7.3 shows the effect of increasing amounts of the 1:1 P(MAA-g-EG) microparticles on the insulin degradation rate in the gastric fluid. The degradation rate constant was almost constant even at high concentration of the particles. This difference in the inhibitory characteristics of the polymer containing 1:1

MAA:EG and the polymer containing 4:1 or 1:0 seemed to be due to the difference in the amount of free MAA units in the polymer network. At low pH, most of the MAA units in the polymer with 1:1 MAA:EG are expected to be complexed with the EG units. However, the polymers with 4:1 or 1:0 MAA:EG contain significant number of free MAA units. The inhibitory behavior may thus be linked to the presence of free MAA units in the network. This hypothesis was further supported by results presented in Figure 7.4. It can be seen that the increase in the amount of PMAA polymer (containing 1:0 MAA:EG) resulted in a decrease in the degradation rate constant. Thus, inhibitory effect of the polymer reached a saturation value, such that at higher concentrations, no further decrease in the degradation rate constants was observed with increasing concentration of PMMA in the solution.

The precise mechanism of this inhibition remains unclear but the observed inhibitory effect may be due to weak hydrophobic interactions of the polymer backbone with the active sites on the protein. Complexation between the MAA units and the pendant EG units reduces this interaction thus reducing inhibition of the enzymes. It is worth noting that the inability of the hydrogels containing 1:1 molar ratio of MAA:EG repeating units to inhibit the gastric enzyme is a desirable feature because this means that the polymer carriers can protect the entrapped insulin without interfering with the digestion of nutrient proteins by the gastric enzymes. The polymer microparticles with 1:1 MAA:EG are indeed the preferred

carriers for insulin delivery as they typically exhibit better release behavior compared to the microparticles with 4:1 or 1:0 of MAA:EG repeating units [4].

7.3.2 Enzyme inhibition by complexation hydrogels in intestinal fluid

It is well known that several luminally secreted proteases such as trypsin, chymotrypsin, elastase, are present in the small intestine [12]. Insulin is very sensitive to these proteases and is easily inactivated.

7.3.2.1 Insulin degradation in enzyme solution pre-treated with polymer microparticles

To investigate whether P(MAA-g-EG) hydrogels could inhibit the insulin degradation in the intestinal fluid, insulin degradation in the intestinal fluid was studied. To avoid the interaction between the P(MAA-g-EG) hydrogels and insulin, the intestinal fluid was preincubated in the presence or absence of P(MAA-g-EG) microparticles at 37 ^{0}C for 1 h. After adjusting pH of the fluid to 7.4 to avoid the effect of changes of pH, insulin was incubated with the fluid at 37 ^{0}C. The results are shown in Figure 7.5(a). The degradation rate constants were determined from the slopes (shown in Figure 7.5(b)).

The results indicated that in the intestinal fluid containing no hydrogels, insulin was rapidly degraded and less than 50 % of insulin was detected at 30 min. The degradation rate constant was $1.12 \pm 0.03 \times 10^{-2}$ min^{-1}. On the other hand, in the intestinal fluid treated with P(MAA-g-EG) hydrogels with 1:1, 4:1, or

1:0 molar ratio of MAA:EG repeating units or Carbopol 934P, insulin remaining as significantly higher and the degradation rate constants were $0.76 \pm 0.05 \times 10^{-2}$ min^{-1}, $0.44 \pm 0.06 \times 10^{-2}$ min^{-1}, $0.36 \pm 0.03 \times 10^{-2}$ min^{-1} and $0.02 \pm 0.01 \times 10^{-2}$ min^{-1}

It is interesting to note that the enzyme inhibitory action of these hydrogels in the intestinal fluid was dependent on the density of the ionized carboxylic groups in the hydrogel structure. Carbopol 934P was previously reported to strongly inhibit the protease activities [6, 13]. The enzyme inhibition activities of P(MAA-g-EG) hydrogels were lower compared to that of Carbopol 934P.

7.3.2.2 Calcium binding and protein binding by hydrogels in intestinal fluid

It is thought that the main reason for the observed enzyme inhibitory effect is the Ca^{2+} deprivation of the enzyme structures. For instance, trypsin is a serine protease in the intestinal fluid, which has a binding site for calcium [14]. Calcium plays an important role in maintaining the thermodynamic stability of this enzyme. Therefore, if the calcium is removed from the enzyme structure, the activity is inhibited [13]. In addition, some direct interactions between the hydrogels and enzymes such as the incorporation of the enzymes into hydrogels may explain this inhibitory effect. Therefore, in order to investigate the exact mechanism of this inhibitory effect, protein binding studies and Ca^{2+} binding studies in the intestinal fluid were performed. The intestinal fluid was incubated in the presence or absence of P(MAA-g-EG) microparticles at 37 ^{0}C for 1 h. The changes in the

Ca^{2+} levels or the protein levels were then estimated. The results are shown in Figure 7.6, and Figure 7.7. No changes in the intestinal protein levels were detected in the presence of microparticles, suggesting that the direct interaction between the hydrogels and enzymes was negligible.

On the other hand, in the intestinal fluid treated with all the three hydrogels and Carbopol 934P, significant reduction of Ca^{2+} levels was observed (Figure 7.7). Moreover, the Ca^{2+} binding activity of these hydrogels was dependent on the amount of the carboxylic groups in the hydrogel structure. Madsen and Peppas [6] also reported that the affinity of the polymers toward calcium was dependent on the density of the ionized carboxylic groups. The amount of Ca^{2+} sequestered from the solution in the present study was lower but comparable.

The results shown in Figure 7.5, 7.6, and Figure 7.7, establish that the insulin degradation inhibitory effect correlates with the Ca^{2+} binding activity in the intestinal fluid. These results are summarized in Figure 7.8. A linear relationship (r^2 = 0.9931) was observed between the degradation rate and the reduction in the Ca^{2+} levels in the solution. It is evident that the decrease in the insulin degradation rate correlates well with the Ca^{2+} reduction, suggesting that higher the affinity toward Ca^{2+}, stronger is the enzyme inhibition. Thus the Ca^{2+} binding by the hydrogels plays an important role in the inhibition of the intestinal enzymes.

7.3.3 Insulin release from the hydrogels in the intestinal fluid

Insulin release from the ILPs in the intestinal fluid was investigated. The fractional release of insulin, defined here as the ratio of the amount of insulin released at any time, M_t, in the experimental solution to the total amount released in PBS after 1 h, M_∞, is shown in Figure 7.9. It was observed that in all the three hydrogels, the particles rapidly reached the swollen state and burst release of insulin occurred. The released insulin was then gradually degraded in the intestinal fluid. In a preliminary experiment it was determined that insulin was rapidly degraded in the intestinal fluid in the absence of microparticles. The insulin remaining at 15 min, 30 min and 60 min was 70.3 ± 1.2 %, 47.8 ± 4.3 % and 23.3 ± 1.3 %, respectively.

The release profiles in the intestinal fluid were compared to the release profiles in PBS. The observed burst release of insulin in the intestinal fluid implies that in the harsh environment of the intestinal fluid, a condition of 'high insulin concentration' could be maintained for a short time due to the burst release of insulin. Previously, Morishita et al. [8] reported that insulin released from ILPs was rapidly absorbed from the ileal membrane in rats. Therefore, it is believed that maintaining the condition of 'high insulin concentration' in the small intestine for even a short time can increase the oral insulin bioavailability.

As can be seen from Figure 7.9, the enzyme inhibitory action of these hydrogels was also significant. Nevertheless, some amount of insulin released from ILPs was constantly degraded. All the three types of polymers were able to

protect insulin from degradation due to proteolytic attack in the intestinal environment. It was also shown that the degradation rate for the insulin released from the 1:1 MAA:EG formulation into the intestinal solution containing excess calcium was comparable to the degradation rate for control insulin (added to the intestinal solution) (Figure 7.10) . This confirmed the earlier observation that the inhibition of the enzyme activity is mediated through calcium binding by the hydrogels.

7.4 Conclusions

It was shown in these studies that the complexation hydrogels were highly effective in protecting proteolytic degradation of insulin under conditions mimicking the gastric and intestinal lumen. Investigation of the mechanism of insulin protection in the gastric fluid led to the important conclusion that the P(MAA-g-EG) copolymers containing 1:1 molar ratio of MAA:EG repeating units had no direct inhibitory effect on the gastric enzymes. The polymer microparticles limit the degradation of the entrapped insulin primarily by limiting the diffusion of protein into the gastric fluid. This is important because it implies that the 1:1 MAA:EG polymer, which is typically observed to result in higher bioavailabilities compared to other compositions, will not interfere with the gastric digestion of nutrient proteins.

Calcium binding was identified as the most important factor contributing to the observed inhibition of the intestinal enzymes by the hydrogels. Once again, all the polymer formulations stabilized insulin in the intestinal solution. However, some of the insulin released from all the formulations was degraded. This may be one of the factors that limit the bioavailability of insulin administered orally in the form of insulin-loaded polymer particles. Thus, any strategy that enhances the stability of insulin against proteolytic attack in the intestinal lumen may increase the oral bioavailability. Further, if such a strategy could be used in combination with the complexation hydrogels-based delivery system, it may significantly enhance the insulin bioavailability. One such approach based on conjugation of insulin with tryptic-resistant transferrin molecule is discussed in Chapter 8.

References

1 Langguth, P., Bohner, V., Heizmann, J., Merkle, H. P., Wolffram, S., Amidon, G. L. and Yamashita, S. (1997) The challenge of proteolytic enzymes in intestinal peptide delivery. J Control Rel **46**, 39-57

2 Woodley, J. F. (1994) Enzymatic barriers for GI peptide and protein delivery. Crit Rev Ther Drug Carrier Syst **11**, 61-95

3 Peppas, N. A., Bures, P., Leobandung, W. and Ichikawa, H. (2000) Hydrogels in pharmaceutical formulations. Eur J Pharm Biopharm **50**, 27-46

4 Lowman, A. M. and Peppas, N. A. (1997) Analysis of the Complexation/Decomplexation Phenomena in Graft Copolymer Networks. Macromolecules **30**, 4959 -4965

5 Bell, C. L. and Peppas, N. A. (1996) Water, solute and protein diffusion in physiologically responsive hydrogels of poly (methacrylic acid-g-ethylene glycol). Biomaterials **17**, 1203-1218

6 Madsen, F. and Peppas, N. A. (1999) Complexation graft copolymer networks: swelling properties, calcium binding and proteolytic enzyme inhibition. Biomaterials **20**, 1701-1708

7 Nakamura, K., Murray, R. J., Joseph, J. I., Peppas, N. A., Morishita, M. and Lowman, A. M. (2004) Oral insulin delivery using P(MAA-g-EG) hydrogels: effects of network morphology on insulin delivery characteristics. J Control Rel **95**, 589-599

8 Morishita, M., Goto, T., Peppas, N. A., Joseph, J. I., Torjman, M. C., Munsick, C., Nakamura, K., Yamagata, T., Takayama, K. and Lowman, A. M. (2004) Mucosal insulin delivery systems based on complexation polymer hydrogels: effect of particle size on insulin enteral absorption. J Control Rel **97**, 115-124

9 Lowman, A. M., Morishita, M., Kajita, M., Nagai, T. and Peppas, N. A. (1999) Oral delivery of insulin using pH-responsive complexation gels. J Pharm Sci **88**, 933-937

10 Asada, H., Douen, T., Mizokoshi, Y., Fujita, T., Murakami, M., Yamamoto, A. and Muranishi, S. (1994) Stability of acyl derivatives of insulin in the small intestine: relative importance of insulin association characteristics in aqueous solution. Pharm Res **11**, 1115-1120

11 Morishita, M., Lowman, A. M., Takayama, K., Nagai, T. and Peppas, N. A. (2002) Elucidation of the mechanism of incorporation of insulin in controlled release systems based on complexation polymers. J Control Rel **81**, 25-32

12 Bernkop-Schnurch, A. (1998) The use of inhibitory agents to overcome the enzymatic barrier to perorally administered therapeutic peptides and proteins. J Control Rel **52**, 1-16

13 LuBen, H. L., Rentel, C. O., Kotze, A. F., Lehr, C. M., de Boer, A. G., Verhoef, J. C. and Junginger, H. E. (1997) Mucoadhesive polymers in peroral peptide drug delivery. IV. Polycarbophil and chitosan are potent enhancers of peptide transport across intestinal mucosae in vitro. J Control Rel **45**, 15-23

14 Bartunik, H. D., Summers, L. J. and Bartsch, H. H. (1989) Crystal structure of bovine beta-trypsin at 1.5 A resolution in a crystal form with low molecular packing density. Active site geometry, ion pairs and solvent structure. J Mol Biol **210**, 813-828

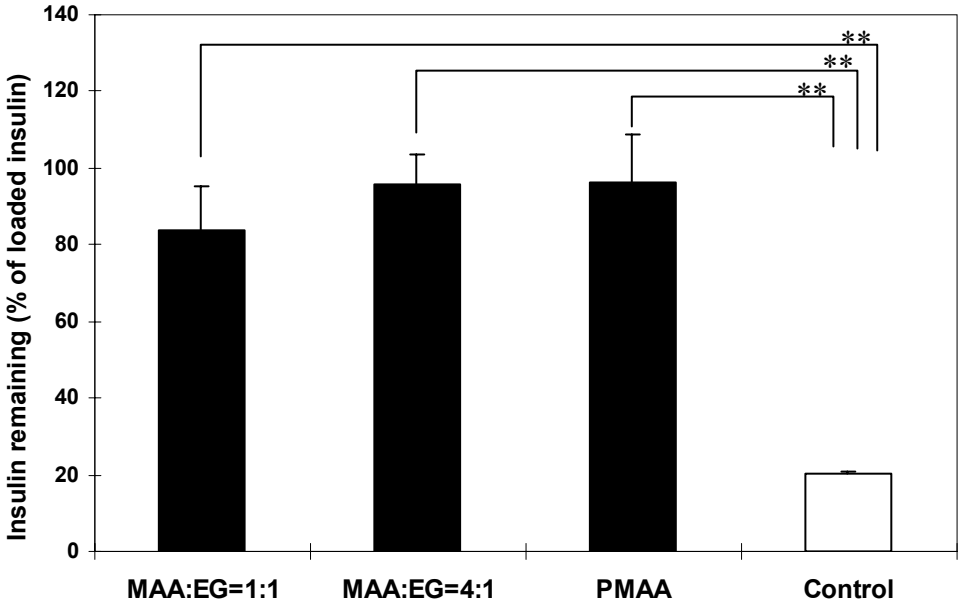

Fig. 7.1 Insulin remaining in the insulin loaded polymer after 1 h exposure to gastric fluid at 37 ^{o}C. A sample of 2 ml of the gastric enzyme solution was incubated for 15 min at 37 ^{0}C. 10 mg of insulin-loaded polymer particles was added to the enzyme solution and incubated for 1 h. Following incubation, the particles were separated and the insulin remaining inside the particles was released in PBS for 3 hours and measured by HPLC. For the control experiments, the amount of insulin equal to the amount incorporated in ILPs, was exposed to 2 ml of gastric fluid at 37 ^{0}C for 1 h. Each value is average of three values

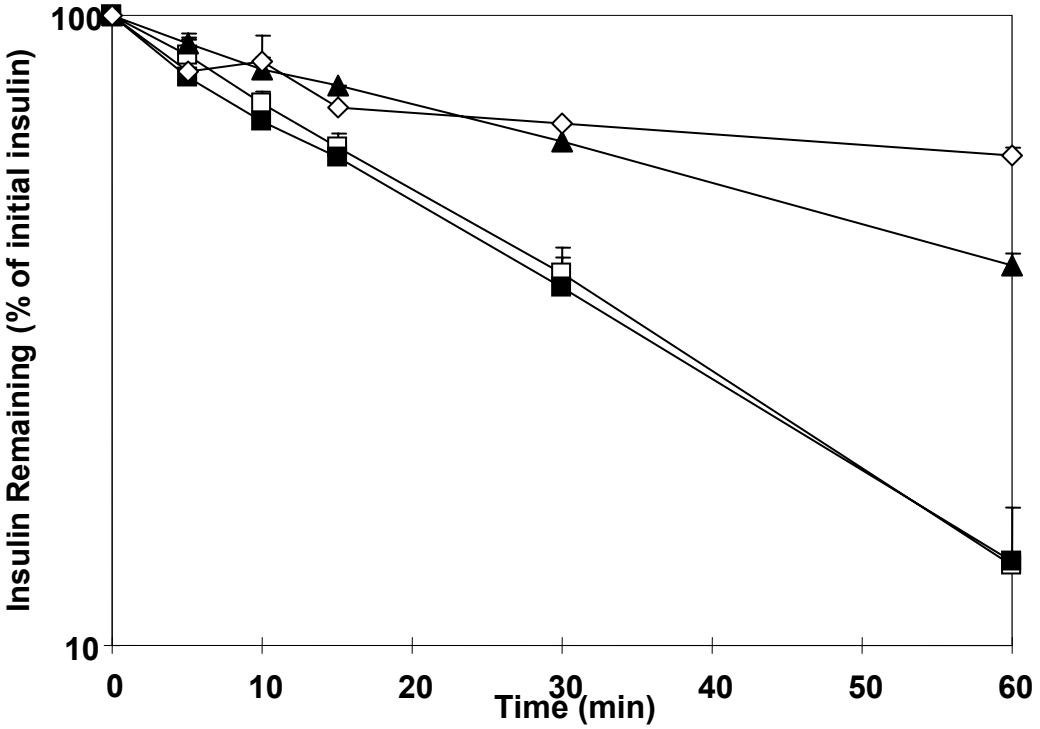

Fig. 7.2(a) Semi-log plot of % insulin remaining in the gastric fluid vs. time. P(MAA-g-EG) microparticles (MAA:EG = 1:1 (■), 4:1(▲), 1:0(◊)) were added to 1.9 ml enzyme solution with100µl insulin solution. Samples were withdrawn at predetermined time intervals and the samples were analyzed with HPLC after stopping the enzyme activity. Control (□) indicates only insulin exposed to gastric fluid. Each reading is average of three values.

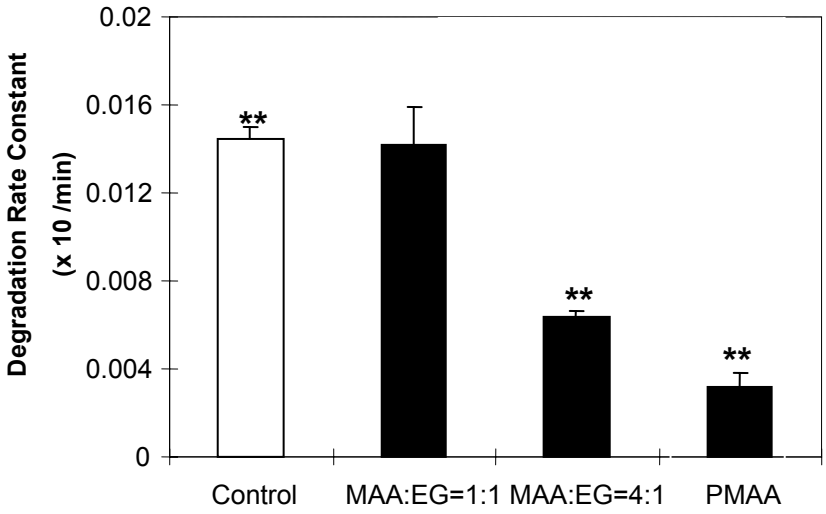

Fig. 7.2(b) Comparison of the effects of hydrogel composition on insulin degradation rate constants. The degradation rate constants were determined from the slope of the semi log plot of the percentage insulin remaining plotted against time in figure 7.2(a). Control indicates only insulin was exposed to gastric fluid. Each value represents average of three values ±S.D. Statistically significant difference: $p<0.01$, **.

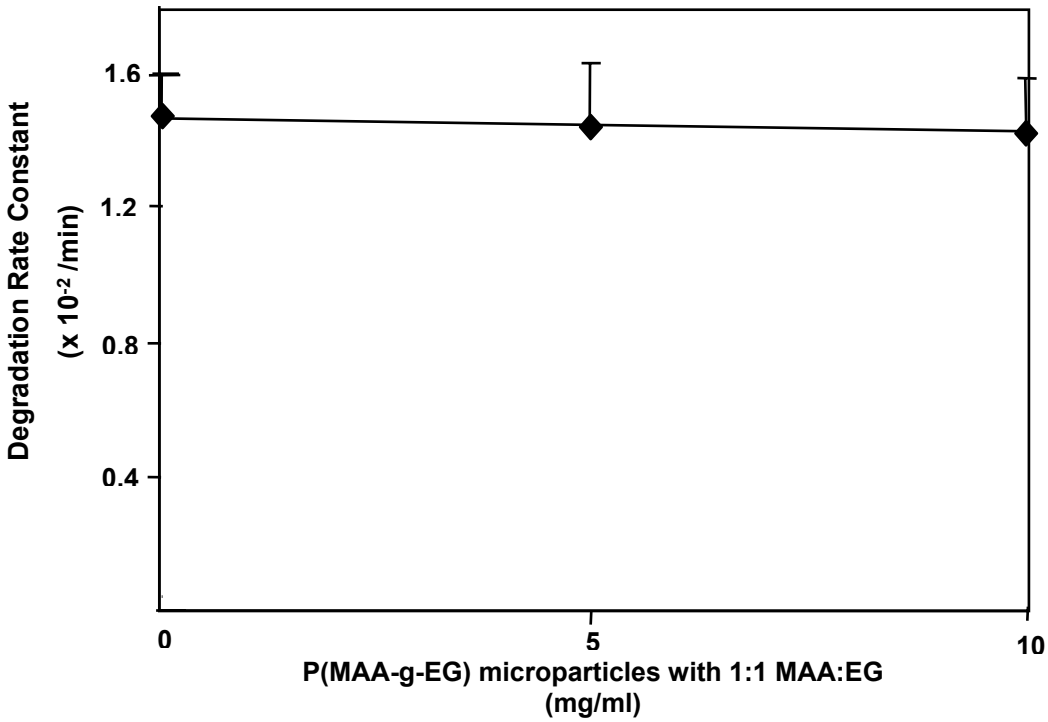

Fig. 7.3 Effect of MAA:EG 1:1 microparticles concentration on insulin degradation rate constant in the gastric fluid. The microparticles were added to 1.9 ml enzyme solution with100µl insulin solution. Samples were withdrawn at predetermined time intervals and the samples were analyzed with HPLC after stopping the enzyme activity. Each value represents average of three values.

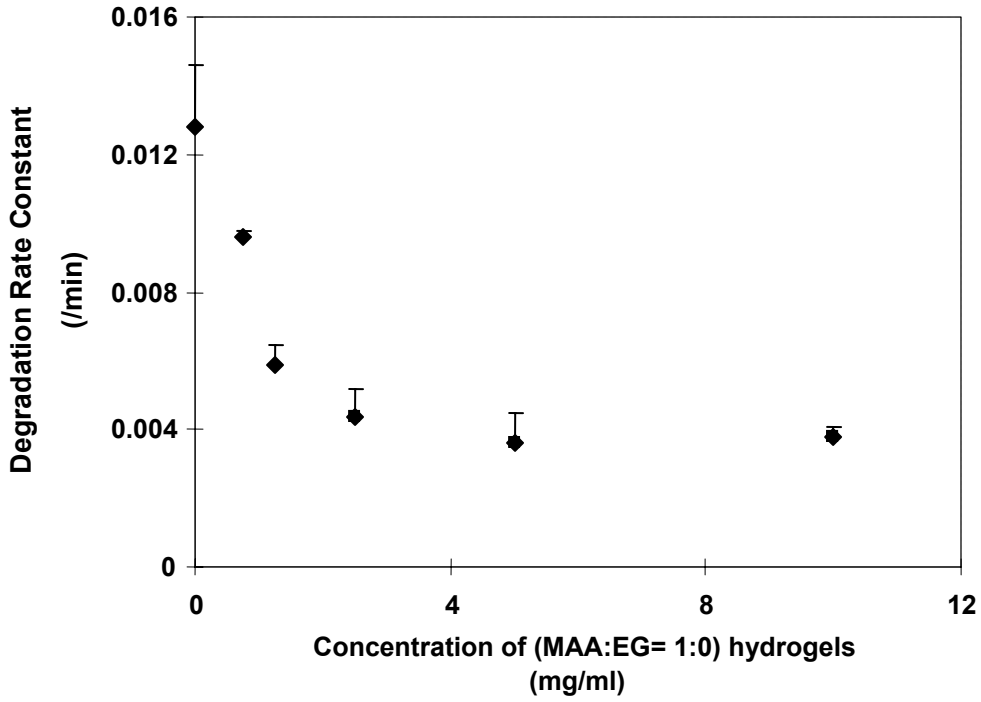

Fig. 7.4 Effect of MAA:EG 1:0 microparticles concentration on insulin degradation rate constant in the gastric fluid. The microparticles were added to 1.9 ml enzyme solution with100µl insulin solution. Samples were withdrawn at predetermined time intervals and the samples were analyzed with HPLC after stopping the enzyme activity. Each value represents average of three values.

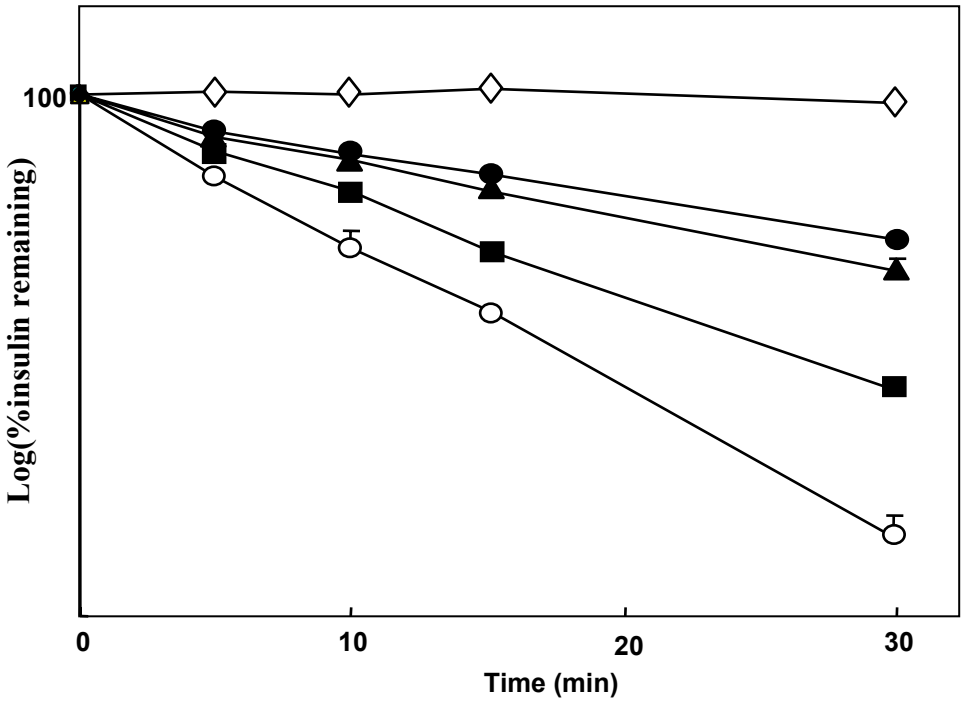

Fig. 7.5(a) Semi-log plot of % insulin remaining in the intestinal fluid vs. time. 2 ml intestinal solution was incubated with 10 mg P(MAA-g-EG) microparticles (MAA:EG = 1:1 (■), 4:1(▲), 1:0(●)) and Carbopol 934P (◊)for 1 hr. The polymers were separated and insulin solution was added to the enzyme solution. Samples were withdrawn at predetermined time intervals and the samples were analyzed with HPLC after stopping the enzyme activity. Control (○) indicates only insulin exposed to intestinal. Each reading is average of three values.

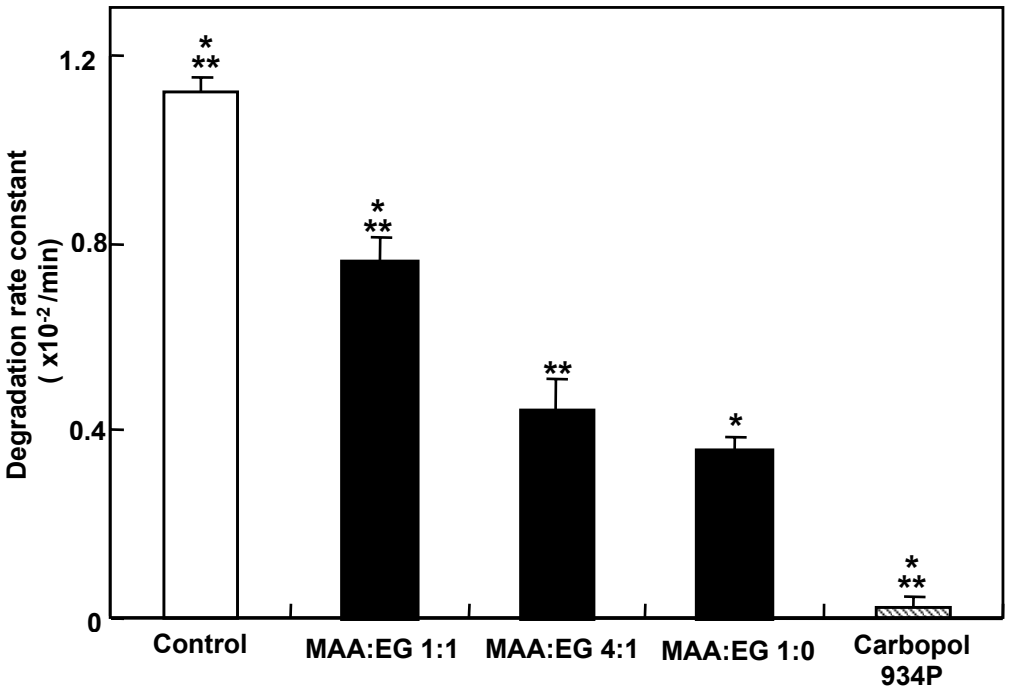

Fig. 7.5(b) Inhibition of insulin degradation by hydrogels in the intestinal fluid; comparison of insulin degradation rate constants. The degradation rate constants were determined from the slope of the semi log plot of the % insulin remaining plotted against time in figure 7.5(a). Control indicates only insulin exposed to intestinal fluid. Each value represents average of three values. Statistically significant difference: $p<0.01$, **

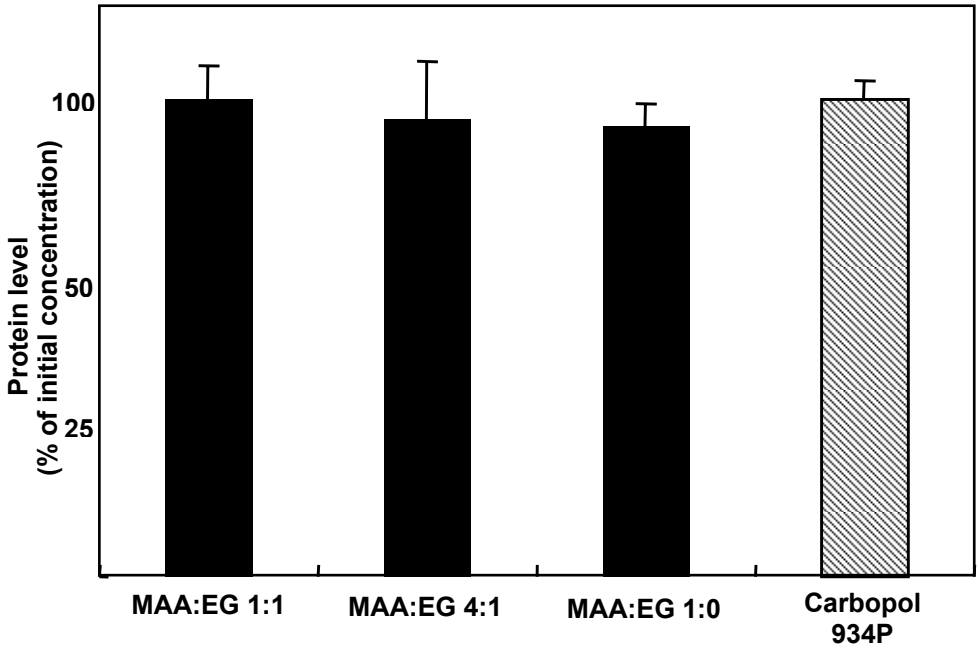

Fig. 7.6 Effect of microparticles on the protein levels in intestinal fluid. 2 ml of the intestinal fluid was incubated at 37 ^{0}C for 15 min. 10 mg of P(MAA-g-EG) microparticles (1:1, 4:1, 1:0 MAA:EG) or Carbopol 934P were added to the fluid and incubated at 37 ^{0}C for 1 h. The concentration of protein in the fluid was then determined by the Protein Quantification Kit. Each value represents average of three values.

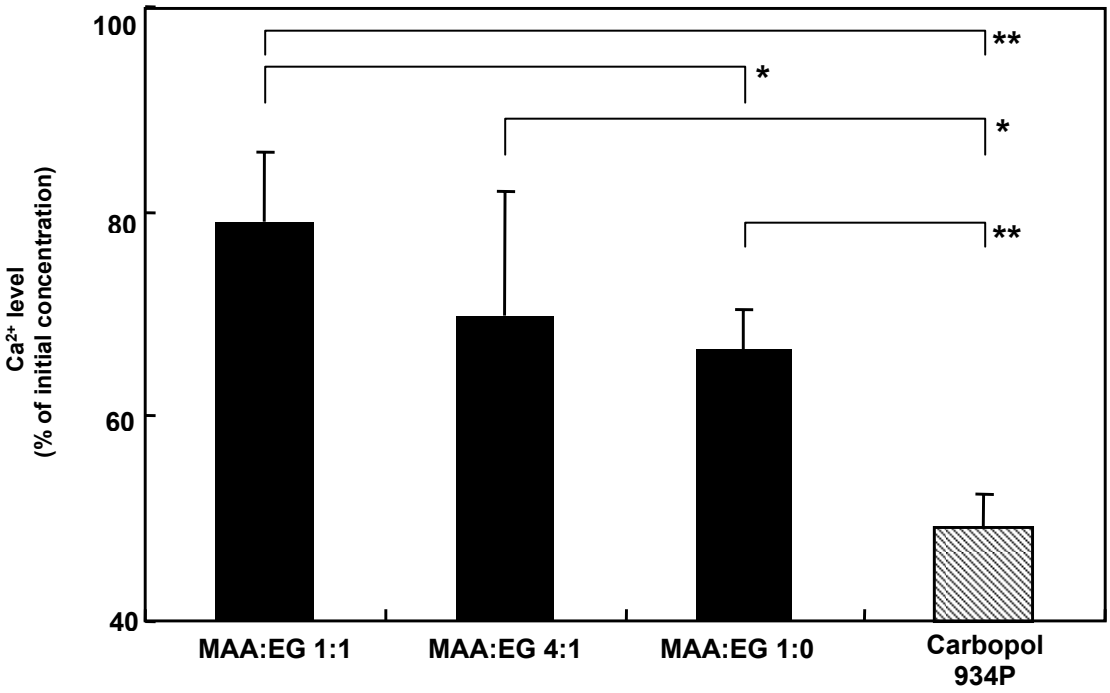

Fig. 7.7 The effect of hydrogels on the Ca^{2+} levels in intestinal fluid. 2 ml of the intestinal fluid was incubated at 37 ^{0}C for 15 min. 10 mg of P(MAA-g-EG) microparticles (1:1, 4:1, 1:0 MAA:EG) or Carbopol 934P were added to the fluid and incubated at 37 ^{0}C for 1 h. The Ca^{2+} concentration was then determined. Each value represents average of three values. Statistically significant difference: $p<0.05$, *, $p<0.01$, **

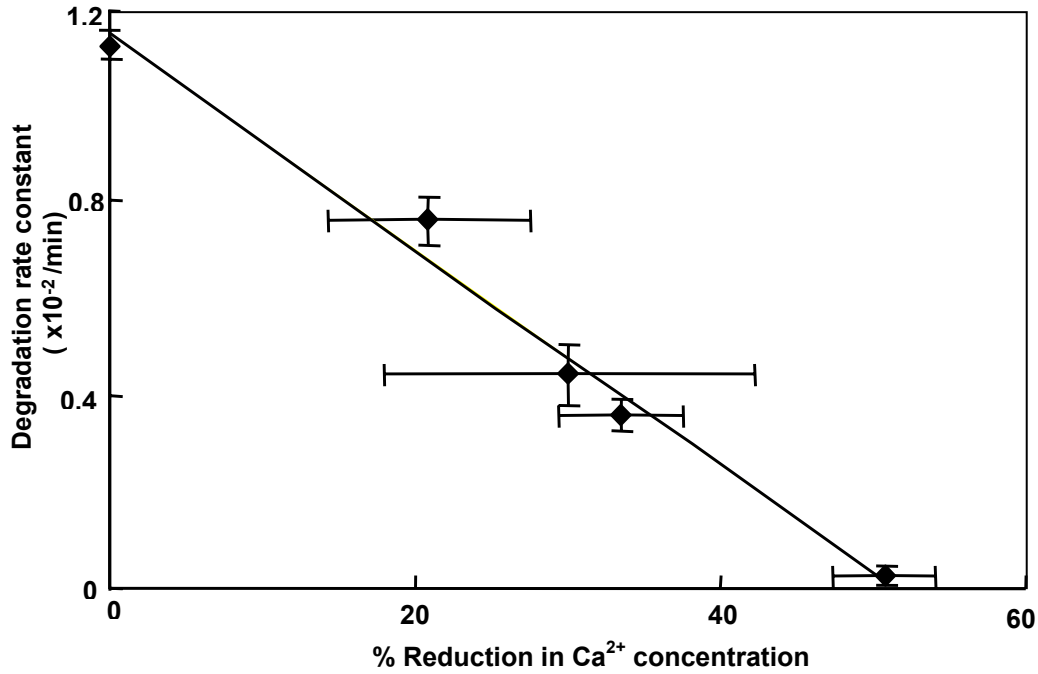

Fig. 7.8 Relationship between the insulin degradation rate constants and the decrease in Ca^{2+} concentration in the intestinal environment. Each value represents average of three values.

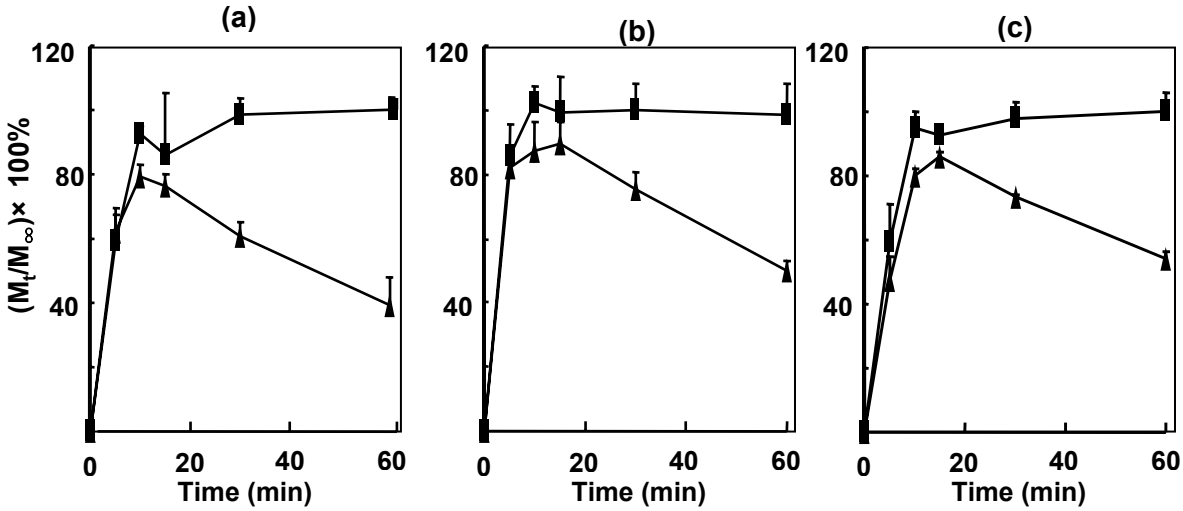

Fig. 7.9 Insulin release profiles from ILPs in the intestinal fluid or PBS. 10 mg of insulin-loaded polymer particles (MAA:EG = 1:1(a), 4:1 (b), and 1:0 (c)) was added to the 20 ml enzyme solution (▲)or PBS (■) and samples were withdrawn at predetermined time intervals up to 60 min. After stopping the enzyme activity, the samples were analyzed by HPLC. The fractional release of insulin from ILPs, defined as the ratio of the amount released at any time (M_t) to the total amount of insulin released after 1 h (M_∞). Each value represents average of three measurements.

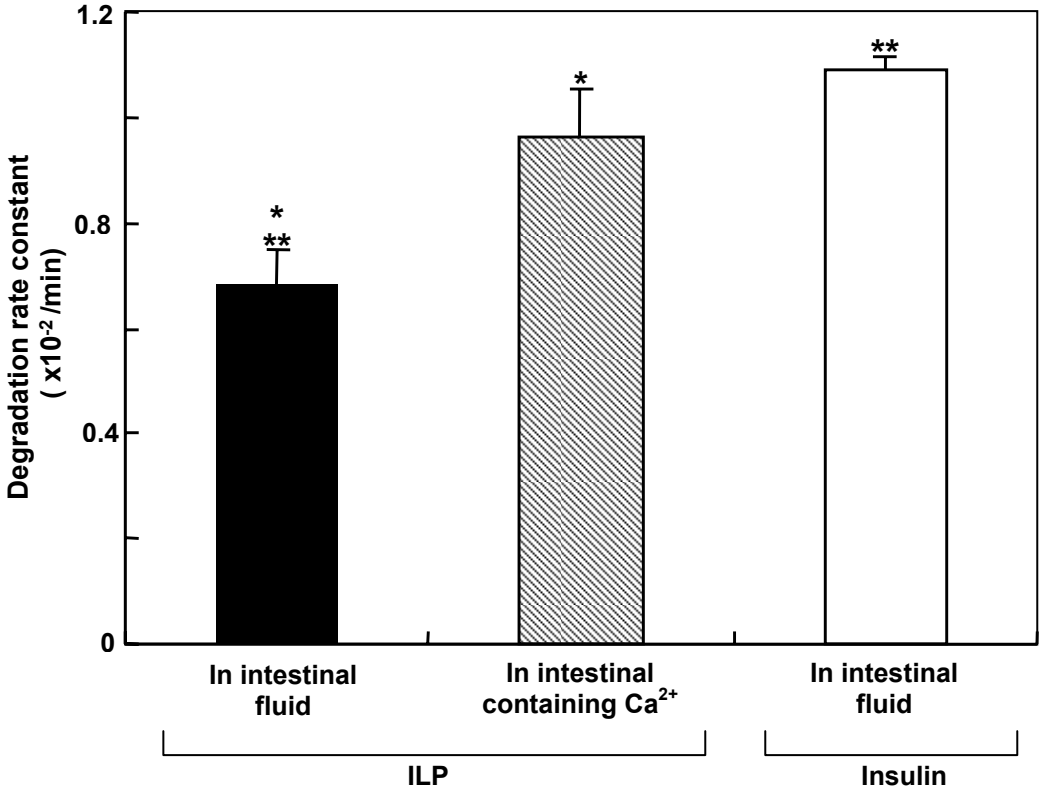

Fig. 7.10 Effect of Ca^{2+} addition on the inhibition of insulin degradation in the intestinal environment by the complexation hydrogels containing 1:1 MAA:EG. ILPs, or only insulin were added to intestinal fluid or intestinal fluid containing Ca^{2+}. The degradation rate constants were determined from the slope of the semi log plot of the percentage insulin remaining plotted against time. Each value represents average of three values. Statistically significant difference: $p<0.01$, *, $p<0.01$, **.

CHAPTER 8

SYNTHESIS AND CHARACTERIZATION OF INSULIN-TRANSFERRIN CONJUGATES

8.1 Introduction

As described in Section 2.4.2, complexation hydrogels developed in our laboratory have emerged as one of the most promising methods for orally delivering therapeutic proteins [1-3]. Both in vitro and in vivo studies with insulin loaded microparticles have demonstrated the efficacy of these hydrogels as vehicles for peroral administration of insulin [1, 4, 5]. The data presented in Chapter 6 and Chapter 7 also indicate that the complexation hydrogels exhibit highly beneficial characteristics for protein oral delivery.

One of the other effective strategies for enhancing bioavailability of proteins exploits the receptor-mediated endocytotic pathway used by the cells for the selective and efficient uptake of specific macromolecules required for various cell processes. By coupling proteins and peptides to ligands that can recognize specific receptors on the epithelial cells, transcellular delivery of these macromolecular biopharmaceuticals may be achieved. Since only those molecules that are conjugated to the ligands are transcytosed, this process eliminates the potential side effects associated with the unspecific transport via the paracellular pathway. Transferrin is one of the most widely investigated proteins for enhancing the cellular uptake of therapeutic agents. It is a naturally

occurring protein involved in iron transport. Absorptive uptake of the iron-bound transferrin is often used to enhance the transcytosis of therapeutic agents and drug carriers across polarized cells such as the epithelial cells and the endothelial cells. Transferrin-receptor (TfR) mediated delivery systems have been widely exploited for delivery of drug carriers [6, 7] neurotoxins, and trophic factors across the blood-brain-barrier for treatment of tumors and neurodegenerative diseases [8, 9].

TfR-mediated cellular uptake has also been exploited for targeted delivery of anticancer drugs, proteins, and therapeutic genes into primary proliferating malignant cells that over express the transferrin receptors [10]. Covalent coupling of transferrin with therapeutic drugs, proteins, or genetic infusion of therapeutic peptides into the structure of transferrin results in complexes with improved specificity and cytotoxicity toward malignant cells and enhanced uptake characteristics [11].

Researchers recently demonstrated improved efficacy of orally administered insulin by conjugating insulin with transferrin through disulfide linkages [12]. Transferrin receptors are present in high density in human GI epithelium, and transferrin can resist tryptic and chymotryptic degradation [12-14]. Shah and Shen [15] showed that insulin conjugated to transferrin via disulfide linkages can be transported across enterocytes-like the Caco-2 cells. The disulfide bond can be cleaved after the conjugate is absorbed into the blood stream, giving rise to free insulin [16]. Xia et al. [12] showed that insulin-

transferrin conjugate exhibited a slow but prolonged hypoglycemic effect compared to that of the native human insulin in streptozotocin-induced diabetic rats.

The object of this study was to develop a delivery system consisting of the complexation hydrogels acting as delivery vehicles for insulin-transferrin conjugates. The use of P(MAA-g-EG)-based microparticles as delivery vehicles for the insulin-transferrin conjugates may constitute a superior transmucosal delivery system for insulin. The system may improve the efficacy of oral insulin administration since: (i) insulin in the conjugated form may be further protected from enzymatic degradation due to steric hindrance created by the conjugated transferrin; (ii) owing to the mucoadhesive nature of the delivery system, most of the conjugate will be released within the localized microenvironment of the small intestine's filamentous brush border creating a high local concentration of the conjugate; (iii) the conjugate will have larger residence time in the small intestine; and (iv) the insulin-transferrin conjugate can cross the intestinal barrier by TfR-mediated transcellular pathway, which may further increase the efficiency of insulin absorption.

This is the first of three chapters that deal with the development of a delivery system based on complexation hydrogels used as carriers for oral delivery of insulin-transferrin conjugates. This chapter focuses on the synthesis of insulin-transferrin conjugates, analysis of the intermediate products, and characterization of the final reaction products. Loading and release of the

conjugates from the complexation hydrogels are given in Chapter 9 and cellular studies are discussed in Chapter 10.

8.2 Materials and Methods

8.2.1 Synthesis of Insulin-Transferrin Conjugates

The protein conjugation method described here has been developed by Carlsson et al. [17] and was used for preparation of insulin-transferrin conjugates by Shah and Shen [15]. Insulin (Ins) was conjugated to transferrin (Tf) through disulfide linkages using a heterobifunctional crosslinker, succinimidyl 3-(2-pyridyldithio)propionate abbreviated as SPDP (Pierce, Rockford, IL). The structure of SPDP and the reaction scheme for conjugation are given in Figure 8.1 and Figure 8.2 respectively.

Insulin modification by DMMA (step I): Insulin was reacted with dimethylmaleic anhydride (DMMA) (Sigma-Aldrich Chemie, Steinheim, Germany) to block the primary amine groups at the n-terminals of insulin chains which can potentially react with SPDP. A sample of 25 mg of bovine insulin (Sigma, St. Louis, MO) was added to a solution containing 1.5 ml of 1N HCl and 3 ml PBS solution (pH 6.9). After completely dissolving insulin, the pH of the solution was adjusted to 6.9 by addition of 1.5 ml of 1N NaOH solution. Dissolved insulin was then reacted with 3.5 mg of DMMA under constant stirring for 0.5 h. The pH of the solution was maintained at 6.8 to 6.9 by addition of 1M Na_2CO_3 solution. Reaction with

DMMA was repeated two more times so that a total of 10.5 mg of DMMA was added to insulin at a controlled pH of 6.8-6.9. A micro-pH meter (IQ Scientific Instruments, San Diego, CA) was used to monitor the pH of the solution during the reaction. The reaction mixture was transferred to dialysis tubing (Float-a-lyzer, MWCO 3500; Spectrum Laboratories, Rancho Dominguez, CA) and dialyzed against PBS buffer (pH 6.9) for 24 hours to remove unreacted DMMA.

Insulin modification with SPDP (step II): Following dialysis, the DMMA-modified insulin was reacted with SPDP to introduce disulfide bonds at primary amine group of lysine at the B29 position of insulin. The pH of modified insulin solution was raised to 9.0 by addition of 1M Na_2CO_3 and 6.0 mg of SPDP dissolved in 150 μl dimethyl formamide (DMF) was added to this solution. The reaction was constantly stirred at 4 ^{0}C for 2 hours. The pH of the reaction was maintained at 8.8-9.0 during the course of the reaction.

The modified insulin was then dialyzed against a PBS buffer (pH 8.0) for 24 hours to remove unreacted SPDP reagent. To measure the average number of moles of 2-pyridyl disulfide groups attached per mole of insulin (PDP: Insulin ratio), 700 μl of Ins-PDP solution was reduced by 25mM dithiothreitol (DTT) (Pierce, Rockford, IL). PDP-modified protein on reduction with DTT releases of 2-pyridinethione chromophore which can be quantitated by measuring the absorbance at 343 nm (A_{343}). A molar extinction coefficient of 8.08 x 10^3 $M^{-1}cm^{-1}$ at 343 nm ($\varepsilon_{343,2\text{-TP}}$) and 5.10 x 10^3 $M^{-1}cm^{-1}$ at 280 nm ($\varepsilon_{280,2\text{-TP}}$) was used for calculations [17, 18]. Protein concentration was determined by measuring the

absorbance at 280 nm (A_{280}). The molar extinction coefficient of 5.8 x 10^3 $M^{-1}cm^{-1}$ at 280 nm was used for insulin. A sample of 40 μl DTT reduced modified insulin solution was diluted to 700 μl and the absorbance was measured in triplicates at 343 nm and 280 nm with a microplate reader (Synergy HT, Bio-Tech Instruments, Winooski, VT). The PDP: protein ratio was determined by the following formula.

$$\text{PDP/protein} = \frac{A_{343} \times \varepsilon_{280,\ \text{protein}}}{(A_{280} \times \varepsilon_{343,2\text{-TP}} - A_{343} \times \varepsilon_{280,2\text{-TP}})} \qquad (8.1)$$

Transferrin modification with SPDP (step III): Transferrin was dissolved in 4 ml phosphate buffer (pH 7.0, 30mM) at a concentration of 20 mg/ml. Four-fold molar excess of SPDP dissolved in 100 μl DMF and added to the transferrin solution under constant stirring. The reaction mixture was stirred for 2 hours at 4 ^oC. The modified transferrin was then dialyzed against phosphate buffer (pH 8.0, 30mM, 3mM EDTA) in Float-a-lyzer dialysis tubing (MWCO 50,000, Spectrum Laboratories, Rancho Dominguez, CA) for 24 hours to remove unreacted SPDP reagent. Following dialysis, entire transferrin solution was reduced by reacting with 25mM DTT for 1 h to generate thiol-containing transferrin (Tf-SH). The PDP: Tf modification ratio was determined by using molar extinction coefficient of 93.0 x 10^3 $M^{-1}cm^{-1}$ at 280 nm ($\varepsilon_{280,Tf}$) as described above.

Conjugation of modified proteins (step IV): The reaction solution from step III containing Tf-SH was immediately purified by elution on D-Salt Dextran Desalting Columns (MWCO 5000, 10 ml, Pierce Biotechnology, Inc., Rockford, IL). Four columns were connected in series to achieve the desired purification. 1 ml fractions were collected using a fraction collector (Spectrum Chromatography Inc, Houston, TX). Phosphate buffer (pH 8.0, 30 mM, 3 mM EDTA) was used to elute the protein from the columns. Fractions with A_{280} values greater than 0.2 were collected. It was important to use EDTA-containing buffer for elution to prevent metal-catalyzed oxidation of free –SH groups of transferrin into disulfide bonds, which may lead to formation of crosslinked transferrin complexes.

Purified Tf-SH was then reacted with Ins-PDP obtained from the reaction step II in a molar ratio of 1:2 of Tf-SH: Ins-PDP. To follow the progress of the reaction, 40 µl of the reaction samples were withdrawn at 0, 5, 10, 30, 60, 90, 120, 150 min and diluted to 700 µl with phosphate buffer. Reaction of each mole of insulin with Tf-SH is accompanied by the release of one mole of 2-pyridinethione. Hence, A_{343} values of the samples were measured with a microplate reader in triplicates to determine the concentration of 2-pyridinethione. To determine the average number of moles of insulin attached to one mole transferrin (Ins: Tf ratio), concentration of the 2-pyridinethione was divided by transferrin concentration in the samples. The A_{343} values used were corrected for the baseline absorbance at 343 nm due to transferrin and insulin. When approximately 2 moles of 2-pyridinethione were released per mole of transferrin,

the reaction was stopped by addition of 4 mg of n-ethylmaleimide (NEM) (MP Biomedicals, Aurora, OH). NEM reacts with free thiol groups [19] and prevents further crosslinking of transferrin molecules via oxidation of unreacted thiols. Following the reaction, the conjugate was purified by dialysis (MWCO 25,000) against phosphate buffer (pH 8.0, 30mM, 3mM EDTA) until no free insulin was detected in the solution by HPLC. Total protein concentration of the final purified conjugate solution was determined by Quick Start™ Bradford assay (Bio-Rad Laboratories, Hercules, CA) using BSA or unmodified transferrin as a reference standard [20]. 20 µl of the protein samples were added to 1 ml of Bradford reagent and the absorbance was detected with a microplate reader at 595 nm. After concentration measurements the conjugate solution was divided into aliquots and stored at -80 ^{o}C until used.

8.2.2 Analysis of the Insulin Modification Reaction

Modifications of the primary amines of insulin due to DMMA reaction (step I) and SPDP modification (step II) was studied here by quantitatively measuring the amount of free primary amine groups of the protein using fluorescamine assay and by identifying the sites of insulin modification by mass spectroscopy. This was important since improper modifications of the protein may lead to decrease n its bioactivity [21].

Fluorescamine assay for measurement of free amine groups of insulin: A primary amine assay utilizing 4-phenylspiro[furan-2(3H),1'-phthalan]-3,3'-dione

(fluorescamine) (Sigma, St. Louis, MO) was performed to estimate insulin primary amine modification by DMMA and by SPDP. 1.08 mM fluorescamine stock solution was prepared by dissolving 0.9 mg fluorescamine in 3 ml acetone. Insulin standard solutions were prepared containing 0.05, 0.1, 0.25, 0.5, 1, and 2 mg/ml native, unmodified insulin in PBS buffer. 50 µl of fluorescamine stock solution was added to 150 µl of insulin standard solutions in 96 well plates and the fluorescence measurements were performed a microplate reader [22]. The excitation wavelength for measurements was 390 nm and the emission wavelength was 470 nm. A standard curve of emission at 470 nm (Em_{470}) vs. insulin concentration (mg/ml) was prepared (Figure 8.5).

Samples were taken from the modification reaction before modification with DMMA (after step I), after purifying the DMMA-modified insulin and after purifying the SPDP-modified insulin intermediate (after step II). The concentrations of the samples were adjusted to account for the dilution caused by dialysis of the modified intermediate products, so that the final concentration in all the samples was 0.75 mg/ml. A plot of Em_{470} vs. concentration (mg/ml) was prepared for all the three samples. Concentrations of 0.75 mg/ml, 0.375 mg/ml and 0.1875 mg/ml were included in the plot of Em_{470} vs. concentration for all the three samples (Figure 8.5). The slopes of standard curve and plots for three samples were calculated and plotted against the expected number of moles of free amines present per mole of insulin samples (Figure 8.6).

Mass spectroscopy analysis of the insulin modification reaction: All chemicals were purchased from Sigma (St. Louis, Mo) without any further purification unless otherwise noted. Sample aliquots were taken before and after the DMMA and SPDP modification steps. Dialysis of each aliquot was performed by Slide-A-Lyzer Mini Dialysis units, 3.5K MWCO (Pierce Biotchnology, Rockford, IL) against 0.5 L deionized H_2O with Triethylamine (TEA) at pH 7.5 for 30 minutes. The dialysis was repeated before dilution for ESI-MS analysis. Dialyzed SPDP modified insulin was digested with immobilized trypsin, TPCK (Pierce Biotechnology, Rockford, IL) treated in 0.1M NH_4OAc buffered to pH 8.5 for 18 hours at 37°C for identification of the SPDP modification sites. The trypsin digest samples were desalted and concentrated with C_{18} ZipTips (Millipore, Billerica, MA). ESI-MS and MS^n experiments were performed on an LCQ Duo quadrupole ion trap mass spectrometer (ThermoFinnigan, San Jose, Ca). All samples were diluted to 10uM and run at 3µl/min for ESI-MS analysis in 99/1/1 MeOH/H_2O/TEA (negative mode) or 99/1/1 MeOH/H_2O/HoAc (positive mode).

8.2.3 Analysis of the Insulin-Transferrin Conjugates

HPLC analysis: A Reversed Phase-HPLC method was established for analysis of the conjugates to be used in quantification of the conjugates in later studies. The same method was used for measurement of insulin and transferrin concentrations. The HPLC system was a Waters 2695 Alliance Separation Module (Waters, Milford, MA) equipped with Waters 2487 Dual λ Absorbance

Detector (Waters, Milford, MA). All the data were collected utilizing Empower Applications version 5.00.00 software. A Symmetry300™ C4 column (particle size 5 µm, 3.9mm i.d. ×150mm length) (Milford, MA) was used for the separations. The solvents used for the analysis were: solvent A (water, 0.1% trifluoroacetic acid (TFA)) and solvent B (HPLC-grade acetonitrile, 0.08% TFA). The mobile phase for the analysis consisted of a linear gradient of 70% of solvent A to 40% of solvent A in 6 min. The gradient was controlled by the Empower software. The column temperature was set at 40 ^{o}C. The flow rate of the mobile phase was set at 0.6 ml/min and the peaks were detected at 215 nm.

SDS-PAGE analysis: For SDS-PAGE, protein samples were diluted in NuPAGE® lithium dodecyl sulfate (LDS) sample buffer (Invitrogen Life Technologies, Carlsbad, CA). Samples were heated to 70 ^{o}C in Eppendorf Thermomixer (Brinkmann Instruments, Westbury, NY) for 10 min before being loaded into wells. Gel electrophoresis was conducted with NuPAGE® Novex 7% Tris-Acetate Gel (1.0 mm, 10 well; Invitrogen Life Technologies, Carlsbad, CA) in NuPAGE® Tris-Acetate SDS Running Buffer (Invitrogen Life Technologies, Carlsbad, CA). The electrophoresis was performed in a Novex X-Cell Surelock Mini-Cell apparatus (Invitrogen Life Technologies, Carlsbad, CA) at 150 V for 2 hours. Relative molecular weights were estimated by comparison with molecular weight standards. Following electrophoresis, the gel was rinsed three times for 5 minutes with 100 ml deionized water (DI water) and stained with Coomassie G-250 SimplyBlue™ SafeStain (Invitrogen Life Technologies, Carlsbad, CA) for 1 h.

The staining solution was then discarded and the gel was placed in DI water for 1hr. At the end of 1 h, 20 ml of 20% NaCl (w/v) solution was added to the water and the gel was stored at room temperature until scanned. The gel was scanned using a digital scanner.

8.2.4 Enzymatic Stability of Insulin-Transferrin Conjugates

The degradation profile of the conjugates was studied in comparison with insulin and transferrin in simulated intestinal fluid. The simulated intestinal fluid was prepared by dissolving trypsin (Sigma, St. Louis, MO) in 50 mM phosphate buffer solution with pH of 7.4 and ionic strength of 154 mM. Insulin and transferrin stock solutions were prepared in the reaction buffer. Conjugate solution was diluted with the reaction buffer to achieve desired concentration. All the solutions were pre-warmed at 37 ^{o}C for 15 minutes. The protein and the trypsin concentrations in the stock solutions were adjusted so that after adding trypsin solution to the insulin, transferrin and conjugate stock solutions, the initial protein concentration in the reaction mixture was 1 mg/ml and the trypsin concentration was 3.2 mg/ml. At time t=0, trypsin stock solution was added to insulin, transferrin and the conjugate solutions at 37 ^{o}C under continuous mixing. 50 µl samples were withdrawn at 0, 5, 10, 15, 30 and 60 min and the enzyme activity in the samples was stopped by addition of 50 µl ice-cold acetic acid solution (50% (v/v) acetic acid in DI water). The samples were then analyzed by

HPLC as described previously. Degradation rate constants were determined from the slope of semi-log plot of the percentage of initial protein remaining vs. time.

8.3 Results and Discussion

8.3.1 Synthesis of Insulin-Transferrin Conjugates

Insulin was conjugated to transferrin using SPDP (Figure 8.1), a heterobifunctional, cleavable cross-linker that reacts with primary amines and sulfhydryl groups [23]. The reaction scheme for conjugation is shown in Figure 8.2. The amine-reactive portion of SPDP reagents is the n-hydroxysuccinimide (NHS) ester. Upon SPDP reaction with the accessible primary amines of a protein, a mixed disulfide is formed which has free 2-pyridyldithio groups, that can react with free sulfhydryl groups from other proteins. This results in formation of conjugates of different proteins (heteroconjugates), without unwanted cross-reaction products such as the homoconjugates of individual proteins. This crosslinker is especially applicable to this research since the disulfide linkages are inherently unstable in the plasma [24]. Hence disulfide linkages linking the two proteins may be cleaved once the conjugate reaches systemic circulation [16, 25, 26]. Xia et al. [12] showed that free insulin was released within 5 minutes of incubation of the insulin-transferrin conjugates with rat liver slices. Free insulin was also detected in the rat serum 4 hours after oral administration of the insulin-transferrin conjugates.

Step I of the conjugation involves modification of the n-terminal primary amines of insulin by reaction with DMMA. Insulin has three primary amine moieties: at A1-Glycine (A1Gly), B1- Phenylalanine (B1Phe) and at B29-Lysine (B29-Lys) (Figure 8.10). All the primary amines can potentially react with SPDP reagent at a pH where most of the amine groups are deprotonated so that the $-NH_2$ group can act as a nucleophile and react with the electron-deficient carbon atom of the succinimidyl group of SPDP (Figure 8.1). However, Lindsay and Shall [27] reported that acetylation of insulin at the A1Gly position resulted in decrease in the biological activity of insulin. Hence insulin modifications involving primary amines are usually directed at either B1Phe or B29Lys positions [28]. In this work SPDP modification was carrier out at the B29 lysine group of insulin. Hence it was necessary to block the n-terminal primary amines before reacting insulin with SPDP. This was done by reacting insulin with DMMA at a controlled pH of 6.8-6.9. The pKa of the n-terminal amine residues is around 7.5-8.0, whereas the pKa of the lysine group is around 10.5 [29]. Thus, at the reaction pH a significant number of terminal amine groups were in their deprotonated state, and were able to react with DMMA through nucleophilic attack (Figure 8.2, step I). However, since the pH was more 2 units below the pKa of the lysine residue, most of the lysine residues remained unreacted. The DMMA modification of insulin is acid-labile and the amino acid residues can be regenerated by making the solution slightly acidic.

SPDP modification of the purified intermediate from step I was carrier out at the pH of 9.0 to generate the Ins-PDP intermediate. The modification was measured by UV spectroscopy after reducing a small aliquot of purified Ins-PDP by 25 mM DTT dissolved in pH 4.5 sodium-acetate buffer. At this concentration, the DTT is able to selectively reduce the -S-S- bonds in the crosslinker without affecting the protein disulfide linkages. The modification ratio (PDP: Ins) calculated from equation 8.1 was (0.95 ± 0.05): 1. Modification ratio for transferrin (PDP: Tf) was approximately 4: 1.

After reducing the Tf-PDP intermediate to generate thiol containing transferrin (Tf-SH), the intermediate was purified by size exclusion. 2 moles of Ins-PDP was added per mole of Tf-SH. Figure 8.3 shows the progress of the reaction followed by measuring the A_{343} for determining 2-pyridinethio released. When added Ins-PDP was almost entirely reacted releasing 2 moles of 2-pyridinethio, the reaction was stopped by addition of NEM to prevent crosslinking of the Ins-Tf conjugates due to oxidation of excess –SH on insulin-conjugated transferrin. The conjugation ratio of 2:1 Ins:Tf was chosen since excessive modification of transferrin by insulin attachment will result in a bulky complex which may adversely affect the diffusion characteristics of the conjugate in the polymer network reducing loading and release efficiencies of the conjugate.

Little or no insulin was detected in the reaction mixture by HPLC at the end of the reaction. The conjugate was extensively dialyzed to remove unreacted residual insulin. The concentration of purified conjugate was determined using

Bradford assay [20]. In this assay, the negatively charged Coomassie blue reagent binds the positive charges on protein, which results in absorbance shift from 465 nm to 595 nm. The protein concentration can be determined by measuring the absorbance at 595 nm. Because many proteins have nearly identical response curve, the methods can be applied widely using a single set of standards [20]. BSA and transferrin were used as standards to calculate the concentration of conjugate in the purified conjugate solution. This was done to verify that BSA or transferrin could be used as a reference standard to measure concentration of the conjugate. As expected, both the proteins had approximately the same slopes for A_{595} vs. concentration plots. Figure 8.4 shows the standard curves of BSA and transferrin.

8.3.2 Analysis of the Insulin Modification Reaction

Cellular studies performed by Shah and Shen [15] showed that conjugate molecules containing up to 3 insulin molecules per molecule of transferrin were able to get transported across the Caco-2 cell monolayers by transcellular mechanism. This means that the modification of transferrin did not decrease its ability to bind the transferrin receptors on the cell surfaces and get transported across the cell monolayers by receptor-mediated transcytosis. Thus, SPDP modification of the surface exposed lysine residues of transferrin does not decrease its biological activity. However, improper modification of insulin by DMMA or SPDP may result inhibition of its physiological activity. Hence sites of

modification of insulin were verified here by fluorescamine assay and mass spectroscopy analysis of the insulin modified by step I (DMMA modification) and step II (SPDP modification).

8.3.2.1 Fluorescamine assay for quantification of the primary amine groups

Fluorescamine, a non-fluorescent compound, rapidly reacts rapidly with primary amines in proteins, such as the terminal amino groups and the ε-amino groups of lysine residues, to form fluorophors which are excited at 390 nm and fluoresce at 475 nm [30]. The reaction is completed in 100-500 ms and excess reagent is quickly hydrolyzed to nonfluorescent products. The fluorescent product is stable for several hours.

Figure 8.5 shows the plot of Em_{470} vs. concentration for insulin standards, unmodified insulin (before step I), DMMA-modified insulin (after step I), and SPDP-modified insulin (after stem II). As can be seen from the Figure, the calibration plots for standard curve and unmodified insulin overlap and have comparable slopes. The slopes of the calibration curves greatly reduced after DMMA modification, indicating that the number of free amino groups per mole of insulin has reduced. Fluorescence values for corresponding concentrations of the SPDP-modified insulin are even lower indicating that the SPDP-modified derivative of insulin has fewer amino groups that are free to react with fluorescamine than the DMMA-modified insulin.

Ideally, PDP-insulin should not react with fluorescamine since a successfully modified insulin molecule should not have any free amino groups. But in actual reaction, some unreacted amino groups are to be expected that can react with fluorescamine to form the fluorophors. In Figure 8.6 the slopes of the calibration plots from Figure 8.5 are plotted against the expected number of free amino groups per mole of insulin for various samples. A linear correlation (r^2 = 0.9808) was observed indicating that the fluorescence drop correlated well with the conversion of free amino groups into intermediates that were unreactive towards fluorescamine.

This was an important finding since it established that the primary amines were indeed getting converted into intermediates owing to DMMA and SPDP modifications. However this assay did not provide much information about the reaction site specificity of the modification agents. Hence, mass spectroscopy analysis was performed on the insulin intermediates to confirm the modifications and to evaluate the specificity of the reagents for reaction with the primary amines.

8.3.2.1 Mass spectroscopy analysis of the insulin modifications

Figure 8.7 shows the mass spectra of unmodified bovine insulin in the negative mode. The mass to charge ratio (m/z) for the 4^- state was 1432 corresponding to the molecular weight of 5728 Da.

Mass spectra of the DMMA-modified insulin: Figure 8.8 shows the close up of the 4^- state MS spectra for DMMA-modified insulin in 50/50/1 H2O/MeOH/TEA. As can be seen from the spectra, most of the insulin was in 2:1 DMMA: insulin form indicated by the peak at 1495.3 m/z. Importantly, no peak was identified for 3:1 derivative of insulin indicating that the n-terminal amines were the main modification sites of DMMA at the pH of 6.8-6.9. Satellite peaks from the water loss from the original molecule can also be identified in the spectra.

Mass spectra of the SPDP-modified insulin: Figure 8.9 shows the SPDP-modified insulin intermediate. The 2:1:1 DMMA: Insulin: PDP peak can be identified at 1544.3 m/z ratio. It is interesting to note that a peak for 3:1 DMMA: insulin can be identified in the spectra. This could be due to the reaction of the residual DMMA at pH 9.0 with the lysine group. This samples analyzed by mass spectroscopy was not subjected to dialysis step for removal of unreacted DMMA before reacting the insulin with SPDP. This may explain the appearance of the 3:1 DMMA: insulin peak in the spectra.

Mass spectra of the trypsin digest of PDP-insulin intermediate: To further identify the sites of modification more accurately, mass spectra of the trypsin-digested modified insulin intermediate was studied. Figure 8.10 shows the sites of DMMA and SPDP modifications and the amide bonds digested by trypsin. As shown in the Figure, trypsin can digest the insulin molecule at the amide bond between B23Arg and B24Gly groups forming a 43 amino acid long peptide (Ins-43) containing the n-terminals and a smaller 8 amino acid peptide (Ins-8) containing

the B chain c-terminal of the original molecule. These peptide fragments were then individually analyzed. Figure 8.11 shows the mass spectra of the Ins-43 peptide fragment (3^- state). As expected peaks corresponding to both 1:1 and 2:1 DMMA: Ins were identified in the spectra, but no peak was identified for PDP attached to Ins-43. This indicates that the PDP did not attach at the n-terminal primary amines.

The mass spectra for Ins-8 is shown in Figure 8.12. The 8 amino acid peptides (G-F-F-Y-T-P-K-A) were further fragmented into smaller peptides by collision induced dissociation. From the fragments generated, two peptide fragments were analyzed; Y4 (T-P-K-A) and B7 (G- F- F-Y-T-P-K), such that both the peptides contained the lysine residue. The table inserted in Figure 8.12 shows the expected m/z ratio for the PDP attached states of Ins-8, (GFFYTPKA)-PDP; Y4, (TPKA)-PDP and B7, (GFFYTPK)-PDP. As seen in the spectra, PDP attachment was identified to all the peptide fragments. This indicated that the PDP was attached to amino acid residues common to Y4 and B7 (T, P,K).

Further analysis of a smaller peptide segment containing only the two terminal amino acids (Y2, K-A) indicates that the PDP was attached to the lysine residue of the insulin molecule (Figure 8.13). This is a very important result since the site of PDP modification site is verified as the B29 lysine group by isolating only the two terminal amine groups from the insulin macromolecular structure.

The data from mass spectroscopy and fluorescamine assay together provide evidence that the SPDP modification is primarily at B29Lys and the

DMMA modification sites are A1Gly and B1Phe. These are very important results since improper modification may result in reduction or complete loss of insulin activity. Further evidence of the biological activity of insulin in the conjugated form is given in chapter 11.

8.3.3 Analysis of the Insulin-Transferrin Conjugates

8.3.3.1 HPLC analysis the Insulin-Transferrin Conjugates

It was important to develop a HPLC method for quantitative determination of the conjugate for subsequent studies. Figure 8.14 shows the HPLC chromatogram for insulin, transferrin and the purified conjugate. The insulin eluted from the C4 column due to the applied gradient with a retention time of approximately 3.4 min, where as the transferrin and the conjugates eluted at around 4.5 and 7.5 min respectively. More importantly, the chromatogram of the purified conjugate did not show any peak for transferrin or insulin, indicating that the conjugate was essentially pure and did not contain either of the unmodified proteins. Based on these results, a standard curve for conjugate was prepared.

8.3.3.2 SDS-PAGE analysis of the In-Tf conjugate

SDS-PAGE analysis of the conjugate revealed a single band for the conjugate at around 90 kDa (Figure 8.15). This was close to the expected molecular weight of about 91.6 kDa for the conjugate which contains two

molecules of 5.73 kDa insulin attached to one molecule transferrin (80 kDa). No peak for the unmodified transferrin was observed in the lane for the conjugate. Bovine serum albumin (BSA) was run along with the conjugate and transferrin for comparison.

8.3.4 Enzymatic Stability of Insulin-Transferrin Conjugates

Intact insulin-transferrin conjugate has been shown to reach systemic circulation in diabetic rats [12]. In these studies insulin and insulin transferrin conjugates were orally administered in diabetic rats in a 30 mg/ml $NaHCO_3$ solution to neutralize the gastric acidity and to protect digestion of proteins in the stomach. However there was no mechanism to reduce the degradation of insulin or the conjugate in the intestinal milieu. Even in the absence of such a mechanism, the conjugate was able to reach the systemic circulation without getting completely degraded. This provides an indirect evidence of increased stability of the conjugated insulin against tryptic and chymotryptic attack. However this improvement in the stability of the conjugate in enzymatic solution has not been demonstrated experimentally. Hence in this study, the degradation profiles of insulin, transferrin and the conjugate were evaluated in a solution containing trypsin. As can be seen from Figure 8.16, Most of the insulin degraded due to tryptic attack within 15 minutes of incubation, whereas transferrin was significantly more stable at the same enzyme concentrations. The conjugate degraded at a faster rate as compared to transferrin, but was more stable than

the unmodified insulin. The degradation rate constants were calculated from the slope of the semi-log plot of the percentage of initial protein remaining vs. time (Figure 8.17 and Table 8.1). The degradation rate constant calculated was 21.1 x 10^{-3} min^{-1} for insulin and 0.73 x 10^{-3} min^{-1} and 6.17 x 10^{-3} min^{-1} for the transferrin and the conjugate, respectively. These data indicated that the stability of insulin was significantly increased due to its conjugation with transferrin. This may be one of the important factors contributing to the observed hypoglycemic effect of the orally administered conjugates. Although the reasons behind the observed increase in stability of the conjugate are not clearly understood, this may be due to the shielding effect of the transferrin which limits enzymatic degradation of insulin. Transferrin has been shown to be resistant to tryptic and chymotryptic digestion [13]. Thus the large transferrin molecule may stabilize the conjugated insulin against enzymes by creating a hindrance for the enzymatic attack.

As shown in chapter 8, the complexation hydrogels are able to protect protein degradation in both gastric and intestinal environments. Orally administered conjugate in the form of conjugate-loaded polymer microparticles may have even higher stability from proteolytic attack, due to limited diffusion of the conjugate out of the microparticles into the stomach and inhibition of the intestinal enzymes by the polymer microparticles.

8.4 Conclusions

Insulin-transferrin conjugate was synthesized by site-specific modification of insulin and modification of transferrin by a heterobifunctional crosslinker. Proper modification of the insulin molecule, which is critical to its physiological function, was verified through fluorescence photometry and mass spectroscopy. The conjugation resulted in a macromolecular heteroconjugate of controlled stoichiometry consisting of two insulin molecules and one transferrin molecule. A HPLC-based method was established to be used in quantitative determination of conjugate in subsequent studies. Insulin in the conjugated form also exhibited enhanced stability against proteolytic attack. This, combined with ability of complexation hydrogels to prevent protein degradation in gastric and intestinal environment, should further enhance the stability of insulin.

References

1 Lowman, A. M., Morishita, M., Kajita, M., Nagai, T. and Peppas, N. A. (1999) Oral delivery of insulin using pH-responsive complexation gels. J Pharm Sci **88**, 933-937

2 Morishita, M., Lowman, A. M., Takayama, K., Nagai, T. and Peppas, N. A. (2002) Elucidation of the mechanism of incorporation of insulin in controlled release systems based on complexation polymers. J Control Rel **81**, 25-32

3 Lowman, A. M. and Peppas, N. A. (1997) Analysis of the Complexation/Decomplexation Phenomena in Graft Copolymer Networks. Macromolecules **30**, 4959 -4965

4 Lopez, J. E. and Peppas, N. A. (2004) Effect of poly (ethylene glycol) molecular weight and microparticle size on oral insulin delivery from P(MAA-g-EG) microparticles. Drug Dev Ind Pharm **30**, 497-504

5 Lopez, J. E. and Peppas, N. A. (2004) Cellular evaluation of insulin transmucosal delivery. J Biomater Sci Polym Ed **15**, 385-396

6 Gosk, S., Vermehren, C., Storm, G. and Moos, T. (2004) Targeting anti-transferrin receptor antibody (OX26) and OX26-conjugated liposomes to brain capillary endothelial cells using in situ perfusion. J Cereb Blood Flow Metab **24**, 1193-1204

7 Vinogradov, S. V., Batrakova, E. V. and Kabanov, A. V. (2004) Nanogels for oligonucleotide delivery to the brain. Bioconjug Chem **15**, 50-60

8 Burdo, J. R., Antonetti, D. A., Wolpert, E. B. and Connor, J. R. (2003) Mechanisms and regulation of transferrin and iron transport in a model blood-brain barrier system. Neuroscience **121**, 883-890

9 Bickel, U., Yoshikawa, T. and Pardridge, W. M. (2001) Delivery of peptides and proteins through the blood-brain barrier. Adv Drug Deliv Rev **46**, 247-279

10 Qian, Z. M., Li, H., Sun, H. and Ho, K. (2002) Targeted drug delivery via the transferrin receptor-mediated endocytosis pathway. Pharmacol Rev **54**, 561-587

11 Li, H. and Qian, Z. M. (2002) Transferrin/transferrin receptor-mediated drug delivery. Med Res Rev **22**, 225-250

12 Xia, C. Q., Wang, J. and Shen, W. C. (2000) Hypoglycemic effect of insulin-transferrin conjugate in streptozotocin-induced diabetic rats. J Pharmacol Exp Ther **295**, 594-600

13 Azari, P. R. and Feeney, R. E. (1958) Resistance of metal complexes of conalbumin and transferrin to proteolysis and to thermal denaturation. J Biol Chem **232**, 293-302

14 Banerjee, D., Flanagan, P. R., Cluett, J. and Valberg, L. S. (1986) Transferrin receptors in the human gastrointestinal tract. Relationship to body iron stores. Gastroenterology **91**, 861-869

15 Shah, D. and Shen, W. C. (1996) Transcellular delivery of an insulin-transferrin conjugate in enterocyte-like Caco-2 cells. J Pharm Sci **85**, 1306-1311

16 Thorpe, P. E., Wallace, P. M., Knowles, P. P., Relf, M. G., Brown, A. N., Watson, G. J., Blakey, D. C. and Newell, D. R. (1988) Improved antitumor effects of immunotoxins prepared with deglycosylated ricin A-chain and hindered disulfide linkages. Cancer Res **48**, 6396-6403

17 Carlsson, J., Drevin, H. and Axen, R. (1978) Protein thiolation and reversible protein-protein conjugation. N-Succinimidyl 3-(2-pyridyldithio)propionate, a new heterobifunctional reagent. Biochem J **173**, 723-737

18 Stuchbury, T., Shipton, M., Norris, R., Malthouse, J. P., Brocklehurst, K., Herbert, J. A. and Suschitzky, H. (1975) A reporter group delivery system with both absolute and selective specificity for thiol groups and an improved fluorescent probe containing the 7-nitrobenzo-2-oxa-1,3-diazole moiety. Biochem J **151**, 417-432

19 Faulstich, H., Zobeley, S., Heintz, D. and Drewes, G. (1993) Probing the phalloidin binding site of actin. FEBS Lett **318**, 218-222

20 Bradford, M. M. (1976) A rapid and sensitive method for the quantitation of microgram quantities of protein utilizing the principle of protein-dye binding. Anal Biochem **72**, 248-254

21 Mei, H., Yu, C. and Chan, K. K. (1999) NB1-C16-insulin: site-specific synthesis, purification, and biological activity. Pharm Res **16**, 1680-1686

22 Lorenzen, A. and Kennedy, S. W. (1993) A fluorescence-based protein assay for use with a microplate reader. Anal Biochem **214**, 346-348

23 Garnett, M. C. (2001) Targeted drug conjugates: principles and progress. Adv Drug Deliv Rev **53**, 171-216

24 Melton, R. G. and Sherwood, R. F. (1996) Antibody-enzyme conjugates for cancer therapy. J Natl Cancer Inst **88**, 153-165

25 Saito, G., Swanson, J. A. and Lee, K. D. (2003) Drug delivery strategy utilizing conjugation via reversible disulfide linkages: role and site of cellular reducing activities. Adv Drug Deliv Rev **55**, 199-215

26 Thorpe, P. E., Wallace, P. M., Knowles, P. P., Relf, M. G., Brown, A. N., Watson, G. J., Knyba, R. E., Wawrzynczak, E. J. and Blakey, D. C. (1987) New coupling agents for the synthesis of immunotoxins containing a hindered disulfide bond with improved stability in vivo. Cancer Res **47**, 5924-5931

27 Lindsay, D. G. and Shall, S. (1971) The acetylation of insulin. Biochem J **121**, 737-745

28 Nakashima, K., Miyagi, M., Goto, K., Matsumoto, Y. and Ueoka, R. (2004) Enzymatic and hyperglycemia stability of chemically modified insulins with hydrophobic acyl groups. Bioorg Med Chem Lett **14**, 481-483

29 Mohammed, A. and Dent, A. (1998) Bioconjugation: protein coupling techniques for the biomedical sciences. Grove's Dictionaries, New York

30 Udenfriend, S., Stein, S., Bohlen, P., Dairman, W., Leimgruber, W. and Weigele, M. (1972) Fluorescamine: a reagent for assay of amino acids, peptides, proteins, and primary amines in the picomole range. Science **178**, 871-872

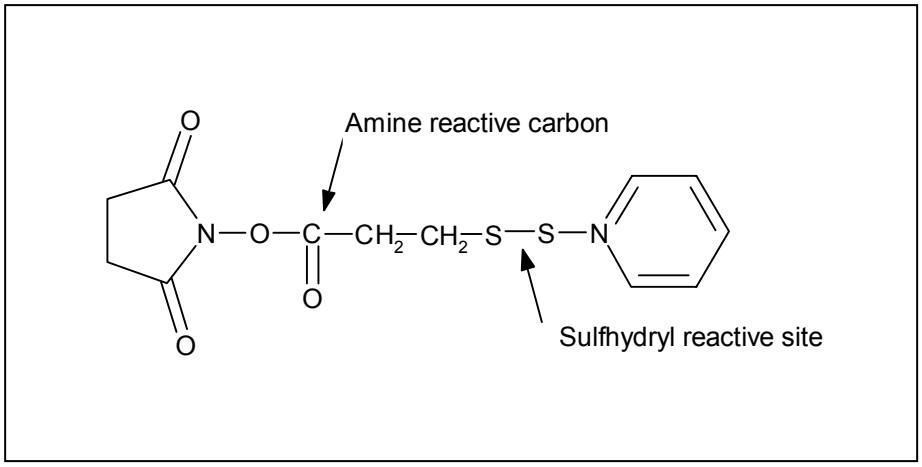

Figure 8.1 Succinimidyl 3-(2-pyridyldithio)propionate (SPDP), a heterobifunctional, cleavable crosslinker for protein crosslinking. Contains amine-reactive N-hydroxysuccinimide (NHS) ester, and sulfhydryl reactive pyridyldithio groups.

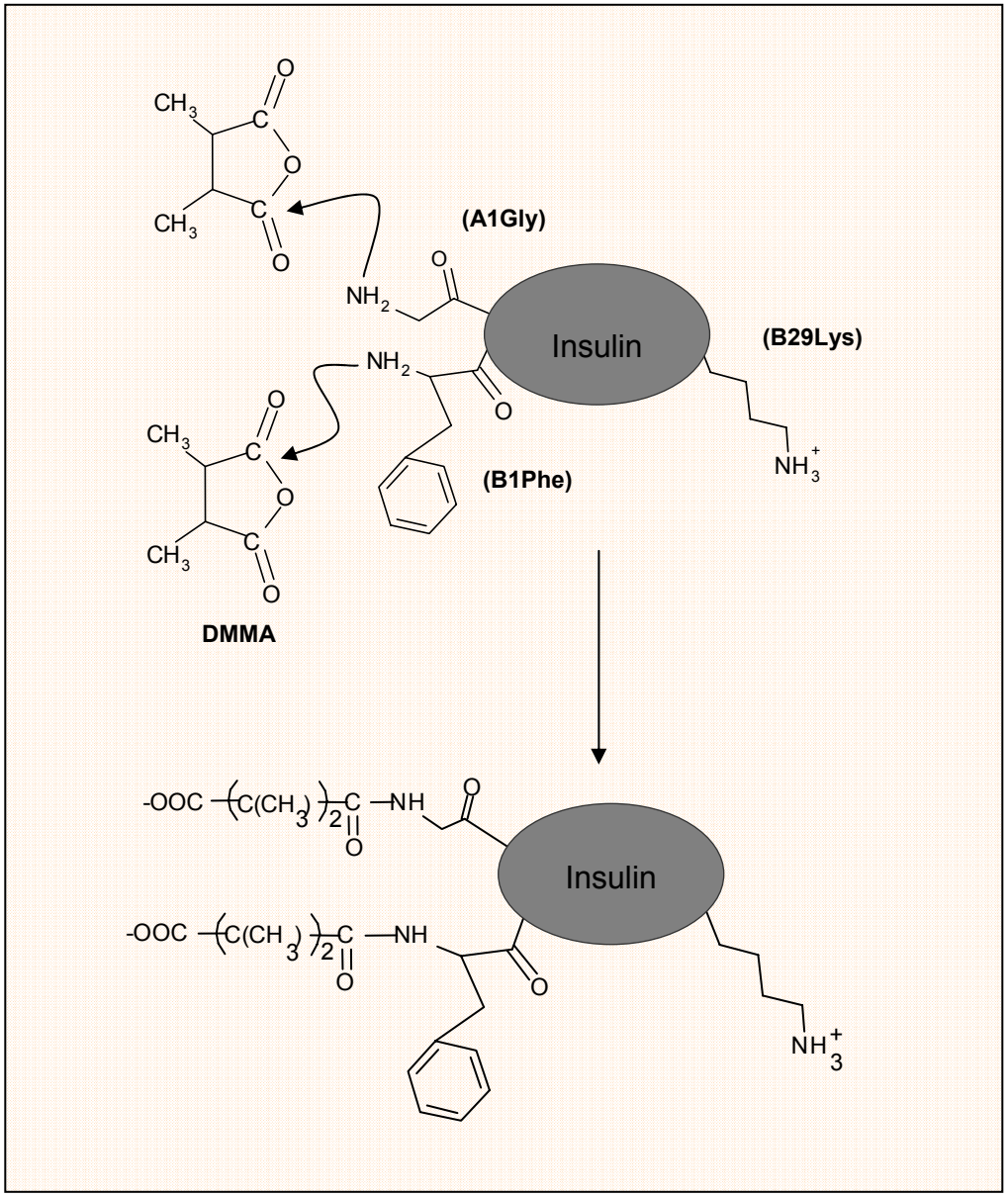

Figure 8.2A Conjugation reaction, step I (DMMA blocking of the n-terminal amine groups). DMMA reaction with insulin at pH of 6.8-6.9. Only the primary amines at n-terminal are deprotonated and are able to react with DMMA. Primary amine at B29 lysine residue is protonated and does not react with DMMA.

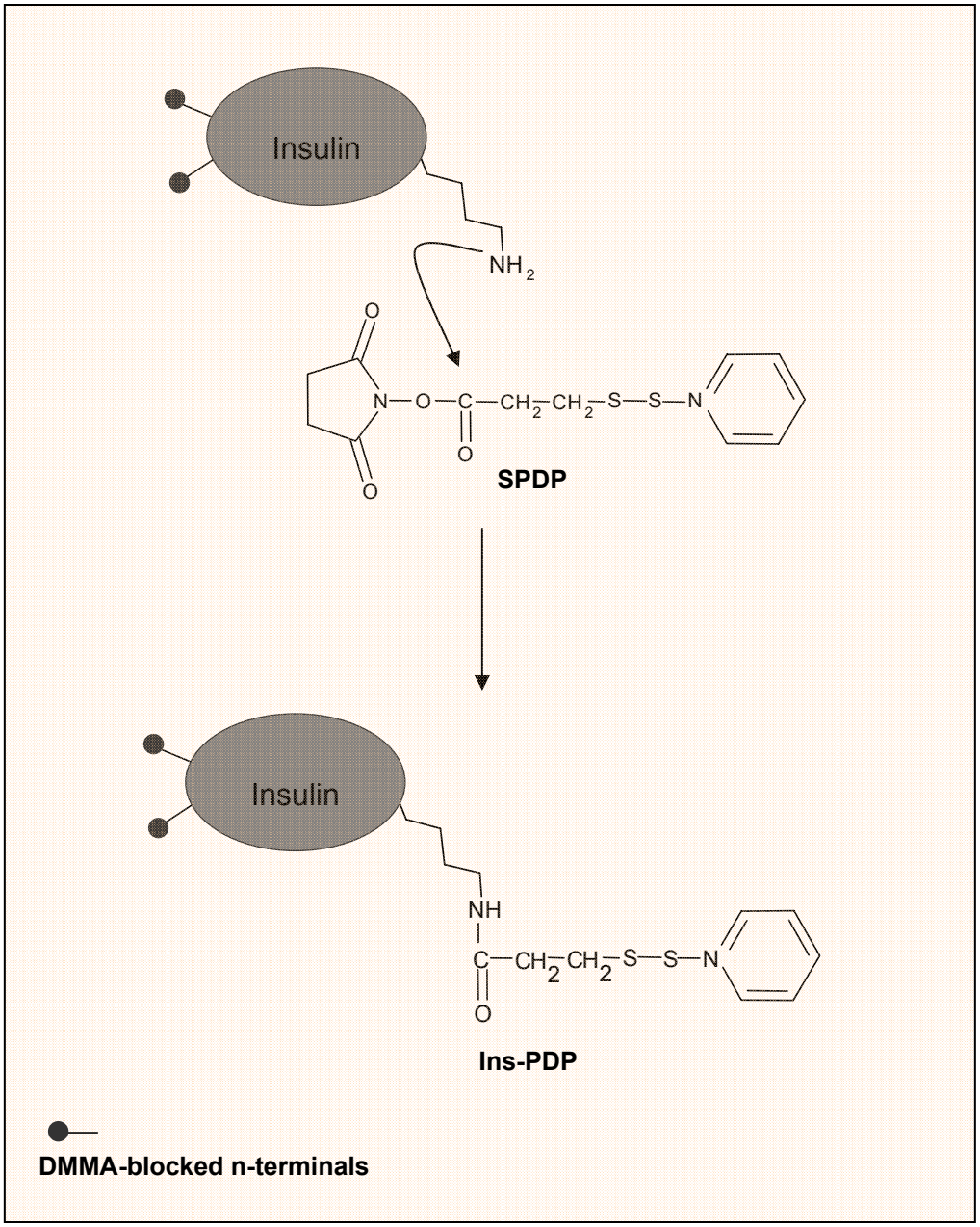

Figure 8.2B Conjugation reaction, step II (SPDP reaction with DMMA-modified insulin). SPDP reacts with DMMA-modified insulin at pH 9.0 to form Insulin-PDP.

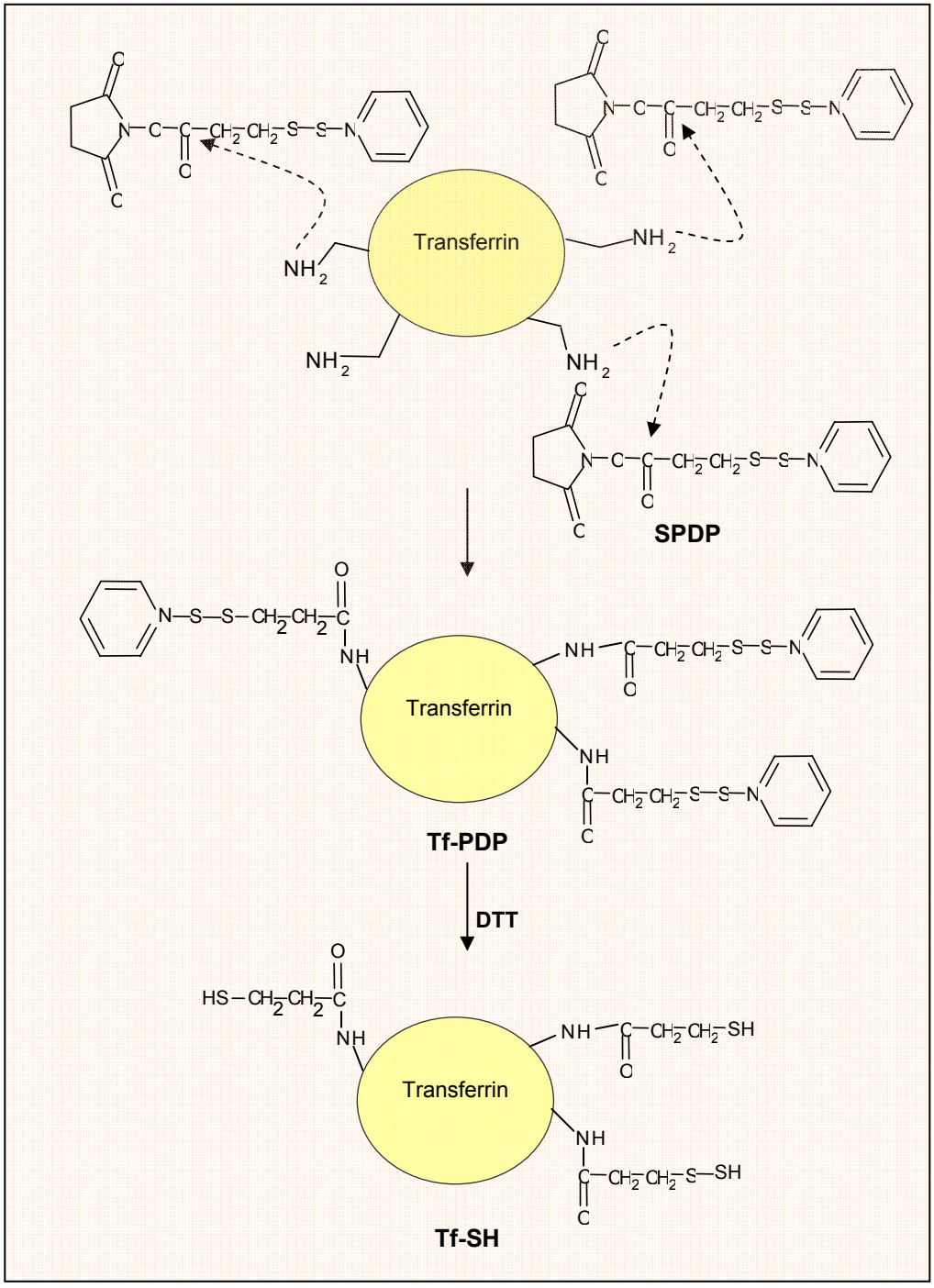

Figure 8.2C Conjugation reaction, step III (SPDP modification of transferrin). SPDP reacts with transferrin at pH 7.0 to form Tf-PDP. The modification ratio can be controlled by altering the amount of SPDP reacted with transferrin. Purified Tf-PDP is then reacted with DTT to generate free thiol groups on transferrin (Tf-SH)

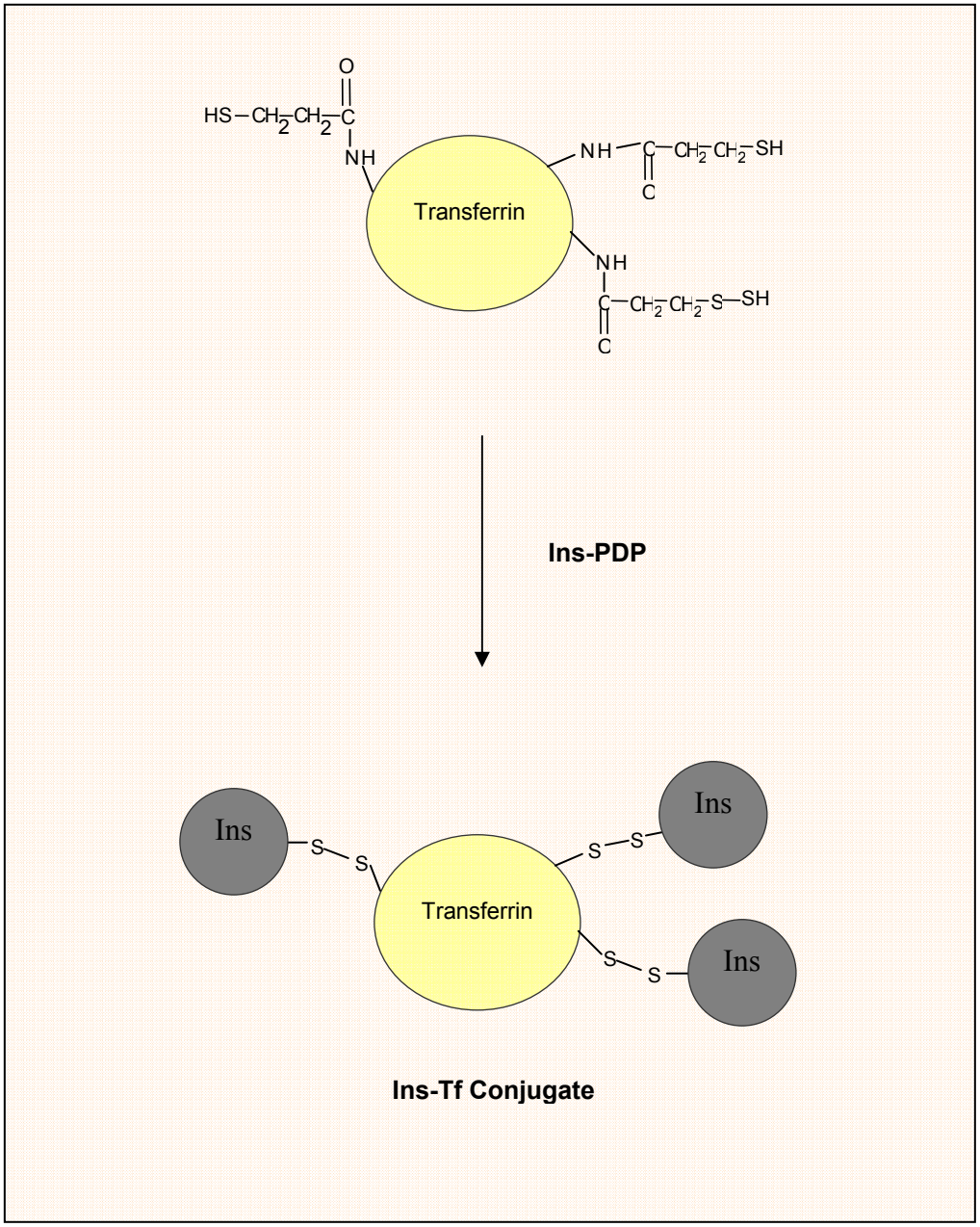

Figure 8.2D Conjugation reaction, step IV (Ins-PDP reaction with Tf-SH). Purified Tf-SH reacts with Ins-PDP obtained from step II to form Ins-Tf conjugate.

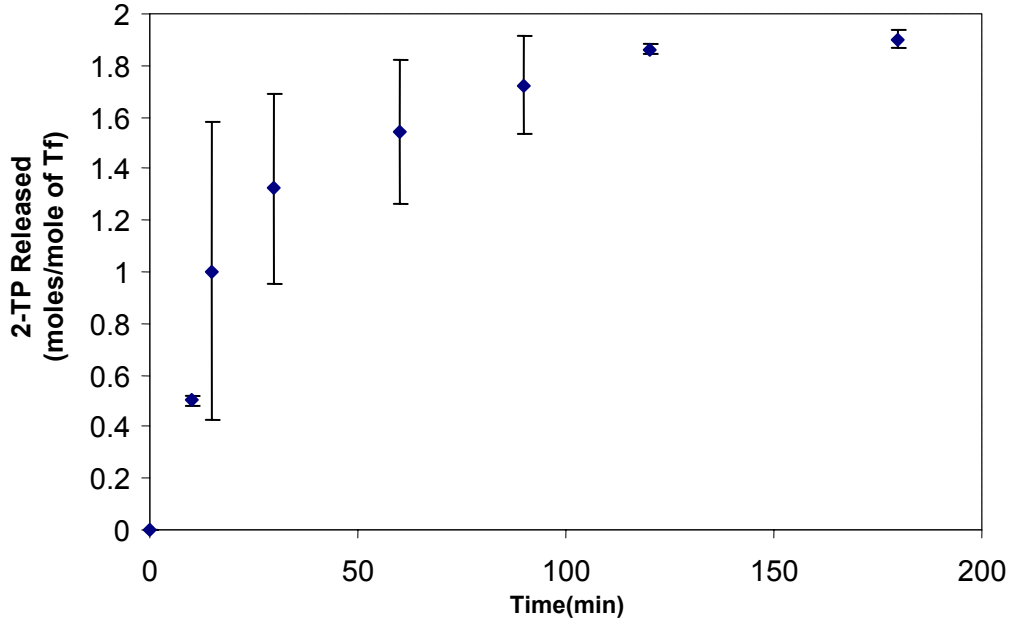

Figure 8.3 Conjugation reaction progress monitored by release of 2-pyridinethio (2-TP) released per mole of transferrin. 40 µl samples were withdrawn at predetermined time intervals and diluted with 660 µl phosphate buffer. Absorbance of the samples was measured by a microplate reader (n=2).

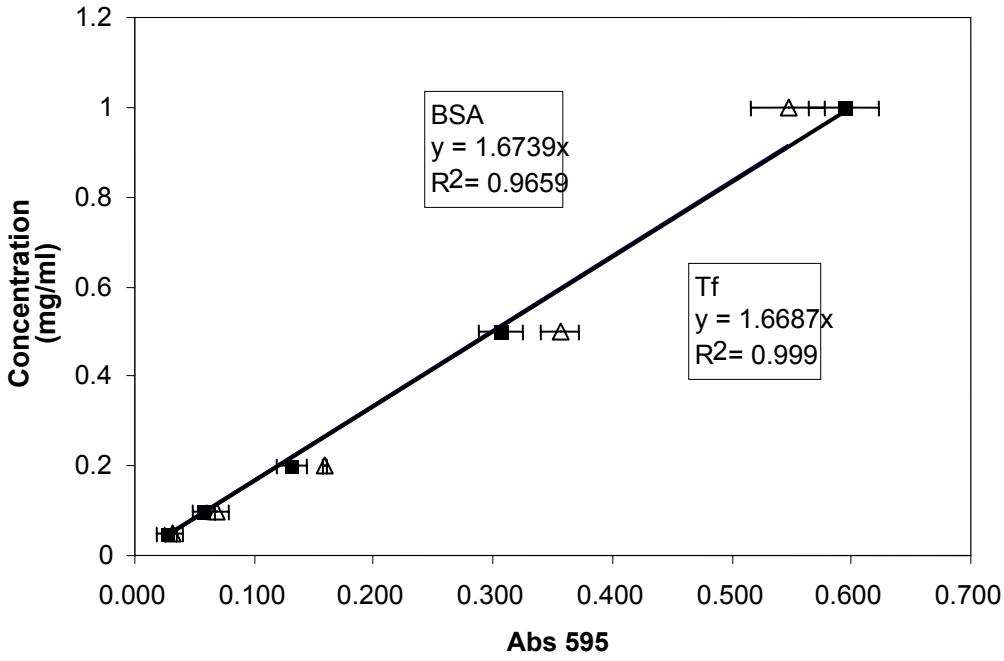

Figure 8.4 Bradford assay standard curves for measurement of conjugate concentration. 20 µl of the protein samples (BSA standard Δ or transferrin standard ■) were added to 1 ml of bradford reagent and the absorbance was detected with a microplate reader at 595 nm (n=2).

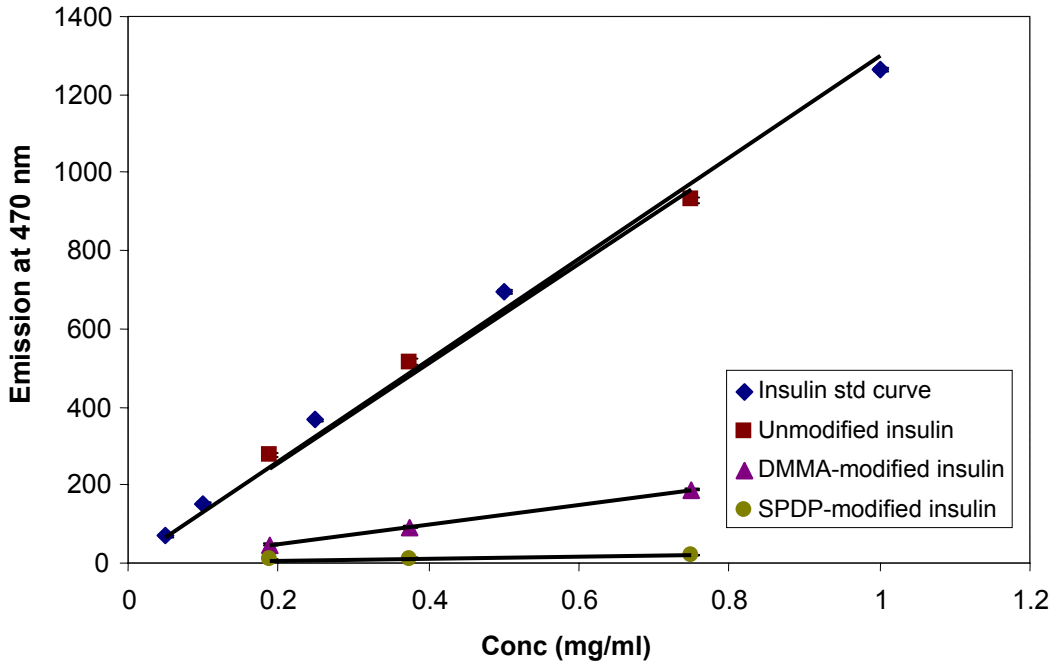

Figure 8.5 Fluorescamine assay for determination of free amine groups of insulin. 50 µl of 1.08 mM fluorescamine in acetone was added to 150 µl protein samples (insulin standard, unmodified insulin, DMMA-modified insulin, or SPDP-modified insulin) in a microplate reader. The fluorescence associated with the samples was measured with a microplate reader (Excitation at 390 nm and emission at 470 nm) (Error bars smaller than the symbols n=3).

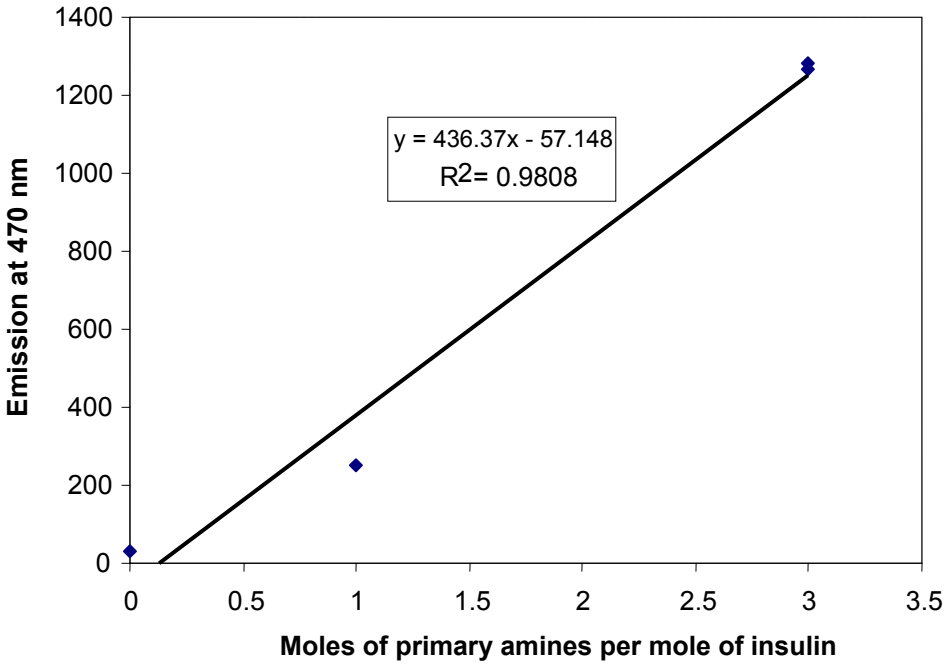

Figure 8.6 Fluorescamine assay for determination of free amine groups of insulin. Slopes of the linear relationship between emission at 470 nm vs. concentration for various insulin samples (insulin standard, unmodified insulin, DMMA-modified insulin, or SPDP-modified insulin) plotted against the expected number of moles of free amine groups per mole of insulin.

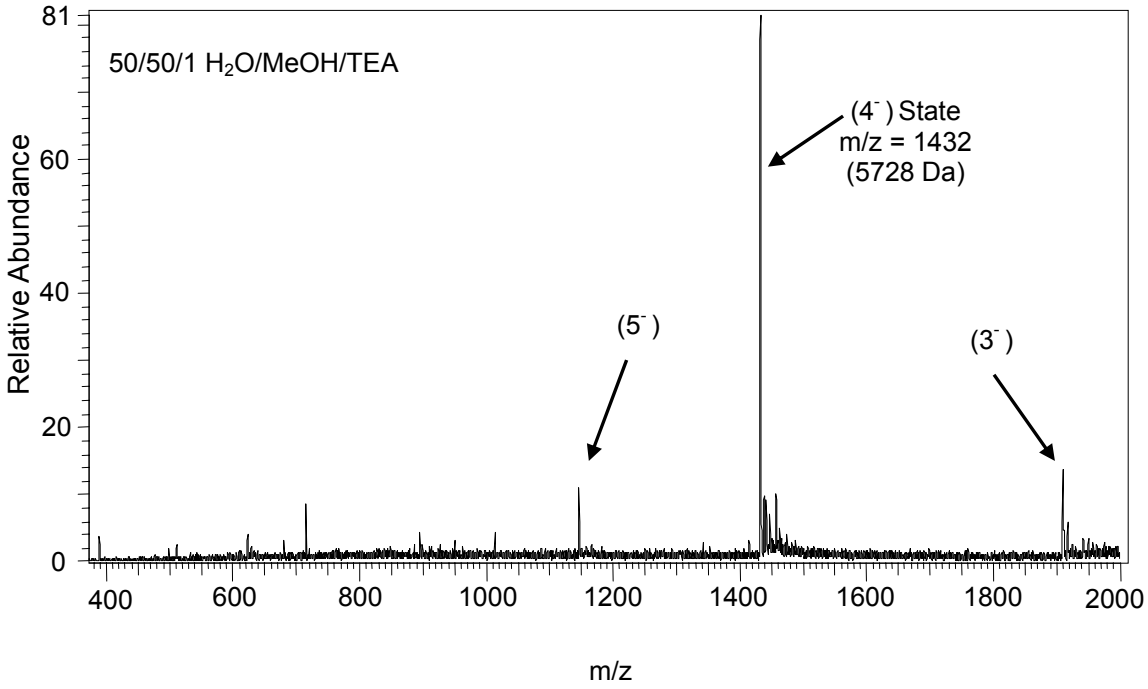

Figure 8.7 Mass spectra of unmodified bovine insulin showing various charged state. The 4^- state with a mass to charge ratio of 1432 corresponds to 5728 Da

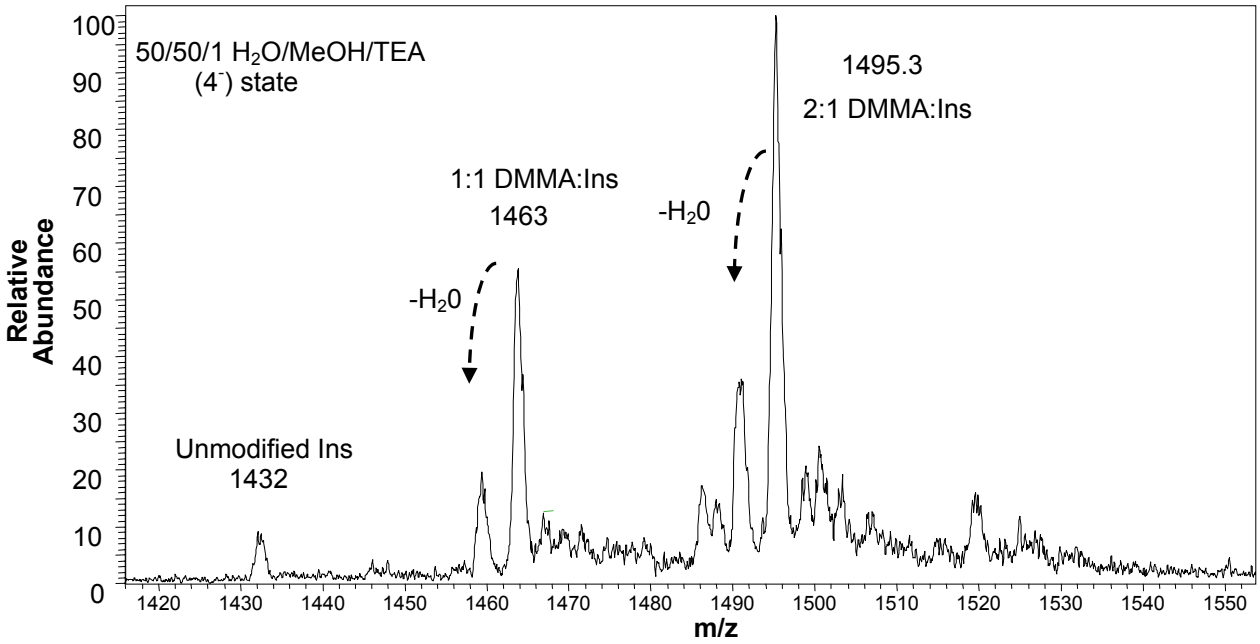

Figure 8.8 Mass spectra of the DMMA-modified bovine insulin (4^- state) in 50/50/1 H_2O/MeOH/TEA. Peak for the 2:1 DMMA: insulin is identified at 1495.3 m/z ratio.

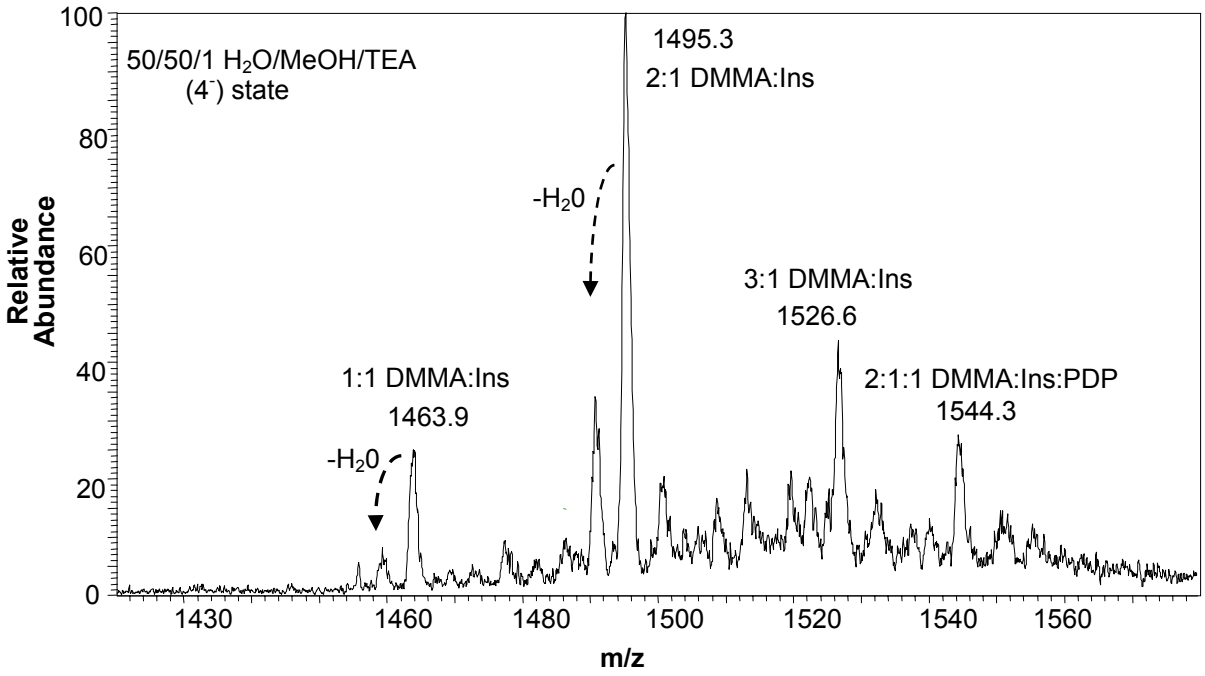

Figure 8.9 Mass spectra of the SPDP-modified bovine insulin (4^- state) in 50/50/1 H_2O/MeOH/TEA. Peak for the 2:1:1 DMMA: insulin: PDP is identified at 1544.3 m/z ratio. No peak for 2:1 PDP is seen in the spectra

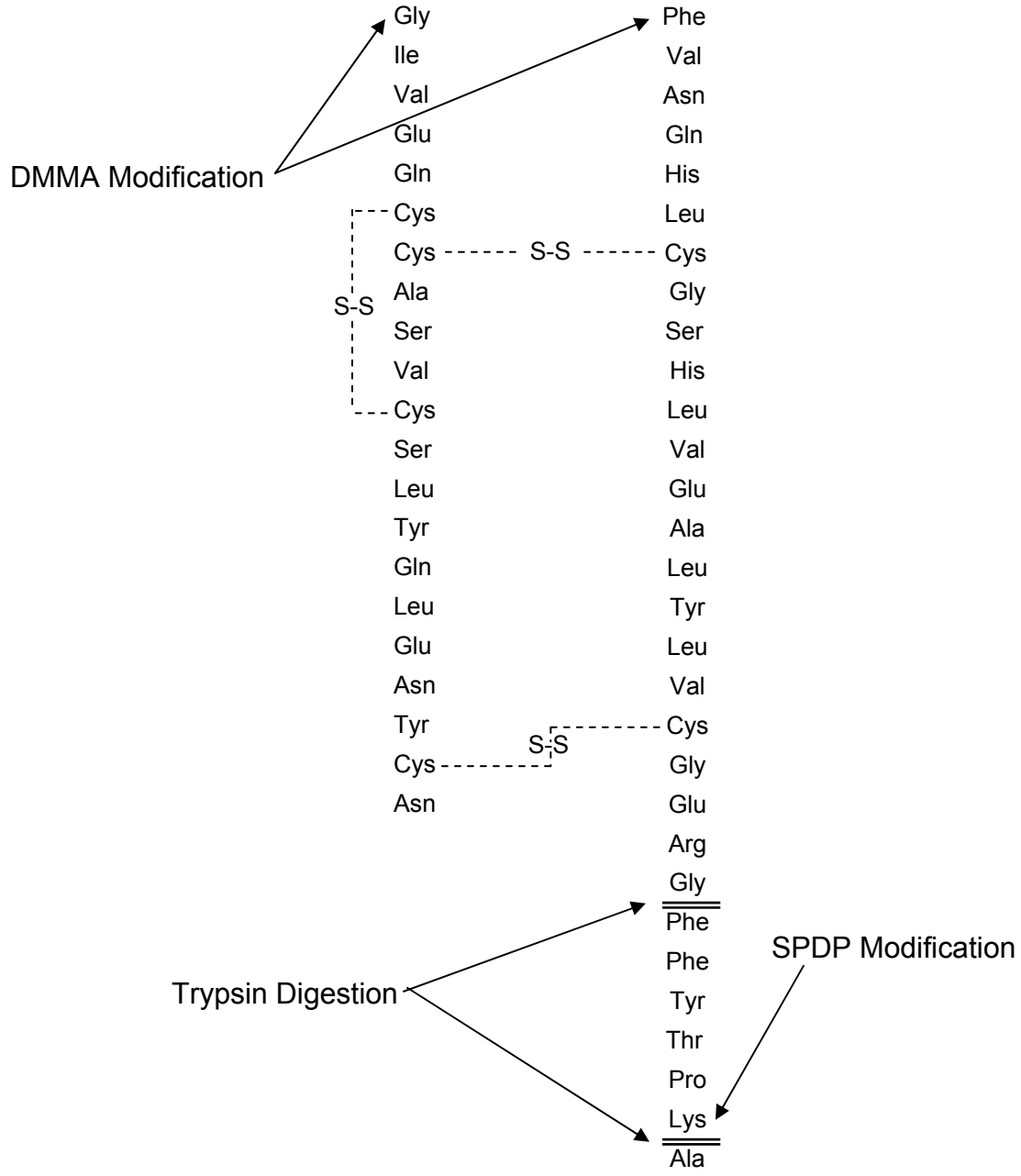

Figure 8.10 Insulin primary structure showing modification sites of DMMA, SPDP and sits of trypsin digestion.

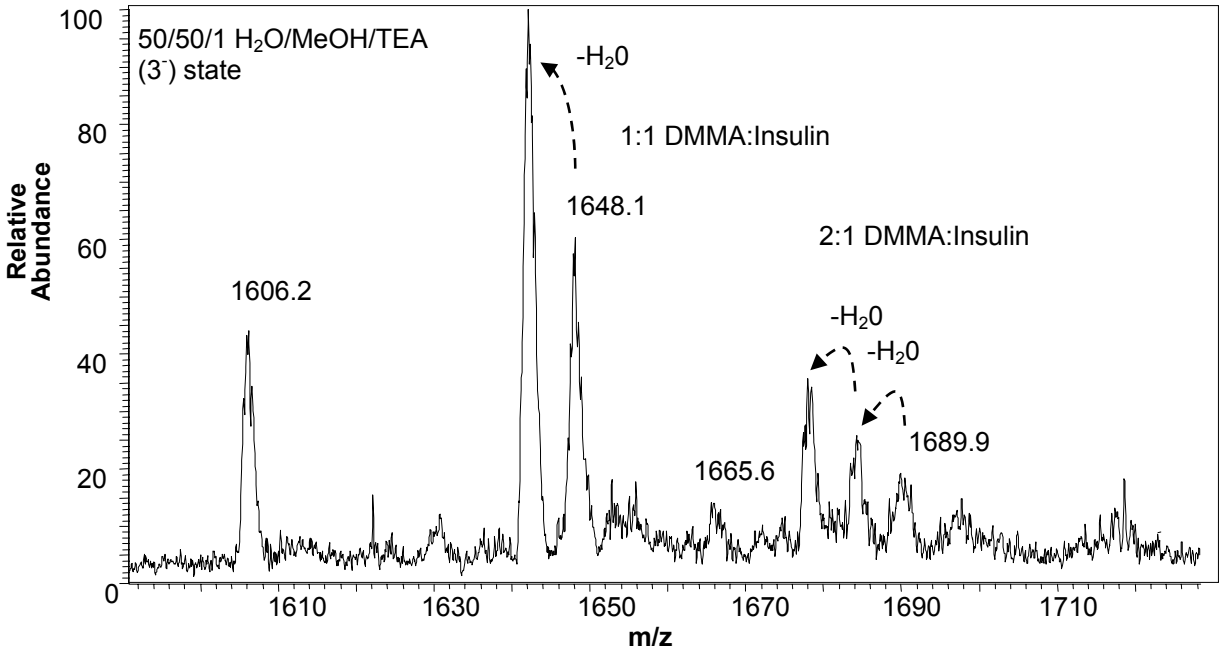

Figure 8.11 Mass spectra of the trypsin digest of the larger peptide formed after trypsin digestion (Ins-43). The spectra was obtained in 50/50/1 H2O/MeOH/TEA and the charge state was 3-. No peak for PDP derivative of Ins-43 was identified in the mass spectra

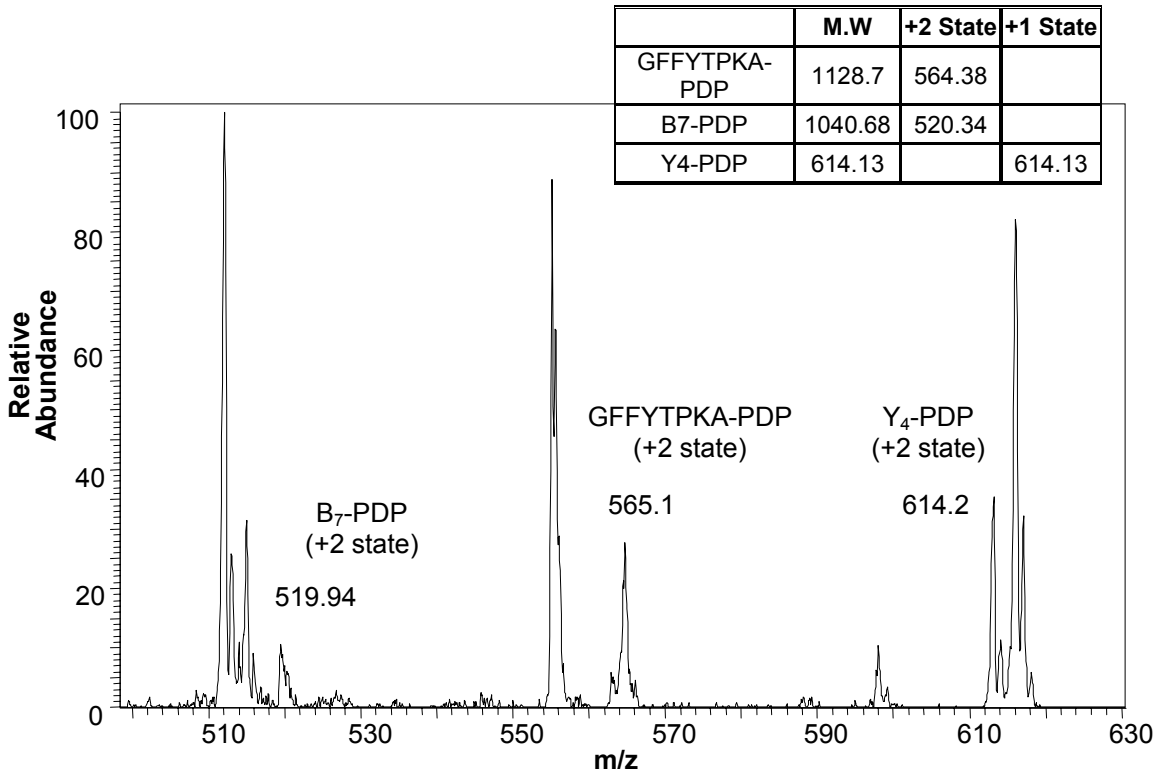

Figure 8.12 Mass spectra of the trypsin digest of the smaller peptide formed after trypsin digestion (Ins-8). The inserted table shows the estimated molecular weights of the PDP-attached peptide fragments in +2 or +1 states. The molecular weights are estimate based on the molecular weights of individual amino acids in the fragments and the molecular weight of PDP.

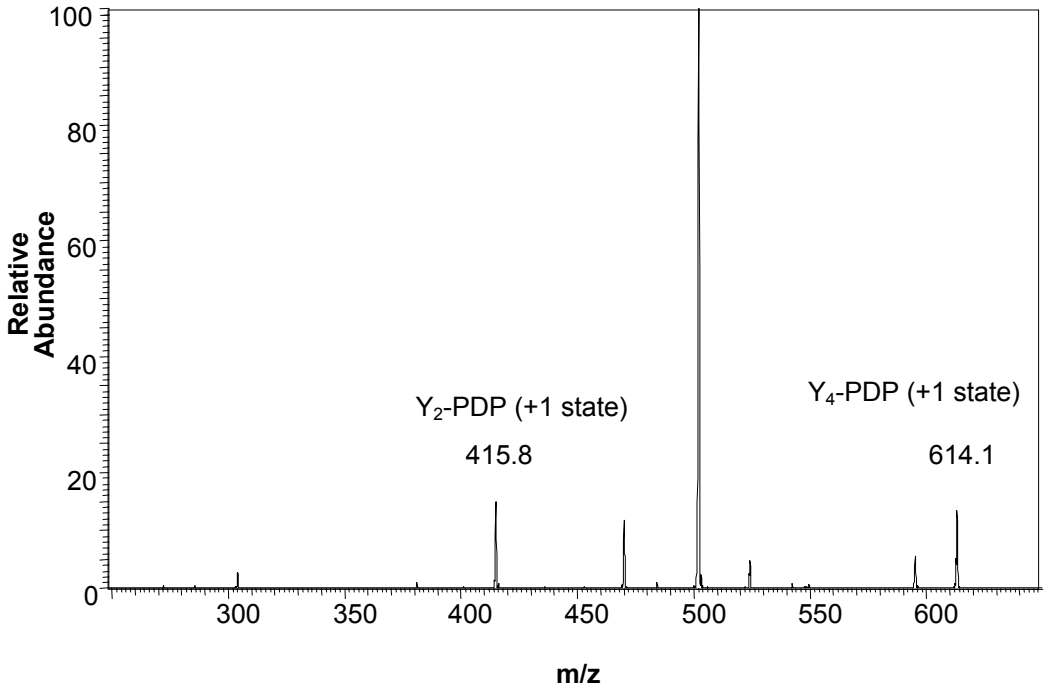

Figure 8.13 Mass spectra of the n-terminal peptide fragments of insulin obtained by collision induced dissociation of the trypsin digest. +1 charge states of Y2-PDP, (KA)-PDP; and Y4-PDP, (TPKA)-PDP are identified.

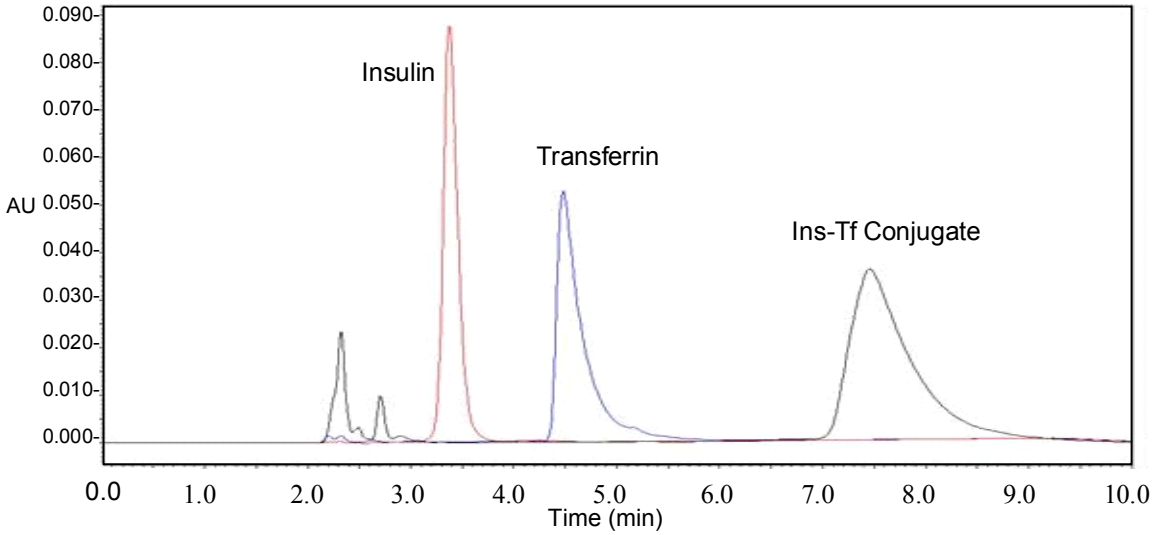

Figure 8.14 HPLC chromatograms of insulin, transferrin and insulin-transferrin conjugate. The mobile phase for the analysis consisted of a linear gradient of 70% of solvent A to 40% of solvent A in 6 min. A Symmetry300™ C4 column (particle size 5 μm, 3.9mm i.d. ×150mm length) was used for the separation.

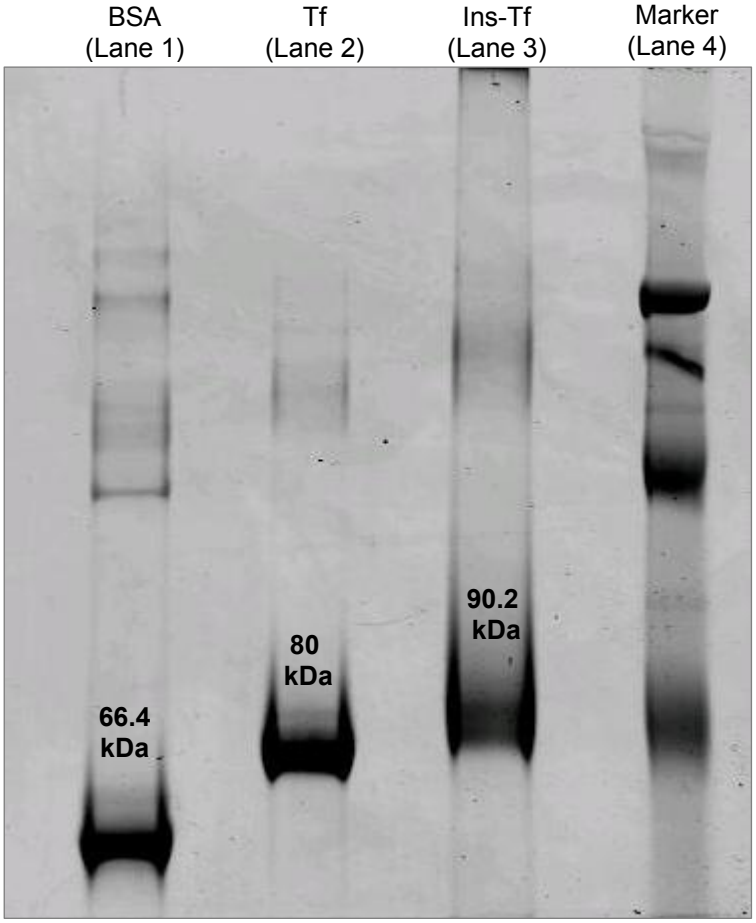

Figure 8.15 SDS-PAGE analysis of the insulin-transferrin conjugate. 5 µl of 1mg/ml protein solutions mixed with 10 µl sample buffer and 25 µl DI water and heated at 70 ^{o}C for 10 minutes. 25 µl of each solution was then loaded into the wells. The gel was run at 150 V for 2 hours and then stained with Coomassie G-250 after washing the gel. After 1 hr of staining the gel was washed in DI water for 1 hr.

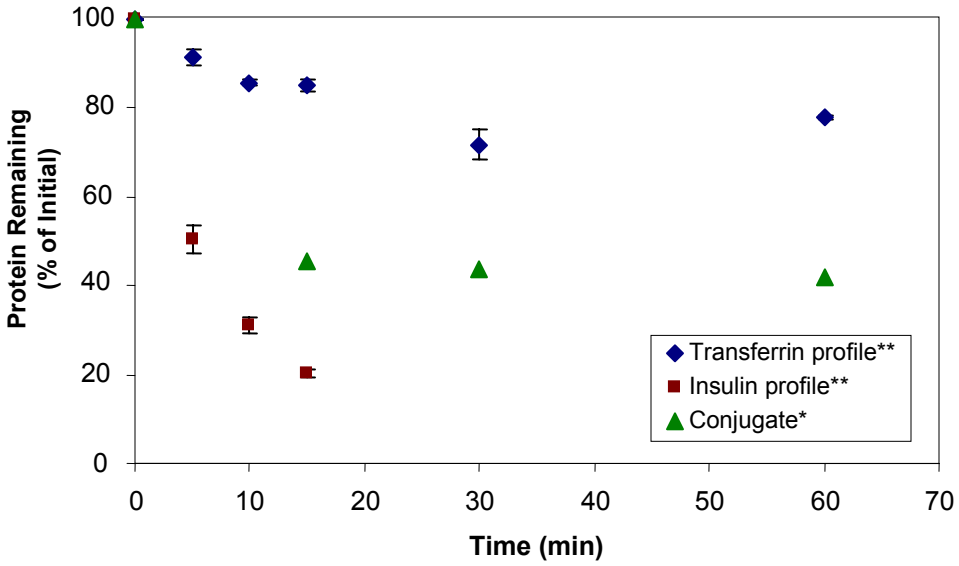

Figure 8.16 Protein degradation profiles in the simulated intestinal fluid. Initial protein concentrations in the reaction was 1 mg/ml and the trypsin concentration was 3.2 mg/ml. The total reaction volume was 5 ml and the pH was 7.4. 50 µl samples were withdrawn at different time intervals and the trypsin activity in the samples was stopped by addition of equal volumes of 50% acetic acid solution. ** n=3, * n=1

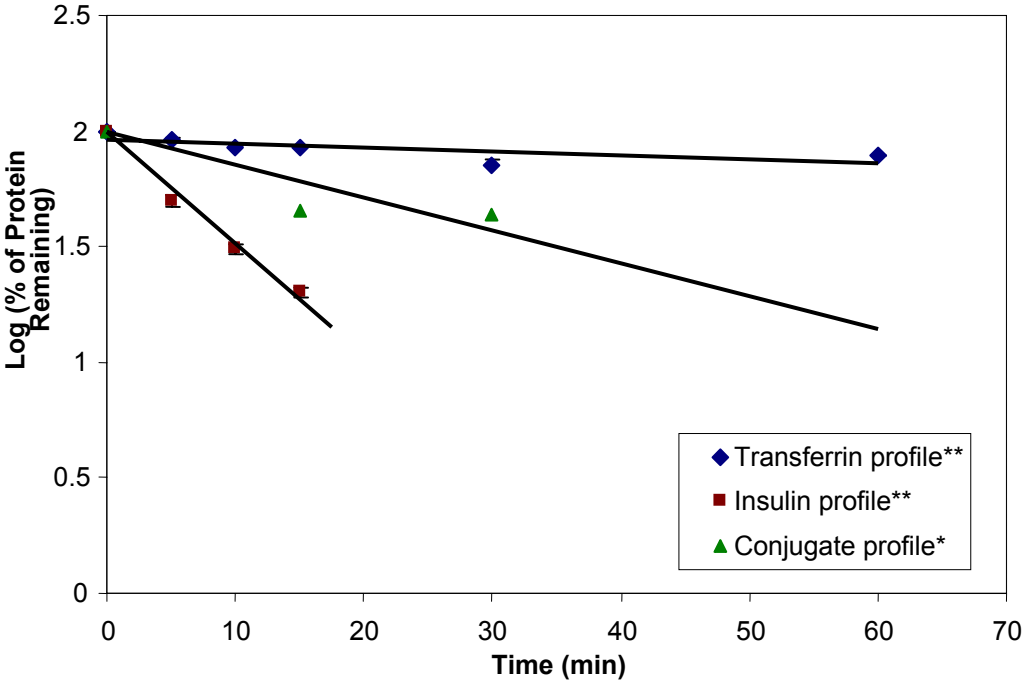

Figure 8.17 Log of %protein remaining vs. time (min). Initial protein concentrations in the reaction was 1 mg/ml and the trypsin concentration was 3.2 mg/ml. The total reaction volume was 5 ml and the pH was 7.4. 50 µl samples were withdrawn at different time intervals and the trypsin activity in the samples was stopped by addition of equal volumes of 50% acetic acid solution. ** n=3, * n=1

Table 8.1 Degradation rate constants for insulin, transferrin and conjugate in the presence of trypsin. Rate constants were calculated from the slope of semi-log plot of %protein remaining vs. time (Figure 8.18).

Protein	**Slope (min^{-1})**	**Degradation rate constant (K) (min^{-1}) x 10^3**
Insulin	-0.0486	21.10
Transferrin	-0.0017	0.73
Conjugate	-0.0142	6.17

CHAPTER 9

LOADING AND RELEASE OF INSULIN-TRANSFERRIN CONJUGATES FROM COMPLEXATION HYDROGELS

9.1 Introduction

The loading and release of Ins-Tf conjugate from the complexation hydrogels is described in this chapter. The P(MAA-g-EG) complexation hydrogels have been specifically designed for optimized oral delivery of small molecular weight drugs and therapeutic proteins. The complexation/decomplexation phenomenon in these polymer networks renders them pH responsive. The pH increase upon transit from the gastric environment into the upper small intestine causes the network to swell, resulting in an increase in the mesh size of the network. The entrapped molecules can be released from the networks at the increased pH.

Thus, optimizing the delivery systems for the specific drug molecule of interest is an important step in developing oral delivery formulations. The complexation hydrogels can be tailored for optimized delivery of both small molecular weight drugs and large molecular weight proteins and peptides. In our laboratory, polymeric carrier systems have been developed for oral delivery of both small molecules, such as theophylline (MW 180.17 Da) and bleomycin (MW 1400 Da), and large molecular weight peptides and proteins such as salmon calcitonin (MW 3500 Da), and insulin [1-8]. The process of loading of a molecule

into the polymer particles and subsequent release of the loaded molecules is limited by the diffusion of the molecule in the polymeric microparticles. Thus, by controlling the mesh size of the polymer network, desired release profiles may be obtained for a drug molecule. The mesh size of the network is greatly influenced by the density and the nature of the crosslinker added to the monomer mixture during the synthesis step. For instance, changing the crosslinker from ethylene glycol dimethacrylate (EGDMA) to poly(ethylene glycol)600 dimethacrylate (PEG600DMA, where 600 represents the molecular weight of the PEG chain in the monomer), while maintaining the same crosslinking density, should increase the mesh size of the resulting network in the swollen state. Thus, the crosslinker EGDMA could be used at high crosslinking density for release of small molecular weight drugs, whereas PEG600DMA used at low crosslinking density will result in a network that is more suited for delivery of high molecular weight compounds.

One important problem in using the P(MAA-g-EG) microparticles developed in our laboratory for insulin delivery, for the present application of Ins-Tf conjugate delivery was the size of the conjugate. The hydrodynamic radius of insulin is ~20 Å whereas the transferrin molecule has hydrodynamic radius of ~40 Å. Thus the diffusion coefficient of the conjugate molecules, containing two molecules of insulin attached to a transferrin molecule, may be significantly lower compared to the native insulin. Thus, one of the objectives of this work was to optimize the polymeric carrier system for delivery of the conjugates.

9.2 Materials and Methods

Synthesis of P(MAA-g-EG) microparticles: Microparticles were synthesized with three different crosslinkers added to the monomer mixture at the same crosslinking density. The crosslinkers used in this work were: Tetra(ethylene glycol) dimethacrylate (TEGDMA), poly(ethylene glycol)400 dimethacrylate (PEG400DMA) and poly(ethylene glycol)600 dimethacrylate (PEG600DMA). All the crosslinkers were purchased from Polysciences, Inc. (Warrington, PA). The monomers used in this reaction are shown in Figure 9.5.

Polymer films were prepared by UV-initiated free radical solution polymerization of methacrylic acid (MAA) (Aldrich Chemical Company, Milwaukee, WI) and poly(ethylene glycol) ether monomethacrylate (PEGMA) (Polysciences, Inc. Warrington, PA). PEGMA was used as received whereas MAA was vacuum distilled at 47°C/25 mmHg to remove the inhibitor hydroquinone monomethyl ether.

MAA and PEGMA were mixed in the molar ratio of 1:1. PEGMA with PEG molecular weight of 1000 was used in this synthesis. The crosslinkers were added at a concentration of 0.80 mol% of the total monomers. The photoinitiator, 1-hydroxy-cyclohexl-phenylketone, (Irgacure-184) (Ciba-Geigy Co. Hawthorne, NY), was added in the amount of 0.1wt % of the total amount of monomers. To inhibit auto acceleration in the polymerization reaction, monomer mixture was diluted with a mixture of 50 % v/v ethanol and deionized water (Milli-Q Plus

system, Millipore). Oxygen dissolved in the monomer mixture, which acts as free radical scavenger, was removed by bubbling the monomer solution with nitrogen for 25 minutes. The mixture was then pipetted into glass plates separated by Teflon spacers with a thickness of 0.9 mm. The polymerization was carried out by exposing the glass plates containing the monomer mixture to a UV light (16 mW/cm^2 at 365 nm) under nitrogen environment for 35 minutes. After the completion of the reaction, the polymer films were washed in deionized water for approximately 7 days in order to remove unreacted monomers, crosslinking agent, initiator and sol fraction. After washing the polymer films were dried at room temperature for a day and then placed in a vacuum oven at 27 °C for 2 days. The dry polymer films were then crushed by using a mortar and pestle and then sieved to 150-212 μm. All the particles were stored in a desiccator until further use.

Transferrin loading into the polymer microparticles: Transferrin loading and release studies were performed to evaluate if a large molecular weight protein could be loaded and release from the P(MAA-g-EG) microparticles. Transferrin loading into the microparticles was achieved by equilibrium partitioning from a concentrated protein solution.

Transferrin (Sigma Chemical Co., St. Louis, MO) stock solution was prepared by dissolving the protein in PBS buffer at pH 7.4 at a concentration of 1 mg/ml. The loading was performed in glass beakers that were previously siliconized with Sigmacote (Sigma Chemical Co., St. Louis, MO) to minimize the

adhesion of protein to the glass surface during the experiment. Polymer microparticles were added to 20 ml of the transferrin stock solution at a concentration of 7 mg/ml and the solution was stirred overnight on a plate shaker. At the end of this period, the particles were collapsed by addition of 20 ml 0.1 N HCl solution to reduce the pH. The particles were then filtered with a 0.45 (m filter paper (Millipore, Billerica, MA) and washed with 10 ml deionized water to remove the surface attached protein. The loading efficiency was calculated based on the transferrin concentration before and after the loading. The protein concentrations were determined by HPLC.

The HPLC system was a Waters 2695 Alliance Separation Module (Waters, Milford, MA) equipped with Waters 2487 Dual λ Absorbance Detector (Waters, Milford, MA). All the data were collected utilizing Empower Applications version 5.00.00 software. A Symmetry300™ C4 column (particle size 5 μm, 3.9mm i.d. ×150mm length) (Milford, MA) was used for the separations. The solvents used for the analysis were: solvent A (water, 0.1% trifluoroacetic acid (TFA)) and solvent B (HPLC-grade acetonitrile, 0.08% TFA). The mobile phase for the analysis consisted of a linear gradient of 70% of solvent A to 40% of solvent A in 6 min. The gradient was controlled by the Empower software. The column temperature was set at 40 ^{o}C. The flow rate of the mobile phase was set at 0.6 ml/min and the peaks were detected at 215 nm.

The microparticles were stored overnight at -4 ^{o}C and freeze dried to obtain dry, transferrin loaded microparticles. The microparticles were stored inside a desiccator at -4 ^{o}C until used.

Transferrin release from the polymeric carriers at pH 7.4: Transferrin release studies were performed in a dissolution apparatus (Distek model 2100B, Distek Inc., North Brunswick, NJ) by using the paddle method. 10 mg of the transferrin-loaded microparticles were placed in 50 ml dimethyl glutaric acid (DMGA) (Sigma, St. Louis, MO) buffer at pH 7.0. The ionic strength of the solution was 0.1M. 200 μl samples were withdrawn at predetermined time intervals up to 2 hours and analyzed with HPLC as described above. After each sample 200 μl buffer was added to maintain a constant volume. The temperature of the solution was maintained at 37 ^{o}C and the solutions were stirred at 100 r.p.m.

Ins-Tf conjugate loading into the polymer microparticles: Ins-Tf conjugate was loaded into the microparticles similar to transferrin loading. In this experiment, 70 mg of the polymer microparticles were added to 10 ml of 1 mg/ml solution of conjugate in PBS. The conjugate solution for loading (1 mg/ml conjugate in PBS) was prepared by the dilution of the conjugate stock solution which was stored at -4 ^{o}C after the synthesis of the conjugate (Chapter 8). After loading the conjugate for 12 hours, the pH was dropped by addition of 10 ml of 1N HCl. The particles were then filtered and washed with 1 ml deionized water. The particles were stored in a desiccator at -4 ^{o}C until used.

Release of the Ins-Tf conjugates from the polymeric carriers under dynamic pH conditions: The release of the conjugate from the microparticles was performed under dynamic pH conditions to mimic the transit of the polymer particles through the GI tract. Conjugate release studies were performed in the dissolution apparatus using the paddle method. 10 mg of the conjugate-loaded microparticles were placed in 50 ml DMGA buffer at pH 3.2. The ionic strength of the solution was 0.1 M. Samples of 200 μl were withdrawn at predetermined time intervals up to 1 h. The pH of the solution was increased to 7.0 by addition of 1N NaOH to the solution. 200 μl samples were withdrawn at predetermined time intervals up to 3 hours and analyzed with HPLC as described above. After each sample 200 μl buffer of corresponding pH was added to maintain a constant volume. The temperature of the solution was maintained at 37 ^{o}C and the solutions were stirred at 100 r.p.m.

Mesh size measurements for the polymer networks: The mesh size measurements for the polymers containing TEGDMA, PEG400DMA and PEG600DMA crosslinkers were performed according to the method described by Hassan et al. [14] Polymer films were prepared by the method described above. Immediately after the synthesis of the polymer films, 12 mm discs were cut and weighed in air and in n-heptane. The weight in heptane was obtained by weighing the discs in a stainless steel mesh basket suspended in heptane. The sample discs were then washed in deionized water for 5 days and transferred into pH 7.0 DMGA buffer used for the release studies and allowed to swell for 4

days. The weight measurements were performed in air and in heptane. The weights of the dried disks were measured after drying the polymer disks under vacuum for 2 days.

9.3 Results and Discussion

9.3.1 Transferrin Loading and Release from the Microparticles

This study was performed to verify that a large molecular weight protein can be successfully loaded and release from the polymer microparticles. This was necessary since insulin was thus far the largest protein that we have successfully loaded and released from the polymer microparticles. Since the conjugate formed after crosslinking of insulin to transferrin was significantly bigger than the native, unmodified insulin, its diffusion into and out of the polymer network could be significantly hindered. Thus, the loading and release study using transferrin served as step to verify that proteins that are much larger than insulin can be delivered by the complexation hydrogels.

When insulin is loaded into the polymer microparticles, loading efficiencies as high as 90% are achieved [9, 10]. In the present study, the loading efficiency for the microparticles containing TEGDMA, PEG400DMA, and PEG600DMA were 61.9 ±1.2 %, 52.9 ±4.3 %, and 51.9 ± 3.2 %, respectively. The concentration of transferrin in the loading solution decreased by approximately 90% of its initial value for all the three polymers in the 12 hours of experiment. However, after HCl addition and the wash step to remove any protein attached to

the surface, the efficiencies reduced. This is probably because the protein that was either attached to the surface of the polymer or was near the surface of the polymer inside the microparticles was washed out during the wash step.

The release profiles of transferrin from the three polymers tested is shown in Figure 9.2. In all the three polymers, most of the protein was released in the first hour of the experiment. The release efficiencies, defined here as the percentage of the loaded amount that is released into the buffer, increased with the increasing length of the cross linker. The microparticles containing PEG600DMA had the highest release efficiency of about 60%.

This study confirmed that the microparticles could be used for releasing large molecular weight proteins. While successful release of transferrin in this study did not necessarily mean that the conjugate could be delivered using the complexation hydrogels, but it did imply that the polymeric carriers could be tailored to release proteins with much higher molecular weight than insulin. The loading and release studies for the conjugate are discussed below.

9.3.2 Ins-Tf Conjugate Loading and Release from the Microparticles

Figure 9.3 shows the loading efficiencies of the conjugate before and after the HCl wash step. In comparison with the loading efficiencies of unmodified transferrin (Figure 9.1), two important differences can be noted. Firstly, the percentage decrease in the protein concentration after 12 hours of the experiment was lower for the conjugate compared to the transferrin. In addition,

the efficiencies did not drop significantly after the addition of HCl and the wash step. This data indicated that the native transferrin molecule partitioned better in the polymer microparticles compared to the conjugate, but once the conjugate entered the polymer network, it could not diffuse out easily during the wash step. Interestingly, the overall loading efficiency was higher for the conjugate compared to transferrin.

The release profiles for the conjugate are shown in Figure 9.4. It should be noted that the release of the conjugate was performed under dynamic pH conditions. The pH of the release buffer was changed from 3.2 to 7.0 after 1 h incubation at pH 3.2. This was done to mimic the transition of the polymer formulations from the gastric environment to the upper small intestine. However, in all the three polymers tested, no conjugate was detected by the HPLC measurements in the release buffer at pH 3.2. Hence, only the profile for release at the neutral pH is shown in Figure 9.4. This is significant since it implies that most of the protein will be released in the upper small intestine which is the targeted site for absorption. This will minimize any possible degradation of the conjugated insulin in the stomach.

For the microparticles loaded with insulin, a small portion of the loaded insulin is typically released at low pH [10]. The mesh size of the network at the gastric pH is approximately 70 Å [11]. Thus, the insulin molecule with a hydrodynamic radius of about 20 Å, may get released at the low pH. However, in

case of the conjugate, the large size of the molecule may not allow any diffusion into the low pH environment.

Once again, the release efficiencies of the conjugate increased with the increase in the length of the crosslinker from TEGDMA to PEG600DMA. The overall release efficiencies were significantly lower than for transferrin in the corresponding polymers. The maximum release efficiency was approximately 36%.

9.3.3 Mesh size measurements for the polymer networks

Measurements of the mesh sizes in the three polymers tested at the pH of the release experiment were performed using the Peppas-Merrill equation [12-14]. The polymer volume fraction in the gel immediately after preparation (relaxed state), $v_{2,r}$ and the polymer volume fraction of the swollen gels (swollen state), $v_{2,s}$, were determined as follows:

$$\upsilon_{2,r} = \frac{V_p}{V_{g,r}} \tag{9.1a}$$

$$\upsilon_{2,s} = \frac{V_p}{V_{g,s}} \tag{9.1b}$$

$V_{g,r}$ and $V_{\mathrm{g,s}}$ were the volumes of the gel in the relaxed state and the swollen state, respectively and V_p was the volume of the polymer in dry state. These volumes were determined by buoyancy measurements in heptane by the following equation:

$$V = \frac{W_a - W_h}{\rho_h} \tag{9.2}$$

where, W_a and W_h were the weights of the gel in air and in heptane, and ρ_h was the density of heptane. The number average molecular weight between crosslinks was calculated as follows

$$\frac{1}{\overline{M_c}} = \frac{2}{\overline{M_n}} - \frac{\frac{\bar{\upsilon}}{V_1}\cdot\left[\ln(1-\upsilon_{2,s}) + \upsilon_{2,s} + \chi\cdot\upsilon_{2,s}^2\right]}{\upsilon_{2,r}\cdot\left[\left(\frac{\upsilon_{2,s}}{\upsilon_{2,r}}\right)^{1/3} - \frac{1}{2}\left(\frac{\upsilon_{2,s}}{\upsilon_{2,r}}\right)\right]} \tag{9.3}$$

In this equation, $\overline{M_n}$ is the number average molecular weight of the linear polymer produced without crosslinking agent under the same conditions of polymerization. V_1 is the molar volume of water (18.1 cm^3/mol); $\bar{\upsilon}$ is the specific volume of the polymer defined as the ratio between the weight of the polymer,

$W_{a,r}$, in air before swelling and the volume, V_p. The Flory polymer-solvent interaction parameter, χ, was calculated as a weighted average of the values for PMAA (χ = 0.5987) and PEG (χ = 0.55) in water [14].

The correlation length or the mesh size of the polymer network (ξ), was calculated as:

$$\xi = \upsilon_{2,s}^{-1/3}\left(\bar{r}_o^2\right)^{1/2} \tag{9.4}$$

Here, $\left(\bar{r}_o^2\right)^{1/2}$ is the root-mean-square, unperturbed, end-to-end distance of the polymer chains between two neighboring crosslinks. The unperturbed end-to-end distance of the polymer chain between two adjacent crosslinks can be calculated using Equation 9.5

$$\left(\bar{r}_o^2\right)^{1/2} = l\left(C_n N\right)^{1/2} \tag{9.5a}$$

$$N = \frac{2\overline{M}_c}{M_r} \tag{9.5b}$$

where C_n is the Flory characteristic ratio (PMAA= 14.6 and PEG = 3.8), l is the length of the bond along the polymer backbone (1.54 Å) and N is the number of links per chain. M_r is the molecular weight of the repeating units.

The results of this analysis are given in Table 9.1. The polymer films containing TEGDMA crosslinker had and average mesh size of 209 Å where as the films containing PEG400DMA and PEG600DMA crosslinkers had almost the same mesh size (226 Å and 227 Å, respectively). Experimental errors may be one of the reasons why the polymers containing PEG400DMA and PEG600DMA crosslinkers had so similar mesh sizes. However, the difference in the mesh size of films containing TEGDMA and PEG600DMA was significant. Whether this difference in the calculated mesh sizes was the only reason behind the observed differences in the release profiles is not known. One other possible explanation for this observed difference in release efficiencies is that the hydrophilicity of the crosslinkers increases from TEGDMA to PEG600DMA. The PEG600DMA has approximately 13 ethylene glycol units where as PEG400DMA and PEG600DMA have ~9, and 4 ethylene glycol units, respectively. Incorporating crosslinkers with higher hydrophilicity may help the network swell to a greater extent in the aqueous medium thus releasing the more of the entrapped protein.

9.4 Conclusions

In this study, the polymeric carriers were optimized for delivery of large molecular weight proteins. The insulin-transferrin conjugate was successfully

loaded and released from the polymer microparticles. Both loading and release efficiencies were lower in comparison to the typical efficiencies for insulin [10]. However, since the conjugate released from the microparticles in the upper small intestine will have better stability and permeability characteristics, as will be shown in the next chapter, overall efficacy of this formulation should be higher. Based on the analysis presented in this chapter, the polymer carriers containing PEG600DMA crosslinker were chosen for the cellular evaluation of the conjugate permeability which is discussed in Chapter 10.

References

1 Peppas, N. A., Wood, K. M. and Blanchette, J. O. (2004) Hydrogels for oral delivery of therapeutic proteins. Expert Opin Biol Ther **4**, 881-887

2 Torres-Lugo, M., Garcia, M., Record, R. and Peppas, N. A. (2002) pH-Sensitive hydrogels as gastrointestinal tract absorption enhancers: transport mechanisms of salmon calcitonin and other model molecules using the Caco-2 cell model. Biotechnol Prog **18**, 612-616

3 Blanchette, J. and Peppas, N. A. (2005) Oral chemotherapeutic delivery: design and cellular response. Ann Biomed Eng **33**, 142-149

4 Brannon-Peppas, L. and Blanchette, J. O. (2004) Nanoparticle and targeted systems for cancer therapy. Adv Drug Deliv Rev **56**, 1649-1659

5 Blanchette, J. and Peppas, N. A. (2005) Cellular evaluation of oral chemotherapy carriers. J Biomed Mater Res A **72A**, 381-388

6 Lowman, A. M. and Peppas, N. A. (1997) Design of oral delivery systems for peptides and proteins using complexation graft copolymer networks. AIChE, New York

7 Lowman, A. M., Morishita, M., Kajita, M., Nagai, T. and Peppas, N. A. (1999) Oral delivery of insulin using pH-responsive complexation gels. J Pharm Sci **88**, 933-937

8 Lopez, J. E. and Peppas, N. A. (2004) Cellular evaluation of insulin transmucosal delivery. J Biomater Sci Polym Ed **15**, 385-396

9 Nakamura, K., Murray, R. J., Joseph, J. I., Peppas, N. A., Morishita, M. and Lowman, A. M. (2004) Oral insulin delivery using P(MAA-g-EG) hydrogels:

effects of network morphology on insulin delivery characteristics. J Control Rel **95**, 589-599

10 Morishita, M., Lowman, A. M., Takayama, K., Nagai, T. and Peppas, N. A. (2002) Elucidation of the mechanism of incorporation of insulin in controlled release systems based on complexation polymers. J Control Rel **81**, 25-32

11 Lowman, A. M. and Peppas, N. A. (1997) Analysis of the Complexation/Decomplexation Phenomena in Graft Copolymer Networks. Macromolecules **30**, 4959 -4965

12 Peppas, N. A. and Barr-Howell, B. D. (1986) In Hydrogels in Medicine and Pharmacy (Peppas, N. A., ed.), pp. 28-55, CRC Press, Boca Raton, FL

13 Brannon-Peppas, L. and Peppas, N. A. (1991) Equilibrium swelling behavior of pH-sensitive hydrogels. Chem Eng Sci **46**, 715-722

14 Hassan, C. M., Doyle, F. J. and Peppas, N. A. (1997) Dynamic Behavior of Glucose-Responsive Poly(methacrylic acid-g-ethylene glycol) Hydrogels. Macromolecules **30**, 6166-6173

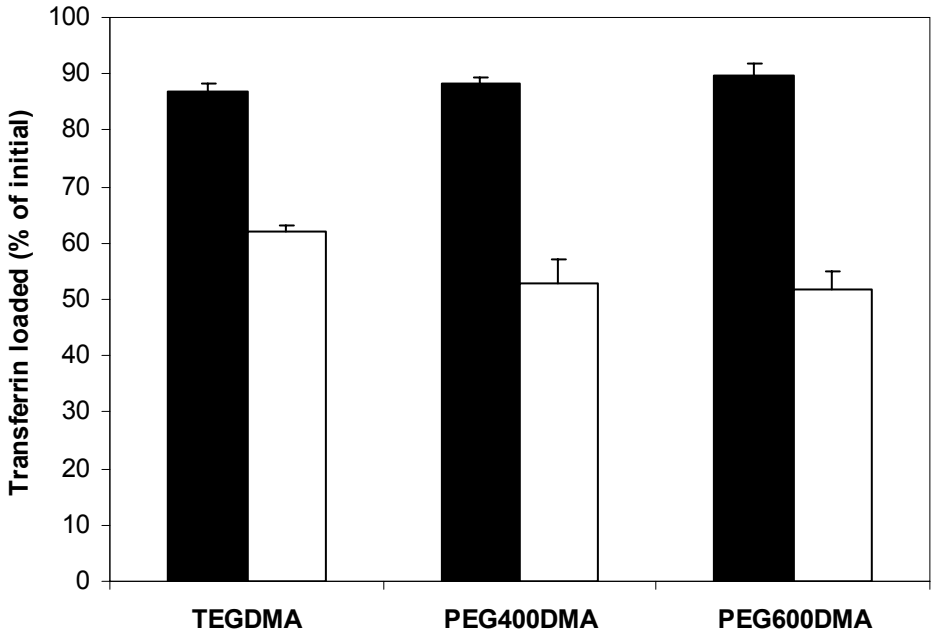

Figure 9.1 The effect of crosslinker in the polymer on the loading efficiencies of transferrin. Transferrin was loaded into the polymer particles by equilibrium partitioning. 140mg microparticles were placed in 20 ml PBS solution containing 1 mg/ml transferrin. The particles were collapsed by addition of 1N HCl after 12 hours. The particles were filtered and washed with deionized water. The percentage of transferrin loaded after incubation for 12 hours (black) and after the wash step (white) was measured. Concentrations were measured by HPLC. Each value represents average of 3 values

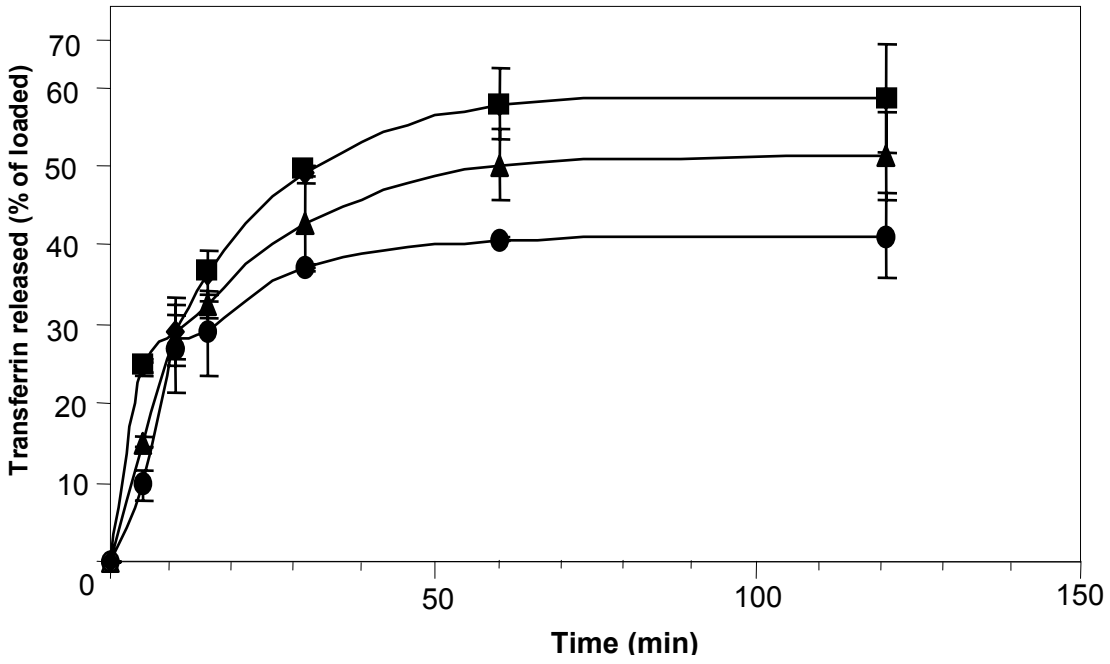

Figure 9.2 Percentage of the loaded transferrin released at pH 7.4. The effect of crosslinker used on the release profile of the transferrin. 10 mg conjugate loaded microparticles containing TEGDMA (●) PEG400DMA (▲) and PEG600DMA (■) were placed in pH 7.0 buffer and 0.2 ml samples were withdrawn at different time intervals. The protein released was measured by HPLC. Each value represents average of 3 values

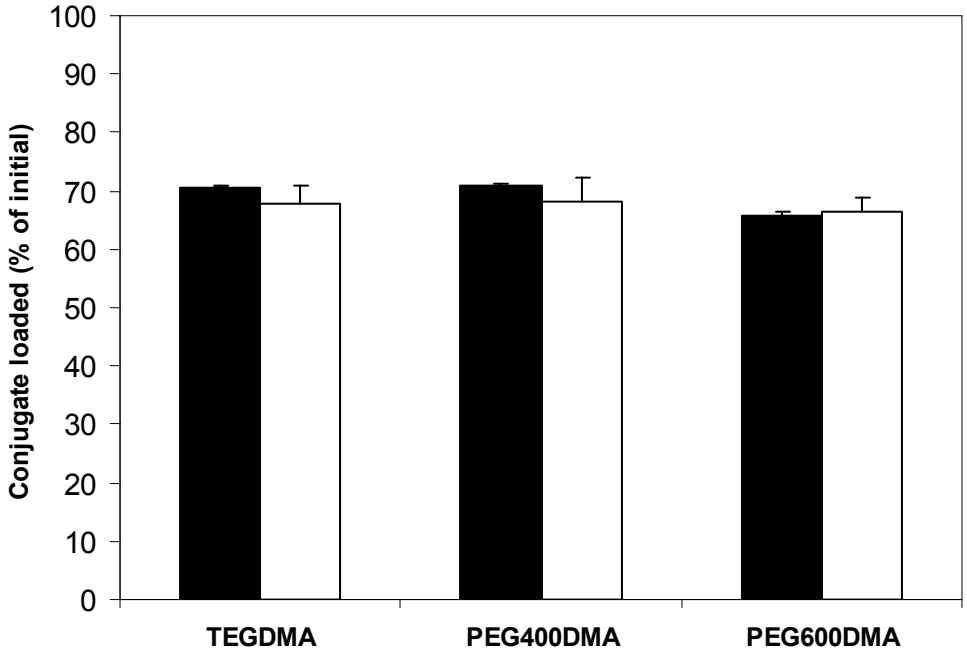

Figure 9.3 The effect of crosslinker used on the loading efficiencies of the Ins-Tf conjugate. Conjugate was loaded into the polymer particles by equilibrium partitioning. 70 mg microparticles were placed in 10 ml PBS solution containing 1 mg/ml transferrin. The particles were collapsed by addition of 1NHCl after 12 hours. The particles were filtered and washed with deionized water. The percentage of conjugate loaded after incubation for 12 hours (black) and after the wash step (white) was measured. Concentrations were measured by HPLC. Each value represents average of 3 values

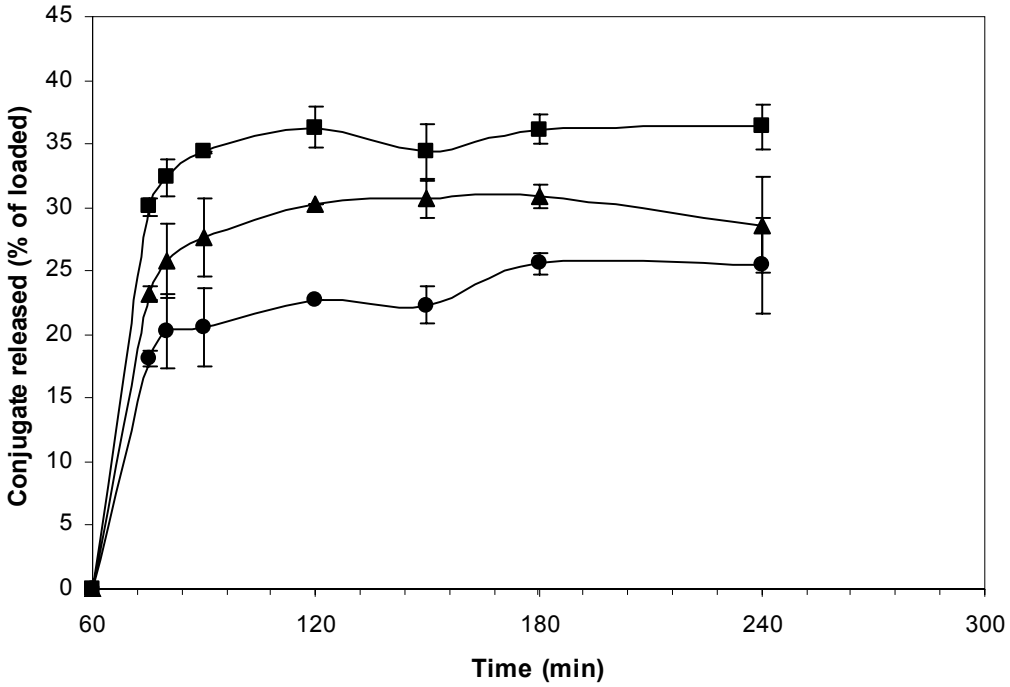

Figure 9.4 Percentage of the loaded conjugate released at pH 7.4. The effect of crosslinker used on the release profile of the Ins-Tf conjugate. 10 mg conjugate loaded microparticles containing TEGDMA (●) PEG400DMA (▲) and PEG600DMA (■) were placed in pH 3.2 buffer and 0.2 ml samples were withdrawn at 20, 30, 60 min. The pH of the buffer was then increased 7.0 buffer and 0.2 ml samples were withdrawn at different time intervals. The protein released was measured by HPLC. Each value represents average of 3 values

Table 9.1 Mesh size of the polymer films containing TEGDMA, PEG400DMA and PEG600DMA crosslinkers. Polymer films were swollen in pH 7.0 for 4 days and the mesh sizes were calculated as described in Section 9.3.3. Each value represents average of 4 values.

Crosslinker in the polymer	**Mesh size (Å)**
TEGDMA	209.2 ± 6.3
PEG400DMA	226.1± 2.4
PEG600DMA	227.0 ±1.4

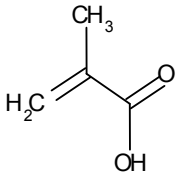

Methacrylic Acid

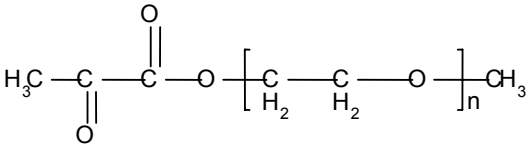

Poly(ethylene glycol) (n) monomethylether monomethacrylate (PEGMA)

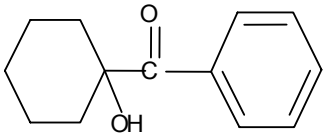

1-hydroxycyclohexyl phenyl ketone

(Irgacure-184)

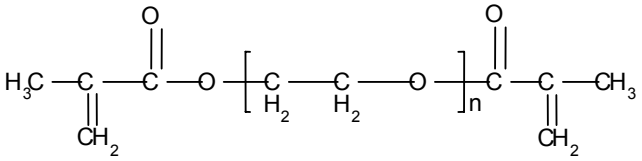

n = 4; Tetraethylene glycol dimethacrylate (TEGDMA)
n ~ 9; Poly(ethylene glycol) 400 dimethacrylate (PEG400DMA)
n ~ 13; Poly(ethylene glycol) 600 dimethacrylate (PEG600DMA)

Figure 9.5 Monomers for synthesis of the complexation hydrogels. Irgacure 184 acts as an initiator, MAA and PEGMA are added in 1:1 molar ratio of MAA:EG units. The crosslinkers are added at 0.80 mol% of the total monomer.

CHAPTER 10

CELLULAR EVALUATION OF FORMULATIONS BASED ON COMPLEXATION HYDROGELS FOR ORAL DELIVERY OF INSULIN-TRANSFERRIN CONJUGATES

10.1 Introduction

In vitro evaluation of the cellular permeability of the insulin-transferrin conjugates in the presence of the complexation hydrogels was an important goal of this work. As described in Chapter 8, the conjugates were synthesized through disulfide crosslinking [1, 2]. Further, the conjugates were successfully loaded and released from the complexation hydrogels optimized for delivery of large molecular weight proteins. In this chapter the cellular studies for in vitro evaluation of the transport of the conjugates across cellular barrier in presence or in absence of the polymer microparticles is presented. Establishing the effectiveness of a formulation by performing in vitro permeability studies is an important step in the development of oral delivery formulations.

The in vitro model used for these studies was Caco-2 cells grown on permeable supports. Caco-2 cell line, which originates from a human colonic adenocarcinoma, is the most widely used cell culture model for in vitro permeability studies [3-6]. These cell lines are used as rapid screening tools for comparing different strategies for enhancing drug permeability [7]. By placing the drug formulation on the apical side of the cell monolayers and measuring the

cumulative fraction of the drug transported across the barrier, the permeability of the drug can be estimated (Fig. 10.1).

Caco-2 cells have morphological and functional characteristics similar to the absorptive enterocytes of the intestinal epithelium [6]. One of the main disadvantages of these cells is that they lack heterogeneity of the intestinal epithelium. The small intestinal epithelium consists of six distinct cell types: the enterocytes or absorptive cells, mucin producing goblet cells, endocrine cells, paneth cells, M cells, tuft and cup cells [8], whereas the Caco-2 cells consist of the enterocytes cells. Since they lack the goblet cells, the mucus layer that covers the intestinal epithelial cells is absent in the monolayers of the Caco-2 cells. This is sometimes seen as a major disadvantage of this model since the presence of mucus can greatly affect the diffusion of some molecules across the cell barrier [9, 10]. To address this issue, cocultures consisting of Caco-2 cells and HT29-MTX cells (mucus producing goblet cell clone consisting of large population of mature goblet cells), have been developed [11]. Even though this coculture provides an alternative to the Caco-2 cells, it has not been fully characterized to compare the in vitro permeability data with the in vivo permeability of drugs. Hence, Caco-2 cell line remains the most applicable cell line for permeability studies.

The transport of therapeutic agents or proteins across the intestinal gut wall may take place via various pathways (Figure 10.2) [12]. The molecules can cross the cellular barrier through the cell membrane of the enterocytes

(transcellular transport), or via the tight junctions between the cells (paracellular transport). The transcellular pathway can be further classified into carrier-mediated transport, passive diffusion and receptor-mediated transcytosis. Confocal microscopy evidence presented in Chapter 5 showed that the predominant mechanism of transport for native insulin across the Caco-2 cell monolayer was the paracellular pathway. The complexation hydrogels are known to induce reversible increase in the permeability of the tight junctions between the Caco-2 cells. P(MAA-g-EG) microparticles placed with insulin on the apical side of the cell monolayers increased the permeability of insulin across the barrier approximately two-folds [13]. The insulin permeability enhancement was attributed to the ability of the hydrogels to reversibly increase the tight junctional permeability. Furthermore, as discussed in Section 2.4.4 and Chapter 8, the insulin-transferrin (Ins-Tf) conjugate has been shown to increase the insulin permeability across the epithelial barrier through the transferrin receptor (TfR)-mediated transcellular pathway [1]. Thus, in the formulations developed in this work, consisting of hydrogels loaded with the Ins-Tf conjugates, the changes in the insulin permeability may be due to both the transcellular and the paracellular pathways.

Hence, the specific objectives of this study were to evaluate the changes in the permeability of insulin due to its conjugation to transferrin, and to measure the changes in the Ins-Tf conjugate permeability due to the presence of the microparticles. Upon oral administration of the conjugate-loaded microparticles,

the overall increase in the permeability of the conjugated insulin across the intestinal epithelium may be due to (i) the transcellular component of the transport because of the conjugated transferrin, and (ii) the paracellular component of transport due to the reversible increase in tight junctional permeability caused by the microparticles. Hence it was important to evaluate the improvement in insulin transport due to conjugation and due to the presence of the microparticles.

10.2 Materials and Methods

Development of the Caco-2 cell monolayers: The cells were cultured in 75 cm^2 culturing flasks (VWR Scientific, West Chester, PAs) with 10 mL of Dulbecco's Modified MEM, culture media, DMEM (Bio Fluids, Biosource International). The seeding density for cultivation was $2.5x10^5$ cells/flask. The cells were maintained in an incubator at 37 °C temperature, 95 % relative humidity, and 5 % CO_2. The culture medium was replaced with fresh medium every other day for about 6 or 7 days, until the cells reached 70-80% confluency. A passage operation was performed after the cells reached 60-80% confluency. In the passage operation, the cells were detached from the culturing flask by trypsinization, counted and transferred at the desired seeding density to a new culturing flask or experimental wells. In these cells studies, cells with passage numbers between 60 and 65 were used.

For transport studies, Caco-2 cells were grown in 6-well Transwell® plates (4.71 cm^2/well) (Costar, Corning Incorp., Corning NY). The culturing cell density was 2.35 x 10^5 cells/well. The cells were grown in a DMEM culture medium containing fetal bovine serum (FBS) for 21 to 24 days until they achieved a constant transepithelial electrical resistance, which indicated that the tight junctions had formed in the monolayer [14, 15]. The medium was changed every other day and the electrical resistance was monitored using a voltmeter with a chopstick electrode (World Precision Instrument, Sarasota, FL). The experimental setup is shown in Figure 10.1. Each well consisted of two chambers: the apical (top) and the basolateral (bottom), which were separated by a membrane with 3.0 μm pore size.

On the day of the experiment, the cell membranes were allowed to equilibrate for one hour with the experimental medium, Hanks' balanced salt solution (HBSS), with Ca^{2+}. 2.0 ml of the HBSS was placed in the apical chamber and 2.5 ml was placed in the basolateral chamber. It was important to use medium containing Ca^{2+} since decrease in the extracellular Ca^{2+} concentrations can deplete the intracellular Ca^{2+} which can induce dilations of the tight junctions. After one hour of incubation, the cell monolayer achieved a constant electrical resistance after the change of the medium.

Conjugate transport across the Caco-2 cell monolayer: Insulin was dissolved in pre-warmed HBSS solution at a concentration of 0.2 mg/ml. The conjugate stock solution was diluted by addition of pre-warmed HBSS to yield a final

concentration of 0.2 mg/ml. To establish the mechanism of conjugate transport across the cell barrier, a solution containing the Ins-Tf conjugate at the final concentration of 0.2 mg/ml and unmodified transferrin at the final concentration of 2 mg/ml in HBSS was prepared. Since the conjugate is believed to be transported across the cell monolayer by TfR-mediated transcytosis, excess unmodified transferrin present in the apical side should compete with the conjugate for the receptors on the cell surface. This should reduce the permeability of the conjugate across the cell monolayer.

After equilibrating the cell monolayers with HBSS for one hour as described above, the HBSS from both the apical and the basolateral sides was removed. 2.5 ml of fresh, pre-warmed HBSS was placed in the basolateral chamber of each cell monolayer. 2.0 ml of solutions prepared above containing either insulin (control), Ins-Tf conjugate, or Ins-Tf conjugate with transferrin in HBSS were placed in the apical sides of monolayers. The Transwell® plates were then placed in the incubator at 37 ^{o}C. At 0.5, 1, 2, and 3 hours, the cells were removed from the incubator and 100 µl samples were withdrawn from the basolateral chambers. 100 µl samples were also withdrawn at 0 h and 3 hours to measure the changes in the apical concentrations during the course of the experiment. The transepithelial electrical resistance (TEER), which depends on the permeability of the tight junctions, was measured after each sample measurement. During the measurements, the plates were laced on a heating mat at 37 ^{o}C. This was important because changes in the temperature can induce

changes in the tight junctional permeability. Changes in temperature can also affect the energy-dependent transcellular transport of the conjugate. The samples were placed in vials and stored at -4 ^{o}C until analyzed. The concentration measurements were performed using ELISA assay.

Protein transport across the Caco-2 cell monolayer in the presence of P(MAA-g-EG) microparticles: Protein transport in the presence of microparticles was studied to evaluate the effect of microparticles on the permeability of insulin or the Ins-Tf conjugate. The polymer microparticles used in this study were prepared as described in Chapter 9 and contained PEG600DMA as the crosslinker. This polymer formulation was used since it was shown in Chapter 9 to be optimal for the release of the large molecular weight conjugates.

For the transport studies, insulin and the conjugate solutions (0.2 mg/ml) in HBSS were prepared as described above. After removing the HBSS from the apical and the basolateral chambers, 2.0 ml of the protein solutions and 2.5 ml HBSS were added to the apical and the basolateral chambers, respectively. Immediately after addition of the protein-containing HBSS, 10 mg dry polymer microparticles were added to the apical side. 100 µl samples were withdrawn at 0.5, 1, 2, and 3 h as described above and analyzed by ELISA assay as described below.

Transport of the conjugate loaded in the microparticles across the cell monolayer: This study was performed to establish that the conjugate released from the microparticles into the apical HBSS medium could cross the Caco-2 cell

monolayer. The monolayers were incubated with HBSS for 1 h at 37 ^{o}C as described previously and the HBSS medium was then replaced with fresh HBSS. 10 mg of the conjugate loaded microparticles were placed in the apical side of the cell monolayers. 100 µl samples were withdrawn at 0.5, 1, 2, 3, and 4 h and analyzed with ELISA.

ELISA assay measurements of the transported insulin and Ins-Tf conjugate: Measurements of free and transferrin-bound insulin transported across the cell monolayers were performed using a sandwiched enzyme-linked immunosorbent assay (ELISA) for bovine insulin (Alpco Diagnostics, Windham, NH). This assay allows accurate determination of insulin concentrations in 0.25-6 ng/ml range. ELISA standard curves were prepared for both free insulin and the Ins-Tf conjugate.

Preliminary experiments were carried out to determine the dilution factors required to adjust the concentrations in the ng/ml range. The samples obtained from the basolateral sides containing free insulin were diluted 10 times whereas the samples containing the transferrin-bound insulin (Ins-Tf conjugate) were used without any dilutions. This was done because 1.0 mg/ml concentration of the conjugate is equivalent to approximately 0.125 mg/ml of the bond insulin. Thus a 1 mg/ml conjugate solution contains same free insulin as a 10 times diluted 1 mg/ml insulin sample.

The ELISA assay measurements were performed according to the protocol provided by Alpco Diagnostics. A sample of 25 µl of standards and

samples was pipetted into the microplate wells coated with mouse monoclonal antibody for bovine insulin. A sample of 50 µl of the conjugate working solution containing peroxidase conjugated mouse monoclonal anti-insulin was added to each well. The plate was incubated at room temperature for 2 hours at under constant shaking. The wells were washed 6 times to remove the unreacted peroxidase-conjugated anti-insulin antibody by filling all the wells with wash solution and discarding the solution after each washing step. A sample of 200 µl of 3,3',5,5'-tetramethylbenzidine substrate (TMB) solution was added to each well and allowed to react for 15 min. 50 µl of stop solution containing sulfuric acid was pipetted into each well and allowed to react for 10 seconds. The optical density was measured at 450 nm using a microplate reader (Synergy HT; Bio-Tech Instruments, Winooski, VT).

10.3 Results and Discussion

Evaluation of the transport characteristics of the insulin in the free and the transferrin-conjugated form was performed here. The efficacy of the Ins-Tf conjugate and polymeric microparticles to transport the bound and free insulin, respectively, was compared. The measurements of the apparent permeability (P_{app}) were performed according to the following standard analysis.

In this analysis, the cellular monolayer barrier is approximated to a chemically homogeneous slab. By applying Fick's first law to the diffusion

process across the monolayers, following relationship between the rate of protein transported from the donor (apical) and receiver (basolateral) compartments and the concentration gradient is obtained:

$$\frac{dQ(t)}{dt} = \frac{K \times D}{h} \times A \times [C_D(t) - C_R(t)] \qquad (10.1)$$

where, Q(t) is the cumulative amount of protein transported to the receiver compartment (mg); K is the distribution coefficient between the medium in the barrier and the aqueous donor and receiver solutions; D is the diffusion coefficient (cm^2/s); h is the thickness of the barrier to diffusion (cm); A is the area of the cell monolayer (cm^2); and C_D and C_R are the concentrations of protein in the apical and the basolateral compartments (mg/ml). The apparent permeability (P_{app}) was defined as:

$$P_{app} = \frac{K \times D}{h} \qquad (10.2)$$

Further simplification of the equation is achieved by approximating the receiver compartment to a 'perfect sink'. Ideally this would mean that the concentration in the basolateral compartment is always zero (which can be achieved by constantly removing the basolateral solution and replacing it with a fresh medium). However, conventionally a condition where the value of C_R remains below 10% of the C_D is acceptable. With these further simplifications, P_{app} is approximated by:

$$P_{app} = \frac{dQ(t)}{dt} \times \frac{1}{A \times C_{D0}} \tag{10.3}$$

where, C_{D0} is the initial concentration in the donor compartment. The term dQ/dt is the slope of the linear relationship between the cumulative amount of protein transported (mg) vs. time (s).

10.3.1 Enhancement of Insulin Transport across the Cell barrier due to the Complexation Hydrogels

Previous studies performed in our lab have demonstrated that the complexation hydrogels placed in the apical compartment of monolayers with insulin caused 4-20 fold increase in the permeability of insulin [13, 16]. Foss et al. [13] reported 2-fold increase in permeability of insulin whereas Ichikwa and Peppas [16] reported about 20-fold increase in the permeability due to the presence of microparticles. Significant variability is typically observed in the results obtained from in vitro transport experiments because of differences in experimental conditions, passage numbers, and other factors. Hence the data presented here is not compared with the earlier results obtained in our laboratory. However, reliable comparisons can be made within the same experimental set while comparing different formulations.

Figure 10.3 shows the cumulative amount of insulin transported across the cell monolayer in the control wells (no polymer). The apparent permeability P_{app}

was 1.08 ± 0.15 x 10^{-9} cm/s as calculated from Eq. 10.3 using the slope the plot in Figure 10.3. Figure 10.4 shows the cumulative amount of insulin transported across the cell barrier in the presence of the P(MAA-g-EG) microparticles. The P_{app} value for insulin in this case was 6.44 ± 1.3 x 10^{-9} cm/s. The permeability values of various formulations are given in Table 10.1. Thus, as expected, the microparticles caused increase in the permeability of insulin. Approximately 6-fold increase in insulin P_{app} was observed.

It can be observed from Figure 10.4 that there was an initial lag in the transport of insulin across the cellular barrier (0.5 and 1 h readings). This can be explained by changes in the TEER values of the cell monolayer due to the presence microparticles (Figure 10.5). As mentioned previously, the TEER value is a measure of the permeability of the tight junctions. Higher the permeability, lower is the TEER value of a monolayer. The reduction in TEER values has been shown to correlate with the increase in P_{app} values of insulin across the monolayers [13, 17, 18]. In Figure 10.5 the reduction in the TEER values is noticed to start after around 1 h after the start of the experiment. This correlates with the observed lag in insulin transport in Figure 10.4 implying that the permeability increase is primarily due to the opening of the tight junctions.

10.3.2 Enhancement of Insulin Transport across the Cell barrier due to Conjugation with Transferrin

Shah and Shen [19] reported a15-fold increase insulin permeability due to its conjugation to transferrin. It was also shown that the primary mechanism of

transport of the conjugates is the TfR-mediated transcytosis of the conjugated insulin. Hence one of the important goals of this study was to assess the transport characteristics of the Tf-bound insulin. The concentration measurements were performed using ELISA for bovine insulin. This was possible because insulin in the conjugated configuration was still able to bind the antibodies targeted at two different antigenic determinants on the insulin molecule. Figure 10.6 shows the cumulative Ins-Tf conjugate transported (ng) across the monolayers as a function of time (h). Ins-Tf conjugation caused a 15-fold increase in the insulin permeability. The overall permeability of the conjugate across the monolayer was calculated to be $16.3 \pm 2 \times 10^{-9}$ cm/s.

As seen from the plot, unlike for the transport process in the presence of the microparticles (Figure 10.4), there is no lag time in the transport process of the conjugate. This was expected since the transport of the conjugate is a receptor-mediated process, compared to the transport process in due to the polymer.

10.3.3 Enhancement of Insulin Transport across the Cell barrier due to Conjugation with Transferrin and the Complexation hydrogels

Figure 10.7 shows the combined effect of conjugation and the microparticles on the transport of insulin across the cellular barrier. The changes in the TEER values as a percentage of the initial TEER are plotted against time in Figure 10.8. The P_{app} value calculated from the slope of the plot in Figure 10.7

was 24 ± 0.05 x 10^{-9} cm/s. Thus the permeability of the conjugate increased due to the presence of the microparticles (approximately 1.5-fold increase in the permeability of the conjugate due to the microparticles). However, the enhancing effect of the hydrogels on the conjugation permeability was less pronounced than seen for unmodified insulin, where a 6-fold permeability enhancement was observed. One of the reasons for this behavior is that the paracellular pathway is size-dependent. Smaller molecules may diffuse easily across this pathway compared to large proteins such as the Ins-Tf conjugate. In the absence of any enhancing agents, only molecules with radius less than 11 Å are effectively transported via the paracellular pathway [20]. Thus the transport of the conjugated protein consisting insulin (~ 20 Å hydrodynamic radius) and transferrin (~ 40 Å hydrodynamic radius) may be limited by this route, even if the permeability of the tight junctions is increased due to the microparticles.

More importantly, a 22-fold increase in the transport of insulin was observed due to the combined effect of conjugation and the presence of the microparticles (Table 10.1). This is a very important result since it demonstrates the effectiveness of combining the two strategies based on utilization of TfR-mediated transcytosis and the use of complexation hydrogels for improved oral delivery.

The ability of the Ins-Tf conjugate released from P(MA-g-EG) microparticles to traverse the Caco-2 cell barrier was also tested in this work. This was done to show that the process of loading the conjugate into the

microparticles did not adversely affect the conjugate's ability to get transported across the cellular barrier. However, permeability measurements were not performed for this set, since due to the experimental conditions in this study, the standard method for P_{app} measurements did not apply. For instance, the assumption of constant concentration in the apical side ($C_D(t) = C_{D0}$) was not valid here. This is because at initial time, when the conjugate-loaded microparticles were added to the donor compartment, the concentration of the conjugate in this compartment is zero. The conjugate is released over time and hence the concentration changes with time. Figure 10.9 shows the total conjugate released in the apical side and the conjugate transported across the barrier as a function of time. These results indicate that the polymer slowly released the protein conjugate into the apical side. This was followed by uptake and transport of the released conjugate across the cell monolayer. Thus, the process of loading the conjugate, drying the loaded microparticles and subsequent release of the protein did not adversely affect its ability to get transported across the cellular barrier.

10.3.4 Competitive Transport of Ins-Tf Conjugate and Unmodified Transferrin across the Cell Barrier

To establish that the transport of the Ins-Tf conjugate molecules across the cells is mediated by the TfR receptors, transport of the conjugate was evaluated in the presence of 20-fold excess transferrin by weight in the donor

compartment. HBSS solution containing 0.2 mg/ml conjugate with 2 mg/ml Tf was placed on the apical side and the permeability of the conjugate was measured (Figure 10.10). The addition of Tf to the apical side reduced the permeability of the conjugate from 16.3 ± 2 x 10^{-9} cm/s to 0.97 ± 0.18 x 10^{-9} cm/s. The significant decrease in the conjugate permeability was attributed to the competitive binding of the excess Tf to its receptors thus reducing the permeability of the conjugate across the cells. Thus, it was established that the transport of the conjugate across the barrier was primarily mediated via the transferrin receptors.

10.3.5 Indirect Evidence of Insulin Stability in the Conjugated form by ELISA Analysis

An indirect evidence of intact secondary structure of insulin in the transferrin-bound state was provided in this work through successful quantitative determination of the conjugate concentration by ELISA assay. The ELISA assay used here was based on the direct sandwich technique in which two monoclonal antibodies are directed against separate antigenic determinants (or epitopes) on the bovine insulin molecule. In the assay, insulin in the sample reacts with peroxidase-conjugated anti-insulin and the anti-insulin immobilized on the well surfaces. Thus for successful determination of insulin, either in free or Tf-conjugated form would require that both the antibodies, bind to their respective epitopes on the insulin molecule. Further, disruption of the secondary structure of

the protein may adversely affect its ability to bind to the antibodies via the antigenic determinants. Since we were able to use the ELISA assay for quantitative determination of the Ins-Tf conjugate, this means that the insulin in the conjugated form has secondary structure similar to the native, unmodified insulin. Even though this can not be accepted as a conclusive evidence of the biological activity of insulin, it does indicate that the secondary structure of insulin was unchanged due to its conjugation to transferrin.

10.4 Conclusions

The in vitro evaluation of the formulation consisting of polymer microparticles as carriers for the Ins-Tf conjugates was performed using Caco-2 cell model. The effect of conjugation and the presence of microparticles on insulin permeability were separately studied. Transferrin receptor-mediated transcytosis was identified as the primary mechanism of transport of the conjugate across the cell barrier. The microparticles increased the permeability of both insulin and the conjugate, most probably through enhancement in the paracellular transport induced by dilations of the tight junctions. The observed 22-fold net increase in insulin permeability due to the combined effect of transferrin conjugation and the presence of the microparticles implies that this formulation can result in significant increase in the oral bioavailability of insulin. This permeation enhancing effect, combined with the increased stability of the

conjugate against proteolytic degradation, should enhance the overall efficacy of oral administration of insulin.

References

1 Xia, C. Q., Wang, J. and Shen, W. C. (2000) Hypoglycemic effect of insulin-transferrin conjugate in streptozotocin-induced diabetic rats. J Pharmacol Exp Ther **295**, 594-600

2 Carlsson, J., Drevin, H. and Axen, R. (1978) Protein thiolation and reversible protein-protein conjugation. N-Succinimidyl 3-(2-pyridyldithio)propionate, a new heterobifunctional reagent. Biochem J **173**, 723-737

3 Ungell, A.-L. B. (2004) Caco-2 replace or refine? Drug Discovery Today: Technologies **1**, 423-430

4 Artursson, P. and Borchardt, R. T. (1997) Intestinal drug absorption and metabolism in cell cultures: Caco-2 and beyond. Pharm Res **14**, 1655-1658

5 Artursson, P., Lindmark, T., Davis, S. S. and Illum, L. (1994) Effect of chitosan on the permeability of monolayers of intestinal epithelial cells (Caco-2). Pharm Res **11**, 1358-1361

6 Artursson, P., Palm, K. and Luthman, K. (2001) Caco-2 monolayers in experimental and theoretical predictions of drug transport. Adv Drug Deliv Rev **46**, 27-43

7 Audus, K. L., Bartel, R. L., Hidalgo, I. J. and Borchardt, R. T. (1990) The use of cultured epithelial and endothelial cells for drug transport and metabolism studies. Pharm Res **7**, 435-451

8 Madara, J. L. and Trier, J. S. (1986) Functional morphology of the mucosa of the small intestine. In Physiology of the Gastrointestinal Tract (Johnson, L. R., ed.), pp. 1209-1250, Raven Press, New York

9 Wikman, A., Karlsson, J., Carlstedt, I. and Artursson, P. (1993) A drug absorption model based on the mucus layer producing human intestinal goblet cell line HT29-H. Pharm Res **10**, 843-852

10 MacAdams, A. (1993) The effect of gastro-intestinal mucus on drug absorption. Adv Drug Deliv Rev **11**, 201-220

11 Walter, E., Janich, S., Roessler, B. J., Hilfinger, J. M. and Amidon, G. L. (1996) HT29-MTX/Caco-2 cocultures as an in vitro model for the intestinal epithelium: in vitro-in vivo correlation with permeability data from rats and humans. J Pharm Sci **85**, 1070-1076

12 Balimane, P. V., Chong, S. and Morrison, R. A. (2000) Current methodologies used for evaluation of intestinal permeability and absorption. J Pharmacol Toxicol Methods **44**, 301-312

13 Foss, A. C. and Peppas, N. A. (2004) Investigation of the cytotoxicity and insulin transport of acrylic-based copolymer protein delivery systems in contact with Caco-2 cultures. Eur J Pharm Biopharm **57**, 447-455

14 Gumbiner, B. (1987) Structure, biochemistry, and assembly of epithelial tight junctions. Am J Physiol **253**, C749-758

15 Denker, B. M. and Nigam, S. K. (1998) Molecular structure and assembly of the tight junction. Am J Physiol **274**, F1-9

16 Ichikawa, H. and Peppas, N. A. (2003) Novel complexation hydrogels for oral peptide delivery: In vitro evaluation of their cytocompatibility and insulin-transport enhancing effects using Caco-2 cell monolayers. J Biomed Mat Res **67A**, 609-617

17 Lopez, J. E. and Peppas, N. A. (2004) Effect of poly (ethylene glycol) molecular weight and microparticle size on oral insulin delivery from P(MAA-g-EG) microparticles. Drug Dev Ind Pharm **30**, 497-504

18 Lopez, J. E. and Peppas, N. A. (2004) Cellular evaluation of insulin transmucosal delivery. J Biomater Sci Polym Ed **15**, 385-396

19 Shah, D. and Shen, W. C. (1996) Transcellular delivery of an insulin-transferrin conjugate in enterocyte-like Caco-2 cells. J Pharm Sci **85**, 1306-1311

20 Fasano, A. and Uzzau, S. (1997) Modulation of intestinal tight junctions by Zonula occludens toxin permits enteral administration of insulin and other macromolecules in an animal model. J Clin Invest **99**, 1158-1164

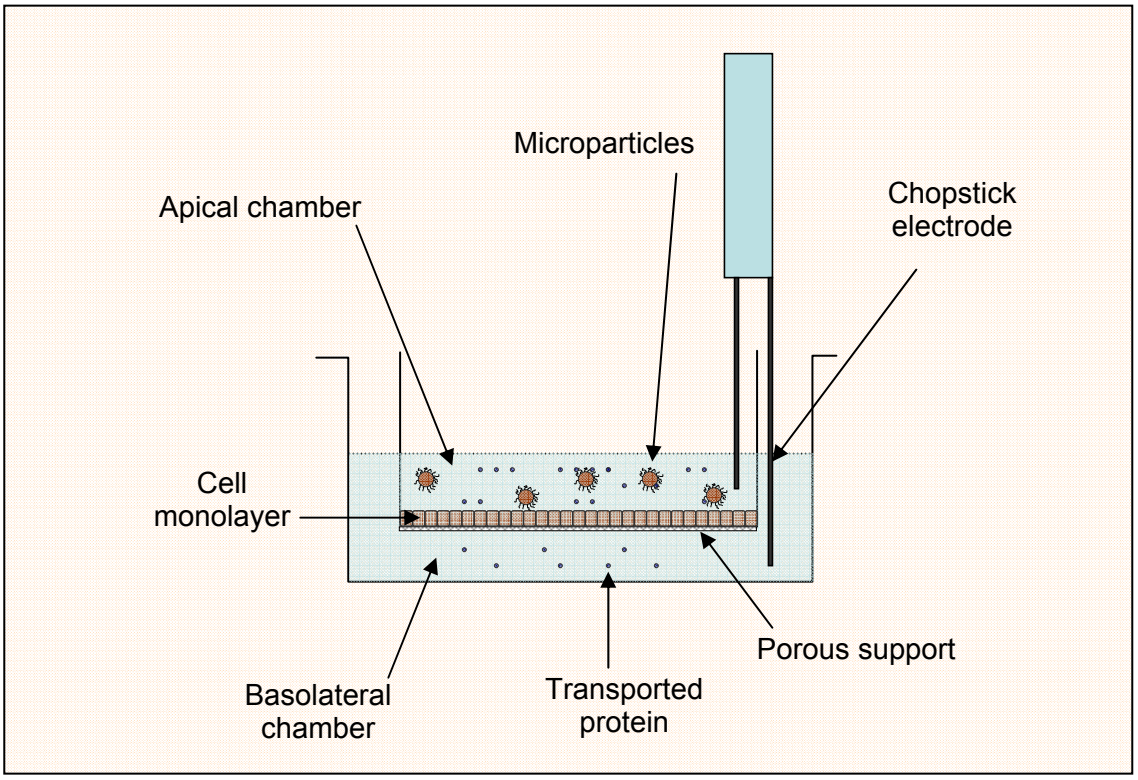

Figure 10.1 Experimental setup for the permeability studies using Caco-2 cells. The cells were grown on Transwell® porous supports in DMEM medium for 21 days. The experiments were performed in HBSS. The particles and the protein solution were placed on the apical side and the samples were withdrawn from the basolateral side. The TEER values of the monolayer were measured using a chopstick electrode. The cell monolayers were incubated at a constant temperature of 37 ^{o}C during the experiment.

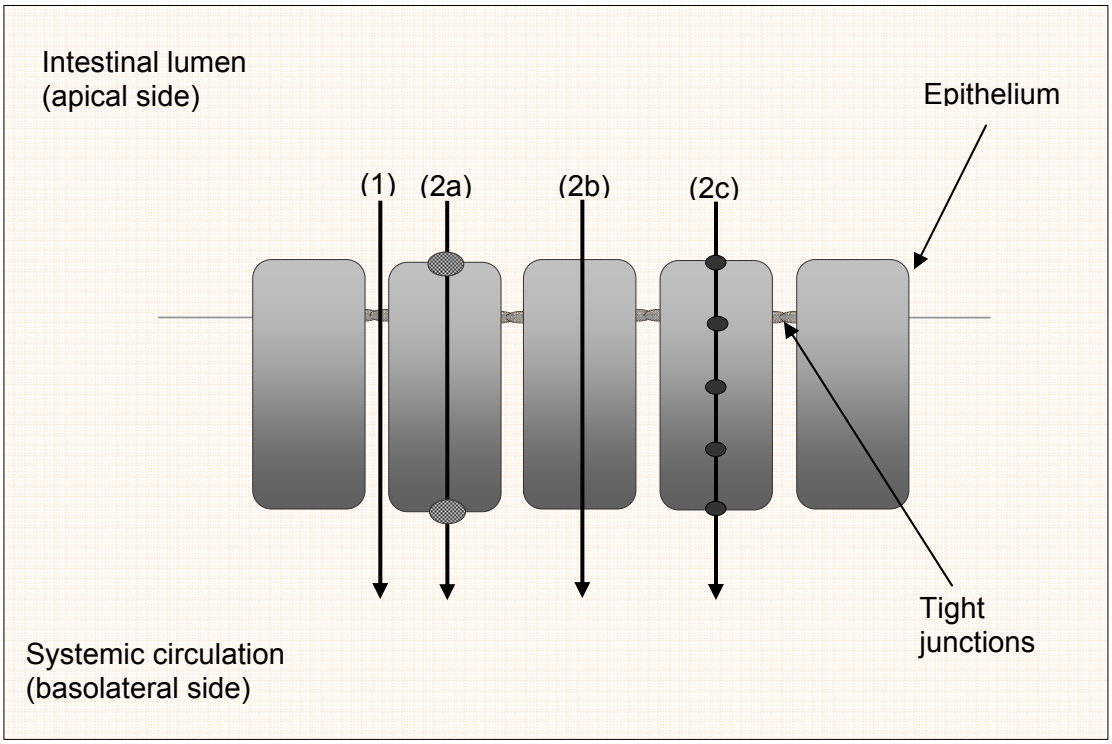

Figure 10.2 Mechanisms of transport across the intestinal epithelium. The epithelial cells separating the luminal side from the systemic circulation are held together by tight junctions. The two main mechanisms of transport are (1) paracellular transport, and (2) transcellular transport. The transcellular transport can be further divided into (2a) carrier-mediated transport, (2b) passive diffusion, and (2c) receptor-mediated transcytosis

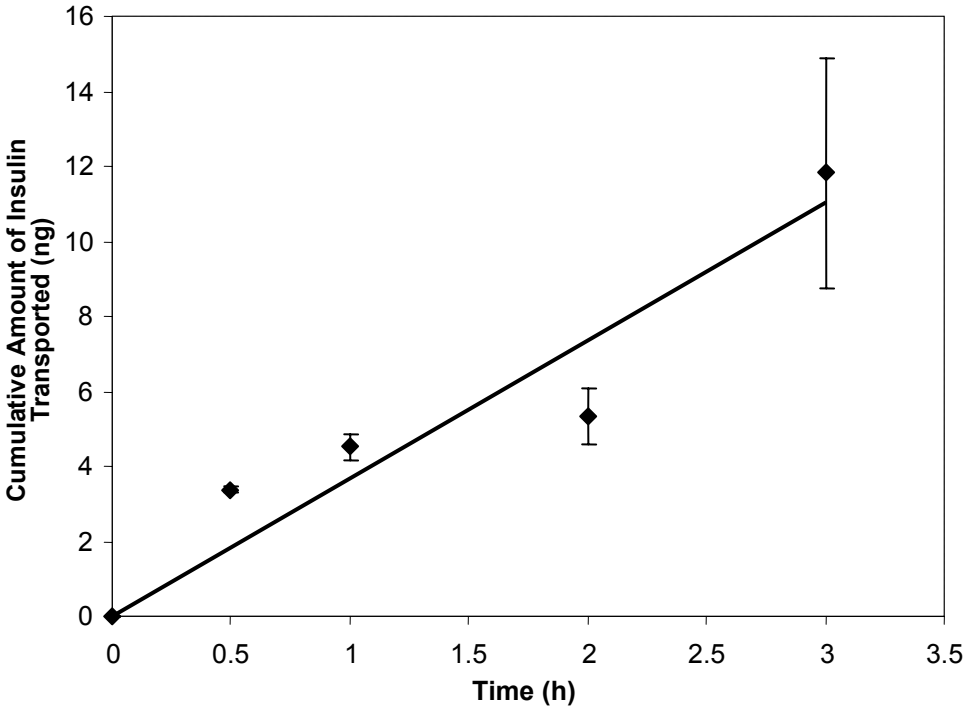

Figure 10.3 The cumulative amount of insulin transported across Caco-2 cell monolayers grown on porous Transwell® filters without microparticles (control experiment). A 0.2 mg/ml insulin solution in HBSS was placed in the apical chamber and 100 µl samples were withdrawn from the basolateral chamber at different time intervals. The samples were analyzed by bovine insulin ELISA. The cell monolayers were incubated at a constant temperature of 37 ^{o}C during the experiment. Each value is average of two cell monolayers, with a deviation that is either indicated as a bar or is smaller than the size of the symbol.

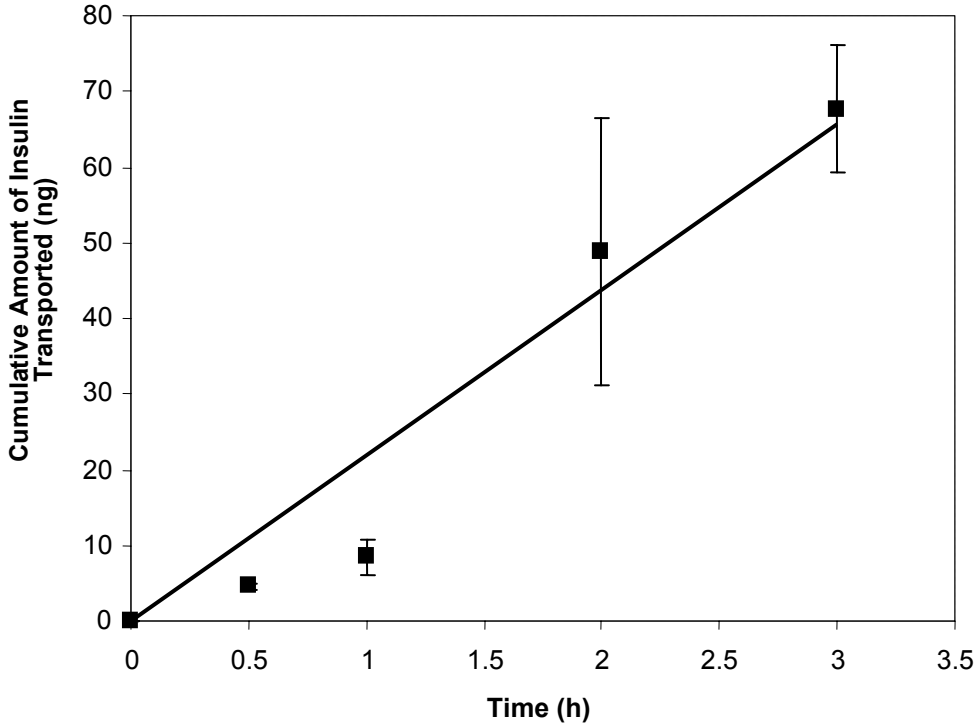

Figure 10.4 The cumulative amount of insulin transported across Caco-2 cell monolayers grown on porous Transwell® filters with microparticles. A 0.2 mg/ml insulin solution in HBSS was placed in the apical chamber with 10 mg P(MAA-g-EG) microparticles containing PEG600DMA crosslinker. 100 µl samples were withdrawn from the basolateral chamber at different time intervals. The samples were analyzed by bovine insulin ELISA. The cell monolayers were incubated at a constant temperature of 37 ^{o}C during the experiment. Each value is average of two cell monolayers, with a deviation that is either indicated as a bar or is smaller than the size of the symbol.

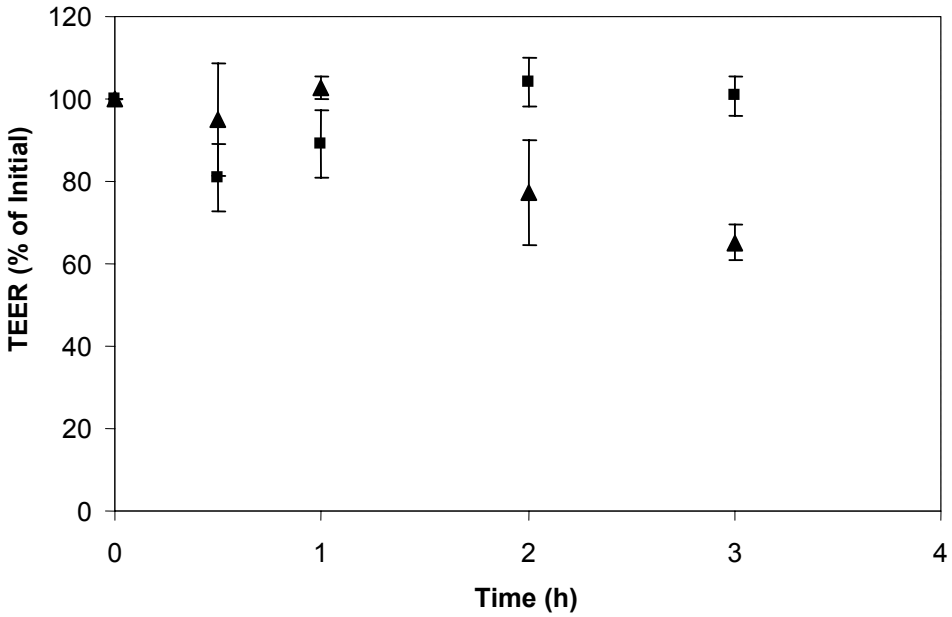

Figure 10.5 Effect of polymer microparticles on the transepithelial electrical resistance of Caco-2 cell monolayers grown on porous Transwell®. A 0.2 mg/ml insulin solution in HBSS was placed in the apical chamber with (triangles) or without (squares) 10 mg P(MAA-g-EG) microparticles containing PEG600DMA crosslinker. The TEER of the cell monolayers was measured immediately after taking samples for permeability measurements. The cell monolayers were incubated at a constant temperature of 37 ^{o}C during the experiment. Each value is average of two cell monolayers, with a deviation that is either indicated as a bar.

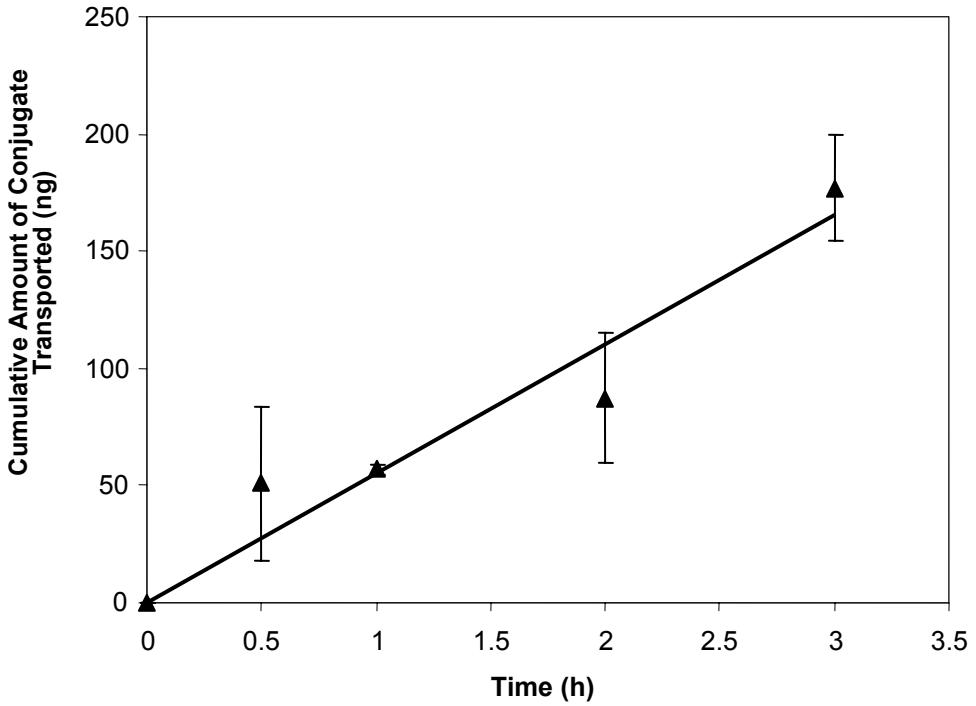

Figure 10.6 The cumulative amount of insulin-transferrin conjugate transported across Caco-2 cell monolayers grown on porous Transwell® filters without the microparticles. A 0.2 mg/ml conjugate solution in HBSS was placed in the apical chamber. 100 µl samples were withdrawn from the basolateral chamber at different time intervals. The samples were analyzed by bovine insulin ELISA. The cell monolayers were incubated at a constant temperature of 37 ^{o}C during the experiment. Each value is average of two cell monolayers, with a deviation that is either indicated as a bar or is smaller than the size of the symbol.

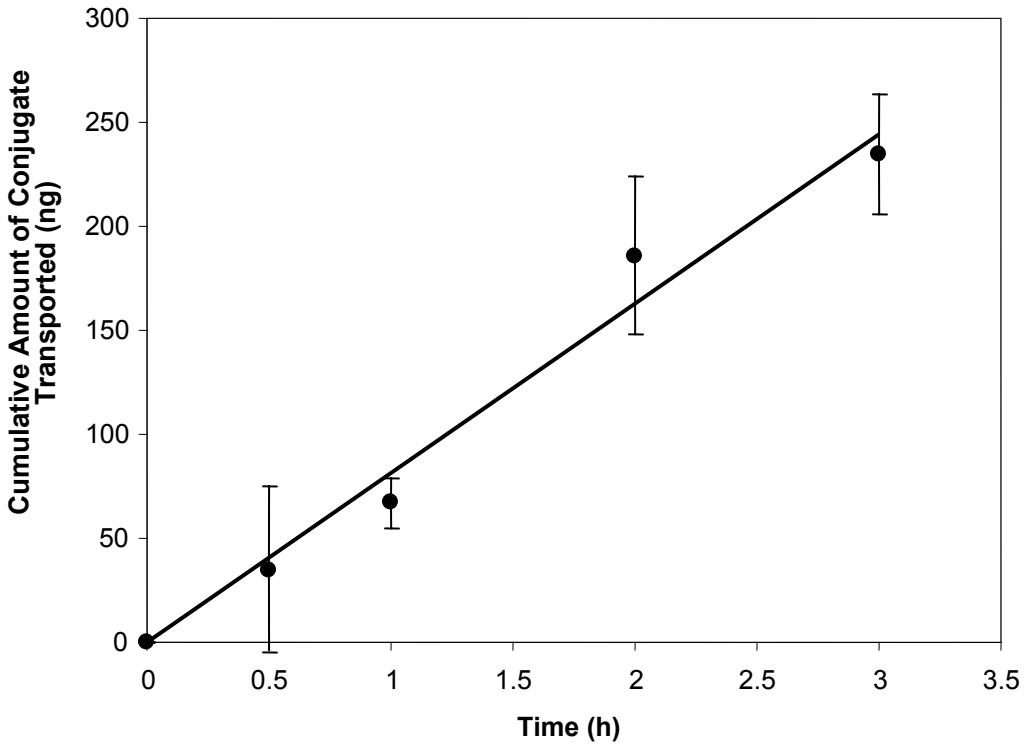

Figure 10.7 The cumulative amount of insulin-transferrin conjugate transported across Caco-2 cell monolayers grown on porous Transwell® filters in the presence of microparticles. A 0.2 mg/ml conjugate solution in HBSS was placed in the apical chamber with 10 mg P(MAA-g-EG) microparticles containing PEG600DMA crosslinker. 100 µl samples were withdrawn from the basolateral chamber at different time intervals. The samples were analyzed by bovine insulin ELISA. The cell monolayers were incubated at a constant temperature of 37 ^{o}C during the experiment. Each value is average of two cell monolayers, with a deviation that is either indicated as a bar or is smaller than the size of the symbol.

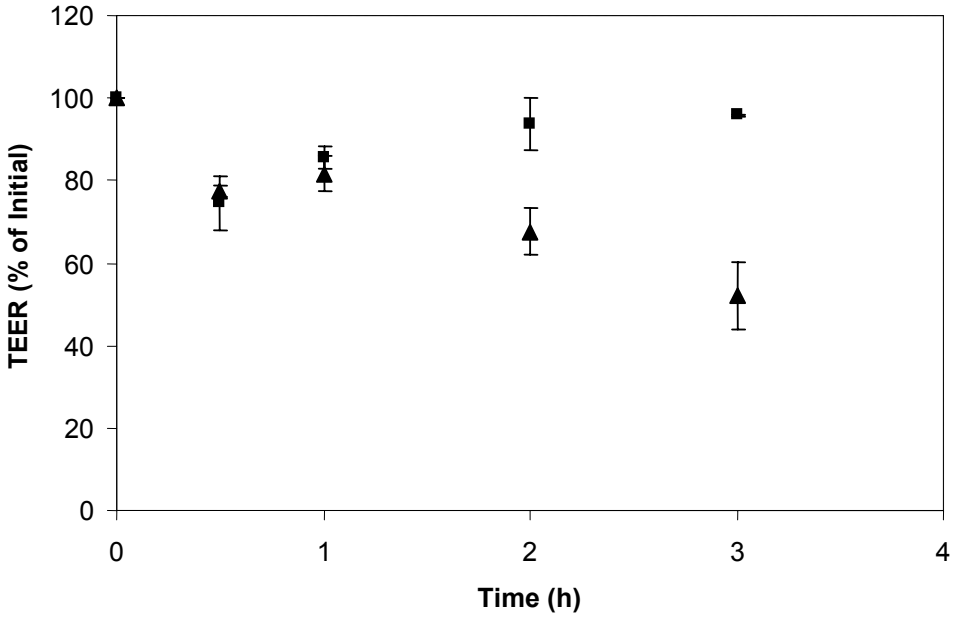

Figure 10.8 Effect of polymer microparticles on the transepithelial electrical resistance of Caco-2 cell monolayers grown on porous Transwell®. A 0.2 mg/ml insulin-transferrin conjugte solution in HBSS was placed in the apical chamber with (triangles) or without (squares) 10 mg P(MAA-g-EG) microparticles containing PEG600DMA crosslinker. The TEER of the cell monolayers was measured immediately after taking samples for permeability measurements. The cell monolayers were incubated at a constant temperature of 37 ^{o}C during the experiment. Each value is average of two cell monolayers, with a deviation that is either indicated as a bar.

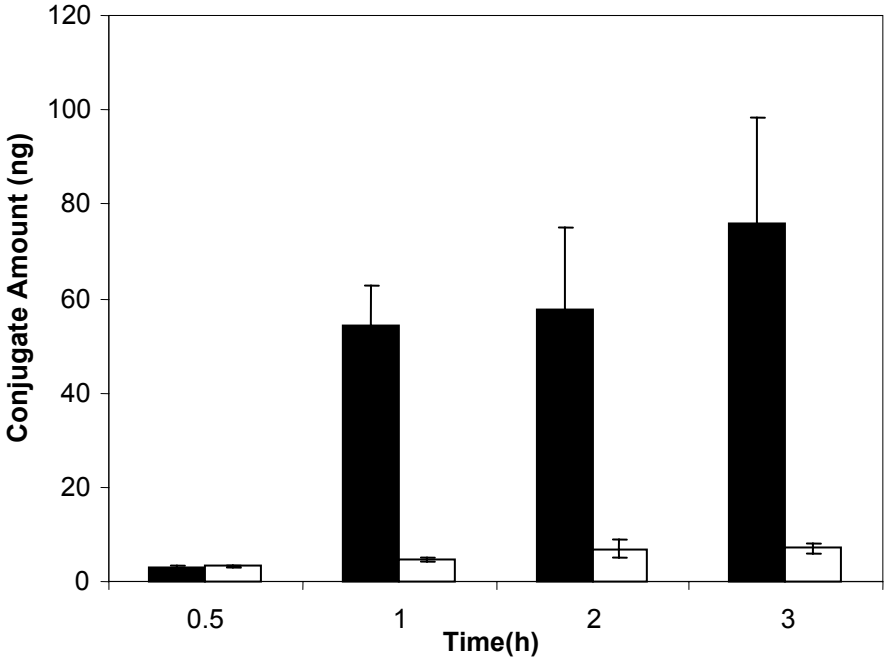

Figure 10.9 Total amount of conjugate in the apical and basolateral chambers. 10 mg conjugate loaded microparticles were added to the apical side and the samples were taken from the apical and basolateral sides at different time points and analyzed with ELISA. The experiment was carried out at a constant temperature of 37 °C. Each value is mean of two values ± deviation.

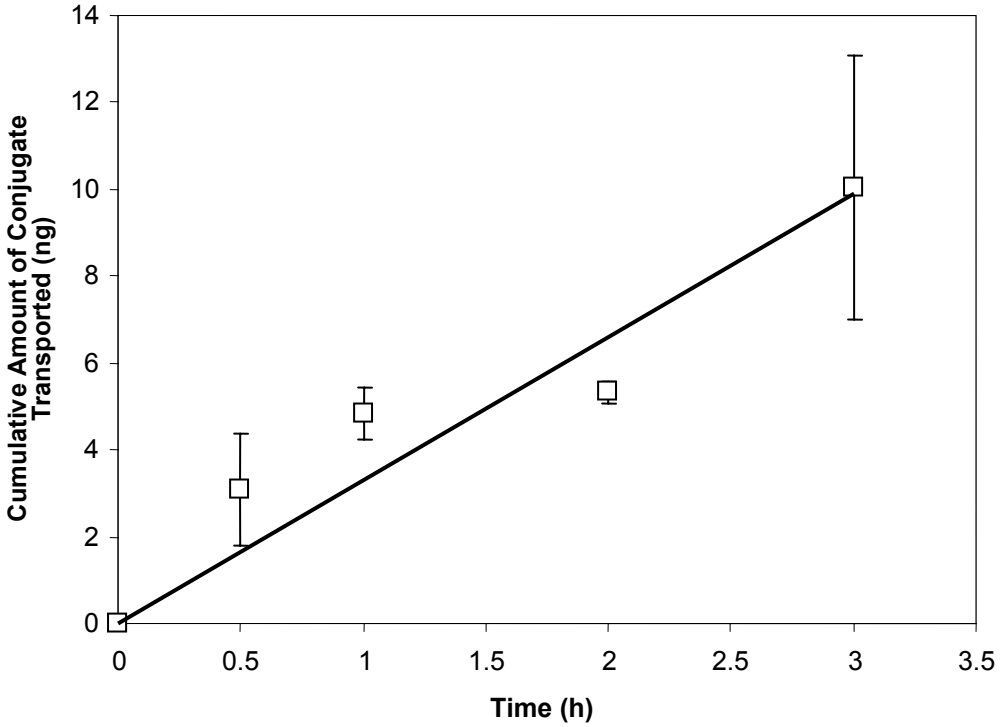

Figure 10.10 The cumulative amount of insulin-transferrin conjugate transported across Caco-2 cell monolayers grown on porous Transwell® filters in the presence of excess unmodified transferrin. A 0.2 mg/ml conjugate solution in HBSS containing 2.0 mg/ml transferrin was placed in the apical chamber of the monolayers. 100 µl samples were withdrawn from the basolateral chamber at different time intervals. The samples were analyzed by bovine insulin ELISA. The cell monolayers were incubated at a constant temperature of 37 ^{o}C during the experiment. Each value is average of two cell monolayers, with a deviation that is either indicated as a bar or is smaller than the size of the symbol.

Table 10.1 Insulin permeability across Caco-2 cell monolayers grown on porous Transwell® filters. Insulin formulations in HBSS were placed on the apical side of the cell monolayers and samples were withdrawn at different time points from the basolateral sides at different time points. The samples were analyzed with ELISA. Apparent permeability was determined from the slopes of linear relationship between amount of protein transported and the time. The experiment was carried out at a constant temperature of 37 °C. Each value is mean of two values ± deviation.

Formulation	**Permeability (P_{app}) (cm/s) x 10^9**
Control (insulin)	1.08 ± 0.15
Polymer + insulin	6.44 ± 1.3
Ins-Tf conjugate	16.3 ± 2
Polymer + conjugate	24 ± 0.05
Conjugate + excess Tf	0.97 ± 0.18

CHAPTER 11

CONCLUSIONS

Oral delivery of proteins has been dubbed the “holy grail of drug delivery” [1, 2]. Oral insulin delivery systems are at the heart of research efforts in the field of oral protein delivery. Development of oral insulin formulations would significantly improve the quality of life of patients suffering from diabetes. The limited bioavailability of therapeutic proteins administered orally is primarily because of their low enzymatic stability and low permeability across the cellular barrier of the intestinal epithelium [3, 4]. Many different approaches, coming from such diverse disciplines as biomaterials, conjugation chemistry, biochemistry, have provided approaches to solve some of the problems associated with oral delivery of proteins.

The complexation hydrogels developed in our laboratory, are one of the most promising classes of materials for use in targeted oral delivery of proteins [4-6]. They exhibit many characteristics that make them ideal candidates for oral delivery applications. Hence, in vivo and in vitro understanding of the functioning of these hydrogels was an important goal since this understanding may lead to newer approaches that may provide even better bioavailability of the orally administered protein. One of the important goals of this work was to carry out in vivo and in vitro studies that could provide valuable information about oral protein delivery using complexation hydrogels.

The two main characteristics of the hydrogels studied in this work were (i) the ability of the PEG chains in the network to increase the gastrointestinal retention of the polymeric carriers (ii) ability of the orally administered hydrogels to protect the degradation of insulin in the gastrointestinal tract.

Evaluation of effect of PEG chains in the P(MAA-g-EG) microparticles on the GI distribution and retention of polymer particles showed that the both the distribution and retention characteristics of the particles were significantly affected due to the presence of PEG chains. The PEG chains increased the retention of the microparticles in both gastric and intestinal environment. Increase in the intestinal retention is a desirable feature since it can potentially improve protein absorption by delaying the clearance of the protein from the GI tract.

Another important goal of this work was to analyze and understand the mechanism behind the ability of polymeric carriers to protect insulin degradation during transit in the GI tract. Our results showed that the hydrogels were very effective in protecting the entrapped insulin in the gastric environment and could also inhibit the intestinal enzymes to certain extent by binding free Ca^{2+} in the intestinal fluid solution.

Results from confocal microscopy analysis of insulin transport in Caco-2 cells indicated that the primary route of transport was the paracellular pathway and that the transcellular component of the transport was insignificant. In addition, studies with sodium caprate, a model permeation enhancer, showed

that using a permeation enhancer with complexation hydrogels may cause permanent damage to the cell monolayer.

Hence, it was proposed that any further enhancement in the overall efficacy of our oral formulations would require

(i) Improved stability of insulin against proteolytic attack in the intestinal environment. This could significantly improve the bioavailability since the enzyme inhibition by complexation hydrogels can also protect the insulin

(ii) Improvement in the permeability characteristics of insulin across the intestinal epithelium, preferably through the specific transcellular pathway

Based on these observation, a strategy was formulated that could further enhance the bioavailability of insulin when administered using complexation hydrogels. Insulin was conjugated to transferrin, which can get transcytosed across the intestinal epithelium by receptor-mediated transcytotis. Work of Shen and coworkers has shown that orally administered insulin-transferrin conjugate (Ins-Tf conjugate) was able to reach the systemic circulation in intact form [7, 8].

We developed a formulation consisting of the complexation hydrogels for delivery of Ins-Tf conjugates. The conjugates were successful synthesized and the polymer microparticles were optimized for the delivery of Ins-Tf conjugates.

Finally, cellular evaluation of the formulation consisting of complexation hydrogels and the Ins-Tf conjugates was carried out. Overall, approximately 24

fold increase in the insulin permeability was demonstrated due to the combined effect of the conjugation and the presence of the complexation hydrogels.

Thus in this work, we have developed a formulation that combines the beneficial characteristics of the Ins-Tf conjugates and the complexation hydrogels. The formulation was demonstrated to have characteristics that make it a very promising candidate for oral insulin delivery.

References

1 Shah, D. and Shen, W. C. (1995) The paradox of transferrin receptor-mediated drug delivery--intracellular targeting or transcellular transport? J Drug Target **3**, 243-245

2 Peppas, N. A., Wood, K. M. and Blanchette, J. O. (2004) Hydrogels for oral delivery of therapeutic proteins. Expert Opin Biol Ther **4**, 881-887

3 Blanchette, J., Kavimandan, N. and Peppas, N. A. (2004) Principles of transmucosal delivery of therapeutic agents. Biomed Pharmacother **58**, 142-151

4 Lowman, A. M., Morishita, M., Kajita, M., Nagai, T. and Peppas, N. A. (1999) Oral delivery of insulin using pH-responsive complexation gels. J Pharm Sci **88**, 933-937

5 Lowman, A. M. and Peppas, N. A. (1997) Design of oral delivery systems for peptides and proteins using complexation graft copolymer networks. In Biomaterials, Carriers for Drug Delivery and Scaffolds for Tissue Engineering (Peppas, N. A., Mooney, D. J., Mikos, A. G. and Brannos-Peppas, L., eds.), pp. 21-23, AIChE, New York

6 Lopez, J. E. and Peppas, N. A. (2004) Cellular evaluation of insulin transmucosal delivery. J Biomater Sci Polym Ed **15**, 385-396

7 Xia, C. Q., Wang, J. and Shen, W. C. (2000) Hypoglycemic effect of insulin-transferrin conjugate in streptozotocin-induced diabetic rats. J Pharmacol Exp Ther **295**, 594-600

8 Shah, D. and Shen, W. C. (1996) Transcellular delivery of an insulin-transferrin conjugate in enterocyte-like Caco-2 cells. J Pharm Sci **85**, 1306-1311

BIBLIOGRAPHY

Amos, A. F., McCarty, D. J. and Zimmet, P. (1997) The rising global burden of diabetes and its complications: estimates and projections to the year 2010. Diabet Med **14 Suppl 5**, S1-85

Anderberg, E. K., Lindmark, T. and Artursson, P. (1993) Sodium caprate elicits dilatations in human intestinal tight junctions and enhances drug absorption by the paracellular route. Pharm Res **10**, 857-864

Anderson, J. M. and Van Itallie, C. M. (1995) Tight junctions and the molecular basis for regulation of paracellular permeability. Am J Physiol **269**, G467-475

Anthony, S., Odgers, T. and Kelly, W. (2004) Health promotion and health education about diabetes mellitus. J R Soc Health **124**, 70-73

Arbit, E. (2004) The physiological rationale for oral insulin administration. Diabetes Technol Ther **6**, 510-517

Artursson, P. and Borchardt, R. T. (1997) Intestinal drug absorption and metabolism in cell cultures: Caco-2 and beyond. Pharm Res **14**, 1655-1658

Artursson, P., Lindmark, T., Davis, S. S. and Illum, L. (1994) Effect of chitosan on the permeability of monolayers of intestinal epithelial cells (Caco-2). Pharm Res **11**, 1358-1361

Artursson, P., Palm, K. and Luthman, K. (2001) Caco-2 monolayers in experimental and theoretical predictions of drug transport. Adv Drug Deliv Rev **46**, 27-43

Asada, H., Douen, T., Mizokoshi, Y., Fujita, T., Murakami, M., Yamamoto, A. and Muranishi, S. (1994) Stability of acyl derivatives of insulin in the small intestine: relative importance of insulin association characteristics in aqueous solution. Pharm Res **11**, 1115-1120

Audus, K. L., Bartel, R. L., Hidalgo, I. J. and Borchardt, R. T. (1990) The use of cultured epithelial and endothelial cells for drug transport and metabolism studies. Pharm Res **7**, 435-451

Aungst, B. J. (2000) Intestinal permeation enhancers. J Pharm Sci **89**, 429-442

Aungst, B. J. and Rogers, N. J. (1988) Site dependence of absorption-promoting actions of laureth-9, Na salicylate, Na2EDTA, and aprotinin on rectal, nasal, and buccal insulin delivery. Pharm Res **5**, 305-308

Aungst, B. J., Saitoh, H., Burcham, D. L., Huang, S. M., Mousa, S. A. and Hussain, M. A. (1996) Enhancement of the intestinal absorption of peptides and non-peptides. J Control Rel **41**, 19-31

Azari, P. R. and Feeney, R. E. (1958) Resistance of metal complexes of conalbumin and transferrin to proteolysis and to thermal denaturation. J Biol Chem **232**, 293-302

Bai, J. P. and Chang, L. L. (1995) Transepithelial transport of insulin: I. Insulin degradation by insulin-degrading enzyme in small intestinal epithelium. Pharm Res **12**, 1171-1175

Bai, J. P., Chang, L. L. and Guo, J. H. (1996) Effects of polyacrylic polymers on the degradation of insulin and peptide drugs by chymotrypsin and trypsin. J Pharm Pharmacol **48**, 17-21

Balimane, P. V., Chong, S. and Morrison, R. A. (2000) Current methodologies used for evaluation of intestinal permeability and absorption. J Pharmacol Toxicol Methods **44**, 301-312

Banerjee, D., Flanagan, P. R., Cluett, J. and Valberg, L. S. (1986) Transferrin receptors in the human gastrointestinal tract. Relationship to body iron stores. Gastroenterology **91**, 861-869

Barnett, A. H. and Owens, D. R. (1997) Insulin analogues. Lancet **349**, 47-51

Bartunik, H. D., Summers, L. J. and Bartsch, H. H. (1989) Crystal structure of bovine beta-trypsin at 1.5 A resolution in a crystal form with low molecular packing density. Active site geometry, ion pairs and solvent structure. J Mol Biol **210**, 813-828

Baudry, B., Fasano, A., Ketley, J. and Kaper, J. B. (1992) Cloning of a gene (zot) encoding a new toxin produced by Vibrio cholerae. Infect Immun **60**, 428-434

Bell, C. L. and Peppas, N. A. (1996) Water, solute and protein diffusion in physiologically responsive hydrogels of poly (methacrylic acid-g-ethylene glycol). Biomaterials **17**, 1203-1218

Bendayan, M., Ziv, E., Ben-Sasson, R., Bar-On, H. and Kidron, M. (1990) Morpho-cytochemical and biochemical evidence for insulin absorption by the rat ileal epithelium. Diabetologia **33**, 197-204

Bendayan, M., Ziv, E., Gingras, D., Ben-Sasson, R., Bar-On, H. and Kidron, M. (1994) Biochemical and morpho-cytochemical evidence for the intestinal absorption of insulin in control and diabetic rats. Comparison between the effectiveness of duodenal and colon mucosa. Diabetologia **37**, 119-126

Benjamin, S. M., Valdez, R., Geiss, L. S., Rolka, D. B. and Narayan, K. M. (2003) Estimated number of adults with prediabetes in the US in 2000: opportunities for prevention. Diabetes Care **26**, 645-649

Bernkop-Schnurch, A. (1998) The use of inhibitory agents to overcome the enzymatic barrier to perorally administered therapeutic peptides and proteins. J Control Rel **52**, 1-16

Bernkop-Schnurch, A., Konig, V., Leitner, V. M., Krauland, A. H. and Brodnik, I. (2004) Preparation and characterisation of thiolated poly(methacrylic acid)-starch compositions. Eur J Pharm Biopharm **57**, 219-224

Beyer, U., Roth, T., Schumacher, P., Maier, G., Unold, A., Frahm, A. W., Fiebig, H. H., Unger, C. and Kratz, F. (1998) Synthesis and in vitro efficacy of transferrin conjugates of the anticancer drug chlorambucil. J Med Chem **41**, 2701-2708

Bickel, U., Yoshikawa, T. and Pardridge, W. M. (2001) Delivery of peptides and proteins through the blood-brain barrier. Adv Drug Deliv Rev **46**, 247-279

Blanchette, J., Kavimandan, N. and Peppas, N. A. (2004) Principles of transmucosal delivery of therapeutic agents. Biomed Pharmacother **58**, 142-151

Blanchette, J. and Peppas, N. A. (2005) Cellular evaluation of oral chemotherapy carriers. J Biomed Mater Res A **72A**, 381-388

Blanchette, J. and Peppas, N. A. (2005) Oral chemotherapeutic delivery: design and cellular response. Ann Biomed Eng **33**, 142-149

Bolli, G. B., Di Marchi, R. D., Park, G. D., Pramming, S. and Koivisto, V. A. (1999) Insulin analogues and their potential in the management of diabetes mellitus. Diabetologia **42**, 1151-1167

Bradford, M. M. (1976) A rapid and sensitive method for the quantitation of microgram quantities of protein utilizing the principle of protein-dye binding. Anal Biochem **72**, 248-254

Brange, J. and Volund, A. (1999) Insulin analogs with improved pharmacokinetic profiles. Adv Drug Deliv Rev **35**, 307-335

Brannon-Peppas, L. and Blanchette, J. O. (2004) Nanoparticle and targeted systems for cancer therapy. Adv Drug Deliv Rev **56**, 1649-1659

Brannon-Peppas, L. and Peppas, N. A. (1991) Equilibrium swelling behavior of pH-sensitive hydrogels. Chem Eng Sci **46**, 715-722

Broadwell, R. D., Baker-Cairns, B. J., Friden, P. M., Oliver, C. and Villegas, J. C. (1996) Transcytosis of protein through the mammalian cerebral epithelium and endothelium. III. Receptor-mediated transcytosis through the blood-brain barrier of blood-borne transferrin and antibody against the transferrin receptor. Exp Neurol **142**, 47-65

Burdo, J. R., Antonetti, D. A., Wolpert, E. B. and Connor, J. R. (2003) Mechanisms and regulation of transferrin and iron transport in a model blood-brain barrier system. Neuroscience **121**, 883-890

Carlsson, J., Drevin, H. and Axen, R. (1978) Protein thiolation and reversible protein-protein conjugation. N-Succinimidyl 3-(2-pyridyldithio)propionate, a new heterobifunctional reagent. Biochem J **173**, 723-737

Cefalu, W. T. (2004) Concept, strategies, and feasibility of noninvasive insulin delivery. Diabetes Care **27**, 239-246

Cefalu, W. T., Rosenstock, J. and Bindra, S. (2002) Inhaled insulin: a novel route for insulin delivery. Expert Opin Investig Drugs **11**, 687-691

Cevc, G., Gebauer, D., Stieber, J., Schatzlein, A. and Blume, G. (1998) Ultraflexible vesicles, Transfersomes, have an extremely low pore penetration resistance and transport therapeutic amounts of insulin across the intact mammalian skin. Biochim Biophys Acta **1368**, 201-215

Chowdary, K. P. and Rao, Y. S. (2003) Design and in vitro and in vivo evaluation of mucoadhesive microcapsules of glipizide for oral controlled release: a technical note. AAPS PharmSciTech **4**, E39

Chowdary, K. P. and Rao, Y. S. (2004) Mucoadhesive microspheres for controlled drug delivery. Biol Pharm Bull **27**, 1717-1724

Clark, M. A., Hirst, B. H. and Jepson, M. A. (2000) Lectin-mediated mucosal delivery of drugs and microparticles. Adv Drug Deliv Rev **43**, 207-223

Clement, S., Dandona, P., Still, J. G. and Kosutic, G. (2004) Oral modified insulin (HIM2) in patients with type 1 diabetes mellitus: results from a phase I/II clinical trial. Metabolism **53**, 54-58

DeAscentiis, A., Bettini, R., Colombo, P. and Peppas, N. A. (1996) [Mucoadhesive properties of hydrophilic polymer microparticles]. Boll Chim Farm **135**, 101-103

DeAscentiis, A., Colombo, P. and Peppas, N. A. (1995) Screening of potentially mucoadhesive polymer microparticles in contact with rat intestinal mucosa. J Pharmacol Biopharmacol **41**, 229-334

DeAscentiis, A., de Grazia, J. L., Bowman, C. N., Colombo, P. and Peppas, N. A. (1995) Mucoadhesion of poly(2-hydroxyethyl methacrylate) is improved when linear poly(ethylene oxide) chains are added to the polymer network. J Control Rel **33**, 197-201

De Groot, M., Schuurs, T. A. and van Schilfgaarde, R. (2004) Causes of limited survival of microencapsulated pancreatic islet grafts. J Surg Res **121**, 141-150

De la Torre, P. M., Enobakhare, Y., Torrado, G. and Torrado, S. (2003) Release of amoxicillin from polyionic complexes of chitosan and poly(acrylic acid). Study of polymer/polymer and polymer/drug interactions within the network structure. Biomaterials **24**, 1499-1506

De la Torre, P. M., Torrado, G. and Torrado, S. (2005) Poly (acrylic acid) chitosan interpolymer complexes for stomach controlled antibiotic delivery. J Biomed Mater Res B Appl Biomater **72**, 191-197

Denker, B. M. and Nigam, S. K. (1998) Molecular structure and assembly of the tight junction. Am J Physiol **274**, F1-9

Dominguez, L. J. and Licata, G. (2001) [The discovery of insulin: what really happened 80 years ago]. Ann Ital Med Int **16**, 155-162

Dorkoosh, F. A., Stokkel, M. P., Blok, D., Borchard, G., Rafiee-Tehrani, M., Verhoef, J. C. and Junginger, H. E. (2004) Feasibility study on the retention of superporous hydrogel composite polymer in the intestinal tract of man using scintigraphy. J Control Release **99**, 199-206

Drejer, K., Vaag, A., Bech, K., Hansen, P., Sorensen, A. R. and Mygind, N. (1992) Intranasal administration of insulin with phospholipid as absorption enhancer: pharmacokinetics in normal subjects. Diabet Med **9**, 335-340

Fasano, A. (1998) Novel approaches for oral delivery of macromolecules. J Pharm Sci **87**, 1351-1356

Fasano, A. and Uzzau, S. (1997) Modulation of intestinal tight junctions by Zonula occludens toxin permits enteral administration of insulin and other macromolecules in an animal model. J Clin Invest **99**, 1158-1164

Faulstich, H., Zobeley, S., Heintz, D. and Drewes, G. (1993) Probing the phalloidin binding site of actin. FEBS Lett **318**, 218-222

Fix, J. A. (1996) Strategies for delivery of peptides utilizing absorption-enhancing agents. J Pharm Sci **85**, 1282-1285

Foldvari, M. (2000) Non-invasive administration of drugs through the skin: challenges in delivery system design. Pharm Sci Technol Today **3**, 417-425

Foss, A. C., Goto, T., Morishita, M. and Peppas, N. A. (2004) Development of acrylic-based copolymers for oral insulin delivery. Eur J Pharm Biopharm **57**, 163-169

Foss, A. C. and Peppas, N. A. (2004) Investigation of the cytotoxicity and insulin transport of acrylic-based copolymer protein delivery systems in contact with Caco-2 cultures. Eur J Pharm Biopharm **57**, 447-455

Frizzell, R. A. and Schultz, S. G. (1972) Ionic conductances of extracellular shunt pathway in rabbit ileum. Influence of shunt on transmural sodium transport and electrical potential differences. J Gen Physiol **59**, 318-346

Gabbe, S. G. and Graves, C. R. (2003) Management of diabetes mellitus complicating pregnancy. Obstet Gynecol **102**, 857-868

Gabor, F., Schwarzbauer, A. and Wirth, M. (2002) Lectin-mediated drug delivery: binding and uptake of BSA-WGA conjugates using the Caco-2 model. Int J Pharm **237**, 227-239

Gabor, F., Stangl, M. and Wirth, M. (1998) Lectin-mediated bioadhesion: binding characteristics of plant lectins on the enterocyte-like cell lines Caco-2, HT-29 and HCT-8. J Control Rel **55**, 131-142

Gabor, F., Wirth, M., Jurkovich, B., Haberl, I., Theyer, G., Walcher, G. and Hamilton, G. (1997) Lectin-mediated bioadhesion: Proteolytic stability and binding-characteristics of wheat germ agglutinin and Solanum tuberosum lectin on Caco-2, HT-29 and human colonocytes. J Control Rel **49**, 27-37

Gallo-Payet, N. and Hugon, J. S. (1984) Insulin receptors in isolated adult mouse intestinal cells: studies in vivo and in organ culture. Endocrinology **114**, 1885-1892

Ganong, W. (1995) Review of medical physiology. Appleton & Lange, Stamford, CT

Garnett, M. C. (2001) Targeted drug conjugates: principles and progress. Adv Drug Deliv Rev **53**, 171-216

Genuth, S., Alberti, K. G., Bennett, P., Buse, J., Defronzo, R., Kahn, R., Kitzmiller, J., Knowler, W. C., Lebovitz, H., Lernmark, A., Nathan, D., Palmer, J., Rizza, R., Saudek, C., Shaw, J., Steffes, M., Stern, M., Tuomilehto, J. and Zimmet, P. (2003) Follow-up report on the diagnosis of diabetes mellitus. Diabetes Care **26**, 3160-3167

Gingerich, R. L., Gilbert, W. R., Comens, P. G. and Gavin, J. R., 3rd (1987) Identification and characterization of insulin receptors in basolateral membranes of dog intestinal mucosa. Diabetes **36**, 1124-1129

Goldraich, M. and Kost, J. (1993) Glucose-sensitive polymeric matrices for controlled drug delivery. Clin Mater **13**, 135-142

Gordon, G. S., Moses, A. C., Silver, R. D., Flier, J. S. and Carey, M. C. (1985) Nasal absorption of insulin: enhancement by hydrophobic bile salts. Proc Natl Acad Sci U S A **82**, 7419-7423

Gosk, S., Vermehren, C., Storm, G. and Moos, T. (2004) Targeting anti-transferrin receptor antibody (OX26) and OX26-conjugated liposomes to brain

capillary endothelial cells using in situ perfusion. J Cereb Blood Flow Metab **24**, 1193-1204

Guevara-Aguirre, J., Guevara, M., Saavedra, J., Mihic, M. and Modi, P. (2004) Oral spray insulin in treatment of type 2 diabetes: a comparison of efficacy of the oral spray insulin (Oralin) with subcutaneous (SC) insulin injection, a proof of concept study. Diabetes Metab Res Rev **20**, 472-478

Gumbiner, B. (1987) Structure, biochemistry, and assembly of epithelial tight junctions. Am J Physiol **253**, C749-758

Gupta, V. K., Assmus, M. W., Beckert, T. E. and Price, J. C. (2001) A novel pH- and time-based multi-unit potential colonic drug delivery system. II. Optimization of multiple response variables. Int J Pharm **213**, 93-102

Gupta, V. K., Beckert, T. E. and Price, J. C. (2001) A novel pH- and time-based multi-unit potential colonic drug delivery system. I. Development. Int J Pharm **213**, 83-91

Hassan, C. M., Doyle, F. J. and Peppas, N. A. (1997) Dynamic Behavior of Glucose-Responsive Poly(methacrylic acid-g-ethylene glycol) Hydrogels. Macromolecules **30**, 6166-6173

Hayakawa, E., Yamamoto, A., Shoji, Y. and Lee, V. H. (1989) Effect of sodium glycocholate and polyoxyethylene-9-lauryl ether on the hydrolysis of varying concentrations of insulin in the nasal homogenates of the albino rabbit. Life Sci **45**, 167-174

Hill, R. A., Strat, A. L., Hughes, N. J., Kokta, T. J., Dodson, M. V. and Gertler, A. (2004) Early insulin signaling cascade in a model of oxidative skeletal muscle: mouse Sol8 cell line. Biochim Biophys Acta **1693**, 205-211

Heinemann, L., Pfutzner, A. and Heise, T. (2001) Alternative routes of administration as an approach to improve insulin therapy: update on dermal, oral, nasal and pulmonary insulin delivery. Curr Pharm Des **7**, 1327-1351

Hermansen, K., Ronnemaa, T., Petersen, A. H., Bellaire, S. and Adamson, U. (2004) Intensive therapy with inhaled insulin via the AERx insulin diabetes management system: a 12-week proof-of-concept trial in patients with type 2 diabetes. Diabetes Care **27**, 162-167

Huang, Y., Leobandung, W., Foss, A. and Peppas, N. A. (2000) Molecular aspects of muco- and bioadhesion: tethered structures and site-specific surfaces. J Control Rel **65**, 63-71

Ichikawa, H. and Peppas, N. A. (2003) Novel complexation hydrogels for oral peptide delivery: In vitro evaluation of their cytocompatibility and insulin-transport enhancing effects using Caco-2 cell monolayers. J Biomed Mat Res **67A**, 609-617

Jones, A. T., Gumbleton, M. and Duncan, R. (2003) Understanding endocytic pathways and intracellular trafficking: a prerequisite for effective design of advanced drug delivery systems. Adv Drug Deliv Rev **55**, 1353-1357

Kan, K. S. and Coleman, R. (1988) The calcium ionophore A23187 increases the tight-junctional permeability in rat liver. Biochem J **256**, 1039-1041

Kendzierski, K. S., Pansky, B., Budd, G. C. and Saffran, M. (2000) Evidence for biosynthesis of preproinsulin in gut of rat. Endocrine **13**, 353-359

Kilpatrick, D. C., Pusztai, A., Grant, G., Graham, C. and Ewen, S. W. B. (1985) Tomato lectin resists digestion in the mammalian alimentary canal and binds to intestinal villi without deleterious effects. FEBS Letters **185**, 299-305

King, H., Aubert, R. E. and Herman, W. H. (1998) Global burden of diabetes, 1995-2025: prevalence, numerical estimates, and projections. Diabetes Care **21**, 1414-1431

Kissel, T. and Werner, U. (1998) Nasal delivery of peptides: an in vitro cell culture model for the investigation of transport and metabolism in human nasal epithelium. J Control Rel **53**, 195-203

Lacaz-Vieira, F. (1997) Calcium site specificity. Early Ca2+-related tight junction events. J Gen Physiol **110**, 727-740

Lafont, J., Rouanet, J. M., Gabrion, J., Assouad, J. L., Zambonino Infante, J. L. and Besancon, P. (1988) Duodenal toxicity of dietary Phaseolus vulgaris lectins in the rat: an integrative assay. Digestion **41**, 83-93

Lamprecht, A., Saumet, J. L., Roux, J. and Benoit, J. P. (2004) Lipid nanocarriers as drug delivery system for ibuprofen in pain treatment. Int J Pharm **278**, 407-414

Langguth, P., Bohner, V., Heizmann, J., Merkle, H. P., Wolffram, S., Amidon, G. L. and Yamashita, S. (1997) The challenge of proteolytic enzymes in intestinal peptide delivery. J Control Rel **46**, 39-57

Langkjaer, L., Brange, J., Grodsky, G. M. and Guy, R. H. (1998) Iontophoresis of monomeric insulin analogues in vitro: effects of insulin charge and skin pretreatment. J Control Rel **51**, 47-56

Le, L., Kost, J. and Mitragotri, S. (2000) Combined effect of low-frequency ultrasound and iontophoresis: applications for transdermal heparin delivery. Pharm Res **17**, 1151-1154

Lee, V. H. (1988) Enzymatic barriers to peptide and protein absorption. Crit Rev Ther Drug Carrier Syst **5**, 69-97

Lee, V. H. L. and Yamamoto, A. (1989) Penetration and enzymatic barriers to peptide and protein absorption. Adv Drug Deliv Rev **4**, 171-207

Lee, V. H., Yamamoto, A. and Kompella, U. B. (1991) Mucosal penetration enhancers for facilitation of peptide and protein drug absorption. Crit Rev Ther Drug Carrier Syst **8**, 91-192

Lehr, C. M. (2000) Lectin-mediated drug delivery: the second generation of bioadhesives. J Control Rel **65**, 19-29

Li, H. and Qian, Z. M. (2002) Transferrin/transferrin receptor-mediated drug delivery. Med Res Rev **22**, 225-250

Lillioja, S., Mott, D. M., Spraul, M., Ferraro, R., Foley, J. E., Ravussin, E., Knowler, W. C., Bennett, P. H. and Bogardus, C. (1993) Insulin resistance and insulin secretory dysfunction as precursors of non-insulin-dependent diabetes mellitus. Prospective studies of Pima Indians. N Engl J Med **329**, 1988-1992

Lindmark, T., Nikkila, T. and Artursson, P. (1995) Mechanisms of absorption enhancement by medium chain fatty acids in intestinal epithelial Caco-2 cell monolayers. J Pharmacol Exp Ther **275**, 958-964

Lindmark, T., Schipper, N., Lazorova, L., de Boer, A. G. and Artursson, P. (1998) Absorption enhancement in intestinal epithelial Caco-2 monolayers by sodium caprate: assessment of molecular weight dependence and demonstration of transport routes. J Drug Target **5**, 215-223

Lindsay, D. G. and Shall, S. (1971) The acetylation of insulin. Biochem J **121**, 737-745

Lopez, J. E. and Peppas, N. A. (2004) Cellular evaluation of insulin transmucosal delivery. J Biomater Sci Polym Ed **15**, 385-396

Lopez, J. E. and Peppas, N. A. (2004) Effect of poly (ethylene glycol) molecular weight and microparticle size on oral insulin delivery from P(MAA-g-EG) microparticles. Drug Dev Ind Pharm **30**, 497-504

Lowman, A. M., Morishita, M., Kajita, M., Nagai, T. and Peppas, N. A. (1999) Oral delivery of insulin using pH-responsive complexation gels. J Pharm Sci **88**, 933-937

Lowman, A. M. and Peppas, N. A. (1997) Design of oral delivery systems for peptides and proteins using complexation graft copolymer networks. AIChE, New York

Lowman, A. M. and Peppas, N. A. (1997) Analysis of the Complexation/Decomplexation Phenomena in Graft Copolymer Networks. Macromolecules **30**, 4959 -4965

Lorenzen, A. and Kennedy, S. W. (1993) A fluorescence-based protein assay for use with a microplate reader. Anal Biochem **214**, 346-348

LuBen, H. L., Rentel, C. O., Kotze, A. F., Lehr, C. M., de Boer, A. G., Verhoef, J. C. and Junginger, H. E. (1997) Mucoadhesive polymers in peroral peptide drug delivery. IV. Polycarbophil and chitosan are potent enhancers of peptide transport across intestinal mucosae in vitro. J Control Rel **45**, 15-23

MacAdams, A. (1993) The effect of gastro-intestinal mucus on drug absorption. Adv Drug Deliv Rev **11**, 201-220

Madara, J. L. and Trier, J. S. (1986) Functional morphology of the mucosa of the small intestine. In Physiology of the Gastrointestinal Tract (Johnson, L. R., ed.), pp. 1209-1250, Raven Press, New York

Madara, J. L. and Pappenheimer, J. R. (1987) Structural basis for physiological regulation of paracellular pathways in intestinal epithelia. J Membr Biol **100**, 149-164

Madsen, F. and Peppas, N. A. (1999) Complexation graft copolymer networks: swelling properties, calcium binding and proteolytic enzyme inhibition. Biomaterials **20**, 1701-1708

Malmberg, K. (1997) Prospective randomised study of intensive insulin treatment on long term survival after acute myocardial infarction in patients with diabetes mellitus. DIGAMI (Diabetes Mellitus, Insulin Glucose Infusion in Acute Myocardial Infarction) Study Group. Bmj **314**, 1512-1515

McAulay, V. and Frier, B. M. (2003) Insulin analogues and other developments in insulin therapy for diabetes. Expert Opin Pharmacother **4**, 1141-1156

McCarthy, A. A. (2004) New approaches to diabetes disease control, insulin delivery, and monitoring. Chem Biol **11**, 1597-1598

McChesney, L. P. (1999) Advances in pancreas transplantation for the treatment of diabetes. Dis Mon **45**, 88-100

Mei, H., Yu, C. and Chan, K. K. (1999) NB1-C16-insulin: site-specific synthesis, purification, and biological activity. Pharm Res **16**, 1680-1686

Mellman, I., Fuchs, R. and Helenius, A. (1986) Acidification of the endocytic and exocytic pathways. Annl Rev Biochem **55**, 663-700

Melton, R. G. and Sherwood, R. F. (1996) Antibody-enzyme conjugates for cancer therapy. J Natl Cancer Inst **88**, 153-165

Mitragotri, S., Blankschtein, D. and Langer, R. (1995) Ultrasound-mediated transdermal protein delivery. Science **269**, 850-853

Miyazaki, Y., Ogihara, K., Yakou, S., Nagai, T. and Takayama, K. (2003) In vitro and in vivo evaluation of mucoadhesive microspheres consisting of dextran derivatives and cellulose acetate butyrate. Int J Pharm **258**, 21-29

Modi, P., Mihic, M. and Lewin, A. (2002) The evolving role of oral insulin in the treatment of diabetes using a novel RapidMist System. Diabetes Metab Res Rev **18 Suppl 1**, S38-42

Mohammed, A. and Dent, A. (1998) Bioconjugation: protein coupling techniques for the biomedical sciences. Grove's Dictionaries, New York

Mohan, V. (2002) Which Insulin to Use? Human or Animal? Current Science **83**, 1544-1547

Morishita, M., Goto, T., Peppas, N. A., Joseph, J. I., Torjman, M. C., Munsick, C., Nakamura, K., Yamagata, T., Takayama, K. and Lowman, A. M. (2004) Mucosal insulin delivery systems based on complexation polymer hydrogels: effect of particle size on insulin enteral absorption. J Control Rel **97**, 115-124

Morishita, M., Morishita, I., Takayama, K., Machida, Y. and Nagai, T. (1993) Site-dependent effect of aprotinin, sodium caprate, Na_2EDTA and sodium glycocholate on intestinal absorption of insulin. Biol Pharm Bull **16**, 68-72

Morishita, M., Lowman, A. M., Takayama, K., Nagai, T. and Peppas, N. A. (2002) Elucidation of the mechanism of incorporation of insulin in controlled release systems based on complexation polymers. J Control Rel **81**, 25-32

Mudaliar, S. and Edelman, S. V. (2001) Insulin therapy in type 2 diabetes. Endocrinol Metab Clin North Am **30**, 935-982

Mun, G. A., Nurkeeva, Z. S., Khutoryanskiy, V. V., Sergaziyev, A. D. and Rosiak, J. M. (2002) Radiation synthesis of temperature-responsive hydrogels by copolymerization of [2-(methacryloyloxy)ethyl]trimethylammonium chloride with N-isopropylacrylamide. Radiation Physics and Chemistry **65**, 67-70

Nagahora, H., Harata, K., Muraki, M. and Jigami, Y. (1995) Site-directed mutagenesis and sugar-binding properties of the wheat germ agglutinin mutants Tyr73Phe and Phe116Tyr. Eur J Biochem **233**, 27-34

Nagai, T. (1986) Topical mucosal adhesive dosage forms. Med Res Rev **6**, 227-242

Nakamura, K., Murray, R. J., Joseph, J. I., Peppas, N. A., Morishita, M. and Lowman, A. M. (2004) Oral insulin delivery using P(MAA-g-EG) hydrogels: effects of network morphology on insulin delivery characteristics. J Control Rel **95**, 589-599

Nakashima, K., Miyagi, M., Goto, K., Matsumoto, Y. and Ueoka, R. (2004) Enzymatic and hyperglycemia stability of chemically modified insulins with hydrophobic acyl groups. Bioorg Med Chem Lett **14**, 481-483

Naisbett, B., Woodley, J. and Department of Biological Sciences, U. o. K. S. U. K. (1990) Binding of tomato lectin to the intestinal mucosa and its potential for oral drug delivery. Biochemical Society transactions. **18(5)**, 879-880

Nam, I. K., Mun, G. A., Urkimbaeva, P. I. and Nurkeeva, Z. S. (2003) Gamma-induced synthesis of hydrogels of vinyl ethers with stimuli-sensitive behavior. Radiation Physics and Chemistry **66**, 281-287

Noah, N. D., Bender, A. E., Reaidi, G. B. and Gilbert, R. J. (1980) Food poisoning from raw red kidney beans. British Medical Journal **281**, 236-237

Nolte, M. S., Taboga, C., Salamon, E., Moses, A., Longenecker, J., Flier, J. and Karam, J. H. (1990) Biological activity of nasally administered insulin in normal subjects. Horm Metab Res **22**, 170-174

Ohkubo, Y., Kishikawa, H., Araki, E., Miyata, T., Isami, S., Motoyoshi, S., Kojima, Y., Furuyoshi, N. and Shichiri, M. (1995) Intensive insulin therapy prevents the progression of diabetic microvascular complications in Japanese patients with

non-insulin-dependent diabetes mellitus: a randomized prospective 6-year study. Diabetes Res Clin Pract **28**, 103-117

Oliva, A., Farina, J. and Llabres, M. (2000) Development of two high-performance liquid chromatographic methods for the analysis and characterization of insulin and its degradation products in pharmaceutical preparations. J Chromatogr B Biomed Sci Appl **749**, 25-34

Opara, E. C. and Kendall, W. F., Jr. (2002) Immunoisolation techniques for islet cell transplantation. Expert Opin Biol Ther **2**, 503-511

Owens, D. R. (2002) New horizons--alternative routes for insulin therapy. Nat Rev Drug Discov **1**, 529-540

Owens, D. R., Zinman, B. and Bolli, G. (2003) Alternative routes of insulin delivery. Diabet Med **20**, 886-898

Owens, D. R., Zinman, B. and Bolli, G. B. (2001) Insulins today and beyond. Lancet **358**, 739-746

Palmieri, G. F., Michelini, S., Di Martino, P. and Martelli, S. (2000) Polymers with pH-dependent solubility: possibility of use in the formulation of gastroresistant and controlled-release matrix tablets. Drug Dev Ind Pharm **26**, 837-845

Park, K. S. (2004) Prevention of type 2 diabetes mellitus from the viewpoint of genetics. Diabetes Res Clin Pract **66 Suppl 1**, S33-35

Patton, J. S., Bukar, J. and Nagarajan, S. (1999) Inhaled insulin. Adv Drug Deliv Rev **35**, 235-247

Peppas, N. A. (2004) Devices based on intelligent biopolymers for oral protein delivery. Int J Pharm **277**, 11-17

Peppas, N. A. and Barr-Howell, B. D. (1986) In Hydrogels in Medicine and Pharmacy (Peppas, N. A., ed.), pp. 28-55, CRC Press, Boca Raton, FL

Peppas, N. A., Bures, P., Leobandung, W. and Ichikawa, H. (2000) Hydrogels in pharmaceutical formulations. Eur J Pharm Biopharm **50**, 27-46

Peppas, N. A., Huang, Y., Torres-Lugo, M., Ward, J. H. and Zhang, J. (2000) Physicochemical foundations and structural design of hydrogels in medicine and biology. Annu Rev Biomed Eng **2**, 9-29

Peppas, N. A. and Klier, J. (1991) Controlled release by using poly(methacrylic acid-g-ethylene glycol) hydrogels. J Control Rel **16**, 203-214

Peppas, N. A., Lowman, A. M. (1998) Protein Delivery from Novel Bioadhesive Complexation Hydrogels. In Protein and Peptide Drug Research (Frøkjær, S., Christup, L., Krogsgaard-Larsen, P., ed.), pp. 206-216, Munksgaard, Copenhagen

Peppas, N. A., Wood, K. M. and Blanchette, J. O. (2004) Hydrogels for oral delivery of therapeutic proteins. Expert Opin Biol Ther **4**, 881-887

Pillion, D. J., Ganapathy, V. and Leibach, F. H. (1985) Identification of insulin receptors on the mucosal surface of colon epithelial cells. J Biol Chem **260**, 5244-5247

Podual, K., Doyle, F. J., 3rd and Peppas, N. A. (2000) Dynamic behavior of glucose oxidase-containing microparticles of poly(ethylene glycol)-grafted

cationic hydrogels in an environment of changing pH. Biomaterials **21**, 1439-1450

Ponchel, G. and Irache, J. (1998) Specific and non-specific bioadhesive particulate systems for oral delivery to the gastrointestinal tract. Adv Drug Deliv Rev **34**, 191-219

Qian, Z. M., Li, H., Sun, H. and Ho, K. (2002) Targeted drug delivery via the transferrin receptor-mediated endocytosis pathway. Pharmacol Rev **54**, 561-587

Qiu, Y. and Park, K. (2001) Environment-sensitive hydrogels for drug delivery. Adv Drug Deliv Rev **53**, 321-339

Reseland, J. E., Holm, H., Jacobsen, M. B., Jenssen, T. G. and Hanssen, L. E. (1996) Proteinase inhibitors induce selective stimulation of human trypsin and chymotrypsin secretion. J Nutr **126**, 634-642

Rini, J. M. (1995) Lectin structure. Biophysical J **24**, 551-577

Rubas, W., Cromwell, M. E., Shahrokh, Z., Villagran, J., Nguyen, T. N., Wellton, M., Nguyen, T. H. and Mrsny, R. J. (1996) Flux measurements across Caco-2 monolayers may predict transport in human large intestinal tissue. J Pharm Sci **85**, 165-169

Saffran, M., Pansky, B., Budd, G. C. and Williams, F. (1997) Insulin and the gastrointestinal tract. J Control Rel **46**, 89-98

Sahlin, J. J. and Peppas, N. A. (1997) Enhanced hydrogel adhesion by polymer interdiffusion: use of linear poly(ethylene glycol) as an adhesion promoter. J Biomater Sci Polym Ed **8**, 421-436

Saito, G., Swanson, J. A. and Lee, K. D. (2003) Drug delivery strategy utilizing conjugation via reversible disulfide linkages: role and site of cellular reducing activities. Adv Drug Deliv Rev **55**, 199-215

Sajeesh, S. and Sharma, C. P. (2004) Poly methacrylic acid-alginate semi-IPN microparticles for oral delivery of insulin: a preliminary investigation. J Biomater Appl **19**, 35-45

Sakai, M., Imai, T., Ohtake, H., Azuma, H. and Otagiri, M. (1997) Effects of absorption enhancers on the transport of model compounds in Caco-2 cell monolayers: assessment by confocal laser scanning microscopy. J Pharm Sci **86**, 779-785

Salzman, R., Manson, J. E., Griffing, G. T., Kimmerle, R., Ruderman, N., McCall, A., Stoltz, E. I., Mullin, C., Small, D., Armstrong, J. and et al. (1985) Intranasal aerosolized insulin. Mixed-meal studies and long-term use in type I diabetes. N Engl J Med **312**, 1078-1084

Sanger, F. (1959) Chemistry of insulin; determination of the structure of insulin opens the way to greater understanding of life processes. Science **129**, 1340-1344

Sato, Y., Kawashima, Y., Takeuchi, H., Yamamoto, H. and Fujibayashi, Y. (2004) Pharmacoscintigraphic evaluation of riboflavin-containing microballoons for a floating controlled drug delivery system in healthy humans. J Control Rel **98**, 75-85

Sayani, A. P. and Chien, Y. W. (1996) Systemic delivery of peptides and proteins across absorptive mucosae. Crit Rev Ther Drug Carrier Syst **13**, 85-184

Schultz, S. G. and Frizzell, R. A. (1976) Ionic permeability of epithelial tissues. Biochim Biophys Acta **443**, 181-189

Scott, D. A. (1934) Crystalline Insulin. Biochem J **28**, 1592-1602

Sedar, A. W. and Forte, J. G. (1964) Effects Of Calcium Depletion On The Junctional Complex Between Oxyntic Cells Of Gastric Glands. J Cell Biol **22**, 173-188

Shah, D. and Shen, W. C. (1995) The paradox of transferrin receptor-mediated drug delivery--intracellular targeting or transcellular transport? J Drug Target **3**, 243-245

Shah, D. and Shen, W. C. (1996) Transcellular delivery of an insulin-transferrin conjugate in enterocyte-like Caco-2 cells. J Pharm Sci **85**, 1306-1311

Shen, W.-C., Wan, J. and Ekrami, H. (1992) (C) Means to enhance penetration: (3) Enhancement of polypeptide and protein absorption by macromolecular carriers via endocytosis and transcytosis. Adv Drug Deliv Rev **8**, 93-113

Simpson, R. W., Shaw, J. E. and Zimmet, P. Z. (2003) The prevention of type 2 diabetes--lifestyle change or pharmacotherapy? A challenge for the 21st century. Diabetes Res Clin Pract **59**, 165-180

Singh, M. (1999) Transferrin As A targeting ligand for liposomes and anticancer drugs. Curr Pharm Des **5**, 443-451

Skyler, J. S. (1986) Lessons from studies of insulin pharmacokinetics. Diabetes Care **9**, 666-668

Skyler, J. S., Cefalu, W. T., Kourides, I. A., Landschulz, W. H., Balagtas, C. C., Cheng, S. L. and Gelfand, R. A. (2001) Efficacy of inhaled human insulin in type 1 diabetes mellitus: a randomised proof-of-concept study. Lancet **357**, 331-335

Smith, R. N., Hansch, C. and Ames, M. M. (1975) Selection of a reference partitioning system for drug design work. J Pharm Sci **64**, 599-606

Soderholm, J. D., Oman, H., Blomquist, L., Veen, J., Lindmark, T. and Olaison, G. (1998) Reversible increase in tight junction permeability to macromolecules in rat ileal mucosa in vitro by sodium caprate, a constituent of milk fat. Dig Dis Sci **43**, 1547-1552

Stephen, R. L., Petelenz, T. J. and Jacobsen, S. C. (1984) Potential novel methods for insulin administration: I. Iontophoresis. Biomed Biochim Acta **43**, 553-558

Stern, M. P., Williams, K. and Haffner, S. M. (2002) Identification of persons at high risk for type 2 diabetes mellitus: do we need the oral glucose tolerance test? Ann Intern Med **136**, 575-581

Stoever, J. A. and Palmer, J. P. (2002) Inhaled insulin and insulin antibodies: a new twist to an old debate. Diabetes Technol Ther **4**, 157-161

Stratford, R. E. and Lee, V. H. L. (1986) Aminopeptidase activity in homogenates of various absorptive mucosae m the albino rabbit: implications in peptide delivery. Int J Pharm **30**, 73-82

Stuart-Harris, C. H. (1958) The frontiers of medicine. Lancet **2**, 427-430

Stuchbury, T., Shipton, M., Norris, R., Malthouse, J. P., Brocklehurst, K., Herbert, J. A. and Suschitzky, H. (1975) A reporter group delivery system with both absolute and selective specificity for thiol groups and an improved fluorescent probe containing the 7-nitrobenzo-2-oxa-1,3-diazole moiety. Biochem J **151**, 417-432

Tan, K. K., Trull, A. K., Uttridge, J. A. and Wallwork, J. (1995) Relative bioavailability of cyclosporin from conventional and microemulsion formulations in heart-lung transplant candidates with cystic fibrosis. Eur J Clin Pharmacol **48**, 285-289

Thorpe, P. E., Wallace, P. M., Knowles, P. P., Relf, M. G., Brown, A. N., Watson, G. J., Blakey, D. C. and Newell, D. R. (1988) Improved antitumor effects of immunotoxins prepared with deglycosylated ricin A-chain and hindered disulfide linkages. Cancer Res **48**, 6396-6403

Thorpe, P. E., Wallace, P. M., Knowles, P. P., Relf, M. G., Brown, A. N., Watson, G. J., Knyba, R. E., Wawrzynczak, E. J. and Blakey, D. C. (1987) New coupling agents for the synthesis of immunotoxins containing a hindered disulfide bond with improved stability in vivo. Cancer Res **47**, 5924-5931

Tomita, M., Hayashi, M. and Awazu, S. (1994) Comparison of absorption-enhancing effect between sodium caprate and disodium ethylenediaminetetraacetate in Caco-2 cells. Biol Pharm Bull **17**, 753-755

Tomita, M., Hayashi, M., Horie, T., Ishizawa, T. and Awazu, S. (1988) Enhancement of colonic drug absorption by the transcellular permeation route. Pharm Res **5**, 786-789

Tomita, M., Shiga, M., Hayashi, M. and Awazu, S. (1988) Enhancement of colonic drug absorption by the paracellular permeation route. Pharm Res **5**, 341-346

Torrado, S., Prada, P., de la Torre, P. M. and Torrado, S. (2004) Chitosan-poly(acrylic) acid polyionic complex: in vivo study to demonstrate prolonged gastric retention. Biomaterials **25**, 917-923

Torres-Lugo, M., Garcia, M., Record, R. and Peppas, N. A. (2002) Physicochemical behavior and cytotoxic effects of p(methacrylic acid-g-ethylene glycol) nanospheres for oral delivery of proteins. J Control Rel **80**, 197-205

Uchiyama, T., Sugiyama, T., Quan, Y. S., Kotani, A., Okada, N., Fujita, T., Muranishi, S. and Yamamoto, A. (1999) Enhanced permeability of insulin across the rat intestinal membrane by various absorption enhancers: their intestinal mucosal toxicity and absorption-enhancing mechanism of n-lauryl-beta-D-maltopyranoside. J Pharm Pharmacol **51**, 1241-1250

Udenfriend, S., Stein, S., Bohlen, P., Dairman, W., Leimgruber, W. and Weigele, M. (1972) Fluorescamine: a reagent for assay of amino acids, peptides, proteins, and primary amines in the picomole range. Science **178**, 871-872

Ungell, A.-L. B. (2004) Caco-2 replace or refine? Drug Discovery Today: Technologies **1**, 423-430

Vial, T. and Descotes, J. (2003) Immunosuppressive drugs and cancer. Toxicology **185**, 229-240

Vinogradov, S. V., Batrakova, E. V. and Kabanov, A. V. (2004) Nanogels for oligonucleotide delivery to the brain. Bioconjug Chem **15**, 50-60

Veuillez, F., Kalia, Y. N., Jacques, Y., Deshusses, J. and Buri, P. (2001) Factors and strategies for improving buccal absorption of peptides. Eur J Pharm Biopharm **51**, 93-109

Walter, E., Janich, S., Roessler, B. J., Hilfinger, J. M. and Amidon, G. L. (1996) HT29-MTX/Caco-2 cocultures as an in vitro model for the intestinal epithelium: in vitro-in vivo correlation with permeability data from rats and humans. J Pharm Sci **85**, 1070-1076

Wan, J., Taub, M. E., Shah, D. and Shen, W. C. (1992) Brefeldin A enhances receptor-mediated transcytosis of transferrin in filter-grown Madin-Darby canine kidney cells. J Biol Chem **267**, 13446-13450

Ward, P. D., Tippin, T. K. and Thakker, D. R. (2000) Enhancing paracellular permeability by modulating epithelial tight junctions. Pharm. Sci. Technol. Today **3**, 346-358

Wikman, A., Karlsson, J., Carlstedt, I. and Artursson, P. (1993) A drug absorption model based on the mucus layer producing human intestinal goblet cell line HT29-H. Pharm Res **10**, 843-852

Woodley, J. F. (1994) Enzymatic barriers for GI peptide and protein delivery. Crit Rev Ther Drug Carrier Syst **11**, 61-95

Woodley, J. F. (2001) Bioadhesion: new possibilities for drug administration? Clin Pharmacokinet **40**, 77-84

Wu, Z. H., Ping, Q. N., Wei, Y. and Lai, J. M. (2004) Hypoglycemic efficacy of chitosan-coated insulin liposomes after oral administration in mice. Acta Pharmacol Sin **25**, 966-972

Xia, C. Q., Wang, J. and Shen, W. C. (2000) Hypoglycemic effect of insulin-transferrin conjugate in streptozotocin-induced diabetic rats. J Pharmacol Exp Ther **295**, 594-600

Ziv, E., Lior, O. and Kidron, M. (1987) Absorption of protein via the intestinal wall. A quantitative model. Biochem Pharmacol **36**, 1035-1039

Definition, diagnosis and classification of diabetes mellitus and its complications. Report of a WHO consultation, Part 1: diagnosis and classification of diabetes mellitus, World Health Organization, Geneva, 1999.

UK Prospective Diabetes Study Group. Intensive blood-glucose control with sulphonylureas or insulin compared with conventional treatment and risk of complications in patients with type 2 diabetes (UKPDS 33). (1998) In Lancet, pp. 837-853

VITA

Nikhil Jayant Kavimandan was born in Nagpur, India on October 15, 1979, the son of Jayant and Nisha Kavimandan. After finishing work at the Shivaji Science Collenge, Nagpur in 1997, he joined the University Department of Chemical Technology (UDCT), Mumbai, India. He received his Bachelor of Chemical Engineering degree from UDCT in 2001. Following graduation, he started his work towards his doctorate in Chemical Engineering with Professor Nicholas A. Peppas at Purdue University in the fall of 2001 and transferred to the University of Texas at Austin with Professor Peppas in January of 2003. He is currently working towards a Doctor of Philosophy degree in Chemical Engineering.

Permanent Address: 3401 Red River, #205, Austin, TX 78705

This dissertation was typed by the author.